



UNIVERSITÀ DELLA CALABRIA



UNIVERSITA' DELLA CALABRIA

Dipartimento di Chimica e Tecnologie Chimiche

SCUOLA DI DOTTORATO DI SCIENZA E TECNICA "BERNARDINO TELESIO"

Indirizzo

Organic Materials of Pharmacological Interest

Con il contributo del Fondo Sociale Europeo (FSE)

CICLO XXVI

*"Solid Phase Microextraction (SPME)
coupled to gas chromatography-mass spectrometry
for bioclinical, environmental and food analysis"*

Settore Scientifico Disciplinare:

Chimica Analitica: CHIM-01

Direttore: Ch.mo Prof. Roberto Bartolino

Coordinatore: Ch.mo Prof. Bartolo Gabriele

Supervisori: Ch.mo Prof. Giovanni Sindona

Dott. Antonio Tagarelli

Dottoranda: Dott.ssa Emanuela Gionfriddo

Emanuela Gionfriddo

Author's Declaration

I hereby declare that I am the sole author of this thesis.

This thesis was co-financed by the European Social Fund-European Commission and the Calabria Region. I am the wholly responsible for the content of this thesis; the European Commission and the Calabria Region are not responsible for the use of the information herein contained.

La presente tesi è cofinanziata con il sostegno della Commissione Europea, Fondo Sociale Europeo e della Regione Calabria. L'autore è il solo responsabile di questa tesi e la Commissione Europea e la Regione Calabria declinano ogni responsabilità sull'uso che potrà essere fatto delle informazioni in essa contenute.

Abstract

The analysis of complex samples consists of several steps typically including sampling, sample preparation, separation, quantification, statistical evaluation and decision making, factors that contribute in sequence to the overall length of analysis time. However, till date, sample preparation remains a major bottleneck for various analytical methods/protocols due to the challenges encountered with critical steps such as separation, purification and pre-concentration of the analytes from a given matrix. Often these steps bear the major source of errors influencing the accuracy, precision and reproducibility of the analytical results. In view of this, there is always the need for new, simple, effective and practical analytical methods that can be applied to the ever-growing complexity of sample matrices. Another critical aspect of any analytical technique is the effective coupling of the sample preparation method with analytical instrumentation for reliable quantitation. With an effective sample preparation method and appropriate analytical instrument, significant success can be attained in bio-clinical and bioanalytical studies, environmental and food analysis, especially food metabolomics, etc.

The objective of this research project focuses on the development of new solid phase microextraction (SPME) methods for bio-clinical, environmental and food analysis. The advantages that the technique offers in comparison to traditional sample preparation techniques include a solvent-free method (environmentally friendly), shorter sample preparation times (higher sample throughput), smaller sample size requirements, automation and minimal or no matrix effects. The technique was effectively coupled to a highly efficient gas-chromatography (GC) separation system in tandem with a sensitive and selective mass spectrometer (MS). The developed approaches definitely will offer new opportunities for simple and reliable determination of tumor biomarker, environmental contaminants and food metabolites.

The approach included investigations of effective derivatization strategies coupled with SPME method for analytes otherwise not amenable to gas chromatographic separation, and the successful application to the determination of biogenic amines in human urine, hydrazine in drinking water and seleno-amino acids in aqueous potatoes extract. Critical in the optimization of these new analytical protocols was the use of the multivariate approach (applying Experimental Design) that allowed simultaneous optimization of multiple parameters, which affect extraction, separation and detection of the analytes by employing relatively small number of experiments.

As an example, the multivariate approach enhanced simultaneous determination and analysis of benzothiazoles, benzotriazoles and benzosulfonamides notwithstanding their chemical diversity, while considering the possible synergistic or antagonistic effects between the parameters on the extraction efficiency.

This thesis also provides further insight into the adsorption mechanism of typical commercially available solid sorbents used as extraction phases for SPME while describing and discussing displacement phenomena for different adsorbents and the newly developed PDMS-modified SPME coatings. This was carried out by using a selected group of compounds as a model, belonging to different chemical classes usually present as metabolites in fruits. Finally but not the least, the analytical performances of new developed polymeric ionic liquid-based coatings were evaluated in order to assess their suitability for food analysis.

Riassunto

L'analisi di matrici complesse prevede diverse procedure analitiche come campionamento, preparazione del campione, separazione, quantificazione e analisi dei dati. Ognuno di questi fattori ha un significativo contributo alla durata totale dell'analisi e influisce sulla propagazione degli errori che possono essere commessi, per questi motivi diventa essenziale l'ottimizzazione delle procedure analitiche nei vari steps che le costituiscono.

La preparazione del campione per l'analisi è una delle fasi più delicate di tutta la procedura analitica e include fasi essenziali come la separazione, la purificazione e la concentrazione degli analiti di interesse. Spesso queste operazioni costituiscono le maggiori fonti di errore dell'intera procedura analitica e, di conseguenza, influiscono sulla precisione e riproducibilità dei risultati dell'analisi strumentale. L'obiettivo di questo progetto di ricerca consiste nello sviluppo di protocolli analitici automatizzabili che minimizzino l'uso di solventi organici e prevedano la simultanea preconcentrazione ed estrazione degli analiti tramite microestrazione in fase solida (SPME) da matrici complesse nei campi bioclinico, ambientale ed alimentare. Tale tecnica non prevede l'uso di solventi e consente di effettuare in un unico step l'estrazione, concentrazione ed analisi in maniera del tutto automatizzata il che comporta un notevole vantaggio sulla riproducibilità della misura effettuata.

I metodi sviluppati hanno previsto l'accoppiamento dell'SPME con sistemi ad alta efficienza separativa e ottima selettività come GC-MS/MS per lo sviluppo e l'ottimizzazione di nuovi protocolli analitici per la determinazione di biomarkers tumorali, contaminanti ambientali e costituenti alimentari. La tecnica del SPME è stata testata considerando diverse strategie di derivatizzazione per la determinazione di analiti altrimenti non idonei all'analisi cromatografica come ammine biogene in urina, idrazina in acque potabili e selenoaminoacidi in patate. Essenziale per l'ottimizzazione di tali metodi analitici è stato l'uso della tecnica multivariata dell'Experimental Design che consente l'ottimizzazione simultanea di parametri relativi ad estrazione, separazione e rivelazione con un numero relativamente esiguo di esperimenti. In particolare durante lo sviluppo di un metodo per la simultanea determinazione di benzotiazoli, benzotriazoli e sulfonammidi svolto in questo lavoro di tesi, l'ottimizzazione mediante Experimental Design ha consentito la determinazione delle migliori condizioni sperimentali generali per tutti gli analiti testati, nonostante la presenza di numerose diverse

funzionalità, tenendo anche conto di possibili effetti sinergici o antagonisti tra le variabili testate.

Questo lavoro di tesi ha inoltre riguardato lo studio dei fenomeni di adsorbimento su rivestimenti SPME adsorbenti ed in particolare su fenomeni di “displacement” per rivestimenti commerciali e nuovi rivestimenti modificati con PDMS, considerando un gruppo di analiti selezionati tra vari metaboliti spesso trovati in matrici alimentari.

Infine è stata condotta un’attenta valutazione delle performance analitiche di nuove fasi estraenti basate su Liquidi Ionici per valutare la loro capacità estrattiva nei confronti di costituenti alimentari.

Acknowledgments

At the end of my PhD I would like to thank all those people who made this experience possible and an unforgettable for me.

First of all, I would like to express my deepest sense of gratitude to my supervisors Prof. Giovanni Sindona and Dr. Antonio Tagarelli, who offered their patient support and encouragement throughout the course of my academic studies and research. I thank them for the systematic guidance and great effort they put into training me in the scientific field.

I am also particularly thankful to Prof. Janusz Pawliszyn, for giving me the opportunity to spend part of my PhD research in his group at University of Waterloo (Ontario, Canada). His trust and support, and continuous stimulus to open my mind to new scientific perspectives, were very important to me.

Sincere thanks also go to my friends and fellow labmates at University of Waterloo: Erasmus Cudjoe, Erica Silva, German Gomez, Nathaly Garces, David Donkor and Jiang Ruifen. I will always remember our time with laughter, tears and mutual encouragement: your friendship and support made my experience abroad unique and unforgettable. In particular, would like to express my gratitude to Erasmus for the care and sincere friendship and to Erica for being a wonderful friend and a great coworker.

I also thank Dr. Barbara Bojko for the happy times we spent together and for supporting my research with many “espresso coffees”.

Last but not the least, I would like to sincerely thank Attilio and my family: your love, unconditional care and continuous encouragements made my life easier and the achievement of this degree possible.

“...il termine libertà ha notoriamente molti sensi,
ma forse il tipo di libertà più accessibile,
più goduto soggettivamente, e più utile al consorzio umano,
coincide con l'essere competenti nel proprio lavoro,
e quindi nel provare piacere a svolgerlo.”

La chiave a stella

Primo Levi

"... The word freedom has notoriously many meanings,
but perhaps the most approachable type of freedom,
the most subjectively enjoyable and useful to human society,
coincides with being competent in our own work,
and thus in the pleasure of doing it. "

La chiave a stella

Primo Levi

Table of Contents

Author's Declaration	i
Abstract.....	ii
Riassunto.....	iv
Acknowledgments	vi
Table of Contents	viii
List of Figures.....	xiv
List of Tables	xix
List of Abbreviations	xxii
Chapter 1	1
Theory, principles and applications of Solid-Phase Microextraction	1
1.1 General Introduction	1
1.2 Solid-Phase Microextraction (SPME).....	2
1.3 Principles and fundamentals of Solid Phase Microextraction.....	5
1.3.1 Principles of extraction	5
1.3.2 Thermodynamic	8
1.3.2.1 Effect of Extraction Parameters on Distribution Constants.....	10
1.3.2.2 Effect of temperature	10
1.3.2.3 Salting and pH	11
1.3.2.4 Presence of organic solvent	12
1.3.3 Kinetics	13
1.4 Types of Commercially Available SPME Coatings.....	16
1.4.1 Absorbent coatings.....	17
1.4.2 Adsorbent coatings.....	18
1.4.3 New developed SPME coatings.....	21

1.4.3.1	PDMS-modified coatings	21
1.4.3.2	Ionic Liquid-based coatings.....	22
1.4.3.3	Polypyrrole fibre coatings	22
1.4.3.4	Mesoporous silica fibre coatings	23
1.4.3.5	Molecularly imprinted polymers for SPME	23
1.4.3.6	Immunosorbents as SPME fibre coatings.....	25
1.4.3.7	SPME fibre coatings synthesised by the sol–gel technique.....	26
1.4.3.8	Carbon nanotubes	29
1.5	Derivatization for GC analysis using SPME.....	29
1.5.1	Pre-Extraction derivatization	30
1.5.2	Post-Extraction derivatization.....	30
1.5.3	Simultaneous extraction/on-fibre derivatization.....	30
1.6	Applications of SPME.....	31
1.6.1	Environmental and on-site analysis	31
1.6.2	Bioanalytical analysis	31
1.6.3	Food analysis.....	32
1.6.4	In-vivo SPME	34
1.7	References	36
Chapter 2		43
Multivariate optimization by Experimental Design		43
2.1	Introduction	43
2.2	Univariate versus multivariate optimization	44
2.2.1	Reasons of performing Experimental Design	47
2.3	Screening designs	48
2.3.1	Factorial designs	48
2.3.2	Placket-Burman Design	55
2.4	Optimization Designs.....	57

2.4.1	Central composite design	58
2.4.2	Mixtures designs	61
2.5	Application experimental designs to the optimization of SPME methods.....	65
2.6	References	67
Chapter 3	68
	Solid-Phase Microextraction combined to gas-chromatography mass-spectrometry in bioclinical, environmental and food analysis	68
3.1	Bioclinical and environmental applications of Solid-Phase Microextraction coupled with GC-QqQ-MS	68
3.1.1	Development of a simple and rapid solid phase microextraction-gas chromatography-triple quadrupole mass spectrometry method for the analysis of dopamine, serotonin and norepinephrine in human urine ¹⁵	71
3.1.1.1	Introduction	71
3.1.1.2	Experimental.....	73
3.1.1.2.1	Materials.....	73
3.1.1.2.2	Instrumentation and apparatus.....	73
3.1.1.2.3	Samples	74
3.1.1.2.4	Analytical procedure	74
3.1.1.2.5	Calibration procedure	74
3.1.1.2.6	Optimization of solid phase microextraction variables.....	75
3.1.1.3	Results and discussion	75
3.1.1.3.1	Derivatization and GC-QqQ-MS/MS analysis.....	75
3.1.1.3.2	Solid phase microextraction	79
3.1.1.3.3	Analytical performances.....	83
3.1.1.3.4	Application to real samples	85
3.1.1.4	Conclusions	86
3.1.2	Simultaneous assessment of benzothiazoles, benzothiazoles and sulfonamides concentration in environmental and biological matrices: development of an high-throughput and reliable SPME-GC-QqQ-MS method	88

3.1.2.1	Introduction	88
3.1.2.2	Experimental section	90
3.1.2.2.1	Materials.....	90
3.1.2.2.2	Instrumentation and apparatus.....	90
3.1.2.2.3	Samples	92
3.1.2.2.4	Analytical procedure	92
3.1.2.2.5	Calibration procedure.....	92
3.1.2.2.6	Optimization of solid phase microextraction variables.....	93
3.1.2.3	Results and discussion.....	93
3.1.2.3.1	GC-QqQ-MS/MS analysis	93
3.1.2.3.2	Solid phase microextraction	94
3.1.2.3.3	Matrix effects	102
3.1.2.3.4	Analytical performances.....	104
3.1.2.3.5	Real samples analysis.....	108
3.1.2.4	Conclusions	108
3.1.3	Multivariate optimization of SPME, derivatization and tandem mass-spectrometric conditions for the determination of hydrazine in drinking water: a powerful tool for health risk assessment	110
3.1.3.1	Introduction	110
3.1.3.2	Experimental section	112
3.1.3.2.1	Materials.....	112
3.1.3.2.2	Instrumentation and apparatus.....	112
3.1.3.2.3	Samples for derivatization and tandem mass spectrometric parameters multivariate optimization	113
3.1.3.2.4	Samples for SPME-GC-MS/MS analysis	113
3.1.3.2.5	Optimization of derivatization reaction, tandem mass spectrometric conditions and solid phase microextraction variables	113
3.1.3.3	Results and discussion.....	114
3.1.3.3.1	Derivatization reaction optimization.....	114
3.1.3.3.2	Optimization of tandem mass spectrometric parameters	121
3.1.3.3.3	Optimization of SPME conditions	123

3.1.3.4	Conclusions	128
3.2	Solid Phase Microextraction in Food Analysis: Nutritional Values Assessment and Investigation on Solid and Ionic Liquid Based Coatings	129
3.2.1	Introduction.....	129
3.2.2	Assessment of selenoamino acids levels in selenized potatoes by DI-SPME-GC- MS/MS ⁶²	131
3.2.2.1	Introduction	131
3.2.2.2	Experimental section	132
3.2.2.2.1	Chemicals	132
3.2.2.2.2	Samples	133
3.2.2.2.3	Instrumentation and apparatus.....	133
3.2.2.2.4	Analytical procedure	134
3.2.2.2.5	Calibration procedure.....	134
3.2.2.2.6	Experimental Design.....	135
3.2.2.3	Result and discussion.....	135
3.2.2.3.1	Derivatization and optimization of SPME conditions.....	135
3.2.2.3.2	GC-QqQ-MS/MS analysis	141
3.2.2.4	Application to real samples	146
3.2.2.5	Conclusion.....	146
3.2.3	Headspace versus direct immersion solid phase microextraction (SPME): investigation of inter-analyte displacement phenomena and consideration for food matrices.....	147
3.2.3.1	Introduction	147
3.2.3.2	Experimental.....	149
3.2.3.2.1	Chemicals and Materials	149
3.2.3.2.2	Standards and Samples Preparation	150
3.2.3.2.3	Preparation of Starch Dispersions and Gels	151
3.2.3.2.4	SPME procedure	152
3.2.3.2.5	Instrumentation.....	152
3.2.3.2.6	Result and discussion	152

3.2.3.2.7	Rational behind the selection of model analytes	154
3.2.3.2.8	Trends in displacement occurrence for commercially solid coatings	155
3.2.3.2.9	Effects of extraction time and extraction mode.....	158
3.2.3.2.10	Evaluation of new PDMS-modified PDMS/DVB and DVB/Car/PDMS coatings	163
3.2.3.2.11	Evaluation of matrix effects using starch based food models.....	167
3.2.3.2.12	Evaluation of sampling mode and extraction time.....	169
3.2.3.2.13	Evaluation of different matrix composition and pH.....	173
3.2.3.3	Conclusions	174
3.2.4	Evaluation of new Polymerized Ionic Liquid coatings in SPME for analysis of food metabolites	175
3.2.4.1	Introduction	175
3.2.4.2	Experimental section	176
3.2.4.2.1	Chemicals	176
3.2.4.2.2	Instrumentation and apparatus.....	176
3.2.4.2.3	Preparation of PIL-Based coatings.....	177
3.2.4.2.4	SPME procedure	178
3.2.4.2.5	Calibration Procedure.....	178
3.2.4.3	Result and discussion.....	179
3.2.4.3.1	Analytical performances.....	180
3.2.4.3.2	Comparison of coatings in terms of extraction sensitivity	182
3.2.4.4	Conclusions	185
3.3	References	187

List of Figures

Figure 1.1 The custom-made SPME device based on Hamilton 7000 series syringe	3
Figure 1.2 Commercial assembly for SPME fibers commercialized by Supelco.....	3
Figure 1.3 Design of the commercial SPME device for a) manual, b) automatic extraction/desorption	4
Figure 1.4 Graphic representation of the SPME/sample system configuration.....	5
Figure 1.5 Two phase SPME/sample system.....	6
Figure 1.6 The effect of pH on the SPME of acid compounds.....	12
Figure 1.7 Extraction versus time profiles: (a) perfect agitation conditions; (b) well agitated and (c) poorly agitated.....	14
Figure 1.8 Boundary layer model configuration.....	14
Figure 1.9 Dimensionless extraction versus time profile, corresponding to mass absorbed from an agitated solution of infinite volume, when the boundary layer controls the extraction rate.	15
Figure 1.10 Chemical structures of common polymers used as SPME coatings.....	17
Figure 1.11 Schematization of absorption and adsorption mechanism for liquid and solid coatings	19
Figure 1.12 Carboxen 1006 tapered pore.....	20
Figure 1.13 Front and lateral section view of a DVB/Car/PDMS coating	20
Figure 1.14 Main approaches to MIP synthesis. Non-covalent approach: (A) mixture of functional monomers, cross-linking agents, polymerisation initiator and templates dissolved on porogenic solvent to form template/functional monomer complex; (B) polymerisation; (C) removal of template (by solvent extraction) and (D) analyte binding (via non-covalent interactions) on the specific imprinted site. Covalent approach: (A') template containing polymerisable groups mixed with cross-linking agent and initiator in proper solvent; (C) removal of template after polymerisation (with	

breaking of covalent bonds between template and polymer) and (D) analyte binding (via covalent bonds) on the specific imprinted site.	24
Figure 1.15 Main reactions involved on sol–gel process for SPME fiber coating. Modified from Malik and co-workers	28
Figure 2.1 Isoresponse plot for the optimization of the yield of a chemical reaction.....	45
Figure 2.2 Lverage plot for the optimization of the yield of a chemical reaction.....	46
Figure 2.3 Graphical representation of a 2 ³ Design	49
Figure 2.4 Isoresponse plot	52
Figure 2.5 Visualization of fractional factorial design	54
Figure 2.6 Construction of a three factor central composite design	58
Figure 2.7 Central composite designs for two and three factors. The gray dots form.....	59
Figure 2.8 The representation of a 3-component mixture, with the lines of the grid	61
Figure 2.9 Isoresponse plots of the two responses of the mixture design (top: breaking	64
Figure 3.1 Reaction between DA (A), 5-HT (B) and NE (C) and the derivatizing agents (R = methyl, ethyl, propyl).....	75
Figure 3.2 Electron ionization (EI) full-scan spectra of the derivatized analytes: DA (A), 5-HT (B) and NE (C).....	76
Figure 3.3 Response surfaces estimated from the full factorial design for amount of pyridine versus amount of propyl chloroformate: peak area of derivatized DA (A), derivatized 5- HT (B) and derivatized NE (C).....	78
Figure 3.4 Peak areas for the three analytes obtained by performing analyses in immersion mode with five different fibers	79
Figure 3.5 Pareto charts obtained from the central composite design for derivatized DA (A), derivatized 5-HT (B) and derivatized NE (C)	82
Figure 3.6 Response surfaces estimated from the central composite design for extraction time versus desorption temperature: peak area of derivatized DA (A), derivatized 5-HT (B) and derivatized NE (C)	83

Figure 3.7 SPME-GC-QqQ-MS (MRM acquisition mode) chromatogram of a real urine sample from an healthy individual (r.t. 16.80 DA; 16.80 DA-d ₃ ; 18.39 5-HT; 18.36 5-HT-d ₄ ; 19.19 NE; 19.17 NE-d ₆).....	86
Figure 3.8 Peak areas obtained by performing analyses in immersion modes with five different fibers. PA, polyacrylate; Car/PDMS, (carboxen/polydimethylsiloxane); DVB/Car/PDMS, (divinylbenzene/ carboxen/ polydimethylsiloxane); PDMS/DVB, (divinylbenzene/ polydimethylsiloxane) and PDMS, polydimethylsiloxane.	94
Figure 3.9 Pareto charts obtained from the central composite design for all the investigated analytes	97
Figure 3.10 Response surfaces estimated from the central composite design	99
Figure 3.11 Chromatogram obtained from the extracts of derivatization of hydrazine with ethyl chloroformate.....	114
Figure 3.12 Mass spectra and molecular structure of A) bi-derivatized, b) tri-derivatized and c) tetra-derivatized hydrazine obtained with ethyl chloroformate.....	116
Figure 3.13 Chromatograms obtained from derivatization by A) propyl- and B) isobutyl chloroformate.....	117
Figure 3.14 Representative response surface for the bi-derivatized product obtained by derivatization reaction with ethyl chloroformate.....	119
Figure 3.15 Evaluation of SPME coatings performances: peak areas for the three derivation products obtained by performing MRM analyses in immersion mode with five different coatings.....	124
Figure 3.16 Pareto chart obtained from the central composite design for tetra-derivatized hydrazine.....	127
Figure 3.17 Response surfaces estimated from the central composite design for tetra-derivatized hydrazine obtained with propylchloroformate: amount of salt added versus adsorption temperature (A), amount of salt added versus desorption temperature (B) and adsorption temperature versus desorption temperature (C).....	128
Figure 3.18 Schematic diagram of the derivatization reaction for SeMet	135

Figure 3.19 Peak areas obtained for SeMet and SeMeSeCys derivatized with three alkylchloroformates and extracted by immersion mode with five SPME fibers.....	137
Figure 3.20 Pareto charts obtained from central composite design for A) SeMeSeCys and B) SeMet.....	139
Figure 3.21 Response surfaces obtained for A) SeMeSeCys and B) SeMet from the central composite design: peak area of derivatized selenoamino acids for desorption temperature versus pH, versus pH and desorption temperature versus % NaCl	140
Figure 3.22 Electron ionization (EI) full-scan spectra of (A) SeMeSeCys (B) SeMet and (C) SeEt.....	142
Figure 3.23 EI-MS/MS spectra of SeMeSeCys, SeMet and SeEt with parent ion at m/z 311 (A), m/z 325 (B) and m/z 339 (C).....	143
Figure 3.24 Comparison of three commercial SPME coatings (PDMS/DVB, DVB/Car/PDMS, Car/PDMS) in terms of occurrence of inter-analyte displacement for a) direct and b) headspace extractions. Error bars represent standard deviation obtained for three replicates	156
Figure 3.25 Comparison of the trends of inter-analyte displacement at different extraction times (15, 30, 60 minutes). The result are expressed as % of analyte displaced.....	159
Figure 3.26 Comparison in terms of percent displaced for PDMS-DVB coating at 15 and 60 minutes of extraction in HS and DI mode at the highest level of alpha-pinene spiked.	159
Figure 3.27 Comparison of the trends of inter-analyte displacement for different extraction modes: direct immersion extraction (right) and headspace extraction (left), performed at 15 minutes of extraction in triplicates using PDMS/DVB coating.....	161
Figure 3.28 Comparison of commercial coatings and PDMS-modified coatings for displacement occurrence in direct immersion analysis.....	164
Figure 3.29 Comparison of commercial coatings and PDMS-modified coatings for displacement occurrence in headspace analysis	166

Figure 3.30 Comparison of extraction mode at 30 minutes of extraction for PDMS/DVB coating	170
Figure 3.31 Comparison of extraction mode in pre-equilibrium and equilibrium extractions...	171
Figure 3.32 Comparison of extraction mode and time for SPME extractions carried out in starch gel matrix. The results shown are expressed in relative % of compound displaced and refer to all the 10 metabolites tested at the highest level of alpha-pinene spiked in the matrix.....	172
Figure 3.33 Comparison of the film thickness normalization of the slope calculated from detector response for all coatings in the extraction of selected analytes	184

List of Tables

Table 1.1 Types of Commercially Available SPME Fibre Coatings.....	16
Table 2.1 The experimental matrix of the 2 ³ factorial design.....	49
Table 2.2 Model matrix response.....	50
Table 2.3 Fractional factorial design	53
Table 2.4 Plackett–Burman design for 11 factors.....	56
Table 2.5 Coded factor levels for central composite designs for two- and three-factor systems .	59
Table 2.6 The experimental matrix and the responses of the mixture design.....	62
Table 3.1 Retention times (r.t.) and electron ionization tandem mass spectrometry (EI-MS/MS) parameters (Collision energies (V) are indicated in parenthesis).....	74
Table 3.2 Design matrix in the full factorial design with three levels for optimization of derivatization reaction.....	78
Table 3.3 Design matrix in the central composite design (CCD) for optimization of SPME parameters.....	81
Table 3.4 Summary of calibration parameters, mean accuracies, relative standard deviations (RSD (%), in parentheses) and limits of detection (LODs) and limits of quantitation (LOQs) in multiple reaction monitoring (MRM) acquisition.....	83
Table 3.5 Retention time (RT) and electron ionization tandem mass spectrometry (EI-MS/MS) parameters (Collision energies (eV) are indicated in parenthesis).	91
Table 3.6 Design matrix of central composite design (CCD) for optimization of SPME parameters.....	96
Table 3.7 Asymmetry factor (AF) of the target compounds analyzed for direct injection of analytes solution and SPME injection in optimized conditions.	101
Table 3.8 Matrix effect (%) evaluated at 20 and 80 µg l ⁻¹ for all the matrices tested	103
Table 3.9 Calibration parameters, LOD and LOQ values for all the matrices tested.....	106

Table 3.10 Mean accuracy and relative standard deviations, RSD (% in parentheses) evaluated at 8, 20 and 80 $\mu\text{g l}^{-1}$ for all the matrices tested.....	107
Table 3.11 Electron ionization tandem mass spectrometry (EI-MS/MS) parameters (Collision energies (eV) are indicated in parenthesis).....	113
Table 3.12 Fragmented ions for the three derivatives obtained derivatizing hydrazine with ethyl chloroformate.....	115
Table 3.13 Fragmented ions for the three derivatives obtained derivatizing hydrazine with propyl chloroformate.....	118
Table 3.14 Fragmented ions for the three derivatives obtained derivatizing hydrazine with isobutyl chloroformate.....	118
Table 3.15 Design matrix in the full factorial design with three levels for optimization of derivatization reaction.....	119
Table 3.16 Design matrix in the full factorial design with three levels for optimization of derivatization reaction.....	120
Table 3.17 optimized amount of derivatization reagent obtained by multivariate optimization	120
Table 3.18 Precursor and product ion selected for mass spectrometric multivariate investigation.	121
Table 3.19 Design matrix in the full factorial design with three levels and three factors for optimization of derivatization reaction.....	122
Table 3.20 Selected SRM transition and their optimized tandem mass spectrometric conditions for bi-derivatized and tetra-derivatized compounds.	123
Table 3.21 Design matrix in the central composite design (CCD) for optimization of SPME parameters.....	126
Table 3.22 Matrix of the central composite experimental design.....	138
Table 3.23 SRM transition evaluated and optimum values of collision energy	144

Table 3.24 Summary of calibration parameters, mean accuracies (%), relative standard deviation RSD (N=3), % in parenthesis and limits of detection (LODs) and limits of quantification (LOQs).....	145
Table 3.25 Target metabolites and their physicochemical properties: molecular weight, log Kow , boiling point, EI quantification ion.....	151
Table 3.26 Comparison between solid coatings tested in terms of relative amount displaced at the highest spiked level of alpha-pinene for HS extraction carried out at the same working conditions.....	157
Table 3.27 Differences in displacement occurrence in direct immersion (DI) and headspace (HS) mode for DVB/Car/PDMS and Car/PDMS coatings.....	162
Table 3.28 Differences in displacement occurrence in direct immersion (DI) and headspace (HS) mode for DVB/Car/PDMS and Car/PDMS coatings.....	167
Table 3.29 Evaluation of different extraction modes for different starch gels systems	173
Table 3.30 Analytes of interest and their physical-chemical properties.....	177
Table 3.31 Structures, abbreviations, and film thicknesses of all sorbent coatings employed in the study.....	178
Table 3.32 Concentration levels of the analytes of interest	179
Table 3.33 Summary of analytical performances and reproducibility values (% RSD) for all the coatings tested.....	181

List of Abbreviations

μSPE	micro solid phase extraction
2-MeBTH	2-methylbenzothiazole
2-MeSBTH	2-(methylthio)benzothiazole
2-NH₂BTH	2-aminobenzothiazole
2-OHBTH	2-hydroxybenzothiazole
2-SHBTH	2-mercaptobenzothiazole
4-MeBTR	4-methyl-1H-benzotriazole
5,6-MeMeBTR	5,6-dimethyl-1H-benzotriazole
5-CIBTR	5-chlorobenzotriazole
5-HT	5-hydroxytryptophan
5-MeBTR	5-methyl-1H-benzotriazole
AED	atomic emission detector
AF	asimmetry factor
BSA	benzenesulfonamide
BTEX	benzene toluene ethylbenzene xylene
BTHs	benzothiazoles
BTRs	benzotriazoles
Car/PDMS	carboxen/polydimethylsiloxane
CCD	central composite design
CE	capillary electrophoresis
CI	chemical ionization
CID	collision-induced dissociation
CL	chemiluminescence detection
CNTs	carbon nanotubes
DA	dopamine
DI	direct immersion
DI-SPME	direct immersion solid phase microextraction
DLLME	dispersive liquid-liquid microextraction

DoE	design of experiments
DVB	divinylbenzene
DVB/Car/PDMS	divinylbenzene/carboxen/polydimethylsiloxane
ECD	electrochemical detector
ECF	extracellular fluid
ECF	ethyl chloroformate
EDMA	ethylene glycol dimethacrylate
EI	electron ionization
ESI-LC-MS/MS	electrospray ionization-liquid chromatography -tandem mass spectrometry
FID	flame ionization detector
FPD	flame photometric detector
FS	fused silica
GC	gas chromatography
GC × GC-ToFMS	comprehensive two-dimensional gas chromatography–time-of-flight mass spectrometry
GC-MS	gas chromatography mass spectrometry
HMDS	hexamethyldisilazane
HPLC	high-performance liquid chromatography
HPTES	3-[bis(2-hydroxyethyl)amino]-propyl-triethoxysilane
HS	headspace
HS-SPME	headspace solid phase microextraction
HZ	hydrazine
IBCF	isobutyl chloroformate
ICP-MS	inductively coupled plasma mass spectrometry
ILs	ionic liquids
LC	liquid chromatography
LC-MS	liquid chromatography-mass spectrometry
LC-MS/MS	liquid chromatography -tandem mass spectrometry
LLE	liquid-liquid extraction
LLOQ	lower limit of quantification

LOD	limit of detection
LOQ	limit of quantitation
MAA	methacrylic acid
MBHFBA	N-methyl-bis(heptafluorobutyramide)
MCF	methyl chloroformate
MCM-41	Mobil Composition of Matter no 41
ME	matrix effect
MEPS	microextraction in packed syringe
MIP-AES	microwave-induced plasma atomic emission spectrometry
MIPs	molecularly imprinted polymers
MRM	multiple reaction monitoring
MS	mass spectrometry
MS/MS	tandem mass spectrometry
M-SPE	miniaturized solid phase extraction
MTMS	methyltrimethoxysilane
MWCNTs	multi-wall carbon nanotubes
NE	norepinephrine
N-Et-p-TSA	N-ethyl p-toluenesulfonamide
OPA	ortho-phthalaldehyde
OVAT	One Variable At a Time
PA	polyacrilate
PAHs	polycyclic aromatic hydrocarbons
PCF	propyl chloroformate
PDMS	polydimethylsiloxane
PDMS-DVB	polydimethylsiloxane/divinylbenzene
PEG	polyethylene glycol
PGC	porous graphitic carbon
PILs	polymeric ionic liquids
PLE	pressurized liquid extraction
Poly([DDMGlu][MTFSI])	N,N-Didecyl-N-methyl-d-glucaminium poly(2-methyl-acrylic acid 2-[1-(3-{2-[2-(3-trifluoromethanesulfonylamino-propoxy)-ethoxy]-ethoxy}-propylamino)-vinylamino]-ethyl ester)

Poly([VBHDIM][NTf2])	Poly(1-vinylbenzyl-3-hexadecylimidazolium) bis[(trifluoromethyl)sulfonyl]imide
POP	persistent organic pollutants
PPY	polypyrrole
p-TSA	p-toluenesulfonamide
PTV	programmed temperature vaporization
QuEChERS	Quick Easy Cheap Effective Rugged Safe
rpm	revolutions per minute
RSD	relative standard deviation
S/N	signal to noise ratio
SE	soxhlet extraction
SeAA	selenoamino acids
SeEt	selenoethionine
SeMeSeCys	selenomethylselenocysteine
SeMet	selenomethionine
SLE	solid-liquid extraction
SPE	solid phase extraction
SPME	solid phase microextraction
SRM	selected reaction monitoring
SWCNTs	single-wall carbon nanotubes
TFA	trifluoroacetic acid
TFME	thin-film microextraction
US EPA	United States Environmental Protection Agency
UV	ultra violet

Chapter 1

Theory, principles and applications of Solid-Phase Microextraction

1.1 General Introduction

The analysis of complex samples consists of several steps, typically including sampling, sample preparation, separation, quantification, statistical evaluation, and decision making factors that contribute in sequence to the overall length of analysis time.

Sample preparation includes critical steps such as separation, purification and pre-concentration of the analytes from a given matrix and always constitutes the major bottleneck in analytical protocols. Often these steps bear the major source of errors influencing the accuracy, precision and reproducibility of the results obtained by instrumental analysis. In addition to the challenges associated with sample preparation, recent protocols require the routine use of simple and high-throughput analytical techniques. Some of the reasons include overall decrease in analysis time, cost and also the combination of any fast separation and detection method with a long and tedious sample preparation procedure is often not practical. On the light of this, the development of fast sample preparation techniques, easily coupled to analytical system of separation and/or detection, is a critical requirement to allow for full implementation of high-throughput methods.

Another important aspect of sample preparation is miniaturization. Some of the advantages of miniaturization include avoidance of the use of large sample sizes, decrease in the invasiveness of the extraction process for *in vivo* applications, improving sampling device portability for direct on-site sampling and the reduction of use of extraction solvents for residue analysis, which is in agreement with the United States Environmental Protection Agency (US EPA) requirements. Conventional methods such as liquid-liquid extraction (LLE), solid-liquid

extraction (SLE), soxhlet extraction (SE), etc., are often too laborious, time consuming and may require the use of large organic solvents. In recent times, relatively newer sample preparation methods such as solid phase extraction (SPE) and solid phase microextraction (SPME) have gained a lot of interest among scientific researchers. This thesis focuses on SPME as a sample preparation method for the analysis complex samples.

1.2 Solid-Phase Microextraction (SPME)

Solid-phase microextraction (SPME) was developed by Pawliszyn and coworkers in 1989 in order to address the need for rapid laboratory and on-site sample preparation, and for efficient integration of sample preparation with separation and detection systems¹. Numerous advantages are associated with this technique for the quantitative and qualitative analyses of organic compounds from various sample matrices. Some of the advantages comprise small sample amount requirements, no/minimal solvent consumption, relatively faster sample throughput, simple and amenable to automation leading to high-throughput analysis, extraction and pre-concentration of analytes from solid, liquid, and gaseous sample matrices, applicable for on-site and *in vivo* investigations². Early work associated with the development of SPME involved the use of fused-silica optical fibers uncoated or coated with polymeric phases. These were dipped into aqueous samples containing target analytes and directly inserted to the gas chromatograph injector for desorption of the extracted analytes¹.

The main limitation associated with this procedure was the introduction and degradation of the coatings in the gas chromatograph system. Despite of this drawback, the approach was still useful since it provided an alternative method for efficiently extracting both polar and nonpolar species from aqueous samples. In the light of these results and since chromatographers already had good knowledge of fused-silica coating methods, the development of SPME accelerated very rapidly by incorporating coated fibers into a Hamilton™ 7000 series microsyringe making desorption in the gas chromatograph injector more reliable and similar to a standard syringe injection. By depressing the plunger the coating/fiber is exposed during extraction and desorption, while it is protected in the needle during storage and penetration of the septum. The schematic illustration of the microsyringe assembly is shown in Figure 1.1

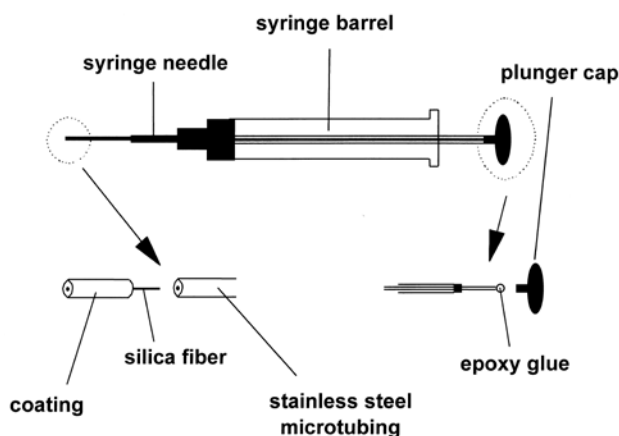


Figure 1.1 The custom-made SPME device based on Hamilton 7000 series syringe

A further optimization of the design led to the development of the assembly showed in Figure 1.2 that avoids the use of more expensive microsyringes. The part of this device that practically is responsive to the extraction and concentration of analytes from sample matrix is a fiber solid support coated with a thin layer of a polymeric stationary phase. The fiber is stored inside the needle, which protects the fiber coating from damage during vial/injector septa penetrations. For practical purposes the SPME fiber assembly, which is a combination of the fiber and needle, also includes a fiber assembly holder available in two different formats to allow for either manual or automated SPME processes Figure 1.3

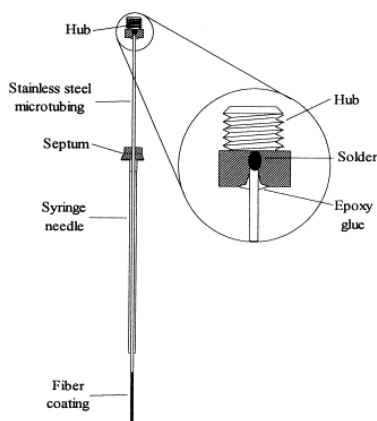


Figure 1.2 Commercial assembly for SPME fibers commercialized by Supelco

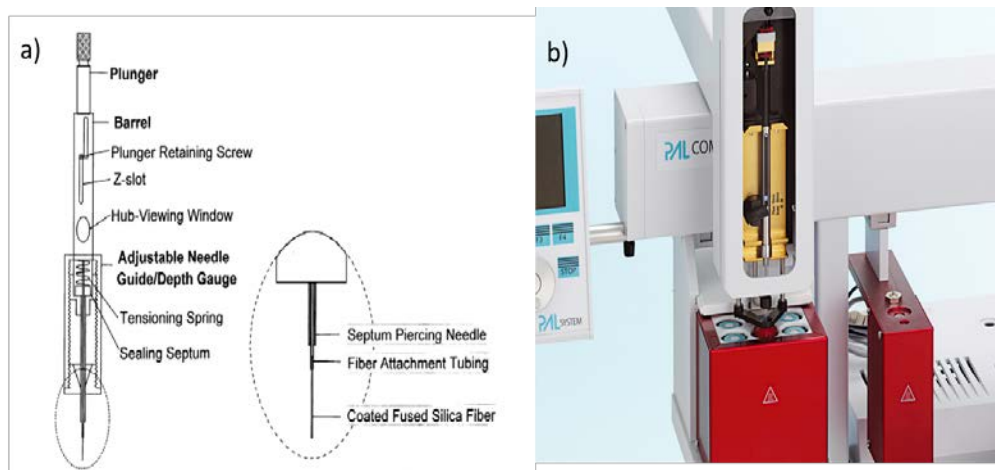


Figure 1.3 Design of the commercial SPME device for a) manual, b) automatic extraction/desorption

This development made the technique more attractive since it completely avoided the use of organic solvents for desorption of analytes and in addition was easily coupled to the gas chromatography (GC) for improved sample throughput analyses in various applications.

Subsequently, the theoretical principles and method development strategies of SPME were developed and established. Currently, development of new SPME devices for various bioanalytical applications, automation, calibration approaches and new extracting phases are still active research areas been explored, and are also improving its suitability for broader range of applications.

Traditionally, SPME has been used routinely in combination with GC and gas chromatography-mass spectrometry (GC-MS). However, the necessity to selectively extract and analyze non-volatile or thermally labile compounds not amenable to GC, led to the hyphenation of the technique to high-performance liquid chromatography (HPLC) and liquid chromatography-mass spectrometry (LC-MS). This led to development of new HPLC interfaces and high-throughput analysis on a 96-well plate format with different geometries and also appropriate sorbents compatible with HPLC solvents³⁻⁶. Today SPME is widely applied to both target and non-target analysis of broad range of organic compounds from various environmental, biological, and food matrices. The versatility of the technique allows its application for on-site analysis as well as *in-vivo* sampling, possible because of the negligible perturbation on living systems^{7,8}.

1.3 Principles and fundamentals of Solid Phase Microextraction

1.3.1 Principles of extraction

SPME was developed to address the need for rapid sample preparation, both in the laboratory and on-site investigations. With the SPME method, a small amount of extracting phase dispersed on a solid support is exposed to the sample for a well-defined period of time. The miniaturized extraction phase geometry enhances rapid mass transfer during extraction and desorption steps. Figure 1.4 shows a graphical representation of the SPME/sample system.

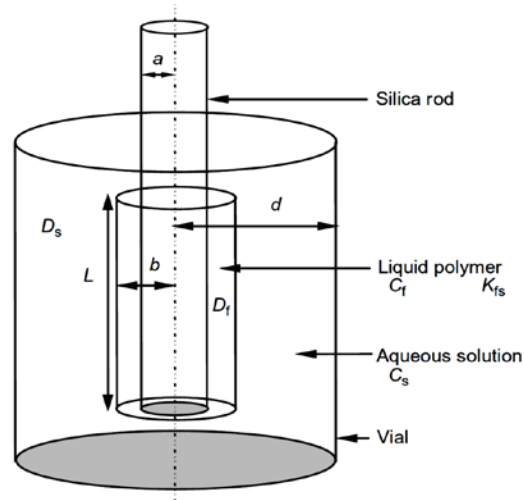


Figure 1.4 Graphic representation of the SPME/sample system configuration

where:

- a and b are the fibre coating inner and outer radius respectively.
- L is the fibre coating length
- d is the vial inner radius
- C_f and C_s are analyte concentration in the fibre coating and in the sample respectively.
- D_f and D_s are analyte diffusion coefficient in the fiber coating and in the sample respectively
- K_{fs} is the analyte distribution coefficient between fibre coating and sample

Contrary to other extraction techniques, exhaustive extraction of analyte from the sample matrix is not achieved by SPME because only a small amount of the analyte is extracted from the given matrix. The amount extracted can be obtained either under equilibrium conditions or at a

specified time (pre-equilibrium) prior to achieving equilibrium. Therefore, SPME operationally is a non-exhaustive, equilibrium or pre-equilibrium extraction method, which can be applied to microextractions from batch and flow-through systems. In view of this, SPME is distinctly different from SPE because SPE techniques, including microSPE (μ SPE) and miniaturized SPE (M-SPE)⁹, are all exhaustive extraction procedures. A simple system of SPME coating immersed in a homogeneous aqueous sample matrix is schematically presented in Figure 1.5

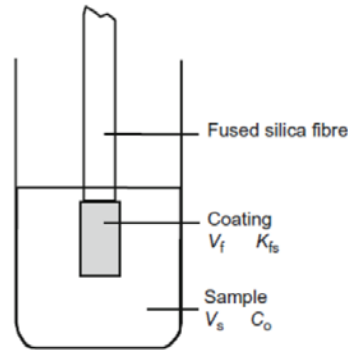


Figure 1.5 Two phase SPME/sample system

where :

- V_f is the volume of fibre coating
- V_s is the volume of sample
- C_o is the initial concentration of the analyte in the sample
- K_{fs} , fibre/sample distribution coefficient

For this two-phase system, the equilibrium conditions can be described according to the law of conservation mass as shown in Equation 1.1

$$C_o V_s = C_f^\infty V_f + C_s^\infty V_s \quad (1.1)$$

Where C_f^∞ and C_s^∞ are respectively the concentrations of the analytes at equilibrium on the fiber coating and in the sample. The fibre/sample distribution coefficient, K_{fs} , is defined as:

$$K_{fs} = \frac{C_f^\infty}{C_s^\infty} \quad (1.2)$$

Combining Equations 1.1 and 1.2 leads to Equation 1.3.

$$C_f^\infty = C_0 \frac{K_{fs}V_s}{K_{fs}V_f + V_s} \quad (1.3)$$

Equation 1.3 can be re-arranged to obtain the number of moles of analyte extracted on the coating at equilibrium

$$n = C_f^\infty V_f = C_0 \frac{K_{fs}V_f V_s}{K_{fs}V_f + V_s} \quad (1.4)$$

Equation 1.4 shows the linear proportionality between the amount of analyte extracted at equilibrium, n , and the initial concentration of the analyte in the sample C_0 , which is the basic principle of quantification using SPME.

When the volume of sample is very large and/or the distribution coefficient very low it happens that $K_{fs}V_f \ll V_s$ and equation 1.4 can be simplified to:

$$n = C_0 K_{fs} V_f \quad (1.5)$$

This equation points out a very useful characteristic of SPME: the amount of analyte extracted is independent of the volume of the sample due to the fact that only a small fraction of the analyte is extracted from the matrix and the coating volume is very small compared to the sample. This feature makes SPME a very versatile sampling technique allowing quantification also when the coating is exposed to the flowing blood (*in-vivo* experiments), ambient air (on-site analysis), water, etc.

With a three-phase system such as the fibre coating, the headspace and a homogeneous matrix for instance pure water or air, the number of moles of analyte extracted on the coating at equilibrium, when the coating is exposed to the headspace, will be:

$$n = \frac{K_{fh}K_{hs}V_f C_0 V_s}{K_{fh}K_{hs}V_f + K_{hs}V_h + V_s} \quad (1.6)$$

The fiber coating/headspace and headspace/sample distribution constants, K_{fh} and K_{hs} , are respectively defined as:

$$K_{fh} = \frac{C_f^\infty}{C_h^\infty} \text{ and } K_{hs} = \frac{C_h^\infty}{C_s^\infty} \quad (1.7)$$

The initial total amount of analyte in the sample at equilibrium can be obtained according the following equation:

$$C_0V_s = C_f^\infty V_f + C_h^\infty V_h + C_s^\infty V_s \quad (1.8)$$

where C_h^∞ and V_h are concentration of analyte in the headspace at equilibrium and volume of headspace.

1.3.2 Thermodynamic

The basic thermodynamic principle common to all the chemical extraction techniques is the partitioning of the analyte between the sample and the extracting phase. When a liquid is used as extracting phase the partitioning equilibrium is described by a distribution constant defined as:

$$K_{es} = \frac{a_e}{a_s} = \frac{C_e}{C_s} \quad (1.9)$$

where a_e and a_s are the activities of analytes in the extraction phase and matrix, respectively, and can be approximated by the appropriate concentrations.

For solid porous extraction phase, the distribution coefficient for the adsorption equilibrium can be written as:

$$K_{es}^s = \frac{S_e}{C_s} \quad (1.10)$$

where S_e is the solid extraction phase surface concentration of adsorbed analytes.

These physicochemical constants, which reflect the chemical composition of the extraction phase, have been discussed in detail in literature for fundamental chromatographic separation. Although chromatography is frequently used to determine distribution constants, sample-preparation techniques (e.g. SPME) can also be used to provide information about the thermodynamics of the partitioning process¹⁰. The partitioning process in GC is analogous to the partitioning process in SPME. A well-defined relationship correlating distribution constants and retention times is given in Equation 1.11:

$$K_{fg} = (t_R - t_A)F \frac{T}{T_m} \cdot \frac{p_m - p_w}{p_m} \cdot \frac{3 \left(\frac{p_i}{p_o}\right)^2 - 1}{2 \left(\frac{p_i}{p_o}\right)^3 - 1} \cdot \frac{1}{V_L} \quad (1.11)$$

where:

- t_R and t_A are the retention times of the solute and an unretained compound,
- respectively
- F is the column flow measured by a soap-bubble flow meter
- T and T_m are the temperatures of the column and flow meter, respectively
- p_m and p_w are the flow meter pressure and the saturated water vapour pressure, respectively
- p_i and p_o are, respectively, the inlet and outlet pressures of the column
- V_L is the column's stationary phase volume.
- Usually, p_m and p_o are equal to atmospheric pressure

The K_{fg} estimated by this method for the polydimethylsiloxane (PDMS) to gas partitioning of benzene agrees within a few percentage points with the value determined by SPME experimentation¹¹.

The fibre coating/water distribution constants can be calculated from the following equation:

$$K_{fw} = K_{fg} * K_{gw} \quad (1.12)$$

where K_{fg} can be calculated from chromatographic data, as discussed above. K_{gw} is the gas/water distribution constant (Henry's constant), which can be obtained from physicochemical tables or can be estimated by the structural unit contribution method¹².

1.3.2.1 Effect of Extraction Parameters on Distribution Constants

Thermodynamic principle is useful to predict how different extraction parameters can affect the partitioning of analytes between coating and sample, thus the distribution constants. Controlling these parameters enhances the optimization of the extraction process for more reproducible and accurate determinations and the correction for variations in extraction conditions without repeating calibration tests for the new conditions. Extraction conditions that affect K_{fs} include temperature, salting, pH and organic solvent content in water.

1.3.2.2 Effect of temperature

The dependence of the distribution coefficient, K_{fs} , from the temperature is described by the following equation:

$$K_{fs} = K_0 e^{-\frac{\Delta H}{R} \left(\frac{1}{T} - \frac{1}{T_0} \right)} \quad (1.13)$$

where K_0 is the distribution constant when both fibre and sample are at temperature T_0 (in degrees Kelvin), ΔH is the molar change in enthalpy of the analyte when it moves from sample to fibre coating and R is the gas constant. Usually the enthalpy change is constant in the temperature range in which SPME operates. When the K_{fs} value for an analyte is greater than 1, the analyte has a lower potential energy in the fibre coating than in the sample, so the analyte partitioning into the fibre must be an exothermic process, implying that ΔH (the molar change in enthalpy of the analyte when it moves from sample to fibre coating) is greater than 0. This means that according to Equation 1.14 increasing the temperature will decrease K_{fs} . However, increasing the sample temperature improves the release of the analytes from the sample matrix, increasing the extraction rate or enhancing the mass transfer in the vapour phase above the sample when headspace extractions are performed. For this reason special attention must be paid in the optimization of this parameter in order to find the best compromise between the matrix modification and the thermodynamic variation of the distribution coefficient. An efficient protocol to enhance the extraction performances of the coating consists in cooling the coating simultaneously with sample heating. With the increase in the temperature gap between fibre

coating and matrix, the amount of analyte increases, as the theory would predict. This SPME device for coating cooling has been automated and the technique called Cooled-fiber SPME. Details of the approach are well discussed elsewhere¹³⁻¹⁶.

1.3.2.3 Salting and pH

Salt addition and pH adjustments of aqueous sample matrices are two common strategies to enhance the extraction of organic species.

Salt addition increases the ionic strength of the sample solution and consequently the activity coefficient of the organic species in the solution decrease; thus, according to Eq. (1.9), it increases the K_{fs} constant and improves sensitivity in most applications, except those involving very polar analytes. The salting-out effect is commonly used for HS-SPME since it causes the analyte molecules to pass more readily from the sample matrix to headspace. For many organic compounds, aqueous solubilities decrease in the presence of large amounts of salt. For compounds whose aqueous solubility does not change, the addition of salt may decrease the amount extracted by decreasing the activity coefficients of the analytes, which adversely affects the partition coefficient between the sample and the SPME coating. The amount of salt added must be carefully evaluated especially when extraction is performed from complex matrices. In some cases, an increase in ionic strength improves extraction efficiency of the target analyte, and also improves extraction of interfering compounds, which is not desirable, especially if a solid (adsorbent) type of coating is used¹⁷. In the analysis of biological samples, to account for the physiological variability of ionic strength of biological fluids, the addition of saturating amounts of sodium chloride minimises the variability in ionic strength between samples and yields more reliable quantitative results¹⁸. However, salt addition can also have an adverse effect on the free concentration of the analytes, since the high amount of salt in the matrix may induce precipitation incorporating the analytes of interest or have negative impact the extraction due to reduced mass transfer¹⁹. The effect of salting-out on SPME has not been examined theoretically, although theories have been developed for the effect of salting on liquid-liquid extraction²⁰.

Adjusting the pH of the sample matrix is critical to improve the method sensitivity since only neutral/undissociated species are extracted by SPME. Therefore, low pH values will improve the extraction of acidic compounds and high pH will improve extraction efficiency for basic compounds. When adjusting sample pH, HS sampling is the preferred extraction mode because direct contact of the fibre coating with sample at very low or high pH levels can damage the fibre

coating. When DI sampling mode is used, extreme pH values should be avoided because they can cause degradation of the coating. For commercially available fibres, the recommended pH range is 2-11, with the exception of PDMS (100 μm), for which pH should be between 2 and 10, and polyethylene glycol (PEG), with a recommended pH range of 2-9. Adjusting the pH will change K for dissociable species, according to the following equation:

$$K = K_0 \frac{[H^+]}{K_a + [H^+]} \quad (1.14)$$

where:

- K_0 is the distribution constant between the sample and the fibre of the undissociated form
- K_a is the acidity constant of the dissociable analyte

This relation was confirmed by Yang and Peppard²¹ whose results for the extraction of acids are illustrated in Figure 1.6

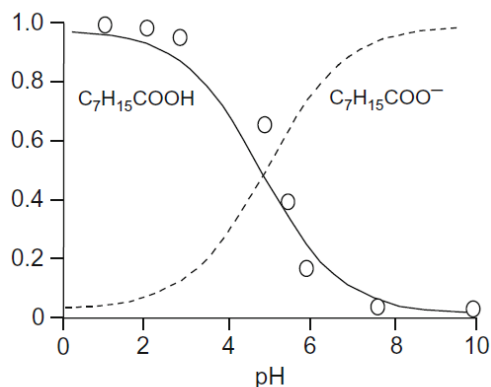


Figure 1.6 The effect of pH on the SPME of acid compounds

1.3.2.4 Presence of organic solvent

Adding organic solvent to an aqueous matrix changes the polarity of the media affecting the distribution coefficient K_{fs} according to the following equation:

$$K_{fs} = K_{fw} 2.303 e^{\left(\frac{P_1 - P_2}{2}\right)} \quad (1.15)$$

where:

- K_{fw} is the distribution constant for the analyte between fibre and pure water
- $P_1=10.2$ is the polarity parameter for water
- $P_2 = cP_s + (1-c)P_1$ is the water/solvent mixture polarity parameter for a solvent of concentration c and polarity parameter P_s

This relationship indicates that the concentration of the solvent must be above 1% to change the properties of water and the distribution constant substantially. The content of organic solvent should always be kept to a minimum because the solvent can compete with the coating for the analytes especially when the polarities of the competing phases are similar. Typically, for optimal extraction efficiencies, organic solvent should not exceed 1-5% of the sample volume. In some cases, a variation in organic solvent content of even below 0.5% of sample volume seriously affected recoveries¹⁸.

Studies conducted¹⁸ highlights the importance of keeping the amount of organic solvent in spiked samples during method validation constant for all samples and all concentration levels tested. Otherwise, significant recovery and precision problems may be observed. For the analysis of drugs from biological fluids, the addition of small amounts of an organic modifier actually improves extraction efficiency because it releases some of the drug that is bound to matrix proteins³.

1.3.3 Kinetics

Kinetic theory of SPME describes the extraction rate of the SPME process and therefore indicates strategies to increase the speed of extraction.

After the immersion of the fibre in solution, there is a rapid increase in the mass absorbed by the fibre. The rate of increase then slows and eventually reaches equilibrium. This trend is shown in all the extraction time profiles in which the amount extracted (absolute or relative to the amount extracted in equilibrium conditions) is plotted versus the extraction time.

In order to enhance mass-transfer of analytes from the sample matrix to the vicinity of the fiber, some type of agitation is usually required. Different degrees of agitation influence the uptake rate during the extraction process as clearly shown in Figure 1.7

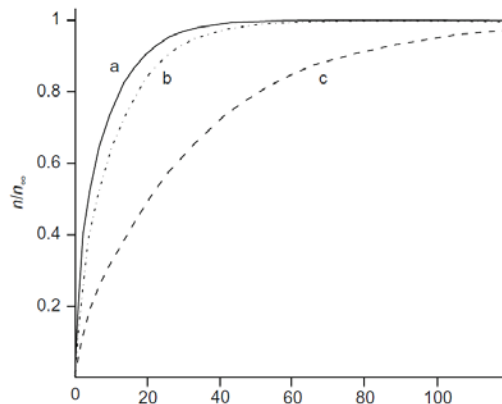


Figure 1.7 Extraction versus time profiles: (a) perfect agitation conditions; (b) well agitated and (c) poorly agitated.

With both gaseous and aqueous samples, independent of the agitation efficiency employed during a particular extraction, the fluid contacting the fiber surface is always stationary and as the distance from the fiber surface increases, fluid movement increases as well, until it corresponds to bulk flow in the sample^{22,23}. In order to model mass transport in such a system, a zone termed the Prandtl boundary layer was defined as a region whose thickness is dependent on both the rate of agitation and viscosity of the fluid constituting the matrix.²³

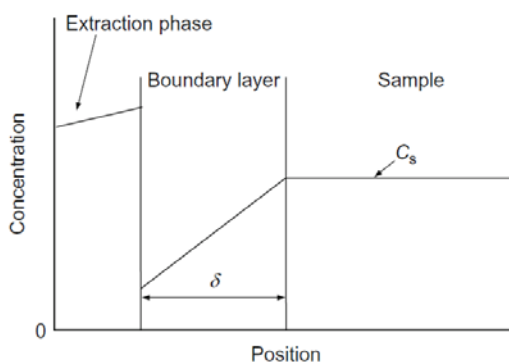


Figure 1.8 Boundary layer model configuration

Therefore, in a single sample, the thickness of the boundary layer (Figure 1.8) is different for different analytes and agitation conditions. However, since the fluid contacting fiber surface is

always stationary in a boundary layer region, analyte flux is progressively more dependent on analyte diffusion and less on agitation, as the extraction phase is approached. Because a thinner boundary layer results in a steeper concentration gradient between the bulk sample and the sorbent, a faster extraction rate occurs. Agitation (convection) conditions are thus critical in reducing the thickness of the boundary layer and increasing the rate of mass-transfer from the sample matrix to the fiber coating. This, in turn, leads to shorter equilibration times and increased overall speed of analysis. The extraction rate in such a system can be estimated by Equation 1.16.

$$t_e = t_{95\%} = 3 \frac{\delta K_{fs}(b-a)}{D_f} \quad (1.16)$$

where $(b-a)$ is the fibre coating's thickness, D_f is the analyte's diffusion coefficient in the sample fluid and K_{fs} is the analyte's distribution constant between fibre and sample. This relationship can be visualized in Figure 1.9.

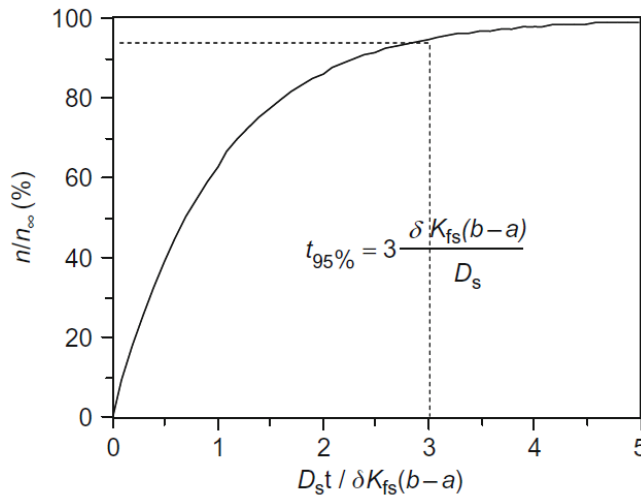


Figure 1.9 Dimensionless extraction versus time profile, corresponding to mass absorbed from an agitated solution of infinite volume, when the boundary layer controls the extraction rate.

1.4 Types of Commercially Available SPME Coatings

Extraction efficiency and selectivity are parameters that depend on the distribution coefficient K_{fs} ; a thermodynamic constant strictly dependent on the chemical properties of the SPME coating type. The SPME coatings commercially available to date have different characteristics and can be classified primarily into two categories: adsorbents and absorbents. The list of SPME coatings commercially available with their characteristics and working conditions ranges is shown in Table 1.1. Polarity of the coating mainly depends on the chemistry of the polymers used as extracting phases; their chemical structures are shown in Figure 1.10.

Table 1.1 Types of Commercially Available SPME Fibre Coatings

Type of Coating	Thickness	Extraction Mechanism	Polarity	Maximum temperature (°C)	Recommended operating temperatures	Recommended pH range
PDMS	7 µm	Absorbent	Non-polar	320	200-320	2-10
PDMS	30 µm	Absorbent	Non-polar	300	200-300	2-11
PDMS	100 µm	Absorbent	Non-polar	300	200-300	2-11
PA	85 µm	Absorbent	Polar	320	220-320	2-11
PEG	60 µm	Absorbent	Polar	250	200-240	2-9
Carbopack Z/PDMS	15 µm	Adsorbent	Bipolar	340	200-340	2-11
PDMS/DVB	65 µm	Adsorbent	Bipolar	270	200-270	2-11
DVB/Car/PDMS	50/30µm	Adsorbent	Bipolar	270	230-270	2-11
Car/PDMS	85 µm	Adsorbent	Bipolar	320	250-320	2-11

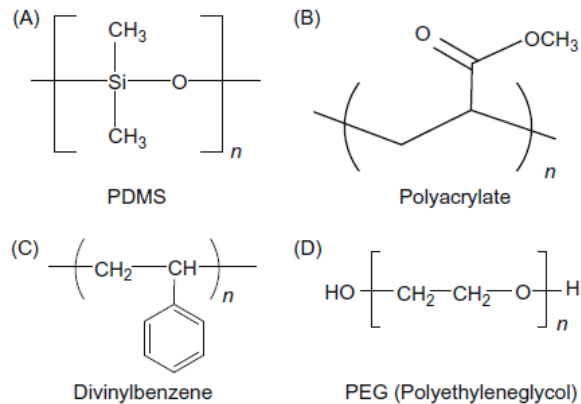


Figure 1.10 Chemical structures of common polymers used as SPME coatings

1.4.1 Absorbent coatings

Absorbent fibre coatings are composed primarily of ‘liquid-like’ polymers. The absorbent can be a gum or viscous oil that contains cross-linking agents. The polymer can be applied in various thicknesses over the fibre core by a cross linking process initiated by heating and/or ultraviolet (UV)-free radical treatment. This produces a stabilized, high-molecular-weight polymer coating with fluid properties.

With absorbent-type fibre coatings, the analytes migrate in and out of the phase coating, and all the bulk of the coating participate to the extraction process. The thickness of the fibre coating governs the retention of the analytes and regulates the capacity of the coating. Polarity is the driving force that governs the migration of the analytes to the coating. When the analytes diffuse into the liquid coating all the extraction phase bulk participate to the extraction process and the analytes can migrate deeper into the coating until they reach the core.

Diffusion coefficient of small analytes can be so high in the extraction phase that their retention by the liquid coating can be difficult unless a thicker coating is used. The three commercial liquid coating commercially available are PDMS (polydimethylsiloxane), PA (polyacrylate) and PEG (polyethyleneglycol).

The most common liquid extraction phase used in solid-phase microextraction is PDMS coating. This non polar polymer it is thermally stable and can be highly cross-linked.

Currently, there are three PDMS fibre coatings commercially available bearing different thickness (7, 30 and 100 μm) suitable for extracting different classes on non-polar compounds.

The thermal stability of the cross-linked polymer allows maximum desorption temperatures of 300 °C (100 and 30 µm) or 320 °C (7 µm). PDMS coatings are stable in water with a pH range from 2 to 11. In the presence of some organic solvents such as chlorinated solvents, hydrocarbons, diethyl ether, etc., the coating will swell up.

PA is a moderately polar coating and is suitable for extraction of a wide range of analytes, both polar and non-polar. This polymer is more rigid than PDMS or PEG, so the migration in and out of this coating is slightly slower. The phase has a high affinity for aromatic compounds and oxygenated analytes. PA coatings have moderate thermal stability and desorption should not be performed above 280°C. Since the phase is constituted by esters is not recommended to directly expose the coating to samples bearing pH above 9.

PEG (Carbowax[®]) fibre coating is the most polar coating available on commercially produced SPME fibres. The coating tends to swell in water samples, but the swelling is reduced if the sample contains a high amount of salt. The fibre has moderate thermal stability. It can be taken up to 250 °C, but it is recommended that it not be used routinely above 240 °C. The recommended pH range for this fibre is 2-9.

1.4.2 Adsorbent coatings

The potential applications for solid phase microextraction technique were enhanced by the introduction of solid adsorbents as coating in 1998. The utility and improved efficiency of these coating were readily confirmed and their use quickly diffused into copious applications²⁴. The main advantage in the use of these coatings is their better suitability for trace analysis as well as the broader molecular mass range of compounds that can be efficiently extracted.²⁵ The mechanism that governs the extraction is adsorption on the active surface of the solid coatings that are characterized by having high degree of porosity (meso and micropore) and high specific surface area (ranging approximately from 750 to 950 m² g⁻¹)²⁶.

The interactions between analytes and active surface of the coating happen by physisorption that involves interaction such as Van der Waals and electrostatic forces. The entire process is exothermic and its activation energy is associated to the transfer between the solution and the coating. Adsorption process generally follows a Langmuir isotherm assuming that molecules adsorb into an immobile state, all sorption sites are equal, each site can hold only one molecule and there are no interactions between molecules adsorbed on adjacent sites.

Conversely to absorption process on liquid coating, the analytes can only be extracted on the active surface of the particles constituting the solid coating as depicted in Figure 1.11

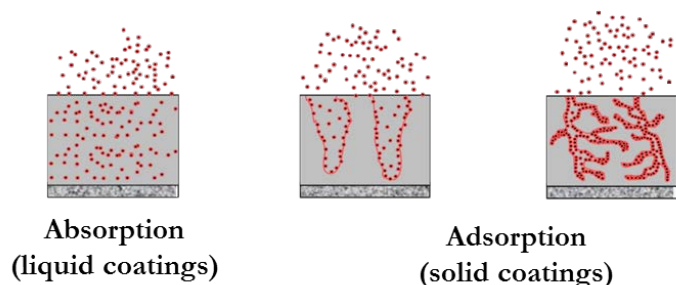


Figure 1.11 Schematization of absorption and adsorption mechanism for liquid and solid coatings

Because of the limited surface area available for the adsorption on solid coating, the number of sorption sites available for adsorption limits the amount of analytes extracted. If substantially occupied, competition between the analytes occurs, where analytes presenting higher affinity for this type of coating will displace analytes with lower K_{fs} values¹². For this reason, in very complex mixtures the equilibrium amount extracted can vary with the concentration of the target analytes and other components, generating biased results and problems for the quantitation. Generally, to overcome this problem shorter extraction times are used in order to avoid the saturation of the coating.

Polydimethylsiloxane/divinylbenzene (PDMS/DVB) coating is constituted by porous particles of DVB polymer glued together by PDMS (that has been shown not participate or influencing the extraction mechanism). DVB particles have a high degree of mesoporosity, but it also has some micropores. The maximum recommended working temperature is 270 °C and pores collapsing may occur at higher temperatures, which compromises the extraction efficiency of the coating. Due to the polymer chemistry, adsorption mainly happens through π - π interactions and generally used for the extraction of semi-volatiles and larger volatile analytes.

Car/PDMS coating consists of Carboxen 1006 particles belonging to a family of carbon molecular sieves. Because of the variety of pore sizes, Carboxen 1006 is an ideal adsorbent for SPME and the micropores present in the particles are narrow enough to retain analytes with shorter carbon chain. This makes the coating applicable for the extraction of volatiles and small molecular weight analytes. The particular design of the pores allows retaining larger analytes

only in the outer portion of the pores. Figure 1.12 shows a schematic of a tapered pore in a Carboxen 1006 particle, called “throughput pore”.

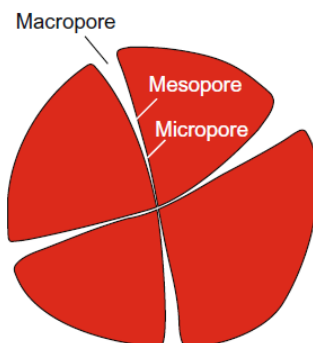


Figure 1.12 Carboxen 1006 tapered pore

The pore has a large opening on the surface and become tapered in proximity of the core of the particle. The pore continues through the particle and widens when it gets close to the surface. This structure allows a much efficient desorption of the analytes. A unique characteristic is that desorption can be carried out at 320 °C without any damage of the coating.

DVB/Car/PDMS consists of layers of DVB and Carboxen particles as depicted in Figure 1.13

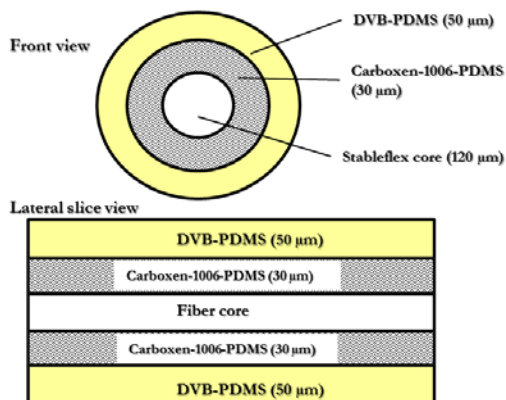


Figure 1.13 Front and lateral section view of a DVB/Car/PDMS coating

The design of this coating follows the principle used in thermal desorption tubes and purge traps. The larger analytes first contact the weaker adsorbent applied on the outer layer (DVB/PDMS) and the smaller analytes migrate through the first layer and into inner layer of Carboxen/PDMS. The larger analytes migrate slowly through the DVB layer remaining in the DVB coating or very

slightly into the Carboxen coating. The smaller analytes should migrate relatively faster through the DVB layer and get trapped in the Carboxen 1006 layer.

1.4.3 New developed SPME coatings

Research focused on the development of new SPME extracting phases is always active. Some of the areas of research include biocompatibility of coatings, improving selectivity and sensitivity limitations of currently available SPME coatings^{27,28}. In addition, there is on-going research on developing new coatings capable of efficiently extracting polar analytes from complex aqueous based matrices. Currently, there are biocompatible coatings for direct *in vivo* applications, which resolved the issue of coating fouling in the direct analysis of complex biological samples.

1.4.3.1 PDMS-modified coatings

Direct immersion SPME (DI-SPME) provides better performances compared to headspace SPME (HS-SPME) for the extraction of polar and low volatile compounds with high affinity with the sample matrix. This concept has been proven for a broad range of application and especially for food metabolomics performed by *in vivo* and *ex vivo* analysis.²⁹ However, especially in food analysis the direct exposure of the coating to the matrix may provoke its deterioration due to irreversible attachment of high-molecular weight compounds (e.g. proteins and carbohydrates) to the surface of the coating. This process leads also to the formation of artefacts at the high-temperature desorption in chromatographic systems.³⁰ For this reasons often the analysis of complex food matrices requires further sample pre-treatment prior SPME extraction or appropriately modifying the coating surface for commercial fibers.

In order to overcome the limitations of performing DI-SPME in complex food with commercial coatings and to avoid any preliminary sample-preparation steps, a new modified SPME-fiber coatings was developed³¹. Existing commercial SPME fiber was coated with a thin layer of PDMS to create a new type of SPME-fiber coating. This improved matrix compatibility of the fiber and enhanced robustness for DI extraction while retaining the original coating sensitivity towards the analytes of interest. The practical aspects of the PDMS-modified coating created new opportunities for SPME application in food analysis and in particular *in-vivo* food metabolomics.

1.4.3.2 Ionic Liquid-based coatings

In recent years ionic liquid have gained increasing interest in the analytical chemistry community because their unique physical and chemical properties. Ionic Liquids (ILs) are organic salts, which consist largely of organic cations paired with organic or inorganic anions. The structure of ILs can be designed to produce desired properties including negligible vapour pressure, elevated thermal stability, tunable viscosity and miscibility with other solvents, as well as the capability of undergoing numerous solvation interactions. In particular when ionic liquid are used as extracting phases their versatility allow to create task-specific ionic liquids with functional groups that impart specific chemical functionality, thus improving specificity.

In recent years, ILs have been used as extracting phases for solid phase microextraction. Recent research demonstrate that ILs show promising potential compared to commercial SPME coatings, due to their tunable physical and chemical properties³². An interesting feature of ILs is their extraction specificity, as presented by Zhao and co-workers in two studies where two Polymeric Ionic Liquids (PILs), namely poly ([ViHIM][NTf₂]) and poly ([ViHIM][taurate]), were used for selective extraction of CO₂³³. In these studies, PILs not only offered enhanced selectivity, but could also more efficiently prevent the loss of analytes from the coating prior throughout the analysis compared to commercial Carboxen fibers. DI-SPME PIL coatings was first reported by Lopez-Darias et al.³⁴ In this study, they employed a poly ([ViHDIM][NTf₂]) PIL- coated fiber for the analysis of a variety of water pollutants, including PAHs and phenols. The sensitivity of the PIL fiber was compared to 30µm PDMS, 100µm PDMS, and 85µm PA fibers. Overall, the 20µm PIL fiber exhibited greater sensitivity than PDMS coatings. Nonetheless, the PA fiber was superior to PIL fiber for mostly polar analytes. However, further improvements in the design of PIL coatings to withstanding complex matrices are needed in order to exploit fully the advantages offered by the technique.

1.4.3.3 Polypyrrole fibre coatings

Polypyrrole (PPY) and its derivatives have also been investigated as possible polymeric SPME coatings³⁵. The polymer is easily synthesized chemically or electrochemically from commercially available monomers³⁶. PPY fibre coatings are mechanically resistant with excellent adhesion to the fibre, however, their instability above 200°C does not make them suitable to be used for the GC thermal desorption of analytes with a high boiling point. PPY

films are usually used to coat metallic fibres made from platinum, gold or stainless steel³⁷ and are highly efficient in the extraction of polar and aromatic compounds³⁸.

1.4.3.4 Mesoporous silica fibre coatings

Mesoporous silica fibre coatings consist of silicates having a large specific surface area ($>100 \text{ m}^2 \text{ g}^{-1}$), mechanically and thermally resistant up to 900°C and have the large pores in their structure that favour the transport of large molecules. They were originally synthesised at Mobil Oil Inc. (Exxon Mobil) in 1992. The main interest in these materials centres on heterogeneous catalysis but they are also applied in adsorption, in catalysis and membrane techniques³⁹. For SPME purposes, coatings made from the material MCM-41 and chemically modified MCM-41 (Mobil Composition of Matter n° 41-mesoporous inorganic solid material with tailored size of the pores) were deposited on stainless steel fibres. These sorbent films were used to extract aromatic hydrocarbons.⁴⁰ One of the latest mesoporous coatings is that made from 3-[bis(2-hydroxyethyl)amino]-propyl-triethoxysilane (HPTES), deposited on a copper fibre, and the nanoporous silicate material SBA-15 containing aminoethyl functional groups. It was used to extract BTEX and phenolic compounds from water samples. Mechanically very strong and resistant to high temperatures, this type of fibre is easy and cheap to produce.⁴¹

1.4.3.5 Molecularly imprinted polymers for SPME

The need to achieve optimum selectivity in sample preparation led to the development of molecularly imprinted polymers (MIPs). MIPs are obtained by copolymerizing monomers with a template, followed by cross-linking of the template monomer complex. After polymerization, the template molecules are flushed out with suitable solvents, leaving in the polymer structure imprints of a given shape and size. When these materials are used for microextraction of analytes, the presence of characteristic functional groups imprinted in the template lend the polymer selectivity and sorption properties corresponding to compounds with a structure exactly the same or similar to the structure of the template^{42,43}.

There are three basic approaches for MIP synthesis: noncovalent, covalent and semi-covalent imprinting (Figure 1.14).

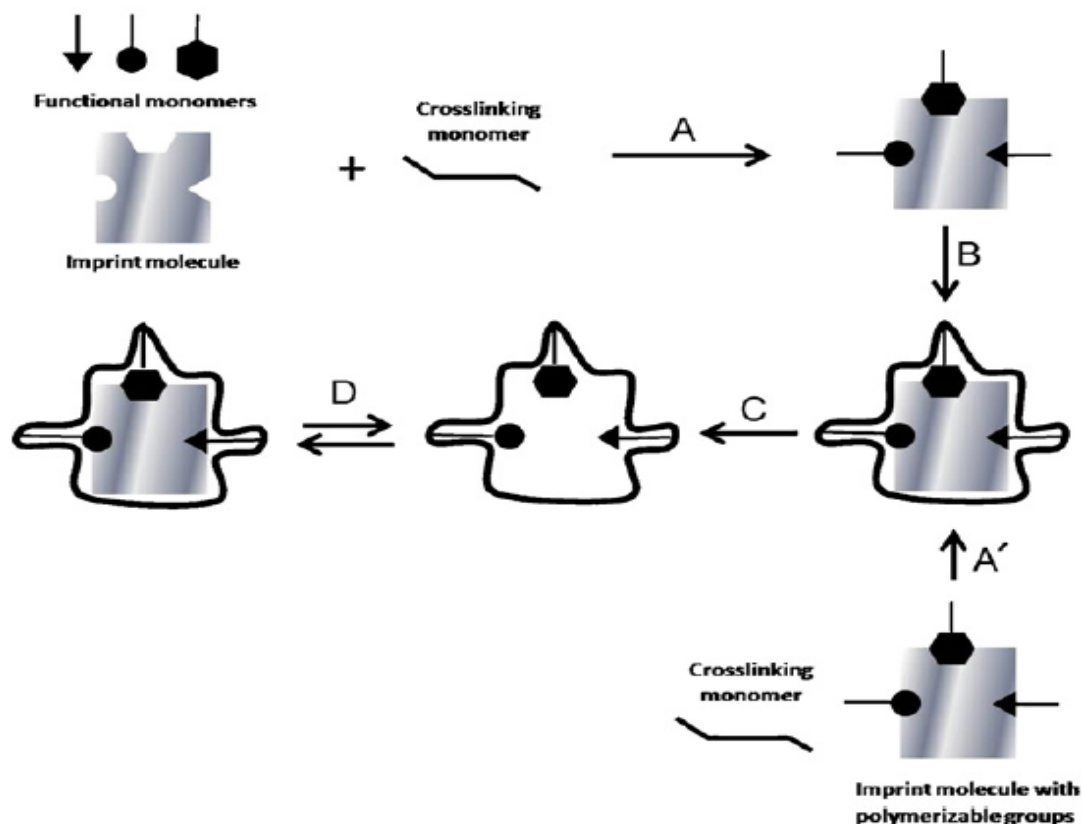


Figure 1.14 Main approaches to MIP synthesis. Non-covalent approach: (A) mixture of functional monomers, cross-linking agents, polymerisation initiator and templates dissolved on porogenic solvent to form template/functional monomer complex; (B) polymerisation; (C) removal of template (by solvent extraction) and (D) analyte binding (via non-covalent interactions) on the specific imprinted site. Covalent approach: (A') template containing polymerisable groups mixed with cross-linking agent and initiator in proper solvent; (C) removal of template after polymerisation (with breaking of covalent bonds between template and polymer) and (D) analyte binding (via covalent bonds) on the specific imprinted site.

In the non-covalent imprinting the most extensively used, due to its relative simplicity, a template (target analyte or structurally related species) is mixed with an appropriate functional monomer, a suitable porogenic solvent, cross-linking agents and catalysts or polymerization initiators. Specific binding sites are formed by self-assembling of template and the functional monomer, which should be capable of forming a fairly stable complex with the template via

dipole interaction, hydrogen bonding, ion pair, etc. After the synthesis, the template is removed from the polymer simply by exhaustive washing with solvents usually on a Soxhlet-type apparatus. For the covalent approach, the template and the functional monomer are covalently bonded prior to polymerization. The template is removed from the polymer matrix after synthesis by cleaving the covalent bonds before the washing step. Sorbents prepared using covalent imprinting tend to have well defined and more homogeneous binding sites than those resulting from non-covalent approach: the interaction between template and functional monomers are much stable during the polymerization. Compared to non-covalent MIP (where analyte binding to imprinted sites take place by weaker interactions), this leads to higher selectivity, with less non-specific retention, and better extraction efficiencies. Finally, on non-covalent MIP preparation the synthesis of the adsorbent is carried out through a covalent procedure but the extraction mechanism is more related to a non-covalently prepared MIP⁴⁴. Semi-covalent imprinting combines the advantages of both covalent and non-covalent approaches: as the template is covalently bound to a polymerizable group whose functionality is recovered after cleavage of the template. Most of the MIP described in the literature for use as specific SPE adsorbents and for other applications are acrylate-based materials prepared by bulk polymerization⁴⁵, using methacrylic acid (MAA) and similar compounds as functional monomers, ethylene glycol dimethacrylate (EDMA) as cross-linker and azo-compounds such as azo(bis)-isobutyronitrile as radicalar polymerization initiator. Advantages of these materials include relatively lower cost, stability across the entire pH range, thermal stability, ease of synthesis and their robustness make them suitable coating for SPME. MIP-SPME were used for sampling pesticides,⁴⁶ triazines,⁴⁷ antibiotics,⁴⁷ as well as many other compounds from samples with a complex matrix composition like blood,⁴⁸ urine,⁴⁹ food⁵⁰ and environmental samples.⁵¹

1.4.3.6 Immunosorbents as SPME fibre coatings

Antibodies are often used as an easy way of recognising organic compounds and for this reason they can be used as a quick and sensitive extraction technique. These materials are based on a high affinity for and selectivity towards antigen-antibody interactions. Highly selective antibodies recognise their counterpart antigens even in the presence of compounds with a very similar structure⁵². A considerable research effort has culminated in the discovery of a way of binding natural antibodies to a solid substrate; the resulting materials, which exhibit immunological affinity (immunosorbents), are used in SPME for extracting analytes from

biological samples with a complex matrix composition⁵³. Immunosorbents can be usefully applied as fibre coatings for the solid-phase microextraction of large molecules: enzymes, proteins, viruses, hormones and other subcellular components of biological fluids,⁵² as well as pesticides and triazines,⁵⁴ narcotics⁵⁵ and PAHs⁵⁶ from samples with diverse matrix compositions, such as water, food, blood, urine and soil.⁵⁴ The determination of small molecules using this technique is much more difficult; moreover, research into immunosorbents is very time-consuming and costly because of the considerable expense and nature of antibody production. Nonetheless, it is becoming more common to use immunosorbent materials as sorbents in SPME techniques and as a column packing and usually combined with LC or with GC and CE applications^{52,57}.

1.4.3.7 SPME fibre coatings synthesised by the sol-gel technique

SPME coating commercially available suffers of some drawbacks such as thermal instability and swelling towards direct exposure to organic solvents, reduced operating temperature and mechanical fragility of the fused silica (FS) support. Some of these problems have been solved by applying the sol-gel technique for binding polymer coatings to the fibre surface. SPME sorptive coatings prepared by sol-gel procedures typically are chemically bonded to the FS-base fibers, being also porous and highly cross-linked; the sorbents are prepared and deposited *in situ* to the surface of raw FS fiber. The first description of sol-gel technology for preparation of SPME fibers was presented by Malik and co-workers in 1997⁵⁸; the organic modifier was hydroxyl-PDMS, and the resulting chemically bonded film was an organically modified silica (ormosil). The procedure involved a preliminary step for activation of the raw fiber surfaces before the deposition and immobilization of the extracting phase. The process occurs on a single-pot operation followed by the deactivation of remaining -OH groups and conditioning. The pre-treatment of the FS surface is necessary to generate free superficial silanol groups, which will act as anchoring points where the sorbent phase will be chemically linked. The coating media usually consisted of a mixture of an alkoxy silane reticulant precursor such as methyltrimethoxysilane (MTMS), a hydroxylated organic modifier-hydroxy-PDMS and small amounts of water and catalyst (trifluoroacetic acid, TFA). Under appropriate conditions, the alkoxy silanes hydrolyze produce silanols (Figure 1.15a), which immediately condensate creating silica aggregates (Figure 1.15b). The hydroxylated organic modifier present in the media can simultaneously condense with the aggregates, being incorporated to the silica network (Figure

1.15c). These organically modified silica nanoparticles form a colloidal suspension on the liquid reagents and reaction products (a sol phase); the continuous growing of the aggregates eventually lead to a silica monolite, where water and the liquid reaction products are trapped (a gel). However, if an activated fiber is exposed to the sol phase before complete gelation, the aggregates may condense with the surface -OH groups on this substrate (Figure 1.15d), forming an ormosil film. In this first publication, the coating thickness obtained was about 10 μ m, and the sorptive film had a highly porous structure, as observed by scanning electronic micrography. A remarkable feature of this fiber was its outstanding thermal stability, when compared to conventional pure polymeric PDMS films: the fibers could be heated up to 320 °C without degradation of their performance or significant bleeding, suggesting that the coating was chemically bonded to the silica core. It was pointed out that since sol-gel ormosil films usually possess microporous structures, they offer a high surface area and offer higher extraction efficiencies even with thin extracting layers, which results also in fast sample/headspace/fiber equilibration times. Sol-gel technology was subsequently applied with success to prepare SPME fibers with different coatings, mostly using FS fibers as support⁵⁹⁻⁶⁵.

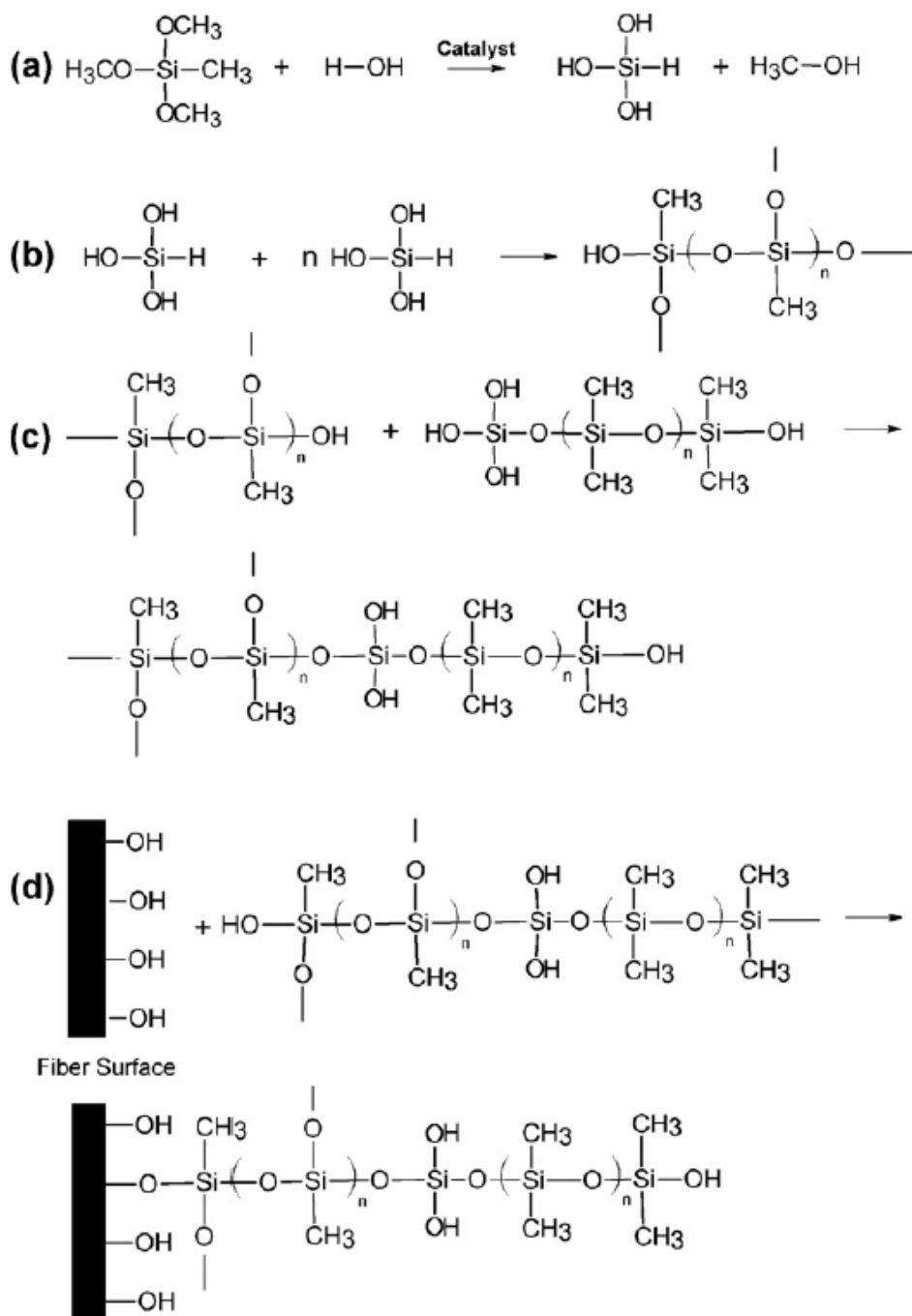


Figure 1.15 Main reactions involved on sol-gel process for SPME fiber coating. Modified from Malik and co-workers

1.4.3.8 Carbon nanotubes

Carbon nanotubes (CNTs) essentially, an allotropic form of graphitic carbon, are needle-like structures comprising a single-rolled graphite lamella forming a tube (single-wall carbon nanotubes, SWCNTs), or several single tubes arranged around a common axis (multi-wall carbon nanotubes, MWCNTs)⁴². The adsorptive behaviour of CNT is similar to other carbon-based alternatives, such as conventional porous graphitic carbon (PGC), which consists of large graphitic lamellae held together by weak intermolecular Van der Waals forces. Both hydrophobic and electronic interactions contribute to retention of analytes by PGC: therefore, non-polar, polar and even ionic analytes may be strongly adsorbed (specially planar species with polar substituents and delocalized electronic charges via π -bonds and free electron pairs)⁶⁶. However, one of the distinctive features of CNT, particularly of the MWCNT, that has a crucial influence on their application for SPME adsorbents, is their large surface-to-volume ratios⁶⁷. As result, compared to other carbon-based adsorbents, the capacity of MWCNT is usually much larger. Feng *et al.*⁶⁸ approached the difficulty in extracting phenols from water samples using CNT-fibers coated on metal wire. Limits of detection (LODs) were much lower than those obtained with commercial fibers. Also, the group reported that such coatings exhibit high thermal stability and robustness when exposed to high temperatures and extreme pHs, organic solvents respectively.

1.5 Derivatization for GC analysis using SPME

Derivatization approaches can be very useful when gas-chromatographic determination need to be carried out on analytes that are largely non-volatile or thermally labile. This is because the derivatization reaction often converts the analyte(s) into more volatile compounds and subsequently amenable to gas-chromatographic applications. Also derivatization reactions can improve SPME coating extraction efficiency for a group of or specific targeted analyte(s) by improving the affinity and increases method sensitivity. However, derivatization reagents may be source of interferences during the extraction, therefore this procedure should be carried out only when strictly necessary and with the minimum amount of reagents needed⁶⁹. Typical procedures of derivatization involve esterification of acidic compounds,⁷⁰ transformation of amines and amphetamines into less polar and more volatile derivatives,⁷¹ aldehydes and ketones

into more stable oximes,⁷² or phenols in acetates⁷³ and metalorganic compounds into more volatile forms⁷⁴ and simultaneous derivatization of acidic and amino moieties in amino acids⁷⁵.

Three different approaches are mainly used as derivatization procedures in SPME applications.

1.5.1 Pre-Extraction derivatization

Pre-Extraction derivatization consists in adding the derivatization reagent into the sample solution. Then the SPME fiber is later exposed to the sample headspace or directly into the sample media and the extraction of the derivatization product occurs followed by their thermal desorption in the gas-chromatographic injection system. The main drawback of this approach is the direct exposure of the coating to the sample media containing the derivatization reagents that may provoke deterioration of the coating as reported by Caruso et al.⁷⁶. However, this can be avoided or diluting the sample or exposing the fiber to the sample headspace when the derivatization products bear enough volatility. This derivatization strategy has been used for determination of sarcosine in urine⁷⁷ as well as for the determination of tumoral biomarker and environmental pollutants⁷⁸⁻⁸⁰. This thesis will also show some applications of pre-extraction derivatization, in Chapter 3, for the determination of dopamine, serotonin and norepinephrine in human urine, hydrazine in drinking water and selenoamino acids in aqueous potato extracts.

1.5.2 Post-Extraction derivatization

Post-Extraction derivatization consists in extracting the analytes from the sample matrix and subsequently derivatizing the analytes extracted on the coating by its exposure to derivatization solution. Post-extraction derivatization can only improve the chromatographic behaviour and detection properties, not the extraction efficiency. This approach was employed in isolation of biphenyls from urea samples,⁸¹ drugs and steroids from water and biological fluids,^{82,83} or herbicides from water samples⁸⁴.

1.5.3 Simultaneous extraction/on-fibre derivatization

In simultaneous extraction/on-fibre derivatization approach the derivatization reagent is pre-loaded by placing the fiber in its vapours or in a suitable solution. Then the fiber is exposed to sample solution and the derivatization reaction allowed proceeding on the fibre simultaneously with the extraction of the analytes. This strategy of derivatization was used in analyses of environmental samples^{85,86} food samples⁸⁷ and biomedical applications^{88,89}.

1.6 Applications of SPME

1.6.1 Environmental and on-site analysis

SPME has been applied extensively to environmental analysis since its introduction with numerous publications in literature yearly. Implementation of SPME for environmental analysis include development of new coatings, new sampling strategies (cold-fiber SPME and in-tube SPME), new derivatization strategies and calibration approaches⁹⁰. Also new SPME approach, thin-film microextraction (TFME) or membrane SPME, was recently developed to achieve higher extraction efficiency and sensitivity. This approach has been successfully applied to field water sampling⁹¹. The main advantages reported in the use of SPME for environmental analysis are the achievement of lower detection and quantitation limits compared to others extraction techniques⁷⁹, the automated, easy and solventless sample preparation that speeds the analytical procedure for routine analyses⁹² and much cleaner chromatograms compared to injection of solvent extracts. The latter approach often hinder detection of target analytes and cause build up of non-volatile deposits in the injector of gas-chromatographic systems⁹³.

The analysis by SPME used for the on-site determination of free and total concentrations can be an ideal alternative to multiple devices-standard approaches. Previously, programming unattended automated desorption sequences was not an included feature in the available autosamplers, and multiple SPME fibre analysis was not entirely exploited. However, new generation of autosamplers developed allow for the sequential extraction and desorption. Undoubtedly, the main advantage of these automated systems is the elimination of errors associated with the manual injection and the considerable reduction of time and labour for the analyst⁹⁴.

1.6.2 Bioanalytical analysis

The simplified nature of SPME including reduced sample handling, solvent use, time, and cost has mainly contributed in the increasing interest of using this technique for pharmaceutical analysis and bioanalysis, especially after the development of biocompatible coatings⁹⁵. Initial applications in drug analysis were primarily for forensic drugs such as amphetamines, opiates, barbiturates, and cannabinoids as well as for therapeutic drugs such as anesthetics, antibiotics, and antidepressants²².

The development of bioanalytical SPME methods has also enabled simplified analysis of such complex samples as tissues for conventional pollutants. Aguinaga *et al.* evaluated SPME for the determination of PAHs in aquatic species such as canned tuna, clam, anchovy, mussel, fresh salmon, and smoked salmon⁹⁶.

Among the early bioanalytical applications of SPME were studies on matrix-analyte binding affinity in a biological system. Because SPME does not disrupt matrix-analyte binding dynamics, which enhances determination of only the free analyte concentration, experiments to study these dynamics were greatly simplified. The theory and application of the method for SPME analysis of several polar compounds in biological matrices have been reported^{97,98}. The monitoring of biological reaction kinetics is also reported, for instance, SPME has been used to investigate drug metabolism in keratinocytes⁹⁹. SPME has also been successfully combined with LC–MS/MS for bioanalytical applications. Notable among them is the simultaneous determination of both free and total concentration from a single specimen using two appropriate calibration curves (matrix-free and matrix-matched). The technique provided excellent sample clean-up, which reduced the potential for ionization suppression effects from the matrix¹⁰⁰. It was recently shown that SPME can meet the most demanding requirements of regulated bioanalysis, such as Food and Drug Administration requirements for bioanalytical method validation, and the introduction of parallel extractions on the 96-well plate format with Concept 96 robotic station enhanced the ability to handle hundreds or thousands of clinical samples a day¹⁰¹.

SPME methodology for global metabolomics studies of whole blood and plasma was also successfully developed¹⁰². These developments are also enabled application of SPME for analysis of other compounds of biomedical and biological interest, such as proteins, peptides, endogenous biological compounds, and biomarkers of health status^{77,78,100}.

1.6.3 Food analysis

Safety and nutritional excellence are topics of major concern for consumers and also with the higher market pricing, the importance of research in food analysis cannot be over emphasized. The accurate assessment of food quality, the freshness of raw materials and the nutritive values of processed food, as well as the determination of food additives (e.g. food preservatives and colours) are especially important to ease anxiety and benefit consumers. For this reason, continuous efforts are made by the analytical chemistry community to develop new analytical

strategies able to respond to customer demands and guarantee reliable results in terms of food components/safety. In most of the cases the main challenges related to the development of new analytical protocols is related to the complexity of food matrices. The effective and fast isolation of the target analytes from foodstuff is critical in order to obtain faster and more accurate analytical procedures. In this case, SPME is one of the most used extraction procedures for food analysis, since it allows efficient isolation of the target analytes from the matrix and simultaneous pre-concentration on the coating, minimizing sample pre-treatment steps and contaminations of the analytical instrumentation used. Proper matrix-specific optimization of SPME parameters enhances ability to obtain highly efficient methods, which upon validation may constitute useful tools to address specific requirements. The applications of SPME in food analysis are mainly related to investigations of their natural composition and presence of contaminants¹⁰³. In particular, admirable results in terms of nutraceutical values assessment¹⁰⁴, traceability purposes^{105,106}, investigation of aroma composition of food and essential oils^{107–109}, and recently also characterization of fruit metabolome²⁹ have been reported. Also, numerous applications of SPME for determining pesticide contamination of foodstuffs from the primary ingredients or contamination from the packaging materials are present in literature and widely reviewed¹¹⁰.

SPME represents an elegant approach to perform the sample preparation in food matrices. However, one of the most challenging steps in reaching the desired objective is the choice of the extraction phase and extraction mode. The proper selection of the extraction phase, performing direct immersion extraction SPME, in combination with a comprehensive two-dimensional gas chromatography–time-of-flight mass spectrometry (GC × GC–ToFMS) allowed the successful metabolite profiling of apples (*Malus × domestica* Borkh.). The study reported 399 tentatively entries including metabolites that were reported for the first time to constitute metabolite composition of apples by applying high-resolution profiling technique.

The selection of the direct immersion mode showed the best result in terms of metabolites coverage, however, the direct immersion mode causes the premature deterioration of the coating especially when very complex food matrices are analyzed²⁹. In view of this, the development of an improved fiber coating dedicated to the analysis of complex matrices, not only has helped to preserve the coating from irreversible early damaging, but has also broaden the spectrum of SPME applied in food analysis. The newly modified SPME coating has been proved for the

analysis of pesticides in grapes and strawberries. When compared to a standard technique (QuEChERS) for the analysis of pesticides in food matrices, the SPME method presented several advantages such as full automation and achievement of limits of quantitation at least one order of magnitude lower than those obtained by QuEChERS method. These new coatings also showed excellent performances in avoiding and limiting the displacement of polar analytes when very complex matrices are analyzed⁹².

Due to its miniaturized format, which often results in minimum disturbance to the investigated system, SPME supports real-time (*in vivo*) measurements of biological systems. Such approach allows for the achievement of an accurate metabolomic snapshot, avoiding the possible presence of enzyme-mediated metabolite conversions. Thus, *in vivo* SPME technique offers numerous unique opportunities for detection and identification of new biomarkers of harvest maturity, fruit ripeness and many other global metabolomics topics in the field of plant biology. The technique also provides an alternative approach to resolving notable displacement effects, which often effects the extraction of the most polar metabolites and their reliable quantification.

1.6.4 In-vivo SPME

In addition to various SPME applications for *in vitro* analysis, SPME also offers some unique possibilities that provide solutions to many future challenges and questions in a variety of research fields. For example, early *in vivo* SPME studies on intravenous blood concentrations of drugs and metabolites in dogs^{111,112} has been reported and this facilitated *in vivo* pharmacokinetic studies in both dogs and rodents^{113–115}. The drug and metabolite concentrations determined by SPME in these studies were thoroughly validated against traditional blood withdrawal followed by solvent precipitation of resulting plasma samples and excellent agreement between the two methods was observed. The main advantage of SPME in this type of study is the fact that no blood is withdrawn, which is particularly important in small rodent studies, which has limited blood volume. In contrast to other traditional methods like protein precipitation, SPME permits multiple sampling of the same animal while keeping constant circulating blood volume. This technology enables multi-compartmental studies to simultaneously extract analytes from the blood and tissue of the same animal without the need anesthetising. Another advantage is that it significantly reduces animal use and overall cost. *In vivo* SPME has also been reported for direct monitoring of environmental pollutants in fish tissues^{116,117} providing also information regarding

the distribution of these species in muscle versus adipose tissue¹¹⁸. The development of this non-lethal sampling methodology, which does not require tissue removal prior to sampling, provides a new, rapid, and simple alternative for bioaccumulation and toxicity studies in fish. *In vivo* SPME was also successfully applied for monitoring of pesticides in plants and in plants metabolomics studies allowing the exclusive detection of metabolites¹¹⁹.

In vivo SPME was recently exploited to study metabolome of whole blood¹²⁰. It was shown that *in vivo* SPME was able to capture unstable metabolites that eluded conventional methodologies based on blood withdrawal, with over 100 unique compounds observed using *in vivo* SPME only. Recently excellent results were obtained by an *in vivo* approach for the simultaneous monitor of changes in the concentrations of multiple neurochemicals in the brain extracellular fluid. The solid phase microextraction method was validated against *in vivo* microdialysis, and both techniques recorded an approximately 3 – 4 fold in basal levels of ECF 5-HT after the administration of the drug¹²¹. All these results demonstrate that *in vivo* SPME is ideally suited a new and important tool in life science research.

1.7 References

- (1) Arthur, C. L.; Pawliszyn, J. *Anal. Chem.* **1990**, *62*, 2145–2148.
- (2) Bojko, B.; Cudjoe, E.; Gómez-Ríos, G. A.; Gorynski, K.; Jiang, R.; Reyes-Garcés, N.; Risticvic, S.; Silva, É. A. S.; Togunde, O.; Vuckovic, D.; Pawliszyn, J. *Anal. Chim. Acta* **2012**, *750*, 132–151.
- (3) Mullett, W. M.; Levsen, K.; Lubda, D.; Pawliszyn, J. *J. Chromatogr. A* **2002**, *963*, 325–334.
- (4) Wu, J.; Tragas, C.; Lord, H.; Pawliszyn, J. *J. Chromatogr. A* **2002**, *976*, 357–67.
- (5) Kataoka, H.; Lord, H. L.; Pawliszyn, J. *J. Chromatogr. B. Biomed. Sci. Appl.* **1999**, *731*, 353–9.
- (6) Cudjoe, E.; Pawliszyn, J. *J. Pharm. Biomed. Anal.* **2009**, *50*, 556–562.
- (7) Pawliszyn, J.; Musteata, F. M.; Vuckovic, D. In *Handbook of Solid Phase Microextraction*; 2012; pp. 399–453.
- (8) Pawliszyn, J. In *Handbook of Solid Phase Microextraction*; 2012; pp. 61–97.
- (9) Mitra, S. *Sample Preparation Techniques in Analytical Chemistry*; John Wiley & Sons, 2004; p. 488.
- (10) Zhang, Z.; Pawliszyn, J. *J. Phys. Chem.* **1996**, *3654*, 17648–17654.
- (11) Martos, P. A.; Saraullo, A.; Pawliszyn, J. *Anal. Chem.* **1997**, *69*, 402–8.
- (12) Górecki, T.; Yu, X.; Pawliszyn, J. *Analyst* **1999**, *124*, 643–649.
- (13) Carasek, E.; Pawliszyn, J. *J. Agric. Food Chem.* **2006**, *54*, 8688–96.
- (14) Carasek, E.; Cudjoe, E.; Pawliszyn, J. *J. Chromatogr. A* **2007**, *1138*, 10–17.
- (15) Guo, J.; Jiang, R.; Pawliszyn, J. *J. Chromatogr. A* **2013**, *1307*, 66–72.
- (16) Jiang, R.; Carasek, E.; Risticvic, S.; Cudjoe, E.; Warren, J.; Pawliszyn, J. *Anal. Chim. Acta* **2012**, *742*, 22–9.
- (17) Zambonin, C. G.; Aresta, A.; Palmisano, F. *J. Chromatogr. B* **2004**, *806*, 89–93.
- (18) Lord, H. L.; Pawliszyn, J. *Anal. Chem.* **1997**, *69*, 3899–3906.
- (19) Kumazawa, T.; Lee, X.-P.; Sato, K.; Suzuki, O. *Anal. Chim. Acta* **2003**, *492*, 49–67.

- (20) Long, F. A.; McDevit, W. F. *Chem. Rev.* **1952**, *51*, 119–169.
- (21) Yang, X.; Peppard, T. *LC GC* **13**, 882–886.
- (22) Lord, H.; Pawliszyn, J. *J. Chromatogr. A* **2000**, *885*, 153–193.
- (23) Pawliszyn, J. In *Handbook of Solid Phase Microextraction*; 2012; pp. 13–59.
- (24) Risticvic, S.; Niri, V. H.; Vuckovic, D.; Pawliszyn, J. *Anal. Bioanal. Chem.* **2009**, *393*, 781–95.
- (25) Pawliszyn, J. *Handbook of Solid Phase Microextraction*; Pawliszyn, J., Ed.; Elsevier.; 2012.
- (26) Nongonierma, A.; Voilley, A.; Cayot, P.; Le Quéré, J.-L.; Springett, M. *Food Rev. Int.* **2006**, *22*, 51–94.
- (27) Vuckovic, D.; Shirey, R.; Chen, Y.; Sidisky, L.; Aurand, C.; Stenerson, K.; Pawliszyn, J. *Anal. Chim. Acta* **2009**, *638*, 175–185.
- (28) Souza Silva, E. A.; Risticvic, S.; Pawliszyn, J. *TrAC Trends Anal. Chem.* **2013**, *43*, 24–36.
- (29) Risticvic, S. *Univ. Waterloo, PhD Thesis* **2012**.
- (30) Adams, A.; Van Lancker, F.; De Meulenaer, B.; Owczarek-Fendor, A.; De Kimpe, N. *J. Chromatogr. B. Analyt. Technol. Biomed. Life Sci.* **2012**, *897*, 37–41.
- (31) Souza-Silva, E. A.; Pawliszyn, J. *Anal. Chem.* **2012**, *84*, 6933–6938.
- (32) Ho, T. D.; Canestraro, A. J.; Anderson, J. L. *Anal. Chim. Acta* **2011**, *695*, 18–43.
- (33) Zhao, Q.; Wajert, J. C.; Anderson, J. L. *Anal. Chem.* **2010**, *82*, 707–13.
- (34) López-Darias, J.; Pino, V.; Anderson, J. L.; Graham, C. M.; Afonso, A. M. *J. Chromatogr. A* **2010**, *1217*, 1236–1243.
- (35) Wu, J.; Pawliszyn, J. *J. Chromatogr. A* **2001**, *909*, 37–52.
- (36) Mohammadi, A.; Yamini, Y.; Alizadeh, N. *J. Chromatogr. A* **2005**, *1063*, 1–8.
- (37) Alizadeh, N.; Zarabadipour, H.; Mohammadi, A. *Anal. Chim. Acta* **2007**, *605*, 159–165.
- (38) Wu, J.; Mullett, W. M.; Pawliszyn, J. *Anal. Chem.* **2002**, *74*, 4855–4859.

- (39) Beck, J. S.; Vartuli, J. C.; Roth, W. J.; Leonowicz, M. E.; Kresge, C. T.; Schmitt, K. D.; Chu, C. T. W.; Olson, D. H.; Sheppard, E. W. *J. Am. Chem. Soc.* **1992**, *114*, 10834–10843.
- (40) Hou, J.; Ma, Q.; Du, X.; Deng, H.; Gao, J. *Talanta* **2004**, *62*, 241–246.
- (41) Beyer, H. K.; Karge, H. G.; Kiricsi, I.; Nagy, J. B.; Roth, W. J.; Kresge, C. T.; Vartuli, J. C.; Leonowicz, M. E.; Fung, A. S.; McCullen, S. B. *Stud. Surf. Sci. Catal.* **1995**, *94*, 301–308.
- (42) Poole, C. F.; Augusto, F.; Carasek, E.; Silva, R. G. C.; Rivellino, S. R.; Batista, A. D.; Martendal, E. *J. Chromatogr. A* **2010**, *1217*, 2533–2542.
- (43) Spietelun, A.; Pilarczyk, M.; Kloskowski, A.; Namieśnik, J. *Chem. Soc. Rev.* **2010**, *39*, 4524–37.
- (44) Spégel, P.; Schweitz, L.; Nilsson, S. *Anal. Bioanal. Chem.* **2002**, *372*, 37–8.
- (45) Ramos, L.; Smith, R. M.; Tamayo, F. G.; Turiel, E.; Martín-Esteban, A. *J. Chromatogr. A* **2007**, *1152*, 32–40.
- (46) Siemann, M.; Andersson, L. I.; Mosbach, K. *J. Agric. Food Chem.* **1996**, *44*, 141–145.
- (47) Turiel, E.; Tadeo, J. L.; Martín-Esteban, A. *Anal. Chem.* **2007**, *79*, 3099–104.
- (48) Koster, E. H. M.; Crescenzi, C.; den Hoedt, W.; Ensing, K.; de Jong, G. J. *Anal. Chem.* **2001**, *73*, 3140–3145.
- (49) Yan, H.; Row, K. H.; Yang, G. *Talanta* **2008**, *75*, 227–232.
- (50) Mohamed, R.; Richoz-Payot, J.; Gremaud, E.; Mottier, P.; Yilmaz, E.; Tabet, J.-C.; Guy, P. A. *Anal. Chem.* **2007**, *79*, 9557–65.
- (51) Andersson, L. I. *Bioseparation* **2001**, *10*, 353–364.
- (52) Hennion, M.-C.; Pichon, V. *J. Chromatogr. A* **2003**, *1000*, 29–52.
- (53) Pichon, V.; Bouzige, M.; Miège, C.; Hennion, M.-C. *TrAC Trends Anal. Chem.* **1999**, *18*, 219–235.
- (54) Pichon, V.; Bouzige, M.; Hennion, M.-C. *Anal. Chim. Acta* **1998**, *376*, 21–35.
- (55) Yuan, H.; Mullett, W. M.; Pawliszyn, J. *Analyst* **2001**, *126*, 1456–1461.
- (56) Cichna, M.; Knopp, D.; Niessner, R. *Anal. Chim. Acta* **1997**, *339*, 241–250.

- (57) Hage, D. S. *J. Chromatogr. B Biomed. Sci. Appl.* **1998**, *715*, 3–28.
- (58) Chong, S. L.; Wang, D.; Hayes, J. D.; Wilhite, B. W.; Malik, A. *Anal. Chem.* **1997**, *69*, 3889–98.
- (59) Wang, Z.; Xiao, C.; Wu, C.; Han, H. *J. Chromatogr. A* **2000**, *893*, 157–168.
- (60) Zhou, F.; Li, X.; Zeng, Z. *Anal. Chim. Acta* **2005**, *538*, 63–70.
- (61) Yu, J.; Dong, L.; Wu, C.; Wu, L.; Xing, J. *J. Chromatogr. A* **2002**, *978*, 37–48.
- (62) Zuin, V. G.; Lopes, A. L.; Yariwake, J. H.; Augusto, F. *J. Chromatogr. A* **2004**, *1056*, 21–26.
- (63) Liu, M.; Zeng, Z.; Tian, Y. *Anal. Chim. Acta* **2005**, *540*, 341–353.
- (64) Oliveira, A. F. de; Silveira, C. B. da; Campos, S. D. de; Campos, E. A. de; Carasek, E. *Chromatographia* **2005**, *61*, 277–283.
- (65) Budziak, D.; Martendal, E.; Carasek, E. *J. Chromatogr. A* **2008**, *1187*, 34–39.
- (66) Hennion, M.-C. *J. Chromatogr. A* **2000**, *885*, 73–95.
- (67) Dai, L.; He, P.; Li, S. *Nanotechnology* **2003**, *14*, 1081–1097.
- (68) Feng, J.; Sun, M.; Xu, L.; Li, J.; Liu, X.; Jiang, S. *J. Sep. Sci.* **2011**, *34*, 2482–8.
- (69) Pawliszyn, J.; Kudlejova, L.; Risticovic, S.; Vuckovic, D. In *Handbook of Solid Phase Microextraction*; 2012; pp. 201–249.
- (70) Wittmann, G.; Van Langenhove, H.; Dewulf, J. *J. Chromatogr. A* **2000**, *874*, 225–234.
- (71) Zimmermann, T.; Ensinger, W. J.; Schmidt, T. C. *Anal. Chem.* **2004**, *76*, 1028–38.
- (72) Cancho, B.; Ventura, F.; Galceran, M. T. *J. Chromatogr. A* **2002**, *943*, 1–13.
- (73) Llompart, M.; Lourido, M.; Landín, P.; García-Jares, C.; Cela, R. *J. Chromatogr. A* **2002**, *963*, 137–148.
- (74) Kaur, V.; Malik, A. K.; Verma, N. *J. Sep. Sci.* **2006**, *29*, 333–345.
- (75) Husek, P. *J. Chromatogr. B. Biomed. Sci. Appl.* **1998**, *717*, 57–91.
- (76) Vonderheide, A. P.; Montes-Bayon, M.; Caruso, J. A. *Analyst* **2002**, *127*, 49–53.

- (77) Cavaliere, B.; Macchione, B.; Monteleone, M.; Naccarato, A.; Sindona, G.; Tagarelli, A. *Anal. Bioanal. Chem.* **2011**, *400*, 2903–12.
- (78) Monteleone, M.; Naccarato, A.; Sindona, G.; Tagarelli, A. *Anal. Chim. Acta* **2013**, *759*, 66–73.
- (79) Cavaliere, B.; Monteleone, M.; Naccarato, A.; Sindona, G.; Tagarelli, A. *J. Chromatogr. A* **2012**, *1257*, 149–57.
- (80) Monteleone, M.; Naccarato, A.; Sindona, G.; Tagarelli, A. *J. Chromatogr. A* **2012**, *1251*, 160–8.
- (81) Hong, J. E.; Pyo, H.; Park, S.-J.; Lee, W. *Anal. Chim. Acta* **2005**, *539*, 55–60.
- (82) Quintana, J. B.; Carpinteiro, J.; Rodríguez, I.; Lorenzo, R. A.; Carro, A. M.; Cela, R. *J. Chromatogr. A* **2004**, *1024*, 177–185.
- (83) Okeyo, P. D.; Snow, N. H. *J. Microcolumn Sep.* **1998**, *10*, 551–556.
- (84) Rodríguez, I.; Rubí, E.; González, R.; Quintana, J. B.; Cela, R. *Anal. Chim. Acta* **2005**, *537*, 259–266.
- (85) Lee, I.-S.; Tsai, S.-W. *Anal. Chim. Acta* **2008**, *610*, 149–155.
- (86) Tsai, S.-W.; Chang, C.-M. *J. Chromatogr. A* **2003**, *1015*, 143–150.
- (87) Pizarro, C.; Pérez-del-Notario, N.; González-Sáiz, J. M. *J. Chromatogr. A* **2007**, *1143*, 26–35.
- (88) Cháfer-Pericás, C.; Campíns-Falcó, P.; Herráez-Hernández, R. *J. Pharm. Biomed. Anal.* **2006**, *40*, 1209–1217.
- (89) Domeño, C.; Ruiz, B.; Nerín, C. *Anal. Bioanal. Chem.* **2005**, *381*, 1576–83.
- (90) Ouyang, G.; Pawliszyn, J. *Anal. Bioanal. Chem.* **2006**, *386*, 1059–1073.
- (91) Mills, D. G. A.; Dean, D. J. R.; Pawliszyn, P. J.; Qin, Z.; Bragg, L.; Ouyang, G.; Pawliszyn, J. *J. Chromatogr. A* **2008**, *1196*, 89–95.
- (92) Souza-Silva, E. A.; Lopez-Avila, V.; Pawliszyn, J. *J. Chromatogr. A* **2013**.
- (93) Schurek, J.; Portolés, T.; Hajslova, J.; Riddellova, K.; Hernández, F. *Anal. Chim. Acta* **2008**, *611*, 163–172.
- (94) Gong, Y.; Eom, I.-Y.; Lou, D.-W.; Hein, D.; Pawliszyn, J. *Anal. Chem.* **2008**, *80*, 7275–82.

- (95) Mullett, W. M.; Pawliszyn, J. *J. Sep. Sci.* **2003**, *26*, 251–260.
- (96) Aguinaga, N.; Campillo, N.; Viñas, P.; Hernández-Córdoba, M. *Anal. Bioanal. Chem.* **2008**, *391*, 1419–24.
- (97) Vaes, W. H. J.; Urrestarazu Ramos, E.; Verhaar, H. J. M.; Seinen, W.; Hermens, J. L. M. *Anal. Chem.* **1996**, *68*, 4463–4467.
- (98) Vaes, W. H.; Ramos, E. U.; Hamwijk, C.; van Holsteijn, I.; Blaauboer, B. J.; Seinen, W.; Verhaar, H. J.; Hermens, J. L. *Chem. Res. Toxicol.* **1997**, *10*, 1067–72.
- (99) Kroll, C.; Borchert, H. H. *Pharmazie* **1998**, *53*, 172–7.
- (100) Vuckovic, D.; Zhang, X.; Cudjoe, E.; Pawliszyn, J. *J. Chromatogr. A* **2010**, *1217*, 4041–60.
- (101) Vuckovic, D.; Cudjoe, E.; Hein, D.; Pawliszyn, J. *Anal. Chem.* **2008**, *80*, 6870–80.
- (102) Vuckovic, D.; Pawliszyn, J. *Anal. Chem.* **2011**, *83*, 1944–54.
- (103) Wardencki, W.; Michulec, M.; Curylo, J. *Int. J. Food Sci. Technol.* **2004**, *39*, 703–717.
- (104) Gionfriddo, E.; Naccarato, A.; Sindona, G.; Tagarelli, A. *Anal. Chim. Acta* **2012**, *747*, 58–66.
- (105) Risticovic, S.; Carasek, E.; Pawliszyn, J. *Anal. Chim. Acta* **2008**, *617*, 72–84.
- (106) Feudo, G. Lo; Macchione, B.; Naccarato, A.; Sindona, G.; Tagarelli, A. *Food Res. Int.* **2011**, *44*, 781–788.
- (107) Pankow, J. F.; Luo, W.; Melnychenko, a. N.; Barsanti, K. C.; Isabelle, L. M.; Chen, C.; Guenther, a. B.; Rosenstiel, T. N. *Atmos. Meas. Tech.* **2012**, *5*, 345–361.
- (108) Belliaro, F.; Bicchi, C.; Cordero, C.; Liberto, E.; Rubiolo, P.; Sgorbini, B. *J. Chromatogr. Sci.* **2006**, *44*, 416–29.
- (109) Jeleń, H. H.; Majcher, M.; Dziadas, M. *Anal. Chim. Acta* **2012**, *738*, 13–26.
- (110) Ahmed, F. E. *TrAC Trends Anal. Chem.* **2001**, *20*, 649–661.
- (111) Lord, H. L.; Grant, R. P.; Walles, M.; Incledon, B.; Fahie, B.; Pawliszyn, J. B. *Anal. Chem.* **2003**, *75*, 5103–5115.
- (112) Musteata, F. M.; Pawliszyn, J. *J. Biochem. Biophys. Methods* **2007**, *70*, 181–93.

- (113) Musteata, F. M.; de Lannoy, I.; Gien, B.; Pawliszyn, J. *J. Pharm. Biomed. Anal.* **2008**, *47*, 907–12.
- (114) Vuckovic, D.; de Lannoy, I.; Gien, B.; Yang, Y.; Musteata, F. M.; Shirey, R.; Sidisky, L.; Pawliszyn, J. *J. Chromatogr. A* **2011**, *1218*, 3367–3375.
- (115) Zhang, X.; Es-haghi, A.; Musteata, F. M.; Ouyang, G.; Pawliszyn, J. *Anal. Chem.* **2007**, *79*, 4507–13.
- (116) Zhang, X.; Cudjoe, E.; Vuckovic, D.; Pawliszyn, J. *J. Chromatogr. A* **2009**, *1216*, 7505–9.
- (117) Zhou, S. N.; Oakes, K. D.; Servos, M. R.; Pawliszyn, J. *Environ. Sci. Technol.* **2008**, *42*, 6073–6079.
- (118) Zhang, X.; Oakes, K. D.; Cui, S.; Bragg, L.; Servos, M. R.; Pawliszyn, J. *Environ. Sci. Technol.* **2010**, *44*, 3417–22.
- (119) Mills, D. G. A.; Dean, D. J. R.; Pawliszyn, P. J.; Zhou, S. N.; Ouyang, G.; Pawliszyn, J. *J. Chromatogr. A* **2008**, *1196*, 46–56.
- (120) Vuckovic, D.; de Lannoy, I.; Gien, B.; Shirey, R. E.; Sidisky, L. M.; Dutta, S.; Pawliszyn, J. *Angew. Chem. Int. Ed. Engl.* **2011**, *50*, 5344–8.
- (121) Cudjoe, E.; Bojko, B.; de Lannoy, I.; Saldivia, V.; Pawliszyn, J. *Angew. Chemie Int. Ed.* **2013**, *52*, 12124–12126.

Chapter 2

Multivariate optimization by Experimental Design

2.1 Introduction

For a long time, the broad range of mathematical and statistical methods has provided an excellent opportunity for the quantitative description of experimental results and effects in natural sciences. It is therefore not surprising that statistical methods are applied as a tool for interpretation of complex data, specifically in scientific research.

First of all, the aim of applying mathematical and statistical methods is to detect and subsequently describe the interrelations between influencing forces and the interrelations between these influences, and the resulting effects. In analytical chemistry, the processes requiring investigation have become increasingly complex. Previously, the acquisition of data was a significant limiting step in the analytical process. However, the situation has changed considerably since the 1950s due to the introduction of various types of analytical instruments. This development has led to the acquisition of larger volumes of data, which require further reduction, clear representation (in the sense of visualization), and extraction of relevant information. This upsurge in data acquired also provided an opportunity for more detailed and quantitative description of systems investigated and structure-activity relationships.

Parallel to the rapid development in analytical instrumentation was the outburst development of computer science and technology, a powerful tool that can provide the solutions for the problems enumerated earlier. It therefore became easier for scientists, and especially analytical chemists, to apply computer tools and models, and advanced statistical and mathematical methods in their field of work. Subsequently, new sub-discipline heavily utilized in analytical chemistry emerged, called chemometrics. Chemometrics can be described as an aspect of science, which relates

measurements made on a chemical system to the condition of the system through the application of mathematical or statistical tools. In order to relate data acquired of any system to its conditions at the time of acquisition, it is critical to carefully optimize the procedure by considering all possible interactions that can occur within the system. It is therefore imperative to perform method optimization.

Method optimizations are useful in all steps of the analytical procedures. Generally, a well thought method optimization entails not necessarily statistical tools, but a set of carefully designed experiments. Method optimizations are not only geared toward the achievement of the highest analytical signal responses but also include prevention of any possible bias that can affect the reliability of the overall data. Thus, well designed experiments with the appropriate statistically tools help to prevent or minimize any form of biases that may occur. Often the approach used involves randomization of the experiments so as to avoid systematic errors in experimentation. The procedure is currently applied in various analysis including food, bioanalytical and environmental analysis. The two major types of method optimizations approaches are known as univariate and multivariate optimizations.

2.2 Univariate versus multivariate optimization

Univariate optimization also called OVAT (One Variable At a Time), involves the optimization of the factors investigated keeping constant all the other variables and optimizing one parameter at time. This approach does not guarantee at all that the real optimum will be reached, since it would be valid only if the variables to be optimized would be totally independent from each other. However, in the most cases this condition is never fulfilled and OVAT optimization will provide information that represents the system considered only in part since the interactions (synergistic or adverse) between variables are not taken into account.

Another important difference between the two approaches is the fact that the analyst performing OVAT decides which experiment to do next on the basis of the outcome of the previous experiments, while with the multivariate optimization there is only a simple grid covering the entire experimental domain. This implies that with OVAT, only a local knowledge is obtained and only the results of the experiments performed could be known with each individual experiment having a degree of uncertainty of experimental error. However, the results obtained

by multivariate optimization, a simple mathematical model could relate the response with the experimental conditions. For example, considering a two-factor system:

$$Y = b_0 + b_1X_1 + b_2X_2 + b_{12}X_1X_2 + b_{11}X_1^2 + b_{22}X_2^2 \quad (2.1)$$

where b_{12} is the coefficient taking into account the interactions between variables. By software computation, it is possible to find the values for all the coefficients by simply replacing X_1 and X_2 with actual values. It is therefore possible to predict the response for each point of the experimental domain, even for those points for which corresponding experiments were not been performed. The model also allows obtaining a graphical representation of the experimental domain investigated as showed in Figure 2.1

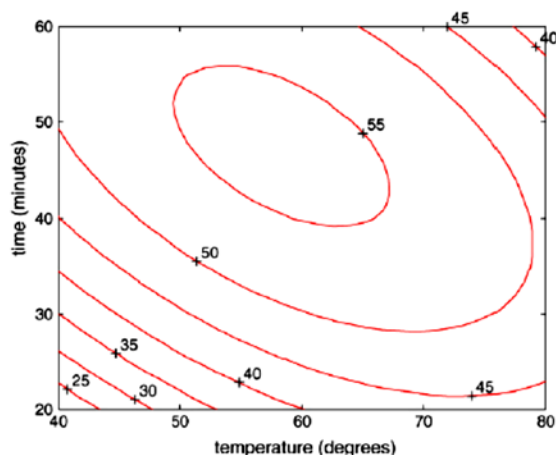


Figure 2.1 Isoresponse plot for the optimization of the yield of a chemical reaction

The iso-response curves connect all points having the same predicted response. By looking at this plot, the general behaviour of the system can be easily understood, and the conditions corresponding to a global maximum effect can be easily identified. For example, in a given experiment with only two variables (temperature and reaction time) with negligible interactions, the best temperature changes with respect to the reaction time could be deduced.

It also very useful taking in consideration the corresponding Leverage plot (Figure 2.2): leverage measures how distant a design point is from the mean of all n runs within the space of the independent variables. The higher the leverage the greater the impact of the point on the fitted

values y will be.

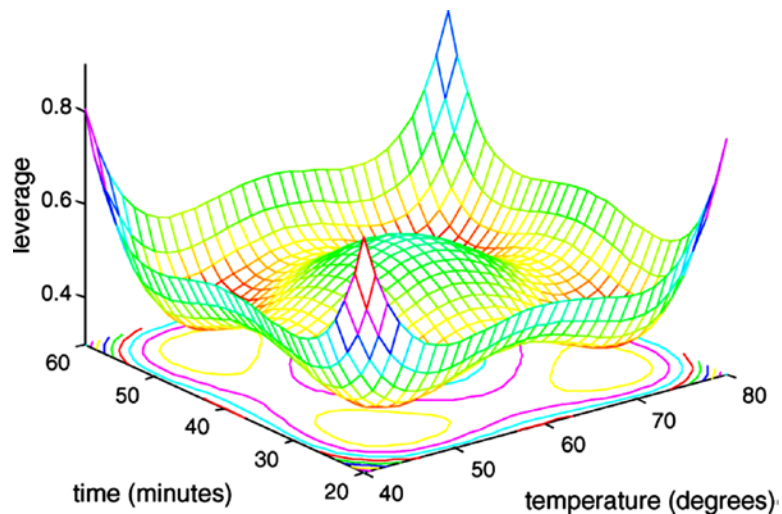


Figure 2.2 Leverage plot for the optimization of the yield of a chemical reaction

Therefore, a leverage of 1 means that the response can be predicted with the same precision of the actual experiment, while leverage < 1 means that the response can be predicted better, if one real experiment would be performed in the same point. Since in the whole experimental domain shown in Figure 2.2 the leverage is always much lower than 1, this means that the response in any point will be known with a better precision by using the prediction from the model obtained by the responses of the nine experiments of the experimental design than by performing an actual experiment in the same point. Since the leverage can be computed before starting to do the experiments, it is possible to know in advance whether the estimated precision will be acceptable or not (of course, to have this knowledge the experimental variance should be known).

Generally the main noticeable differences in information obtained by an OVAT approach with the information obtained by an experimental design by multivariate approach are:

- the experimental design takes into account the interactions among the variables, while the OVAT does not;
- the experimental design provides global knowledge (in the whole experimental domain), while the OVAT gives a local knowledge (only where the experiments have been performed);

- in each point of the experimental domain, the quality of the information obtained by the experimental design (leverage always <1) is greater than the information obtained by the OVAT (leverage = 1, and only for those points where the experiments have been performed);
- the number of experiments required by an experimental design is smaller than the number of experiments performed with an OVAT approach.

2.2.1 Reasons of performing Experimental Design

Performing an experimental design does not only consist in building the experimental matrix, which is the easiest part of the entire optimization but involves multiple logical components. The whole procedure can be summarized in six important steps:

1. Definition of the goal of the experiments; it is important to have clear and final aim of the investigation, and fully understand what the experiments are intended for.
2. Detect all the factors with potential effect; particular attention must be given to the all the variables that may have an effect on the response without exclusions. Any *a priori* exclusion must be based on scientific facts.
3. Choose the proper design to perform based on the number of variables selected and the system in considered.
4. Planning the experiments with carefully chosen factors with well-defined ranges and the model to be applied.
5. Performing the experiments; these are regarded as tools to get results that will be used to build the model.
6. Analyzing the data obtained by the experiments; this step transforms data into information and forms the logical conclusion of the whole process.

It is possible that a single experimental design would not be enough solution of the scientific problem. This often occurs after analyses of the data by the analyst and under such conditions, more accurate experimental design is required. For example, the new approach may incorporate the elimination of some variables from the optimization process since they do not significantly influent on the response or may be necessary a redefinition of the experimental domain¹.

2.3 Screening designs

“Screening Design” is a term referring to an experimental plan that is intended to assess the relative impact of a large number of factors on a response of interest from a list of many potential ones. Alternatively, it is referred to a design whose primary purpose is to identify significant main effects, rather than effects resulting from interactions, the latter being assumed an order of magnitude less important.

Even when the experimental goal is to fit a response surface model, the first experiment set should be a screening design especially for cases where there are many factors to consider. This allows the analyst to perform preliminary evaluations of the variables that carefully needs further optimization and investigation. Screening design give less information compared to optimization design. But they enhance determination of the significance of various variables with a relative small number of experiments compared to “optimization designs” that will be discussed later.

The most used screening designs are Factorial Designs and Plackett-Burman Design.

2.3.1 Factorial designs

A factorial design is the most common way used to study the effect of two or more independent variables². In a factorial design, all levels of each independent variable are combined with all levels of the other independent variables to produce all possible conditions. There are various types of factorial designs. Some of which include a 2x2 (two-by-two) factorial design since there are two independent variables and each has two levels. However, if the first independent variable had three levels instead of 2, then it would be a known as 3x2 factorial design. The number of distinct conditions is formed by combining the levels of the independent variables with the product of the numbers of levels. In a 2x2 design, there are four distinct conditions. In a 3x2 design, there are 6.

The 2^k factorial designs are the simplest possible design; required number of experiments is given as 2^k , where k is the number of variables under study. In these designs each variable has two levels, coded as -1 and $+1$, and the variables can be either quantitative (e.g., temperature, pressure, amount of an ingredient) or qualitative (e.g., type of catalyst, type of apparatus, sequence of operations).

The experimental matrix is usually easy to build even and a typical example is showed in Table 2.1 for a 2^3 full factorial design.

Table 2.1 The experimental matrix of the 2^3 factorial design

Experiment	Reagent A (X1)	Reagent B (X2)	Reagent C (X3)
1	-1	-1	-1
2	1	-1	-1
3	-1	1	-1
4	1	1	-1
5	-1	-1	1
6	1	-1	1
7	-1	1	1
8	1	1	1

The matrix has eight rows with each row corresponding to an experiment, and 3 columns each column corresponding to a variable; in the first column the -1 and $+1$ alternate at every row, in the second column they alternate every second row, in the third column they alternate every fourth row. The same procedure can be used to build any type of factorial design, irrespective of the number of variables. From a geometrical point of view, as shown in Figure 2.3, a 2^3 factorial design explores the corners of a cube, and if the variables are more than three it will be a hypercube. Contrary to what happens in the OVAT approach, in which a variable is changed while maintaining all other variables constant, in the factorial designs all variables are always changed at any point.

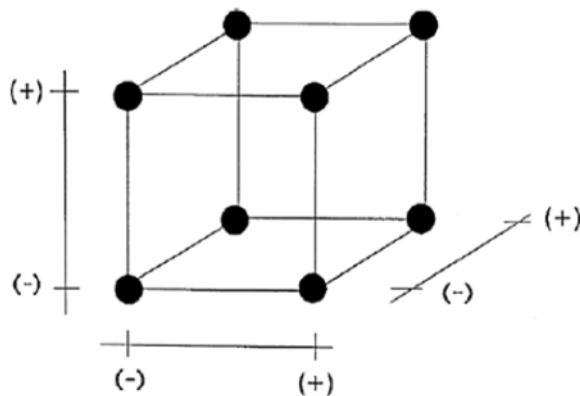


Figure 2.3 Graphical representation of a 2^3 Design

This means that the factorial design is suitable for estimating the interactions between variables. The mathematical model used is given as follows:

$$Y = b_0 + b_1X_1 + b_2X_2 + b_3X_3 + b_{12}X_1X_2 + b_{13}X_1X_3 + b_{23}X_2X_3 + b_{123}X_1X_2X_3 \quad (2.2)$$

Therefore with just eight experiments it is possible to estimate all forms of interactions at each level.

The first step in order to determine the coefficients is to choose a high and low level for each factor and substitute them in the experimental matrix. As in all chemometrics, some advance knowledge of the system is required, so as to make realistic predictions of the system.

To compute the coefficients, it is necessary to use the model matrix (Table 2.2). While the former (experimental matrix) has as many rows as experiments and columns as variables, the latter has as many rows as experiments and columns as coefficients, and can be easily obtained as follows: the first column (b_0) is a column of +1, the columns of the linear terms are the same as the experimental matrix, the columns of the interactions are obtained by a point to point product of the columns of the linear terms of the variables involved in the interaction (e.g., the column b_{12} of the interaction between variables 1 and 2 is obtained by multiplying point to point the column b_1 by the column b_2).

Table 2.2 Model matrix response

Model matrix							
b_0	b_1	b_2	b_3	b_{12}	b_{13}	b_{23}	b_{123}
1	1	-1	-1	1	1	1	1
1	-1	-1	-1	-1	-1	1	1
1	1	1	-1	1	-1	-1	1
1	-1	1	-1	-1	1	-1	1
1	1	-1	1	1	1	1	1
1	-1	-1	1	-1	-1	1	1
1	1	1	1	1	-1	-1	1
1	-1	1	1	-1	1	-1	1

Computing the coefficients for each of them involves multiplying point to point the column corresponding to the coefficient that has to be estimated by the column of the response, and then take the average of the results. For instance, for estimating b_1 (the linear term of X_1), it will be $(-51.8+51.6-51.0 + 42.4-50.2 + 46.6-52.0 + 50.0)/8 = -1.8$. Since every column of the model matrix has four -1 and four $+1$, every coefficient will be computed as half the difference between the average of the four experiments with positive sign and the average of the four experiments with negative sign. This means that each coefficient is computed with the same precision, and the precision, which is the difference of two averages of four values, is better than that of an OVAT experiment. It is clearly evident that the experimental design gives much more information (the interaction terms) of much higher quality (higher precision of the coefficients). Considering the following model:

$$Y = 49.4 - 1.8 X_1 - 0.6X_2 + 0.2X_3 - 0.8X_1X_2 + 0.4X_1X_3 + 1.9X_2X_3 + 1.2X_1X_2X_3 \quad (2.3)$$

since eight coefficients have been estimated with eight experiments with no degrees of freedom and unknown experimental variability, it is impossible to define the statistical significance of the coefficients. Nonetheless, those of the linear term of X_1 (Reagent A) and the interaction X_2, X_3 (Reagent B and Reagent C) have absolute values larger than the other ones.

The large coefficient of X_1 indicates that by increasing the amount of Reagent A, a decrease of the response will be obtained (the sign of the coefficient is negative), and therefore better results are obtained by reducing its amount. Since X_1 is not involved in any relevant interaction, it can be concluded that the effect will be present irrespective of the values of the other two reagents.

The interactions between Reagent B and Reagent C can only be interpreted by looking at the response surface shown in Figure 2.4.

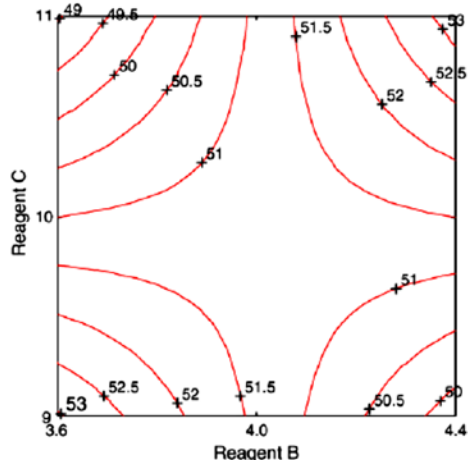


Figure 2.4 Isoresponse plot

Since the response is plotted on the plane defined by two variables, the level of variable 1, which defines the representative response must be defined. Clearly, the effect of Reagent A implies setting the value of X_1 at its lower level (-1).

The geometrical shape of a linear model without interactions is a plane (the iso-response lines are parallel); if relevant interactions are present, then it becomes a distorted plane (the iso-response lines are not parallel). This is the case of the response surface on the plane Reagent B–Reagent C. As shown in the plot, it can be seen that an increase of Reagent B leads to a decrease in response viscosity when Reagent C is at its lower level, while the opposite effect is observed when Reagent C is at its higher level. In the same way, an increase of Reagent C provides a decrease in response when Reagent B is at its lower level, while the opposite effect is observed when Reagent B is at its higher level.

From the plot, it is evident that an OVAT approach will not produce any good results since it does not take into account possible interactions. From the central point outward (corresponding to the original formulation), while changing the amount of either Reagent B or Reagent C, one at a time, by moving parallel to the axes, it becomes evident that irrespective of the type of experiment carried out, no change will be observed. Instead, owing to the strong interaction, relevant variations can only be obtained changing both variables at the same time.

A disadvantage of factorial designs is the large number of experiments that must be performed when the number of factors is large. For example, for a 10 factor design at two levels, 1024 experiments are required. This can be impracticable. However, there could be cases where

carrying out such large number of experiments is inevitable, especially in the screening cases where a large number of factors are of potential interest. There are, fortunately, numerous approaches that can be adopted to reduce the number of experiments.

Consider the case of a three factor with a two-level design. The factors may be, for example, pH, temperature, and concentration, and the yield of a reaction is the response. Eight experiments are listed in Table 2.1 with the coded conditions as usual. The design matrix (Table 2.2) consists of eight possible columns, which equals the number of experiments. Some columns that represent interactions, such as a three-factor interaction, are not relevant. Initial screening, primarily focuses on whether the three main factors have any real influence on the response and not to study the model in detail. In other typical cases, for example, when there may be 10 possible factors, reducing the number of factors to be studied to 3 or 4 makes the next stage of experimentation easier.

To reduce the number of experiments, fractional factorial numbers say 1/2, 1/4, 1/8, etc., of the total can be employed. Using Table 2.1 as an example, a simple but misguided approach to reduce the number of experiments is to perform only the first four experiments of Table 2.1. This, however, restricts the level of the first factor to +1 throughout. The issue with the approach is that the variation of factor -1 is now no longer studied. So any information on how factor -1 influences the response cannot be obtained. However, rules have been developed to produce fractional factorial designs by taking only a subset of the original experiments to enable the study of the other factors.

Table 2.3 illustrates a possible fractional factorial design that enables all factors to be studied.

Table 2.3 Fractional factorial design

Experiments			Matrix of effects							
Factor1	Factor2	Factor3	x_0	x_1	x_2	x_3	$x_1 x_2$	$x_1 x_3$	$x_2 x_3$	$x_1 x_2 x_3$
1	1	1	1	1	1	1	1	1	1	1
1	-1	-1	1	1	-1	-1	-1	-1	1	1
-1	-1	1	1	-1	-1	1	1	-1	-1	1
-1	1	-1	1	-1	1	-1	-1	1	-1	1

There are a number of important features:

- Each of the four columns in the experimental matrix is different.
- In each column, there are an equal number of ‘-1’ and ‘+1’ levels.
- For each experiment at level ‘+1’ for factor 1, there are an equal number of experiments for factors 2 and 3 which are at levels ‘+1’ and ‘-1’, and so on for every combination of factors.

This latter property is sometimes called *orthogonality*. It means that each factor is independent of each other. This is important, otherwise it is not always easy to distinguish the effect of two factors varying separately. The properties of this design can be understood better by visualization Figure 2.5: half the experiments have been removed. For the remainder, each face of the cube now represents two rather than four experiments, and every alternate corner corresponds to an experiment.

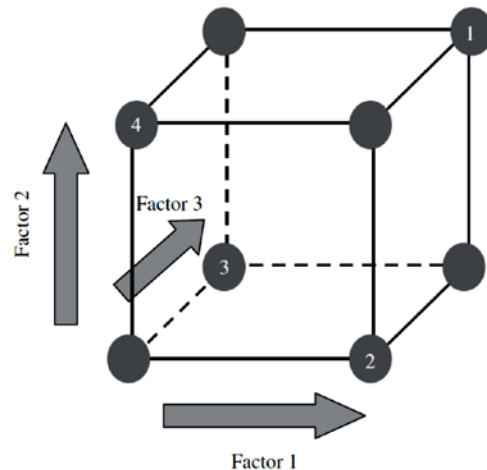


Figure 2.5 Visualization of fractional factorial design

The design matrix of Table 2.3 also has interesting features. Whereas the first four columns are all different, each of the last four corresponds to one of the first four columns. For example the x_1x_2 column is exactly the same as the x_3 column. This implies that as the number of experiments is reduced, the amount of information is correspondingly reduced. Since only four experiments are now performed, it is only possible to measure four unique effects. Thus, four out of the original eight effects can no longer be studied and these effects can subsequently be confused with other most interested effects. The interaction between factors 1 and 2 is said to be *confounded* with factor 3. This may imply, for example, that the interaction between temperature

and pH is indistinguishable from the influence of concentration alone, if these variables correspond to the three factors in the design. However, not all interactions are likely to be significant, and thus by reducing the number of experiments we are banking on some of the interactions not being of primary significance or interest at this point in time.

There are obvious advantages in two level fractional factorial designs, but these do have some drawbacks:

- There are no quadratic terms, as the experiments are performed only at two levels, this also is a weakness of full factorial designs.
- There are no replicates.
- The number of experiments must be a power of two.

Nevertheless, this approach is very popular in many exploratory situations and has the additional advantage that the data are easier to analyze.

2.3.2 Plackett-Burman Design

The main limitation of fractional factorial designs for screening purposes is that the number of experiments must equal a power of two. However, it is possible to set up a design to perform one experiment more than the number of factors being so that the minimum number of experiments required to study, for example 19 factors will be 20. A typical fractional factorial design will require 32 experiments.

Plackett and Burman proposed in 1946 new designs³ constituted by a number of two level factorial designs, whose length (the number of experiments) is a multiple of four and whose width (the number of factors) is one less than the number of experiments. These designs subsequently reduce the overall number of experiments required.

Table 2.4 shows a typical Plackett-Burman design for 11 factors and 12 experiments.

Table 2.4 Plackett-Burman design for 11 factors

Experiments	Factors											
	1	2	3	4	5	6	7	8	9	10	11	
1	-	-	-	-	-	-	-	-	-	-	-	-
2	+	-	+	-	-	-	+	+	+	-	+	
3	+	+	-	+	-	-	-	+	+	+	-	
4	-	+	+	-	+	-	-	-	+	+	+	
5	+	-	+	+	-	+	-	-	-	+	+	
6	+	+	-	+	+	-	+	-	-	-	+	
7	+	+	+	-	+	+	-	+	-	-	-	
8	-	+	+	+	-	+	+	-	+	-	-	
9	-	-	+	+	+	-	+	+	-	+	-	
10	-	-	-	+	+	+	-	+	+	-	+	
11	+	-	-	-	+	+	+	-	+	+	+	
12	-	+	-	-	-	+	+	+	-	+	+	

The first row consists of an experiment at a single level. In the remaining 11 rows, the levels are related diagonally, and it is only necessary to know a row or column to obtain the entire design. The second row is known as “generator”, and Plackett and Burman publish a number of such generators for various different numbers of factors. From the Table 2.4, there are as many high as low levels of each factor over the 12 experiments, as would be expected. The most important property of the design is orthogonality.

Considering factors 1 and 2:

- There are six instances in which factor 1 is at a high level, and six at a low level.
- For each of the six instances at which factor 1 is at a high level, in three cases factor 2 is at a high level, and in the other three cases it is at a low level. A similar relationship exists where factor 1 is at a low level.
- Any combination of two factors is related in a similar way.

Two important implications of the design are:

- The number of experiments must be a multiple of four.

- There are only certain very specific generators that have these properties: there are published generators for different numbers of experiments.

The importance of orthogonality can be illustrated by a simple example, in which factor 1 is always at a high level when factor 2 is low, and vice versa. Under such circumstances, it is impossible to separate the influence of these two factors, i.e., when the first factor increases, the second decreases. For example, if a reaction is always observed either at pH 5 and 30 °C or at pH 3 and 50 °C it is impossible to state whether a change in rate is a result of changing pH or temperature. The only way to be sure is to ensure that each factor is completely independent, or orthogonal, as above. Even small deviations from orthogonality can lead to the influence of different factors getting muddled up.

Standard Plackett-Burman designs exist for 3, 7, 11, 15, 19, etc., factors. If the number of experimental factors is less than the number in a standard design, the final factors can be set as *dummy* factors. Hence, for studies on 10 real factors an 11-factor design must be used with the final factor being considered as a dummy one. This may be a variable that has no influence on the experiment. In fact it is often a good practice to always have one or more dummy factors during screening, because a real factor can be considered insignificant if its influence on the response is less than that of the dummy factor.

2.4 Optimization Designs

It is always useful to obtain more detailed information of the system under investigation, after performing Screening Design.

There are main reasons for proceeding in this direction:

1. Identify the appropriate conditions that result in a maximum or minimum through optimization. An example is improved yield of synthetic reaction.
2. To predict mathematically how a response relates to the values of various factors through the development of detailed quantitative model

Most screening designs do not provide replicate information, or any information on squared or interaction terms. The degrees of freedom for the lack-of-fit for the model are often zero. More informative models are best estimated using a modest number of factors, typically from two to five, to reduce the volume of experimentation..

2.4.1 Central composite design

Central composite designs (CCD) combine⁴ two-level full or fractional factorial designs with additional axial or star points and at least one point at the center of the experimental region being investigated, Figure 2.6. It allows the determination of both linear and quadratic models. The CCD is a better alternative to the full factorial three-level design since it demands a smaller number of experiments while providing more detailed results.

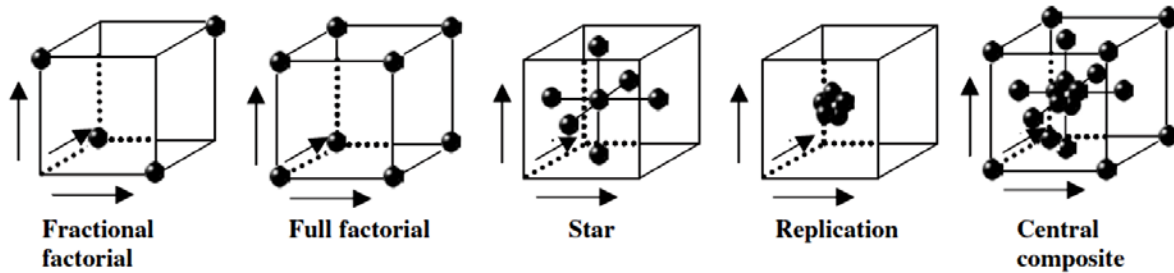


Figure 2.6 Construction of a three factor central composite design

In general, a CCD for k number of factors, coded as (x_1, \dots, x_k) , consists of three parts:

1. A factorial (or cubic) design, containing a total of n_{fact} points with coordinates $x_i = -1$ or $x_i = +1$, for $i = 1, \dots, k$;
2. An axial (or star) part, formed by $n_{\text{ax}} = 2k$ points with all their coordinates null except for one that is set equal to a certain value α (or $-\alpha$);
3. A total of n_c runs performed at the center point, where, of course, $x_1 = \dots = x_k = 0$.

To build a central composite design, it is required to specify each of these three parts. Also, the number of cubic points (α) to use must be evaluated, and how many replicate runs should be conducted at the center point. Two designs are presented in Table 2.5 and Figure 2.7.

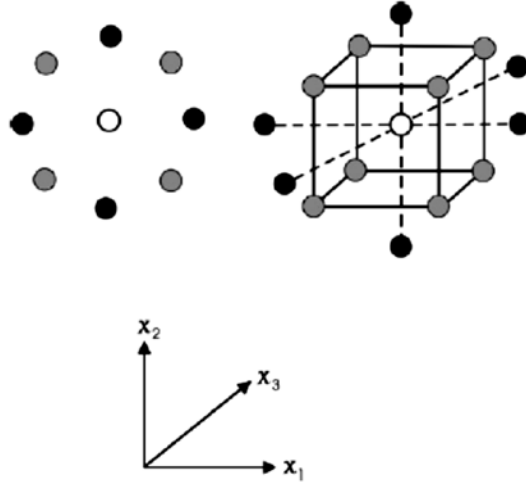


Figure 2.7 Central composite designs for two and three factors. The gray dots form the cubic part the runs of the 2² and 2³ factorial. The black dots represent the star parts.

Table 2.5 Coded factor levels for central composite designs for two- and three-factor systems

Two-factor		Three-factors		
x_1	x_2	x_1	x_2	x_3
-1	-1	-1	-1	-1
1	-1	1	-1	-1
-1	1	-1	1	-1
1	1	1	1	-1
0	0	-1	-1	1
0	0	1	-1	1
0	0	-1	1	1
-1.414	0	1	1	1
0	-1.414	0	0	0
		0	0	0
		-1.683	0	0
		1.683	0	0
		0	-1.683	0
		0	1.683	0
		0	0	-1.683
		0	0	1.683

The design to the left accommodates two factors. The first four runs (2^2 factorial design) make up the cubic part, the star design the last four (with $\alpha = \sqrt{2}$), and there are three replicate runs at the center point. In the case of the three-factor design there are $2^3 = 8$ runs with four center points and six axial points with $\alpha = 1.683$.

The coded values given in Table 2.5 only specify the relative positions of the experimental design points. In part, this determines the precision of the model coefficients and the values predicted by the model.

The cubic points in Table 2.5 and Figure 2.7 are the same as those of full factorial designs although this is not strictly necessary as higher number of factors will require too many experiments.

The total number of distinct levels in a central composite design is $n_{\text{fact}} + 2k + 1$. Therefore, there are $2k + 2k + C_0$ total points where C_0 is the number of center points. For example, with two factors, the model has six parameters. Since the two-factor design in Table 2.1 has nine different combinations of levels, we could estimate all of the model's parameters using only two cubic points, corresponding to one of the two 2^{2-1} fractions. In such a simple design, the economy is very small and hardly justifies destroying the symmetry of the cubic part, but this procedure choosing a fractional design instead of a complete factorial to define the cubic points becomes more attractive as the number of factors increases.

The value of α usually ranges from 1 to \sqrt{k} . When $\alpha = \sqrt{k}$, the cubic and axial points are located on the (hyper) surface of a sphere, and the design is called spherical. This is the case of the two-factor design in Table 2.5 where all of the peripheral points are on the circumference of a circle. At the other extreme, when $\alpha = 1$, the axial points are located at the centers of the sides of the square part of the two-factor design and at the center of the faces of the cubic part of the three-factor design. This type of design is advantageous when the experimental space is square or cubical, which occurs in a natural way when the factors are varied independently of one another. It also has the advantage of requiring only three factor levels, which can be of significance if one of the factors is qualitative. It is important to recognize that these designs are mainly employed for detailed modelling, and also to study interactions and higher order (quadratic) terms. In a nutshell, when the number of experiments becomes excessive as a result of a large number of factors, for example, more than about five significant factors are to be studied, it is only appropriate to initially narrow down the problem using exploratory designs⁵.

2.4.2 Mixtures designs

In the designs described above, each variable could be set at any value inside its range, independently of the value assigned to the other variables. This observation is different for mixture designs. In a mixture design, the implicit constraint is represented by the fact that the sum of all the components must be 1 (or 100%). This means that the components of a mixture cannot be varied independently, since by varying the percentage of one component also the percentages of the other components will change. Another relevant difference with the design for independent variables is that the object of study in these problems is not the effect of the variation of the absolute quantity of the variables, but the effect of the variation of the ratios among the variables. As a result, it is impossible to apply to the problems of mixtures to the experimental designs previously described. The graphical representation of a three-component mixture is shown in Figure 2.8.

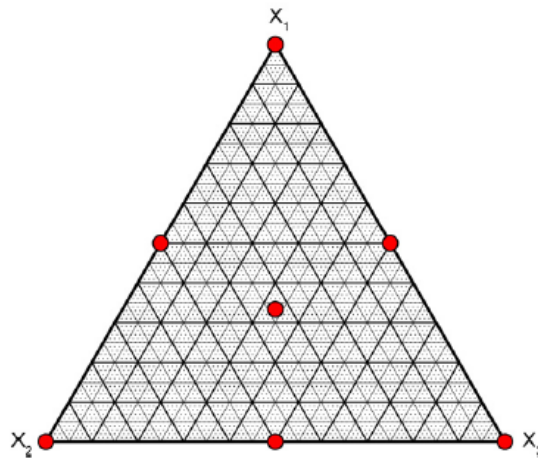


Figure 2.8 The representation of a 3-component mixture, with the lines of the grid drawn at steps of 10% (dark solid lines), 5% (light solid lines) and 1% (dotted lines).

The points of the 7 experiments of the mixture design are reported

It is an equilateral triangle, in which the vertices correspond to the pure components, the sides to the binary mixtures and the internal points to the ternary mixtures. In such a representation, there is a univocal correspondence between the plot and the composition, since to each composition corresponds to one point of the plot, and vice versa. The same is for any number of components of a mixture, whose domain will be the regular figure having as many vertices as components, lying in the space having dimensionality equal to the number of components minus one (the

equilateral triangle is the regular figure having three vertices in a two-dimensional space; the tetrahedron is the regular figure having four vertices in a three-dimensional space). For more than four components, we cannot visualize the whole domain since it lies in a space having more than three dimensions.

Figure 2.8 reports of seven experiments that have been performed, together with the responses that have been obtained, measured on arbitrary units (the experiments are also highlighted in Table 2.6).

Table 2.6 The experimental matrix and the responses of the mixture design

X_1	X_2	X_3	Y_1	Y_2
1	0	0	31	44
0	1	0	113	26
0	0	1	38	52
0.50	0.50	0	42	41
0.50	0	0.50	39	67
0	0.50	0.50	70	30
0.33	0.33	0.33	60	55

By doing these experiments, the coefficients of the following model can be estimated:

$$Y = b_1X_1 + b_2X_2 + b_3X_3 + b_{12}X_1X_2 + b_{13}X_1X_3 + b_{23}X_2X_3 + b_{123}X_1X_2X_3 \quad (2.4)$$

Comparing it with the model for independent variables, it can immediately be seen that the constant is not present. This appears quite logical if the constant corresponds to the response when all the variables zero level. In the case of the designs for independent variables, it has a practical meaning, since it corresponds to the response at the center point. In the case of mixtures, since the sum of all the components must be 1, it is not possible to have a condition in which all the variables have level 0.

The model for the first response is given as:

$$Y = 31X_1 + 113X_2 + 38X_3 - 120X_1X_2 + 18X_1X_3 - 22X_2X_3 + 370X_1X_2X_3 \quad (2.5)$$

It can be noticed that the coefficients of the linear terms correspond to the response obtained with the pure components. The coefficients of the two-term interactions indicate the synergic effect of the two components. In the example described above, the experiment with pure X_1 gave a response of 31, while the experiment with pure X_2 gave a response of 113. If no synergic effect is present, the mixture made by 0.5 X_1 and 0.5 X_2 would give a response of 72 (the average of 31 and 113). Instead, the response of this mixture is 42 (30 units less), meaning that there is a negative synergic effect. This can be observed in the term X_1X_2 , whose coefficient is -120 . It can be seen that the magnitude of the synergic effects of the two-component mixtures is given by the coefficients divided by 4. In the same way, the coefficient of the three-terms interaction, divided by 27, corresponds to the magnitude of the synergic effect of the three components (this is the reason why the coefficients of the higher interactions are usually very large). From the iso-response plot shown in Figure 2.9 it can be seen that X_2 has the greatest effect on Y_1 (breaking load). To understand the effect of each variable one must follow how the response changes when going from a composition without that component to the pure component (without changing the relative amounts of the other components). On the plot, start from the center of the edge opposite to the component under study (i.e., a mixture made by the two remaining components, at 50% each) and go to the vertex representing the pure component. In the case of X_2 , the response at the starting point (no X_2) is 39, and then it goes on increasing quite regularly up to 113 for pure X_2 . Doing the same for X_1 , it can be seen that it has a negative effect: the response is 70 without it, and then regularly decreases down to 31 for pure X_1 .

X_3 is the component with the lowest effect and, owing to the three-component interaction, it has a different behaviour: starting from 42 for the mixture made by 50% X_1 and 50% X_2 , it goes down to 38 for pure X_3 , but the addition of X_3 at first increases the response (up to 60 for the mixture made by 33.3% of each of the components), then decreases it.

The model for the second response is:

$$Y = 44X_1 + 26X_2 + 52X_3 + 24X_1X_2 + 76X_1X_3 - 36X_2X_3 + 206X_1X_2X_3 \quad (2.6)$$

By looking at the coefficients of the interactions it can be understood that the strongest synergic effect is the positive synergy between X_1 and X_3 . By looking at the iso-response plot of Figure

2.9 it can be seen that the highest response corresponds to the mixture made approximately by 50% X1 and 50% X3. Also for this response X2 is the component with the highest effect, since the response decreases from 67 (no X2) to 26 (pure X2). When starting adding X1 the response increases from 30 up to more than 55 (at approximately 50% of X1), then it decreases to 44 (pure X1). X3 is the component with the smallest effect, since the response goes from 41 (no X3) up to about 50 (at approximately 20% of X3), to stay almost constant till the pure X3, having a response of 52.

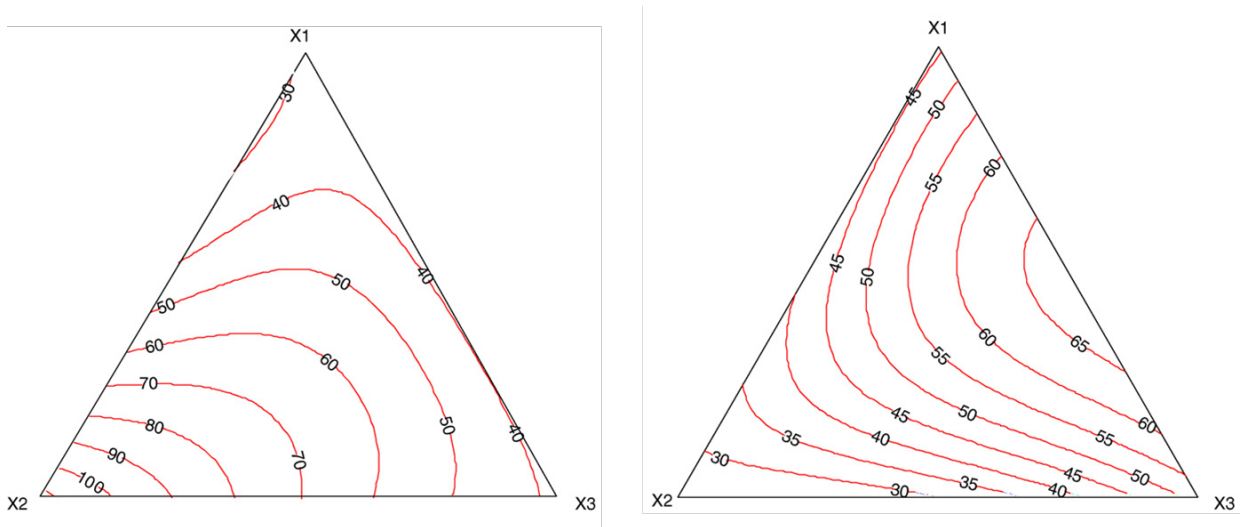


Figure 2.9 Isoresponse plots of the two responses of the mixture design (top: breaking load, bottom: dissolution rate)

In the experimental designs for independent variables we saw that the effect of the factors and the relative importance of the terms can be immediately understood just by looking at the model (the higher the coefficient, the more important the term).

Unfortunately, this is not true in the mixture designs. For instance, in the case of the second response of the previous example, it is clear from the iso-response surface that X_2 is by far the component with the most relevant effect, but its coefficient is the smallest one. This because, as previously explained, the coefficients of the linear terms correspond to the responses with pure components, and therefore have nothing to do with the effects of the components. Considering interactions, for a practical meaning, it should be divided by 4 (in case of a two-term interaction) or 27 (for three-term interactions), or 256 (for four-term interactions).

As a consequence, the only way to understand the meaning of a model is to look at the iso-response surfaces. This is easy in the case of three components (a triangle domain), it becomes more complex but still possible in the case of four components (a tetrahedron domain). It is necessary to take into account “slices” obtained by cutting through with planes parallel to one of the faces, which means keeping one of the components constant. This however is extremely difficult for more than four components (with n components, in order to have a plane, we should cut the experimental domain with hyper-planes obtained by keeping constant $n-3$ components).

This is the reason why the number of components under study in a mixture design usually is not higher than four. In case of a more complex system, it is suggested to split the whole domain into two or more subdomains; each of them with an “acceptable” number of components, and each studied separately. By doing so, it is obvious to realize that the interactions among the components of the different subdomains cannot be studied; a price to pay in order to increase the comprehensibility of the whole system. Mixture designs are extremely important in many fields such as pharmaceutical industry, food products (e.g., formulation of a new recipe), beverages (e.g., formulation of a blend), paintings (e.g., formulation of a painting) and method optimization (e.g., optimal mobile phase for HPLC).

2.5 Application experimental designs to the optimization of SPME methods

The use of multivariate techniques during the method development stage of SPME methods is highly recommended because it is faster and more effective than traditional method development approaches. It requires a much smaller number of experiments and increases the likelihood of finding true optimum values for all the factors tested. In most of the cases all the parameters influencing the SPME process are not independent from each other, in the sense that interactions may exist among them and that can affect the extraction efficiency. Therefore, it is very critical the use of multivariate optimization, since OVAT approaches do not take into account interactions between variables. Usually, in order to identify factors significantly affecting the extraction process, screening design are used and the selected parameters are better investigated by optimization designs such as Central Composite Design (usually not more than three or four factors are selected). The factors not affecting the response can be evaluated by OVAT. For the factors optimized by multivariate optimization, response surfaces will be constructed and the best working conditions estimated. Depending on the number of analytes and the matrix object

of the investigation, different optimum working conditions can be observed. In such cases, careful use of the knowledge of the analyst should lead to the determination of the best compromise between factors in order to ensure good extraction efficiency for all the analytes involved. Example of multivariate optimization of SPME protocols can be found copiously in literature: a very recent application involved the simultaneous determination of trihalomethanes and organochlorine pesticides in water samples by a new developed extraction mode: direct immersion-headspace-solid phase microextraction. The extraction of these analytes was performed by DI-, HS-, and DI-HS-SPME⁶. Central composite design was applied in order to investigate the effect of extraction time, temperature and added volume of aqueous NaCl solution at 20% (*m/v*) for each extraction mode used. Specifically for the DI-HS-SPME, the multivariate optimization allowed the determination of the best compromise working conditions between the two coupled extraction mode, procedure that would have been extremely tedious but not really accurate if performed by OVAT approach.

Similarly, Plackett-Burman design was used to evaluate six factors affecting the efficiency of the simultaneous on-fibre derivatization/SPME extraction⁷.

The use of experimental design during SPME method development is widely documented in literature⁸⁻¹³ and this thesis also demonstrates examples of multivariate optimized SPME methods for bio-clinical, environmental and food analysis in Chapter 3.

2.6 References

- (1) Leardi, R. *Anal. Chim. Acta* 2009, 652, 161–72.
- (2) Brereton, R. G. *Applied Chemometrics for Scientists*; John Wiley & Sons, Ltd: Chichester, UK, 2007.
- (3) Plackett, R. L.; Burman, J. P. *Biometrika Trust* 1946, 33, 305–325.
- (4) Box, G.; Hunter, W.; Hunter, S. *Statistics for Experimenters: An Introduction to Design, Data Analysis, and Model Building*; John Wiley & Sons, 1978.
- (5) Ferreira, S. L. C.; Bruns, R. E.; da Silva, E. G. P.; Dos Santos, W. N. L.; Quintella, C. M.; David, J. M.; de Andrade, J. B.; Breitzkreitz, M. C.; Jardim, I. C. S. F.; Neto, B. B. J. *Chromatogr. A* 2007, 1158, 2–14.
- (6) Merib, J.; Simão, V.; Dias, A. N.; Carasek, E. J. *Chromatogr. A* 2013.
- (7) Herráez-Hernández, R.; Cháfer-Pericás, C.; Verdú-Andrés, J.; Campíns-Falcó, P. J. *Chromatogr. A* 2006, 1104, 40–46.
- (8) Polo, M.; Llompарт, M.; Garcia-Jares, C.; Cela, R. J. *Chromatogr. A* 2005, 1072, 63–72.
- (9) Sousa, E. T.; de M. Rodrigues, F.; Martins, C. C.; de Oliveira, F. S.; de P. Pereira, P. A.; de Andrade, J. B. *Microchem. J.* 2006, 82, 142–149.
- (10) Risticovic, S.; Carasek, E.; Pawliszyn, J. *Anal. Chim. Acta* 2008, 617, 72–84.
- (11) Monteleone, M.; Naccarato, A.; Sindona, G.; Tagarelli, A. *Anal. Chim. Acta* 2013, 759, 66–73.
- (12) Cavaliere, B.; Monteleone, M.; Naccarato, A.; Sindona, G.; Tagarelli, A. J. *Chromatogr. A* 2012, 1257, 149–57.
- (13) Rodrigues, C.; Alves, C.; Santos-neto, A. J.; Fernandes, C.; Lan, F. M. 2007, 1342–1347.

Solid-Phase Microextraction combined to gas-chromatography mass-spectrometry in bioclinical, environmental and food analysis

3.1 Bioclinical and environmental applications of Solid-Phase Microextraction coupled with GC-QqQ-MS

In recent years, there is growing interest in studies related to the identification of biomarkers in biological fluids for disease diagnosis and prognosis. Emerging “omics” technologies such as transcriptomics, proteomics and metabolomics enhances the possibility of measuring and using multiple biomarkers simultaneously to predict or diagnose disease¹.

Biofluids such as urine and blood, plasma and lymph possesses rich information on the overall pathophysiology of the human being. However, screening and analysis of biofluids are among the main challenges in bioanalysis for the development of sensitive and highly selective protocols. In view of this, simultaneous determination of metabolites and their disease biomarkers related to the overall health status of an individual become a challenge. Sample preparation and highly selective detection systems play an important role in the assessment of biomarkers in biofluids. Bioanalytical methods based on mass spectrometry obviously are promising tools for the discovery of novel biomarkers or target biomarker assessment that form the foundation for new clinical tests. One of the essential requirements in bioclinical analysis is the need for precise, selective and accurate detection of the target analytes; clinicians generally recognize triple quadrupole mass analyzer as the gold standard for developing MS-based quantitative methods. Use of tandem mass spectrometric methods based on multiple reaction monitoring (MRM) provide both structural information on the analyte and relative or absolute measurement of analyte concentration when appropriate standards are added²⁻⁸. By combining

with the appropriate sample preparation protocol, the technique will continue to serve as the major tool for bioclinical assays. Currently, SPME has gained significant recognition as a sample preparation tool for various bioanalytical assay⁹. Therefore, SPME combined with MS is a rapidly growing technique in the field applicable to bioclinical investigations.⁹⁻¹²

One of the major factors that influence human health is the environment. This is because human beings are on daily basis exposed to various forms of chemical or biohazards prevalent in the environment due to various human activities and developments. As a result of significant industrialization, the natural environment is strongly affected since emissions from anthropogenic pollutants and/or their decomposition in environment alter natural and delicate biota equilibria and induce adverse health effects on ecosystems. In view of this screening of the environment for potential chemical contaminants is very important.

Without doubt, environmental analytical chemistry research will be essential in order to provide versatile and reliable tools for the fast assessment of pollutants and their degradation products in environmental matrices. Although persistent organic pollutants (POP) and heavy metals had been of paramount concern in the past, recently, they have not received much attention, especially in industrialized countries. This may be due to the fact that drastic reduction of emission has been achieved through the adoption of appropriate measures and elimination of the dominant pollution sources. In recent times there is a paradigm shift in environmental analytical chemistry towards polar organic contaminants. In addition, there is a wide range of so-called “emerging” or “new” unregulated contaminants that have emerged as an environmental problem and subsequently become a major area of concern to environmental analytical chemists¹³.

In the light of this challenge, there is a growing need for newly developed sample preparation methods and analytical techniques to address the recent environmental issue. Currently, some of the conventional methods like soxhlet extraction, solid liquid extraction, etc., do not offer effective sample pretreatment and clean-up for analysis different types of environmental samples. Therefore, extracts from these methods may contain matrix components, which co-elute with the analytes that affect the overall quantitative analysis, or may even require further clean up, making the entire method too laborious. For this reason, efforts have been made in the development of new sample preparation techniques capable of performing sample clean up, extraction and pre-concentration in few and simple steps. The most commonly used methods include solid-phase extraction (SPE) and solid phase microextraction (SPME), especially in

routine analysis. This may be due to the fact that the methods are amenable to automation, can be coupled to various separation and detection systems and also offer shorter sample pre-treatments, to mention a few¹⁴.

Despite the effort made in the development of efficient sample preparation techniques, the complexity of environmental matrices makes relevant the use of efficient separation and highly selective detection system, in order to guarantee accurate identification of analytes. This is because most of these environmental contaminants are in very low concentrations (ultra-trace levels) and thus require reliable and sensitive techniques for detection. Tandem mass spectrometry coupled with high efficiency separation systems such as gas-chromatography (GC) or high-performance liquid chromatography (HPLC) is obvious choice of analytical tool for the development of high-throughput, reliable and versatile protocols for analysis of environmental matrices¹⁴.

This portion of the thesis is describes a newly developed SPME-GC-MS/MS method for bioclinical and environmental analysis. Specifically, a new method for the reliable determination of biogenic primary amines was optimized and developed as an alternative approach for the screening of these biomarkers in human urine. Also, new developed protocols for the simultaneous determination of emerging organic polar contaminants in environmental matrices and human urine have been discussed.

3.1.1 Development of a simple and rapid solid phase microextraction-gas chromatography-triple quadrupole mass spectrometry method for the analysis of dopamine, serotonin and norepinephrine in human urine¹⁵

3.1.1.1 Introduction

Neurotransmitters play an important role in the various activities of endocrine, central and peripheral nervous systems. Catecholamines are hormones and neurotransmitters derived from tyrosine and generated in nerve tissue and adrenal glands. Dopamine (DA) and norepinephrine (NE) are primary amines which belong to this class of biogenic amines and are implicated in several pathological conditions regarding heart disease, stress, neurological disorders and cancerous tumors such as paraganglioma and neuroblastoma¹⁶⁻²³. For example, useful information for diagnoses of Alzheimer's and Parkinson's diseases and schizophrenia may be obtained from the concentration values of these compounds in biological fluids.

Serotonin (5-hydroxytryptamine, 5-HT) is an indolamine neurotransmitter which takes part in the regulation of sleep, mood, sexuality, appetite, blood pressure and smooth muscle contraction.

Since catecholamines and serotonin are of great clinical importance in the diagnosis of several diseases, their simultaneous determination in biological fluids represents a useful tool to identify eventual pathologies at an early stage. The analysis of urine samples is advantageous with respect to plasma both because biological half-life is greater and because urine sampling is less complicated and invasive. Different analytical protocols have been developed for quantification of catecholamines and serotonin in urine. The most adopted methods are based on high performance liquid chromatography (HPLC) interfaced with electrochemical detector (ECD)²⁴⁻³⁰, fluorescent detector³¹⁻³⁵, and mass spectrometer in tandem mass spectrometry (MS/MS) acquisition³⁶⁻⁴¹. During recent years, many studies employed capillary electrophoresis (CE) coupled to UV⁴²⁻⁴⁷, chemiluminescence detection (CL)⁴⁸, fluorescence detection⁴⁹, electrochemical detection⁵⁰⁻⁵² and mass spectrometry (MS)^{42,53}. Only one work based on gas chromatography (GC) technique was recently reported on the analysis of dopamine, norepinephrine and serotonin in urine⁵⁴. It is well known that GC is widely applied in several analytical fields due to its ease of operation, high ability in peak separation at low instrumental cost and good robustness and, for these reasons, gas chromatographic instruments coupled with several detectors are commonly used even in unspecialized laboratories. On the other hand, for some classes of compounds such as amines and hydroxyl group, a derivatization reaction is

required before gas chromatographic analysis to increase volatility, reduce polarity and then improve chromatographic behavior of these compounds. The derivatization of aliphatic amine is usually based on the use of commercially available reagents such as pentafluorobenzaldehyde or pentafluorobenzoyl chloride^{55,56}, N-hydroxylsuccinimidyl phenylacetate⁵⁷, N-succinimidyl benzoate⁵⁸, hexamethyldisilazane (HMDS) and N-Methyl- bis(heptafluorobutyramide) (MBHFBA)⁴². Some studies proved that also alkylchloroformates are strong and rapid derivatizing reagents for amino group⁵⁹. The derivatization reactions with these compounds occurred directly in aqueous media without the requirement of heating, thus simplifying the sample pretreatment and derivatization procedure and therefore improving the batch repeatability. Moreover, it is compatible with the use of solid phase microextraction (SPME) that allows the extraction of analytes directly in the aqueous phase⁶⁰⁻⁶³.

The sample preparation step for the determination of catecholamines and serotonin is usually performed by solid phase extraction (SPE)^{28,29,37,41-43,55}. These methods are tedious, time consuming and, above all, require large volume of organic solvents. Recently, newly developed microextraction techniques such as microextraction in packed syringe (MEPS)^{27,40} and SPME^{38,45} have been used for the extraction of analytes from urine before CE or HPLC analysis. SPME is a well-known sampling technique which allows the simultaneous extraction and preconcentration of organic compounds. An important feature of SPME is its ability to perform extraction without the need to use organic solvents. When SPME is employed in association with gas chromatography, also desorption step can be carried out in absence of organic solvents. Moreover, the relative ease of online coupling to chromatographic system allows the entire analysis process to be automated^{64,65}.

In general, when analytes have to be assayed in complex matrices one of most critical point is represented by interfering species. Tandem mass spectrometry (MS/MS) is by now a recognized technique capable to minimize matrix interference, to obtain reconstructed chromatograms with well-defined chromatographic peaks and, at the same time, to hold unchanged the capability of analyte identification⁶⁶⁻⁶⁸.

The main objective of our work was to develop and validate a simple and rapid method for the analysis of dopamine, serotonin and norepinephrine in human urine by SPME-GC-MS/MS after a derivatization step with propyl chloroformate. The method can be made rapid and easy by a simple derivatization reaction carried out directly in urine sample and a following SPME

analysis in immersion mode in the same vial without use of toxic solvents and further sample treatment. Both derivatization and SPME analysis were optimized by the multivariate approach of “Experimental design”. Moreover, it was evaluated the ability of tandem mass spectrometry (GC-MS/MS) in multiple reaction monitoring (MRM) acquisition mode for the achievement of satisfactory values of validation parameters. This protocol constitutes the first approach for the determination of these important biomarkers using a gas chromatographic system SPME-GC approach.

3.1.1.2 Experimental

3.1.1.2.1 Materials

Dopamine (DA), serotonin (5-HT) and norepinephrine (NE) were purchased from Sigma-Aldrich (Milan, Italy). Dopamine-d₃ (DA-d₃), serotonin-d₄ creatinine sulfate complex (5-HT-d₄) and norepinephrine-d₆ (NE-d₆), used as internal standards, were bought from C/D/N Isotopes (Pointe- Claire, Quebec, Canada). Pyridine, sodium chloride and alkyl chloroformates were obtained from Sigma-Aldrich (Milan, Italy). The tested solid phase microextraction fibers were purchased from Supelco (Bellefonte, PA, USA) and conditioned as recommended by the manufacturer. Aqueous solutions were prepared using ultrapure water obtained from a Milli-Q plus system (Millipore, Bedford, MA). Synthetic urine (negative urine control) was obtained from Cerilliant (Round Rock, TE, USA).

3.1.1.2.2 Instrumentation and apparatus

GC-MS analyses were carried out using a TSQ Quantum GC (Thermo Fischer Scientific) system constituted by a triple quadrupole mass spectrometer (QqQ) Quantum and a TRACE GC Ultra equipped with a TriPlus autosampler. The capillary column was 30 m×0.25 mm i.d., 0.25 μm film thickness Thermo TR-5MS (95% polydimethylsiloxane, 5% polydiphenylsiloxane). The GC oven temperature was initially held at 70 °C for 2 min, then ramped at 16 °C min⁻¹ to 300 °C, and held at this temperature for 7 min. The carrier gas was helium at 1 ml min⁻¹ of purity 99.999% and argon at a pressure of 1.0 mTorr was used as collision gas. For SPME analyses, a Thermo PTV straight Liner 0.75mm × 2.75 mm × 105 mm was used as GC inlet liner. Analyses were performed in splitless mode and by setting the injector temperature at 300 °C. The QqQ mass spectrometer was operated in electron ionization (EI) in multiple reaction monitoring (MRM) mode. The transfer line and ionization source temperatures were set at 290 °C and 300

°C, respectively. The emission current was set at 25 μ A. The scan width and scan time were set at 1.0 m/z and 0.15 s for all segments. Peak width of Q1 was fixed at 0.7 amu. DA and NE signals were acquired in “Profile” mode whereas 5-HT was acquired in “Centroid” mode. Instrumental parameters used in EI-MS/MS acquisition are shown in Table 3.1.

Table 3.1 Retention times (r.t.) and electron ionization tandem mass spectrometry (EI-MS/MS) parameters (Collision energies (V) are indicated in parenthesis)

Compound	Retention time (r.t.)	MRM transition, m/z (collision energy, V)	
		Quantification	Identification
DA	16.80	178→136 (7)	239→136 (9)
5-HT	18.38	245→159 (8)	232→146 (12)
NE	19.20	225→139 (7)	225→183 (5)
DA-d3 (IS)	16.80	181→139 (7)	-
5-HT-d4 (IS)	18.36	249→163 (8)	-
NE-d6 (IS)	19.17	229→143 (7)	-

3.1.1.2.3 Samples

The urine samples were taken as aliquots from the 24-h urine specimens collected from five healthy volunteers (two female and three male) between the ages of 24 and 29 years and stored at – 4 °C until use.

3.1.1.2.4 Analytical procedure

Derivatization procedure was directly carried out in the vial (volume 10 ml) used for autosampler. 600 μ l of urine were spiked with a proper amount of internal standards solution, then 100 μ l of pyridine and 100 μ l of propyl chloroformate were added and the mixture was shaken for 15 min. Afterwards, 8 ml of ultrapure water was added. The vial was then crimped and SPME extraction was performed with 85 μ m polyacrylate (PA) fiber in immersion mode for 45 min at room temperature and the adsorbed analytes were thermally desorbed by introducing the fiber into the injector set at 300 °C for 15 min. A blank analysis has to be performed by using a water solution with derivatizing mixture and without analytes to verify if any peak corresponding to the compounds under investigation is present.

3.1.1.2.5 Calibration procedure

A six-point calibration curves were obtained by spiking ultrapure water with known amounts of analytes and internal standard to cover a concentration range of 10-1000 μ g l⁻¹ with 100 μ g l⁻¹ of

DA-d₃, 5-HT-d₄ and NE-d₆ as internal standards. Each experimental value corresponds to the average of three independent measurements. For DA and NE, a linear regression fit with a weighting factor 1/x was used.

3.1.1.2.6 Optimization of solid phase microextraction variables

The experimental matrix designs were carried out and evaluated using Statistica 8.0 (StatSoft 2007 Edition, Tulsa, USA).

3.1.1.3 Results and discussion

3.1.1.3.1 Derivatization and GC-QqQ-MS/MS analysis

Derivatization of aliphatic amino and phenolic moieties can be carried out in one step by alkyl chloroformates directly in aqueous solution^{59,69}. The formation of the corresponding alkoxy carbonyl compounds is affected by type and amount of alkylchloroformate and amount of pyridine (Figure 3.1).

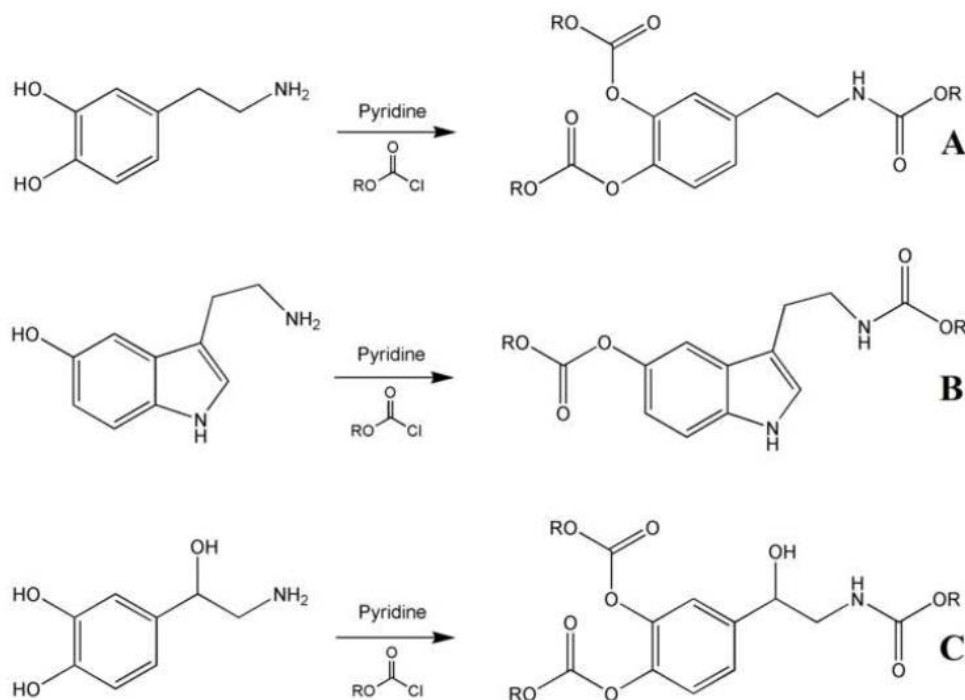


Figure 3.1 Reaction between DA (A), 5-HT (B) and NE (C) and the derivatizing agents (R = methyl, ethyl, propyl)

Preliminary experiments were performed by analyzing the organic extracts (methylene chloride as extraction solvent) containing the analytes derivatized with three alkyl chloroformate (methyl-, ethyl- and propyl-) in the same conditions (synthetic urine spiked at 5 mg l⁻¹, 200 µl of pyridine and 200 µl of alkyl chloroformate). The results obtained clearly showed that more abundant peak areas were obtained employing propyl chloroformate as derivatizing reagent. Three chromatographic peaks were assigned to the corresponding derivatized analytes whose EI mass spectra were shown in Figure 3.2.

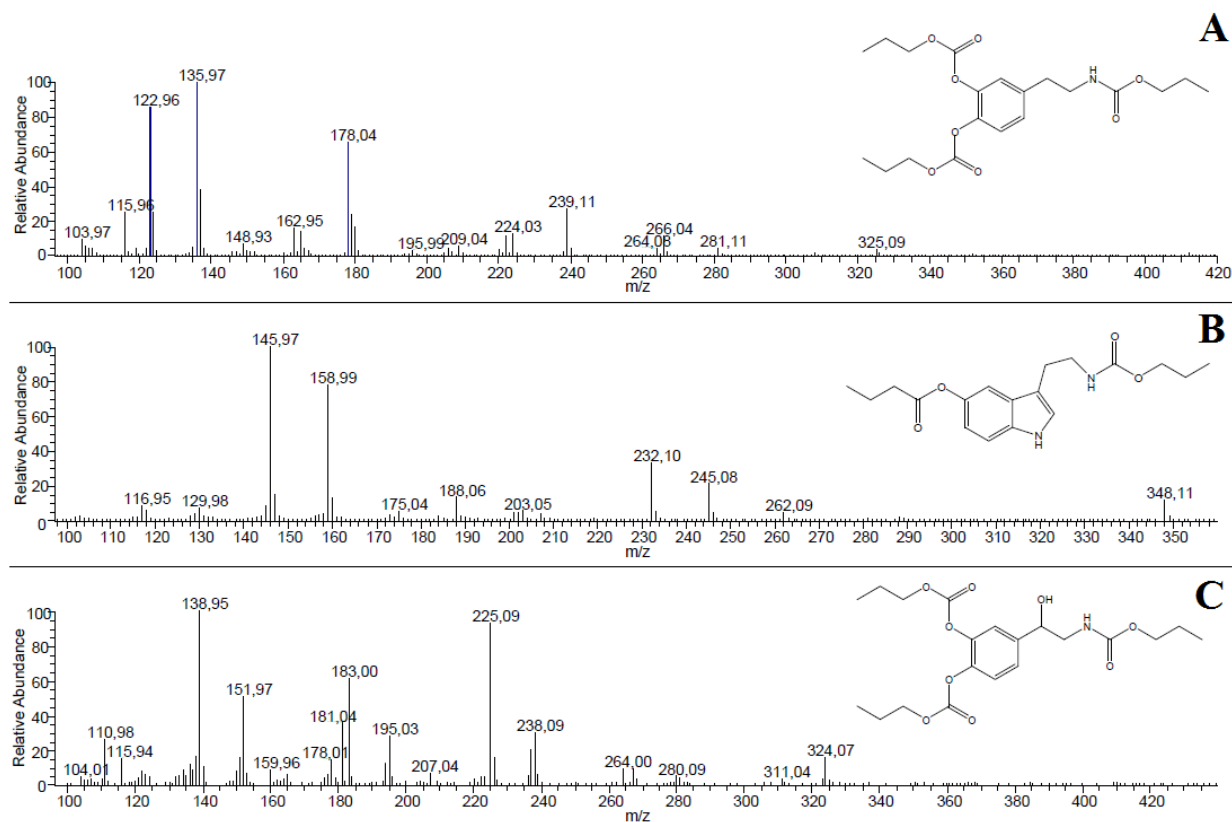


Figure 3.2 Electron ionization (EI) full-scan spectra of the derivatized analytes: DA (A), 5-HT (B) and NE (C)

Mass spectra were evaluated in order to identify without ambiguity the three derivatized analytes. The molecular ion of dopamine propyl derivative (m/z 411) is not present in the corresponding mass spectrum (Figure 3.2-A). The ions at m/z 325 and 239 are species probably obtained by the concerted loss of CH₃CH=CH₂ and CO₂ from the molecular ion and ion at m/z 325, respectively. The fragment at m/z 178 is due to the loss of two groups CH₃CH₂CH₂OCO and one group CH₃CH₂CH₂O from the molecular ion. Finally, the peak at m/z 136 (base peak)

could arise from the ion at m/z 239 by the loss of $\text{CH}_3\text{CH}_2\text{CH}_2\text{OCOO}$ group. The mass spectrum of serotonin derivative shows the molecular ion (m/z 348, Figure 3.2-B). The ions at m/z 262, 245 and 232 arise from the molecular ion by loss of $\text{CH}_3\text{CH}=\text{CH}_2$ and CO_2 , $\text{CH}_3\text{CH}_2\text{CH}_2\text{OCOO}$ group and $\text{CH}_3\text{CH}_2\text{CH}_2\text{OCONHCH}_2$ group, respectively. The base peak (m/z 146) is due to the loss of $\text{CH}_3\text{CH}_2\text{CH}_2\text{OCONHCH}_2$ from m/z 262. Norepinephrine propyl derivative produces a mass spectrum in which ions are generated similarly to dopamine and serotonin derivatives. The peak at m/z 324 arises from the ion at m/z 239 by the loss of $\text{CH}_3\text{CH}_2\text{CH}_2\text{OCOO}$ group and from this ion the concerted loss of $\text{CH}_3\text{CH}=\text{CH}_2$ and CO_2 produces the peak at m/z 238. The same fragmentation results are obtained for ions at m/z 225 and 139 which originate from m/z 311 and 325, respectively.

To acquire data in MRM mode, the parent ions have to be properly chosen to obtain the better compromise between sensitivity (ion with higher abundance) and specificity (ion with higher m/z ratio). According to this criterion, three precursor ions were tested for each analyte: m/z 325, m/z 239, m/z 178 for DA; m/z 348, m/z 245, m/z 232 for 5-HT; m/z 324, m/z 238, m/z 225 for NE. For each tested precursor ion, product ion spectra were acquired by collision-induced dissociation (CID) with argon applying collision energies from 7 to 16 V. The transition yielding the best S/N ratio for each analyte was selected for quantification and the second more sensitive transition was chosen for unambiguous identification of analytes and therefore for preventing false positives (Table 3.1). The use of two MRM transitions for the confirmation of analyte is in line with the European Commission Decision 2002/657/EC⁷⁰. To evaluate possible changes in sensitivity and specificity, for the selected MRM transitions ion currents were acquired both in centroid and profile mode. The results highlighted that an increase of tenfold in sensitivity of DA and NE was observed in profile mode, specificity being equal. On the other hand, a worse specificity was obtained in profile scan type for 5-HT. Therefore, the signals of DA and NE were acquired in profile mode whereas that of 5-HT was acquired in centroid mode.

As already mentioned, the derivatization of phenolic and amino moieties can be significantly affected by amount of pyridine and alkyl chloroformate. Therefore, the derivatization reaction has to be optimized in order to improve its efficiency and increase the sensitivity of analytical measurements. The optimization of these two variables was performed by the multivariate approach of the “Experiment design” which allows the influence of a predefined number of factors in a predefined number of experiments to be evaluated. A full factorial design with three

levels consisting of 3^2 experiments was performed in the range 100-500 μl for both variables (Table 3.2)

Table 3.2 Design matrix in the full factorial design with three levels for optimization of derivatization reaction

Exp	Pyridine (μl)	Propyl chloroformate (μl)
6	300	500
5	300	300
2	100	300
1	100	100
9	500	500
7	500	100
4	300	100
8	500	300
3	100	500

To find the optimal values for the two evaluated variables, response surfaces for each analyte were drawn (Figure 3.3).

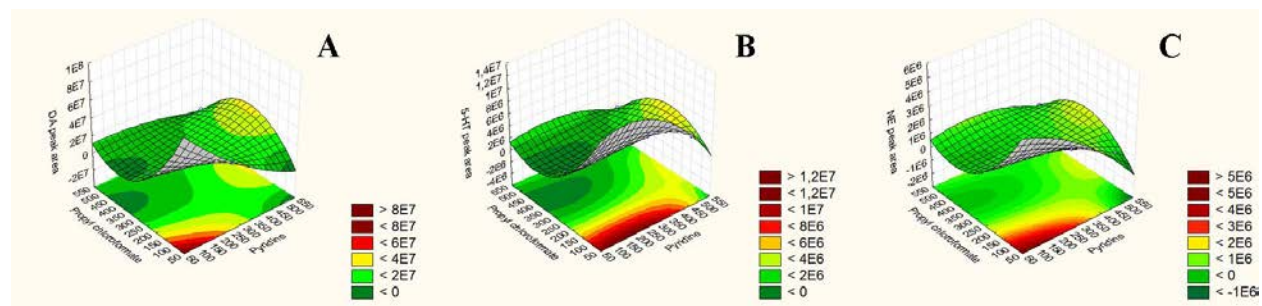


Figure 3.3 Response surfaces estimated from the full factorial design for amount of pyridine versus amount of propyl chloroformate: peak area of derivatized DA (A), derivatized 5-HT (B) and derivatized NE (C)

These graphs showed that a similar trend was obtained for each amine and therefore the optimal conditions are common to the three analytes (100 μl of both pyridine and propyl chloroformate).

3.1.1.3.2 Solid phase microextraction

As it is well-known from the literature, several variables can potentially affect the extraction efficiency of an SPME analysis⁶³. The use of a suitable fiber represents one of the most critical choices of the whole SPME procedure since the affinity of the analytes toward the fiber coating deeply influences the extraction efficiency. Therefore, in analogy with other studies^{60–62,66,67}, the extraction performances of five fibers (polydimethylsiloxane 100 μm (PDMS), polydimethylsiloxane/ divinylbenzene 65 μm (PDMS/DVB), carboxen/polydimethylsiloxane 85 μm (Car/PDMS), polyacrylate 85 μm (PA) and divinylbenzene/carboxen/ polydimethylsiloxane 55/30 μm (DVB/Car/PDMS)) were evaluated by univariate method sampling the analytes in immersion mode under the same condition (synthetic urine spiked at 1 mg L^{-1} , room temperature, extraction time 20 min, analysis acquired in MRM mode in the experimental conditions shown in Table 3.1). An overall evaluation of data showed that more abundant signals were clearly obtained performing analysis with PA fiber (Figure 3.4).

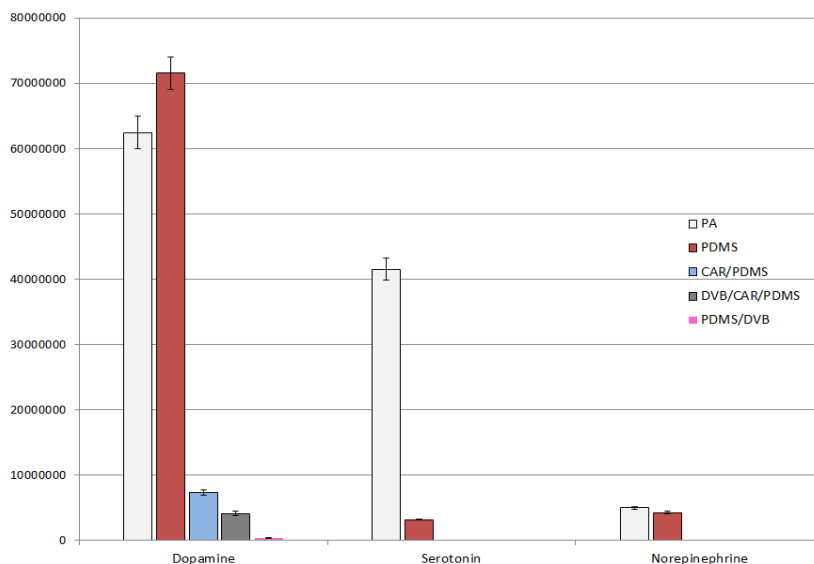


Figure 3.4 Peak areas for the three analytes obtained by performing analyses in immersion mode with five different fibers

According with these results, PA fiber was chosen for applying experimental design to obtain the best experimental conditions of SPME analysis. Desorption temperature, extraction temperature, extraction time and concentration (%) of sodium chloride have been taken in consideration as variables in experimental design. It was chosen to include desorption temperature in the

optimization process since the propyloxycarbonyl derivatives could behave as thermally labile compounds because of the presence of a carbamate moiety. pH was not taken into account since this variable does not significantly affect the extraction of non-ionic compounds. In order to estimate the linear effects, the interactions between pairs of variables and the quadratic effects, a central composite design (CCD) consisting of a 24 factorial design with six star points positioned at $\pm \alpha$ from the center of the experimental domain was performed. The axial distance α was chosen as 2 to establish the rotatability condition, i.e. uniform information in all direction was generated by design and a rotation of the design about the origin does not alter the variance contours. The complete design consisted of 30 randomly performed experiments, six of them in the central point ($24+(2 \times 4)+6$, design matrix was shown in Table 3.3).

Table 3.3 Design matrix in the central composite design (CCD) for optimization of SPME parameters

	Extraction Time (min)	Extraction Temperature (°C)	Desorption temperature (°C)
11	37.5	45	255
9	37.5	45	255
17	15.0	50	270
1	22.5	45	255
22	30.0	50	270
27 (C)	30.0	50	270
16	37.5	55	285
28 (C)	30.0	50	270
5	22.5	55	255
30 (C)	30.0	50	270
26 (C)	30.0	50	270
18	45.0	50	270
20	30.0	60	270
10	37.5	45	285
21	30.0	50	270
13	37.5	55	255
2	22.5	45	285
8	22.5	55	285
23	30.0	50	240
3	22.5	45	255
7	22.5	55	255
15	37.5	55	255
12	37.5	45	285
25 (C)	30.0	50	270
14	37.5	55	285
29 (C)	30.0	50	270
6	22.5	55	285
4	22.5	45	285
24	30.0	50	300
19	30.0	40	270

The ranges of the considered parameters were the following: 15-45 min for extraction time, 40-60°C for extraction temperature, 0-10 % of NaCl, 240-300 °C for desorption temperature. All the design analyses were performed under the same experimental condition used for the fiber screening. The influence of each variable investigated and possible cross-effect among these factors on the response can be evaluated by the Pareto chart. The bar lengths in these graphs are

proportional to the absolute value of the estimated effects and the factors having a significant effect on the response are those beyond the vertical line representing 95% of the confidence interval. Pareto charts obtained for the derivatized analytes were shown in Figure 3.5.

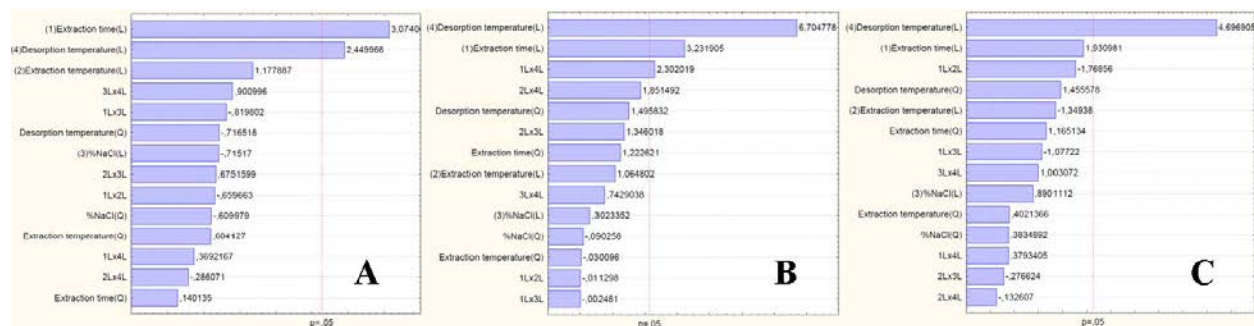


Figure 3.5 Pareto charts obtained from the central composite design for derivatized DA (A), derivatized 5-HT (B) and derivatized NE (C)

These diagrams showed that only linear coefficients of desorption temperature and extraction time were found to be significant for all analytes and their values are positive. This means that high values of these variables involve a significant increase of peak areas. In particular, the positive value of coefficient of desorption temperature indicates that no degradation process occurs in injector and therefore the rise of signals when the injector temperature was increased can be justified by a higher desorption of analytes from fiber. This phenomenon is more important for 5-HT and NE as it was demonstrated by the higher values of coefficient for these two analytes. On the other hand, the signal of analytes was not significantly affected by the presence of NaCl, extraction temperature and interaction terms. Whereas the temperature extraction is often found to be irrelevant for SPME analysis in immersion mode, in some ways the result regarding addition of NaCl is surprising. Indeed, the increase of ionic strength which often promotes a signal increase in this case does not provide significant variation of response and, therefore, there is no “salting out” effect for the derivatized analytes under investigation. To evaluate the trends of the most important factors (desorption temperature and extraction time), response surfaces for the three analytes were drawn in Figure 3.6.

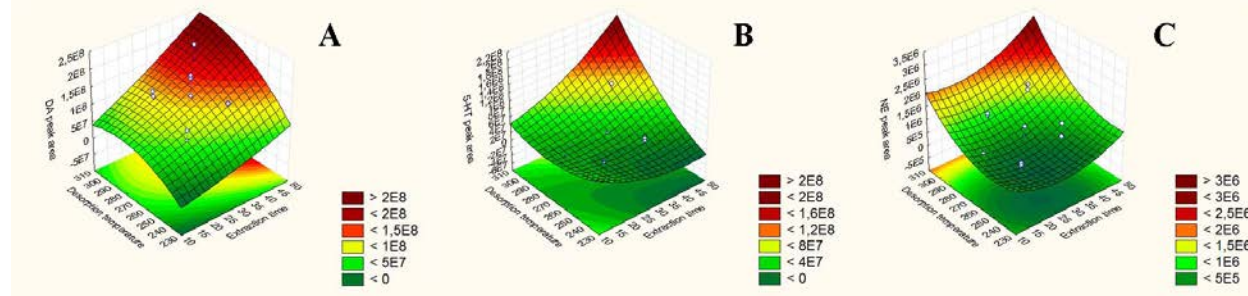


Figure 3.6 Response surfaces estimated from the central composite design for extraction time versus desorption temperature: peak area of derivatized DA (A), derivatized 5-HT (B) and derivatized NE (C)

The optimum working conditions which can be deduced by examining graphics (desorption temperature 300 °C and extraction time 45 min) confirm the observations based on the Pareto Chart. Therefore, in conclusion, the optimized conditions for the SPME analysis were the following: PA fiber, extraction time 45 min at room temperature, desorption temperature 300 °C, no addition of NaCl.

3.1.1.3.3 Analytical performances

The developed method was checked in terms of linearity under the SPME optimized conditions at a concentration range between 10 µg l⁻¹ and 1000 µg l⁻¹ with 100 µg l⁻¹ of each of the deuterated internal standard. Satisfactory linearities were obtained in the considered calibration ranges with correlation coefficient values > 0.99 for all the analytes (Table 3.4).

Table 3.4 Summary of calibration parameters, mean accuracies, relative standard deviations (RSD (%), in parentheses) and limits of detection (LODs) and limits of quantitation (LOQs) in multiple reaction monitoring (MRM) acquisition

Compound	Calibration Curve	R ²	30 µg l ⁻¹	200 µg l ⁻¹	800 µg l ⁻¹	LOD (µg l ⁻¹)	LOQ (µg l ⁻¹)
DA	y=0.01316x+0.01199	0.9995	98.8 (0.97)	96.0 (1.4)	99.4 (0.85)	0.59	0.81
5-HT	y=0.01833x+0.06445	0.9999	97.7 (2.0)	92.8 (0.67)	93.9 (1.4)	0.38	0.74
NE	y=0.00679x+0.02581	0.9987	103.0 (4.5)	102.8 (2.1)	96.5 (0.97)	13.5	21.3

Accuracy and precision between run have been evaluated at three concentration levels (30, 200 and 800 $\mu\text{g L}^{-1}$) by analyzing spiked synthetic urine samples three times every day along a week. Very good values were obtained for both parameters since accuracy were in the range between 92.8 and 103.0% whereas RSD values ranged between 0.67 and 4.5% (Table 3.4). The limit of detection (LOD) and the limit of quantitation (LOQ) were calculated following the directives of IUPAC and the American Chemical Society's Committee on Environmental Analytical Chemistry i.e. the signal at the LOD and the signal at the LOQ are equal to the signal of the reagent blank plus three and ten times the standard deviation for the reagent blank, respectively. The LOD and LOQ values achieved by the proposed method are satisfactory (Table 3.4) because are lower or comparable to those that have been reported in recent literature, even though an eleven-fold dilution of the sample was performed. These results indicate that the proposed method is suitable for the analysis of urine samples that might contain concentrations of DA, 5-HT and NE that are much smaller than those found in healthy adults (65-400 $\mu\text{g L}^{-1}$ for DA, 25-180 $\mu\text{g L}^{-1}$ for 5-HT and 15-80 $\mu\text{g L}^{-1}$ for NE¹⁶). The reliability of developed method was also tested in terms of matrix effect (ME). This phenomenon is a very important aspect above all in the LC-MS analysis of environmental and biological samples that can significantly affect the quantitative analysis. In many cases, if the ME was not overcome the use of the standard addition method is required to achieve acceptable results. The ME was assessed using the method described by Matuszewski et al.⁷¹. Briefly, five raw natural urine samples collected by donors were divided into two aliquot. The first one of each sample was spiked only with 100 $\mu\text{g L}^{-1}$ of internal standards and analyzed as it is (blank sample). The second aliquot was spiked with internal standards and analytes both at 100 $\mu\text{g L}^{-1}$. All samples were analyzed in triplicate accordingly to the final protocol reported in analytical procedure section. The matrix effect was calculated accordingly to Wick et al.⁷² as the percental ratio of the analyte peak area in the spiked sample (A_{spike}) subtracted by the peak area in the non-spiked blank sample (A_{blank}) to the peak area in a non-enriched external standard (A_{std}):

$$ME = \left(\frac{A_{\text{spike}} - A_{\text{blank}}}{A_{\text{std}}} \right) \times 100 \quad (3.1)$$

The ME values obtained showed that no significant matrix effect is present for DA (102%) whereas signal suppression occurs for 5-HT and NE (54% and 55%, respectively). To evaluate the capability of deuterated internal standards to balance matrix effects, the ratio between analytes peak area and internal standards peak area was considered in calculating the matrix effect accordingly to above- mentioned equation. Indeed, if the matrix effect is similar for both analyte and internal standard in all samples the areas ratios should not be affected and therefore the signal reduction should be compensated. In comparison to the previous ME values, the use of internal standards resulted in a noticeable correction of the matrix effect since the values obtained were 93% and 89% for 5-HT and NE, respectively.

3.1.1.3.4 Application to real samples

The applicability of the method to real human urine samples was evaluated by the determination of the target analytes according to the developed protocol in five urine samples (three males and two females) from healthy individuals. Each sample was analyzed in triplicate in accordance with the procedure described in “Experimental” section (a typical chromatogram was shown in Figure 3.7).

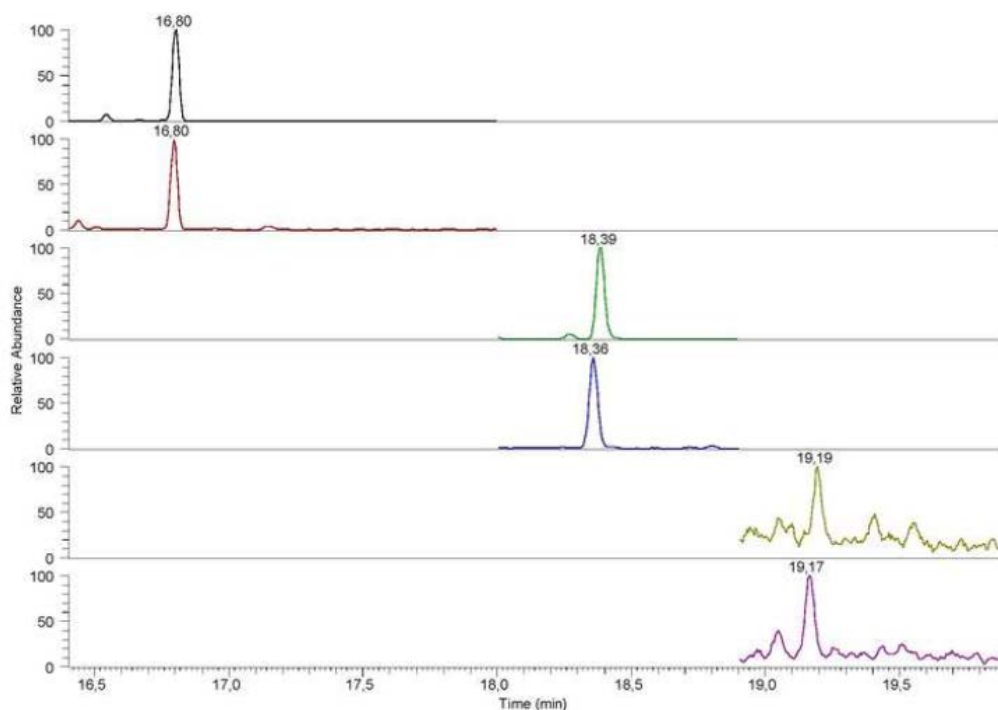


Figure 3.7 SPME-GC-QqQ-MS (MRM acquisition mode) chromatogram of a real urine sample from an healthy individual (r.t. 16.80 DA; 16.80 DA-d₃; 18.39 5-HT; 18.36 5-HT-d₄; 19.19 NE; 19.17 NE-d₆)

The mean values of the concentration of DA, 5-HT and NE were 296, 152 and 63.7 $\mu\text{g l}^{-1}$, respectively, with minimum and maximum values of 216 and 420 $\mu\text{g l}^{-1}$ for DA, 131 and 196 $\mu\text{g l}^{-1}$ for 5-HT, 32.4 and 81.6 $\mu\text{g l}^{-1}$ for NE. The concentrations obtained are in good agreement with the range of normal values in 24 h-human urine¹⁶. To evaluate the applicability of the method to abnormal urine samples, the determination of the target analytes was carried out by assaying the markers naturally present in five real urines from healthy individuals and then spiking the same samples with the analytes at 400 $\mu\text{g l}^{-1}$. These fortified samples were analyzed in triplicate and the values obtained (91.8% for DA, 94.4% for 5-HT and 83.6% for NE) demonstrated that the method is also applicable to samples obtained from diseased individuals.

3.1.1.4 Conclusions

A novel method for a rapid and simple quantification of dopamine, serotonin and norepinephrine in human urine was developed by SPME-GC-QqQ-MS/MS analysis after a preliminary derivatization using propyl chloroformate. The variables influencing the formation of the

corresponding alkoxy carbonyl compounds were reliably optimized by the multivariate approach of “Experimental design” and the derivatized compounds thus formed were extracted by SPME in immersion mode. The commercially available SPME fibers were tested and the optimization of the other parameters affecting the SPME process was again achieved using the experimental design. The present work demonstrated that the combination of alkylchloroformate and SPME represents a convenient approach in the identification and assay of these amines by an easy and automated method involving a minimal handling of sample and no consumption of toxic and not environmentally friendly organic solvents for the extraction of the analytes. Indeed, compared with the longer and more complicated procedures of the published methods, the extraction was directly performed by autosampler in the same vial in which urine sample was put and a rapid and simple derivatization (addition of few microliters of pyridine and propyl chloroformate, 15 min, room temperature) was conducted. Moreover, GC analysis were carried out for the first time using a GC-QqQ-MS instrument in MRM acquisition which has allowed to obtain reconstructed chromatograms with well-defined chromatographic peaks and to achieve high specificity through the selection of appropriate precursor-product ion couples improving the capability in analyte identification. Finally, an overall evaluation in terms of linearity, accuracy, precision and sensitivity shows that the proposed method can represent a suitable tool for epidemiological studies concerning stress pathologies and for clinical diagnosis and treatment of tumors related to the production of these biomarkers.

3.1.2 Simultaneous assessment of benzothiazoles, benzothiazoles and sulfonamides concentration in environmental and biological matrices: development of an high-throughput and reliable SPME-GC-QqQ-MS method

3.1.2.1 Introduction

In recent years, raising concern towards emerging pollutants such as biocides, personal care products and corrosion inhibitors, has become a norm in societies, since their concentration in the environment is increasing due to human activities⁷³. In particular, assessing the contamination of water resources and exposure of humans to these anthropogenic substances is an important and demanding target. Benzotriazoles (BTRs) and benzothiazoles (BTHs) are extensively employed in various industrial and household applications and BTRs have already been classified as emerging pollutants and toxic to aquatic organisms^{73,74}. The main representative compounds of BTRs are 1H-benzotriazole and tolyltriazole i.e. a mixture of 4-methylbenzotriazole and 5-methylbenzotriazole. BTRs are widely used as additives in different processes, principally as corrosion inhibitors, UV stabilizer for plastics and in photography, antifreeze liquids and industrial cooling system⁷⁵⁻⁷⁷. BTHs also are used as corrosion inhibitors and as biocides in paper, lumber and leather industry. Moreover, BTHs are added to antifreezes and cooling liquids and are employed as vulcanizations accelerators and in the production of azo dyes⁷⁸⁻⁸¹. Benzosulfonamides have widespread applications as plasticizers, fungicides and intermediates in the synthesis of pesticides, drugs, sweeteners and dyes⁸²⁻⁸⁴.

Many studies have been reported for the determination of BTRs and BTHs in different waters such as drinking water, rivers, lakes, ground water and wastewaters^{72,74,76-81,85-97}. The majority of these methods are based on high-performance liquid chromatography (HPLC) coupled to mass spectrometry (MS)^{76,78,85,96} or mass spectrometry in tandem acquisition mode (LC-MS/MS)^{72,86,89,91-95} and in fewer cases on gas chromatography (GC)-MS^{74,77,79,80,89,90,97}. Recently, Ying et al. described the determination of BTRs in environmental waters and biosolid samples by GC-MS/MS analysis following a preliminary solid phase extraction (SPE) and pressurized liquid extraction (PLE) step for liquid and solid samples, respectively⁹⁸. Moreover, for the first time an LC-MS/MS method was developed and applied for the quantification of BTRs and BTHs in human urine⁹⁹. Very few studies have been published about the quantification of benzosulfonamides in water and aqueous media^{74,100,101} and, in particular, only one of them is based on gas chromatography technique⁷⁴. Generally, the determination of BTRs and BTHs by

liquid chromatography suffers from some drawbacks because ionic suppression or enhancement in electrospray ion sources can occur due to the organic matter co-extracted in complex aqueous matrices. Indeed, in most of these methods quantification requires use of standard addition procedure. On the other hand, some disadvantages can be related to interfering species also in GC-MS approach even in single ion monitoring because of low mass of the diagnostic ions. Tandem mass spectrometry represents a widely employed technique since MS/MS acquisition increases the sensitivity of analytical method by significantly diminishing the noise and holds unchanged the capability of analyte identification, even in analysis of samples derived from complex matrices^{102,103}. In particular, the triple quadrupole analyzer (QqQ) allows quantitative analysis by operating in multiple reaction monitoring (MRM) acquisition i.e. by selecting a precursor-product ion couples for each target compounds. GC is more widely used in pollutants analysis due to its ease of operation and high separation efficiency. This chromatographic technique in conjunction with triple quadrupole mass spectrometry (GC-QqQ-MS) represents a reliable analytical tool since very satisfactory sensitivity and specificity can be achieved.

The majority of the cited LC and GC approaches provide a solid phase extraction (SPE) step as sample preparation procedure. Since the use of more efficient and environmental friendly extraction methods is increasingly required, in the last years, several microextraction techniques were applied to the determination of different pollutants. Despite this, in only one study microextraction approach (dispersive liquid-liquid microextraction, DLLME) was used to extract BTRs and BTHs from water samples⁹⁴. Solid phase microextraction (SPME) is a microextraction technique which allows the simultaneous extraction and preconcentration of organic compounds. Since its introduction, SPME has gained popularity as a simple, solvent-free, reliable and flexible tool for the sampling of several analytes. Moreover, SPME allows high enrichment factors in the concentration of a variety of volatile and semivolatile compounds and minimizing the sample volume needed compared to solid phase extraction or liquid-liquid extraction. The combined use of SPME and a GC-QqQ-MS system has already allowed developing simple and very sensitive methods for the assay of pollutants, biomarkers and trace food components in aqueous matrices^{61-63,67,68}.

The main objective of the present work was to develop a rapid and versatile method for the simultaneous analysis of BTRs, BTHs and benzosulfonamides by SPME-GC-QqQ-MS in environmental waters and human urine. The joined use of SPME technique and the triple

quadrupole mass spectrometer in multiple reaction monitoring (MRM) acquisition mode was evaluated to achieve a very simple automated method without the need for time consuming step and use of toxic solvents prior to instrumental analysis. Moreover, tandem mass spectrometry was used to obtain a high specific protocol capable of unequivocal identification assay of analytes. The commercially available SPME fibers were tested and the variables affecting the SPME process were optimized by the multivariate approach of “Experiment design”. To the best of our knowledge, there has been no report on the determination of BTRs, BTHs and benzenesulfonamides using SPME and, furthermore, GC-MS/MS approach has never been applied to the analysis of BTHs and benzenesulfonamides in any matrix.

3.1.2.2 Experimental section

3.1.2.2.1 Materials

All analytes [Benzothiazole (BTH), 2-methylbenzothiazole (2-MeBTH), 2-(methylthio)benzothiazole (2-MeSBTH), 2-aminobenzothiazole (2-NH₂BTH), 2-hydroxybenzothiazole (2-OHBTH), 2-mercaptobenzothiazole (2-SHBTH), benzotriazole (BTR), 4-methyl-1H-benzotriazole (4-MeBTR), 5-methyl-1H-benzotriazole (5-MeBTR), 5-chlorobenzotriazole (5-CIBTR), 5,6-dimethyl-1H-benzotriazole (5,6-MeMeBTR), benzenesulfonamide (BSA), p-toluenesulfonamide (p-TSA) and N-ethyl p-toluenesulfonamide (N-Et-p-TSA)] and sodium chloride were purchased from Sigma-Aldrich (Milan, Italy). Benzotriazole-d₄ (BTR-d₄) and p-toluenesulfonamide-d₄ (p-TSA-d₄), used as internal standards, were bought from Sigma-Aldrich and C/D/N Isotopes (Pointe-Claire, Quebec, Canada), respectively. The tested solid phase microextraction fibers were purchased from Supelco (Bellefonte, PA, USA) and conditioned as recommended by the manufacturer. Aqueous solutions were prepared using ultrapure water obtained from a Milli-Q plus system (Millipore, Bedford, MA). The certified reference material “Wastewater” was bought from RTC International (Laramie, WY, USA). Synthetic urine (negative urine control) was obtained from Cerilliant (Round Rock, TE, USA).

3.1.2.2.2 Instrumentation and apparatus

GC-MS analyses were performed using a TSQ Quantum GC (Thermo Fischer Scientific) system constituted by a triple quadrupole mass spectrometer (QqQ) Quantum and a TRACE GC Ultra equipped with a TriPlus autosampler. The capillary column was 30 m × 0.25 mm i.d., 0.25 μm

film thickness Thermo TR-5MS (95% polydimethylsiloxane, 5% polydiphenylsiloxane). The GC oven temperature was initially held at 65 °C for 1 min, then ramped at 10 °C min⁻¹ to 240 °C, then ramped at 50°C min⁻¹ to 290 °C and held at this temperature for 3 min. The carrier gas was helium at 1 ml min⁻¹ of purity 99.999% and argon at a pressure of 1.0 mTorr was used as collision gas. For SPME analyses, a Thermo PTV straight Liner 0.75 mm × 2.75 mm × 105 mm was used as GC inlet liner. Analyses were performed in splitless mode and by setting the injector temperature at 290 °C. The QqQ mass spectrometer was operated in electron ionization (EI) in multiple reaction monitoring (MRM) mode. The transfer line and ionization source temperatures were set at 280 °C and 250 °C, respectively. The emission current was set at 25 μA. The scan width was set at 1.2 m/z for all segments. Peak width of Q1 was fixed at 0.7 amu. All signals were acquired in “Profile” mode. Instrumental parameters used in EI-MS/MS acquisition are shown in Table 3.5.

Table 3.5 Retention time (RT) and electron ionization tandem mass spectrometry (EI-MS/MS) parameters (Collision energies (eV) are indicated in parenthesis).

Compound	Retention time (RT)	Scan time (s)	SRM transition, m/z (collision energy, V)	
			Quantification	Identification
BTH	7.85	0.4	108→69 (20)	108→82
2-MeBTH	8.77	0.4	108→69 (22)	108→82
BTR	11.11	0.1	119→64 (16)	119→91
4-MeBTR	11.87	0.1	133→104 (10)	133→77
BSA	12.15	0.1	157→93 (7)	157→141
5-MeBTR	12.40	0.1	133→104 (10)	133→77
2-MeSBTH	12.74	0.1	181→148 (8)	181→136
2-NH ₂ BTH	12.80	0.1	150→96 (22)	150→123
p-TSA	13.52	0.1	171→91 (16)	171→106
5-CIBTR	13.52	0.1	155→91 (9)	155→109
2-OHBTH	13.64	0.1	151→96 (20)	151→123
N-Et-p-TSA	13.98	0.1	199→155 (10)	199→91
5,6-MeMeBTR	14.07	0.1	147→118 (9)	147→132
2-SHBTH	16.80	0.5	167→123 (12)	167→109
p-TSA-d4 (IS)	13.49	0.1	175→95 (16)	-

3.1.2.2.3 Samples

Five tap water samples were collected from public water supply of Rende (CS, Italy) after flowing for 5 min. Surface water samples were collected at three local rivers sited in Cosenza's City great urban area (CS, Italy) in July 2013. In particular, Campagnano, Crati and Busento were considered. The samples were filled into glass bottles (1 l), stored under refrigerated conditions (4 °C) and then analyzed without any previous treatment. Urban effluent samples were collected in Pizzo Calabro (VV, Italy), Rende (CS, Italy) and Cosenza (CS, Italy). Raw wastewater samples were simulated by spiking the certified reference material "Wastewater" with known amounts of analytes. These samples were filtrated through 0.45 µm filters before the analysis. Urine samples were taken as aliquots from the 24-h urine specimens collected from six healthy volunteers (three females and three males) of age ranging from 23 to 29 years old. All urine samples were collected and stored at -20 °C until analysis.

3.1.2.2.4 Analytical procedure

0.800 g of NaCl was directly weighted in the vial used for autosampler and an amount of real sample was added on the basis of the kind of matrix (8 ml of tap and river water, 1.60 ml of wastewater and 1.33 ml of urine). Afterwards, 0.4 ml of potassium dihydrogen phosphate/dipotassium hydrogen phosphate buffer was added in order to buffer the sample matrices at pH of 9. Also, only for urine and wastewater samples an appropriate volume of ultrapure water to achieve 8 ml as total volume was added. Finally, 80 µl of internal standards solution at 20 µg l⁻¹ were added, the vial was crimped and the solution was stirred to dissolve the salt. SPME extraction was performed with a 85 µm PA (polyacrylate) fiber in direct immersion mode for 45 min at room temperature and the extracted analytes were thermally desorbed by introducing the fiber into the injector set at 290 °C for 10 min.

3.1.2.2.5 Calibration procedure

A six-point calibration curves were obtained by spiking ultrapure water with known amounts of analytes and internal standard to cover a concentration range of 1-100 µg l⁻¹ with 20 µg l⁻¹ of p-TSA-d4 as internal standard. Each experimental value corresponds to the average of three independent measurements.

3.1.2.2.6 Optimization of solid phase microextraction variables

The experimental matrix designs were carried out and evaluated using Statistica 8.0 (StatSoft 2007 Edition, Tulsa, USA).

3.1.2.3 Results and discussion

3.1.2.3.1 GC-QqQ-MS/MS analysis

The presence of significant interferences when BTRs, BTHs and benzosulfonamides are analyzed by GC-MS in TIC or SIM mode in wastewater and in river water was well demonstrated by Jover *et al.*⁷⁴. In this work, a notable overestimation was observed when working with a non-selective detector, as mass spectrometer in full scan mode, above all for more complex matrix like wastewater. However, even if analyses were carried out by a GC-MS system in SIM mode, overestimation can reach 250% in wastewater samples and 79% in river samples. This demonstrates that a more specific analytical approach is necessary to minimize interferences and then improve the reliability of the entire method. The GC-QqQ-MS system represents a trustworthy analytical tool because of the high separation efficiency of gas chromatographic technique and the great sensitivity and specificity of triple quadrupole analyzer in MRM acquisition mode are simultaneously available. To perform analysis in MRM mode, the parent ions have to be properly selected to obtain the better compromise between sensitivity (ion with higher abundance) and specificity (ion with higher m/z ratio). According to this criterion, three precursor ions were tested for each analyte and for each one product ion spectra were acquired by collision-induced dissociation (CID) with argon applying collision energies from 5 to 25 V. The transition yielding the best S/N ratio for each analyte was chosen for quantification and the second more sensitive transition was selected for preventing false positives by an unambiguous identification of analytes (Table 3.5). The use of two MRM transitions for the confirmation of analyte is in line with the European Commission Decision 2002/657/EC.⁷⁰

To evaluate how sensitivity and specificity changed depending on the acquisition mode of ion current, for the selected MRM transitions signals were obtained both in centroid and profile mode. The results highlighted that a significant increase in sensitivity was observed in profile mode for all analytes, specificity being equal and, therefore, this acquisition mode was selected for all the further data collecting.

3.1.2.3.2 Solid phase microextraction

SPME is a simple extraction technique based on the affinity between analytes and the specific polymeric material coating and, therefore, the choice of the more suitable coating represents one of the most critical steps of the entire SPME procedure. In analogy with other studies^{61-63,67,68}, the extraction efficiency of five fibers (polyacrylate 85 μm (PA), carboxen/polydimethylsiloxane 85 μm (Car/PDMS), divinylbenzene/carboxen/polydimethylsiloxane 50/30 μm (DVB/Car/PDMS), polydimethylsiloxane/divinylbenzene 65 μm (PDMS/DVB) and polydimethylsiloxane 100 μm (PDMS)) were evaluated by univariate method sampling the analytes in immersion mode under the same condition (water spiked at 1 mg l⁻¹, room temperature, extraction time 30 min). An overall evaluation of obtained peak areas showed that only PA fiber is capable to extract all analytes (Figure 3.8).

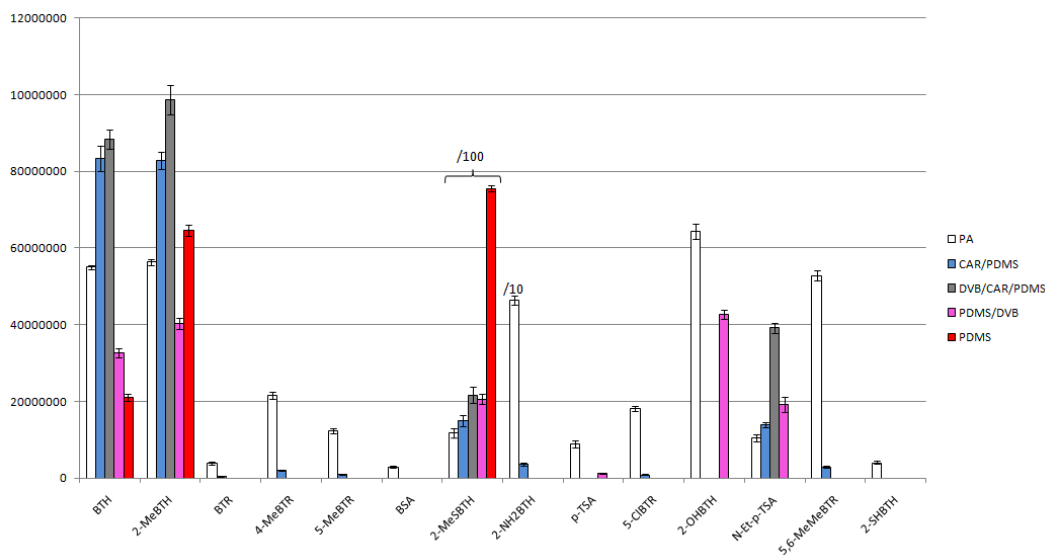


Figure 3.8 Peak areas obtained by performing analyses in immersion modes with five different fibers. PA, polyacrylate; Car/PDMS, (carboxen/polydimethylsiloxane); DVB/Car/PDMS, (divinylbenzene/ carboxen/ polydimethylsiloxane); PDMS/DVB, (divinylbenzene/ polydimethylsiloxane) and PDMS, polydimethylsiloxane.

In particular, BTRs are adsorbed only by PA and Car/PDMS fibers whereas 2-OHBTBTH and p-TSA are extracted by PA and PDMS/DVB fibers. Finally, the extraction of 2-SHBTH and BSA can be carried out exclusively by PA fiber. These results are not surprising given the hydrophilic

character of these analytes that can be deduced from their octanol-water partition coefficients ($\log K_{OW}$).⁷⁴

According to the results shown in Figure 3.8, PA fiber was chosen and used for optimizing the other variables affecting SPME analysis. Considering the literature⁶⁴ several variables can potentially influence extraction efficiency. In this work, extraction time, extraction temperature, pH and percentage of sodium chloride has been considered as variables and the optimization of the experimental conditions of SPME analysis were carried out by the multivariate approach of “Experimental design”. A central composite design (CCD) was employed to determine the optimal conditions for these four factors because the CCD design allows the linear effects, the interactions between pairs of variables and the quadratic effects to be estimated. In particular, a CCD consisting of a 2^4 factorial design with six star points positioned at $\pm\alpha$ from the center of the experimental domain was carried out. The axial distance α was chosen with a value of 2.0 in order to fulfill the rotatability condition i.e. the design generates information uniformly in all directions. The design was completed with six experiments in the central point so that the number of degrees of freedom for the lack-of-fit equals that for replications. Therefore, the complete design consisted of 30 (i.e. $2^4 + (2 \times 4) + 6$) experiments. The range for each selected parameter was determined by preliminary tests and, in according to these experiments, extraction time of 15-45 min, extraction temperature in the range 40-60 °C, pH 2-10 and concentration of NaCl 0-10 % were chosen. All the experiments of the design matrix (Table 3.6, fully randomized) were carried out in MRM acquisition mode using a water sample spiked at $100 \mu\text{g l}^{-1}$.

Table 3.6 Design matrix of central composite design (CCD) for optimization of SPME parameters.

Exp	Extraction time (min)	Temperature extraction (°C)	pH	%NaCl
24	30.0	50.0	6.0	10.0
21	30.0	50.0	2.0	5.0
1	22.5	45.0	4.0	2.5
3	22.5	45.0	8.0	2.5
23	30.0	50.0	6.0	0.0
13	37.5	55.0	4.0	2.5
16	37.5	55.0	8.0	7.5
6	22.5	55.0	4.0	7.5
14	37.5	55.0	4.0	7.5
15	37.5	55.0	8.0	2.5
20	30.0	60.0	6.0	5.0
12	37.5	45.0	8.0	7.5
10	37.5	45.0	4.0	7.5
7	22.5	55.0	8.0	2.5
9	37.5	45.0	4.0	2.5
17	15.0	50.0	6.0	5.0
5	22.5	55.0	4.0	2.5
2	22.5	45.0	4.0	7.5
11	37.5	45.0	8.0	2.5
26 (C)	30.0	50.0	6.0	5.0
27 (C)	30.0	50.0	6.0	5.0
28 (C)	30.0	50.0	6.0	5.0
19	30.0	40.0	6.0	5.0
29 (C)	30.0	50.0	6.0	5.0
4	22.5	45.0	8.0	7.5
22	30.0	50.0	10.0	5.0
25 (C)	30.0	50.0	6.0	5.0
8	22.5	55.0	8.0	7.5
30 (C)	30.0	50.0	6.0	5.0
18	45.0	50.0	6.0	5.0

The Pareto charts were considered to determine the weight of contribution of each factor to response and possible cross-effect among these variables (diagrams of all analytes are shown in Figure 3.9).

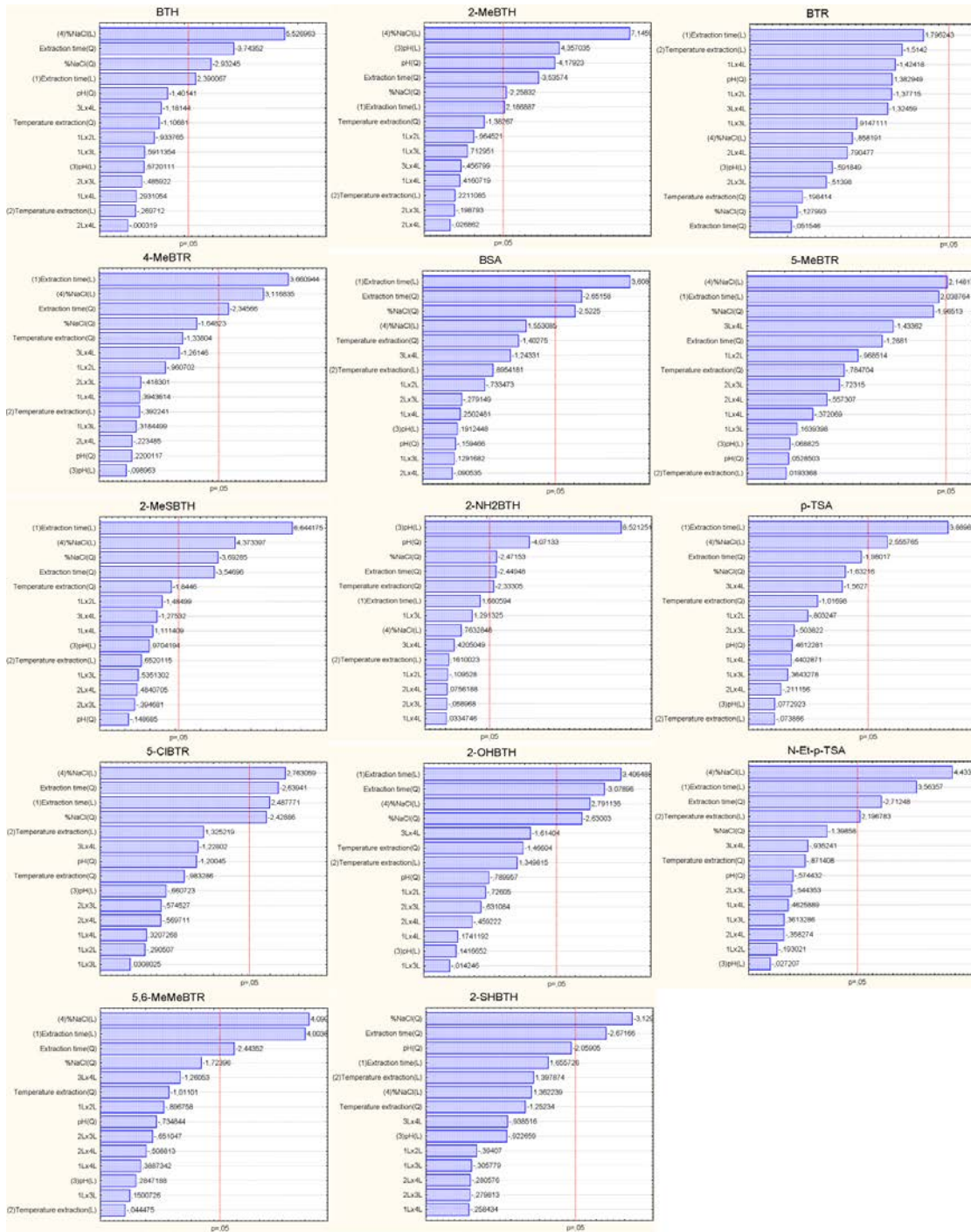


Figure 3.9 Pareto charts obtained from the central composite design for all the investigated analytes

The bar lengths in Pareto charts are proportional to the absolute value of the estimated effects and the vertical line represents 95% of the confidence interval. An effect exceeding this reference line may be considered significant with regard to the response. In general, linear coefficients of extraction time and percentage of NaCl were found to be notably significant for all analytes except BTR and 5-MeBTR and the effects are positive. Moreover, for the majority of the analytes the quadratic term of percentage of NaCl is statistically significant and the sign of coefficient is negative indicating a presence of a maximum in the trend of signal as function of % NaCl. This result could be explained by two opposite factors: i) the classic “salting out” effect that is significant up to about 6%; ii) the variation of activity coefficients that leads to a decrease of the repartition coefficients $K_{\text{coating/solution}}$ when very polar analytes are involved and the concentration of salt is high (in our case percentage greater than about 6%)¹⁰⁴. The linear and quadratic coefficients of pH with positive and negative sign, respectively, were highly significant for the response of 2-NH₂BTH and 2-MeBTH whereas the only quadratic coefficient was close to significance for 2-SHBTH. These results can be easily explained for 2-NH₂BTH and 2-SHBTH given the functional groups with well-known acidic/basic properties. The behavior of 2-MeBTH towards pH variations can be also related to its acid/basic equilibria in aqueous phase at low pH values. This compound, because of the inductive effect of the methyl moiety, bears a higher pK_a value compared to BTH (3.81 and 2.44 respectively) and the concentration of its neutral form (exclusively extracted by the coating) increases critically in the experimental range tested till reaching stability at pH values higher than pK_a+2. The trends of the most important factors for each analytes can be evaluated by the response surfaces shown in Figure 3.10.

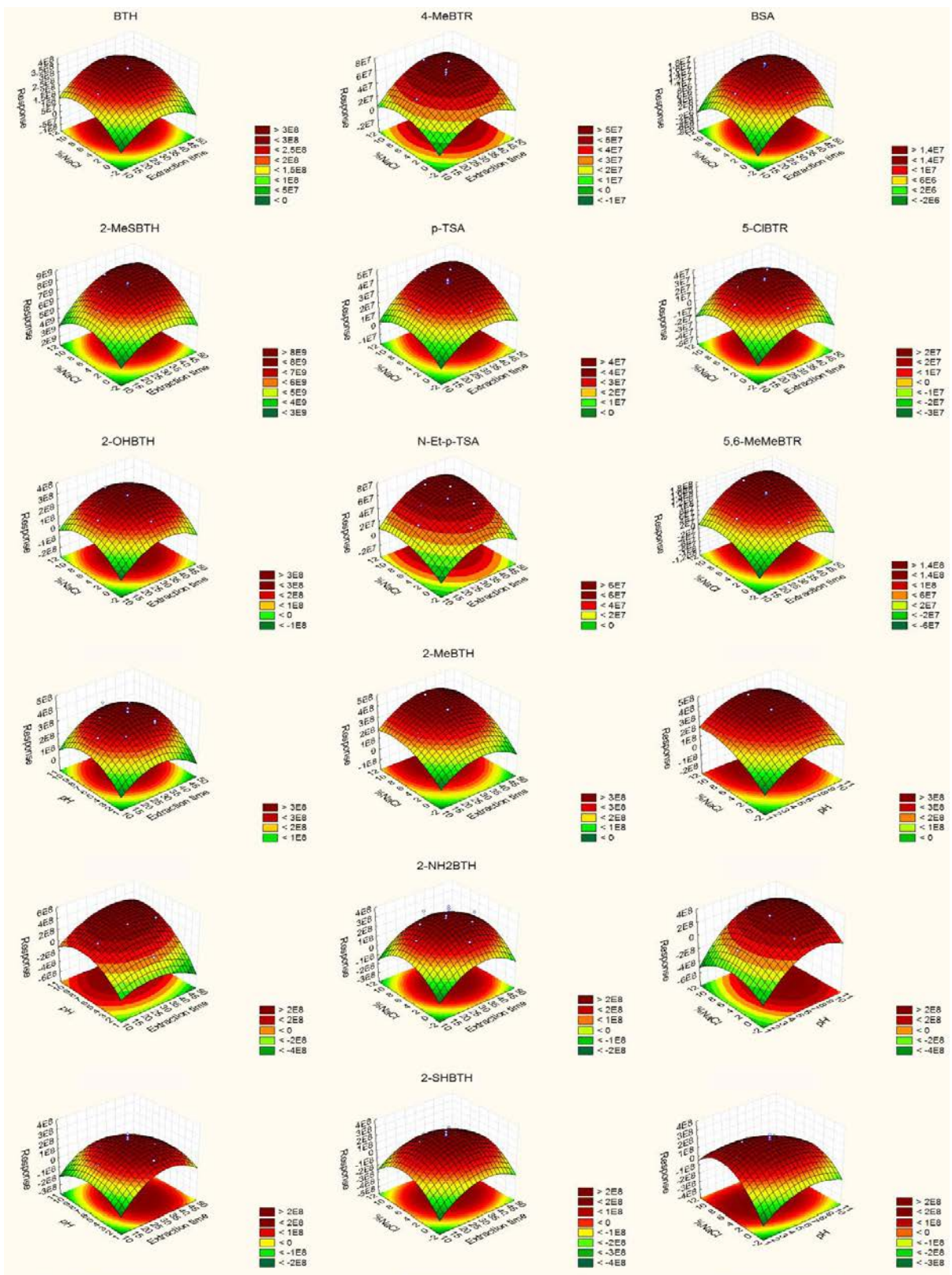


Figure 3.10 Response surfaces estimated from the central composite design

Since the compounds of interest bear a variety of functionalities and physical-chemical properties, the optimum working conditions will differ significantly between them. For this reason it is reasonable setting the system at proper conditions that will lead to the achievement of a compromise among the responses of all the analytes considered. For this purpose, the Derringer's desirability function is proposed in order to convert a multi-response problem into a single-response one.¹⁰⁵ According to this approach, the response is converted into a particular desirability function (d_i) that varies from 0 to 1. Maximum or a fully desired response has the desirability 1 whereas desirability 0 is for non-desirable situations or minimum. The single desirability scores for the predicted values and for each dependent variable are then combined into an overall desirability function D by computing their geometric means of different d_i values:

$$D = \sqrt[n]{d_1^{p_1} \times d_2^{p_2} \times d_3^{p_3} \times \dots \times d_n^{p_n}} \quad (3.2)$$

where p_i is the weight of the response, n is the number of responses and d_i is the individual desirability function of each response. Since the response of each analyte was considered equally important in the overall desirability function, equal weights were given to the responses, i.e. $p_1 = p_2 = p_3 = 1$. The optimum working conditions in terms of desirability score were achieved at the following values: 6.0 % NaCl, extraction time 40 min, pH 7.1, extraction temperature 40.6 °C. Since the extraction temperature do not significantly affects the responses for all the analytes considered, we decide to carry out extractions at room temperature to make the protocol more simple and rapid. The critical evaluation of the asymmetry factor (AF) allows establishing the efficiency of the method in terms of resolution of the peaks obtained for the target analytes and gives information about the capability of accurate and precise quantification taking into account the degree of tailing of the chromatographic peaks. Results obtained by this investigation show that, for all analytes, SPME analysis performed in optimized conditions provided more narrow and symmetric chromatographic peaks than those obtained by direct injection of analytes solution. Two chromatograms were compared: one obtained directly injecting a standard mix solution (methanol as solvent) by syringe and one desorbing the extracts from a standard mix solution in water from the SPME coating. For all the chromatographic peaks obtained both liquid and SPME injection the AF was calculated as follow:

$$AF = \frac{b}{a} \quad (3.3)$$

where b is the distance from the center line of the peak to the back slope and a is the distance from the center line of the peak to the front slope taking all the measurement.

The results obtained, shown in Table 3.7, clearly show an improved chromatographic behavior for peaks obtained by SPME than liquid injection.

Table 3.7 Asymmetry factor (AF) of the target compounds analyzed for direct injection of analytes solution and SPME injection in optimized conditions.

Compound	Asymmetry factor (AF)	
	direct injection of solution	SPME injection
BTH	1.55	1.37
2-MeBTH	1.36	1.27
BTR	9.00	4.83
4-MeBTR	4.56	1.98
BSA	5.03	2.39
5-MeBTR	5.96	2.69
2-MeSBTH	1.00	1.00
2-NH ₂ BTH	2.08	1.64
p-TSA	6.37	1.76
5-CIBTR	6.91	1.93
2-OHBTH	1.00	1.00
N-Et-p-TSA	1.10	1.00
5,6-MeMeBTR	4.13	1.78
2-SHBTH	3.58	3.40

This can be related to the effect of organic solvent on the focusing of the analytes in the head of the chromatographic column. Vaporization of solvent during liquid injection lead to a broader vapor cloud formed in the injector port of the gas-chromatography, in SPME conversely, no solvent is present and the vapor cloud results to be much more compact allowing better focusing of the analytes, thus less tailing. In particular for the most polar compounds such as BTR, 5,6-

MeMeBTR, 5-CIBTR, p-TSA, 5-MeBTR, BSA and 4-MeBTR this effect result to be much more pronounced.

3.1.2.3.3 *Matrix effects*

The effect of matrix components on the analyte ionization process is an important issue which must be evaluated. The evaluation of this effect becomes critical when complex matrices such as biofluids¹⁰⁶ and environmental samples (e.g. wastewater)⁷² need to be analyzed. The presence of the matrix may induce to an enhancement or suppression of the signal since its component may affect the ionization process, invalidating the reliability and accuracy of the analytical method.

The probability of matrix effect is enhanced when sample pretreatment and clean-up procedures are minimized or not performed. In order to test the reliability and versatility towards many matrices of the method herein proposed, a carefully evaluation of matrix effect was conducted, in accordance with the method of Matuszewski et al.⁷¹.

Five raw samples (urine, river water, urban effluent, wastewater and tap water) were collected and divided into two aliquots. One was used as a blank sample, its pH and salt content were adjusted as described in the experimental section, and then it was analyzed according to the optimized condition described earlier. The second aliquot was treated as described above and spiked with the analytes at 20 and 80 $\mu\text{g l}^{-1}$. All samples were analyzed in triplicates by GC-MS/MS according to the procedure described in section 4.1.3.2.4.

Since the analysis of blanks revealed the absence of any peak related to the analytes of interest, the matrix effect was calculated as the percentage ratio of analyte peak area for the spiked sample (A_{spike}) to the peak area for a ultrapure water external standard (A_{std}):

$$ME = \left(\frac{A_{\text{spike}}}{A_{\text{std}}} \right) \times 100 \quad (3.4)$$

ME values less than 100% indicate signal suppression, while values above 100% indicate signal enhancement due to the influence of matrix components. Matrix effect values obtained for all the matrices collected are reported in Table 3.8.

Table 3.8 Matrix effect (%) evaluated at 20 and 80 $\mu\text{g l}^{-1}$ for all the matrices tested

	Tap water		Urban effluent		River water		Waste water*		Urine**	
	20 $\mu\text{g l}^{-1}$	80 $\mu\text{g l}^{-1}$	20 $\mu\text{g l}^{-1}$	80 $\mu\text{g l}^{-1}$	20 $\mu\text{g l}^{-1}$	80 $\mu\text{g l}^{-1}$	20 $\mu\text{g l}^{-1}$	80 $\mu\text{g l}^{-1}$	20 $\mu\text{g l}^{-1}$	80 $\mu\text{g l}^{-1}$
BTH	95.8	96.2	111.3	94.4	106.6	95.7	88.9	92.3	103.2	106.7
2-MeBTH	108.5	96.6	126.3	97.8	114.7	100.2	109.6	94.8	110.9	106.1
BTR	61.3	77.0	56.1	80.7	81.3	75.5	78.1	75.2	74.2	99.2
4-MeBTR	94.1	72.4	95.5	71.9	98.6	72.4	75.8	58.7	86.9	97.7
BSA	100.6	79.7	91.1	76.5	77.7	77.9	68.1	63.5	66.6	102.5
5-MeBTR	95.5	93.6	100.6	90.5	99.6	85.3	78.1	63.0	94.2	113.8
2-MeSBTH	109.8	94.7	115.1	95.6	112.9	95.9	101.0	95.6	95.3	97.1
2-NH2BTH	109.6	92.9	104.4	90.2	99.3	85.8	85.4	75.0	106.6	107.6
p-TSA	104.3	74.5	90.7	71.4	92.3	73.6	79.9	64.3	79.6	106.2
2-OHBTH	103.7	94.9	107.6	92.4	100.7	95.9	92.6	82.9	105.7	110.7
5-CIBTR	105.5	72.2	108.2	70.8	94.2	70.0	78.5	63.0	85.5	104.0
N-Et-p-TSA	125.2	70.4	128.2	72.0	118.9	70.7	99.2	68.8	104.7	112.7
5,6-MeMeBTR	121.5	69.6	103.9	70.1	118.8	66.5	87.9	53.3	121.3	114.6
2-SHBTH	74.3	126.9	80.4	131.6	79.3	132.5	85.2	90.5	106.0	124.7

* 1:5 diluted sample

** 1:6 diluted sample

The results show no significant matrix effect for the majority of the target compounds in all the matrices considered. Significant signal suppression ($< 70\%$) was noticed only in few cases : in tap water and urban effluent at the lowest concentration spiked ($20 \mu\text{g l}^{-1}$) for BTR, in urine for BSA at $20 \mu\text{g l}^{-1}$ and in waste water samples spiked at $20 \mu\text{g l}^{-1}$ for BSA and at $80 \mu\text{g l}^{-1}$ 5-MeBTR, 5-CIBTR, N-Et-p-TSA, 5,6-MeMeBTR 4-MeBTR , p-TSA and BSA also. However, it is worth to mention that the results are not corrected by the internal standard response and cases of significant signal suppression constitute only 10% of the overall evaluation. Also the compounds affected by signal suppression are exclusively benzotriazoles and benzosulfonamides thus their integration it is affected by a pronounced tailing that is characteristic of their chromatographic behavior.

Since matrix effect does not significantly affect the majority of matrices evaluated at concentration levels tested, the protocol herein proposed can be considered potentially suitable for the determination of the analytes investigated in different environmental samples and urine.

On the contrary, other methods based both on gas- and liquid-chromatography, present in literature, are strongly affected by matrix effect, making necessary the use of more complex calibration strategies such as standard additions and matrix matched calibration^{74,81,94,95}.

3.1.2.3.4 Analytical performances

For the assessment of analytical performances two labeled internal standards were initially considered: BTR-d4 and p-TSA-d4. The linearity of method was tested under the SPME optimized conditions at a concentration range between 1 $\mu\text{g l}^{-1}$ and 100 $\mu\text{g l}^{-1}$ with 20 $\mu\text{g l}^{-1}$ of each internal standard. BTR-d4 was discharged since unsatisfactory results were obtained even for the compounds belonging to its same chemical class. This may be related to its poor chromatographic behavior (pronounced tailing) and response. Using p-TSA-d4, satisfactory results were instead obtained in the considered calibration ranges achieving correlation coefficient values > 0.99 for all the analytes except for BRT and 5-MeBTR (Table 3.9).

Three concentration levels (8, 20 and 80 $\mu\text{g l}^{-1}$) were considered to evaluate accuracy and precision between run by analyzing spiked matrices samples three times every day along a week. Both parameters gave satisfactory results (Table 3.10) except in few cases. For benzothiazoles, 2-NH₂BTH shows accuracy comprises between 123.9 and 136.1% at 80 $\mu\text{g l}^{-1}$ in all matrices except river water and 2-SHBTH showed poor reproducibility (26%) and accuracy (130%) at 8 $\mu\text{g l}^{-1}$ respectively in tap water and urine. Among benzotriazoles, the poor chromatographic behavior of BTR and 5-MeBTR led to high RSD value at 8 $\mu\text{g l}^{-1}$ in urban effluent for the former and at 8 $\mu\text{g l}^{-1}$ both in tap water and urban effluent for the latter. Moreover, low accuracy value was observed for 5,6-MeMeBTR at 8 $\mu\text{g l}^{-1}$ (57.3%). In case of benzosulfonamides, low accuracy was achieved for BSA at 8 $\mu\text{g l}^{-1}$ in waste water and at 8 $\mu\text{g l}^{-1}$ and 20 $\mu\text{g l}^{-1}$ in urine (53.5%, 63.1% and 56.5 % respectively). The limit of detection (LOD) and the limit of quantitation (LOQ) were calculated following the directives of IUPAC and the American Chemical Society's Committee on Environmental Analytical Chemistry i.e. the signal at the LOD and the signal at the LOQ are equal to the signal of the reagent blank plus three and ten times the standard deviation for the reagent blank, respectively. The LOD and LOQ values achieved by the proposed method can be considered overall satisfactory (Table 3.9). Generally, very good results were obtained for benzothiazoles since LOD and LOQ values improved of more than one order of magnitude compared to other approaches based on dispersive-LLE and SPE coupled with HPLC^{94,95}. For urine samples, taking into account the 6 fold dilution of the

sample, comparable and lower LODs were obtained for benzothiazoles compared to the results obtained by Asimakopoulus *et al.*⁹⁹.

Table 3.9 Calibration parameters, LOD and LOQ values for all the matrices tested

Compound	Calibration curves	Ranges ($\mu\text{g l}^{-1}$)	R^2	Tap water		Urban effluent		River water		Waste water*		Urine**	
				LOD ($\mu\text{g l}^{-1}$)	LOQ ($\mu\text{g l}^{-1}$)	LOD ($\mu\text{g l}^{-1}$)	LOQ ($\mu\text{g l}^{-1}$)	LOD ($\mu\text{g l}^{-1}$)	LOQ ($\mu\text{g l}^{-1}$)	LOD ($\mu\text{g l}^{-1}$)	LOQ ($\mu\text{g l}^{-1}$)	LOD ($\mu\text{g l}^{-1}$)	LOQ ($\mu\text{g l}^{-1}$)
BTH	$y=0.7757x+2.0577$	1-100	0.9988	0.068	0.134	0.022	0.074	0.021	0.056	0.130	0.200	0.483	0.912
2-MeBTH	$y=0.7422x-0.3535$	1-100	0.9984	0.071	0.140	0.024	0.085	0.022	0.061	0.136	0.208	0.421	0.795
BTR	$y=0.0249x-0.0575$	2.5-100	0.9875	1.96	3.31	2.04	3.07	1.14	2.08	7.50	14.7	2.78	4.91
4-MeBTR	$y=0.1174x-0.0533$	2.5-100	0.9958	0.620	1.49	1.19	2.09	0.629	0.944	3.17	5.21	1.15	1.84
BSA	$y=0.0439x+0.1216$	1-100	0.9997	0.042	0.098	0.025	0.042	0.039	0.089	0.322	0.740	0.253	0.547
5-MeBTR	$y=0.0790x+0.0317$	2.5-100	0.9883	0.921	2.21	1.55	2.44	0.935	1.40	4.71	7.37	1.71	2.72
2-MeSBTH	$y=19.0761x+2.9735$	1-100	0.9999	0.0002	0.0004	0.0001	0.0002	0.0001	0.0003	0.001	0.002	0.003	0.006
2-NH ₂ BTH	$y=0.5875x-0.2562$	1-100	0.9987	0.010	0.020	0.005	0.009	0.004	0.007	0.047	0.096	0.349	0.413
p-TSA	$y=0.0751x+0.1322$	1-100	0.9944	0.354	0.654	0.306	0.532	0.228	0.409	0.973	1.63	0.906	1.73
5-CIBTR	$y=0.1115x-0.0462$	1-100	0.9913	0.242	0.356	0.297	0.551	0.226	0.448	1.00	1.55	2.35	4.85
2-OHBTH	$y=0.6526x+0.4282$	1-100	0.9991	0.083	0.156	0.140	0.263	0.081	0.145	0.459	0.794	0.298	0.453
N-Et-p-TSA	$y=0.0537x+0.0203$	1-100	0.9983	0.063	0.102	0.172	0.328	0.070	0.139	0.611	1.32	0.863	1.45
5,6-MeMeBTR	$y=0.2680x+0.0864$	1-100	0.9919	0.323	0.437	0.282	0.458	0.186	0.251	1.41	2.12	1.61	3.11
2-SHBTH	$y=0.2639x+0.3414$	1-100	0.9921	0.722	1.01	0.890	0.997	0.954	1.23	5.34	6.50	2.56	3.13

* Values calculated according to 1:5 dilution; ** Values calculated according to 1:6 dilution

Table 3.10 Mean accuracy and relative standard deviations, RSD (% , in parentheses) evaluated at 8, 20 and 80 $\mu\text{g l}^{-1}$ for all the matrices tested

	Tap water			Urban effluent			River water			Waste water			Urine		
	8 $\mu\text{g l}^{-1}$	20 $\mu\text{g l}^{-1}$	80 $\mu\text{g l}^{-1}$	8 $\mu\text{g l}^{-1}$	20 $\mu\text{g l}^{-1}$	80 $\mu\text{g l}^{-1}$	8 $\mu\text{g l}^{-1}$	20 $\mu\text{g l}^{-1}$	80 $\mu\text{g l}^{-1}$	8 $\mu\text{g l}^{-1}$	20 $\mu\text{g l}^{-1}$	80 $\mu\text{g l}^{-1}$	8 $\mu\text{g l}^{-1}$	20 $\mu\text{g l}^{-1}$	80 $\mu\text{g l}^{-1}$
BTH	88.5 (4.6)	85.3 (2.2)	87.8 (1.5)	78.5 (5.3)	82.3 (1.8)	85.9 (0.1)	71.7 (10.1)	68.5 (10.5)	87.2 (11.9)	92.1 (0.7)	85.3 (6.9)	112.1 (7.2)	78.9 (4.9)	87.5 (1.8)	84.6 (4.4)
2-MeBTH	85.8 (3.8)	76.4 (5.0)	85.9 (1.3)	87.2 (0.6)	70.5 (1.9)	86.8 (1.7)	82.3 (11.2)	70.5 (12.8)	88.9 (12.4)	93.0 (1.3)	80.0 (6.5)	111.1 (5.3)	74.3 (5.6)	97.7 (1.9)	82.1 (2.7)
BTR	103.6 (6.6)	82.1 (13.0)	70.5 (0.4)	108.8 (26.5)	84.3 (9.5)	73.7 (0.8)	96.0 (14.9)	70.2 (9.8)	69.1 (5.1)	<LOQ	90.1 (7.5)	90.0 (3.3)	112.6 (8.1)	69.6 (9.5)	78.7 (18.2)
4-MeBTR	101.3 (1.4)	117.3 (2.3)	94.5 (1.0)	102.8 (9.3)	106.1 (7.4)	93.7 (1.7)	97.5 (10.5)	100.6 (11.0)	90.4 (6.1)	84.7 (1.5)	110.8 (8.6)	101.0 (2.9)	90.7 (2.2)	73.6 (7.4)	110.8 (19.0)
BSA	93.1 (0.8)	98.5 (12.4)	100.1 (0.1)	76.1 (3.6)	113.8 (3.7)	95.7 (2.4)	69.8 (0.9)	116.0 (4.9)	97.6 (4.8)	53.5 (10.0)	118.4 (9.6)	105.4 (1.5)	63.1 (0.9)	56.5 (3.7)	112.3 (13.8)
5-MeBTR	70.7 (24.6)	102.2 (11.5)	119.7 (0.6)	87.4 (28.9)	90.4 (0.6)	115.5 (1.6)	77.5 (15.0)	87.8 (12.7)	108.9 (2.9)	67.5 (2.5)	72.2 (9.7)	106.4 (3.0)	119.8 (3.1)	79.8 (0.6)	116.7 (8.9)
2-MeSBTH	94.6 (5.7)	82.7 (2.8)	89.8 (1.8)	94.1 (2.9)	74.4 (7.2)	90.5 (1.5)	88.1 (14.6)	70.2 (11.0)	90.7 (4.7)	95.8 (4.6)	82.0 (5.1)	119.8 (1.3)	70.5 (5.7)	80.8 (7.2)	80.1 (0.3)
2-NH ₂ BTH	87.2 (5.9)	113.2 (1.2)	127.8 (0.2)	79.3 (4.4)	108.0 (3.2)	123.9 (0.9)	73.6 (8.3)	102.8 (6.4)	117.8 (4.1)	78.1 (3.4)	103.8 (4.8)	136.2 (4.3)	75.1 (2.7)	90.4(3. 2)	128.8 (5.4)
p-TSA	99.8 (2.0)	99.8 (8.7)	104.5 (0.0)	90.0 (2.8)	120.7 (4.4)	99.8 (2.1)	83.5 (6.1)	109.2 (9.6)	96.5 (3.0)	76.7 (5.1)	116.8 (7.8)	119.4 (5.4)	78.3 (2.0)	87.5 (4.4)	115.2 (16.4)
5-CIBTR	101.9 (4.1)	121.5 (4.8)	118.4 (2.6)	91.9 (2.4)	111.2 (0.5)	115.0 (1.2)	78.7 (7.2)	106.0 (9.9)	119.4 (13.7)	84.9 (8.1)	116.8 (7.1)	116.6 (3.0)	80.7 (2.8)	89.6 (0.5)	120.1 (6.0)
2-OHBTH	106.6 (2.8)	109.3 (5.6)	90.4 (1.3)	100.8 (5.0)	109.4 (5.9)	88.5 (2.5)	94.2 (14.9)	110.7 (7.9)	85.3 (1.0)	89.7 (3.7)	120.0 (14.5)	101.5 (0.3)	89.7 (1.5)	72.5 (5.9)	113.2 (13.7)
N-Et-p-TSA	91.1 (15.1)	108.3 (3.5)	90.6 (3.2)	89.4 (3.4)	111.1 (2.8)	92.5 (2.6)	85.2 (10.1)	101.7 (6.7)	90.9 (3.9)	84.2 (16.4)	116.3 (4.4)	117.0 (6.9)	73.3 (6.9)	88.8 (2.8)	116.5 (2.1)
5,6-MeMeBTR	71.1 (2.0)	102.5 (1.0)	88.9 (1.6)	75.7 (11.0)	102.1 (3.1)	87.3 (0.3)	71.5 (8.4)	82.5 (8.0)	82.8 (1.8)	57.3 (7.1)	79.6 (8.2)	87.8(0. 1)	72.8 (72.8)	114.1 (3.1)	114.6 (0.3)
2-SHBTH	105.5 (24.4)	69.7 (16.1)	115.7 (7.4)	74.9 (16.6)	109.8 (13.0)	105.2 (5.8)	83.2 (9.3)	71.9 (3.9)	106.0 (12.8)	72.0 (0.3)	87.5 (14.6)	95.6 (0.0)	130.3 (5.8)	107.0 (13.0)	90.1 (6.8)

In all the matrices tested the lowest LOD and LOQ values were obtained for 2-MeSBTH achieving results comparable to the values obtained for the same compound in drinking and surface water by SPE-LC-LTQ-FT-Orbitrap/MS system⁸⁵.

3.1.2.3.5 Real samples analysis

The proposed protocol was applied to the analysis of twelve samples of the matrices of interest: six urine samples collected from six healthy volunteers (three females and three males, of age ranging from 23 to 29 years), three river water samples collected from local rivers (Crati, Busento and Campagnano rivers located in Cosenza's urban and rural areas, Italy), three urban waste water samples (collected from urban effluent water in Cosenza, Rende, CS, and Pizzo Calabro, VV, Italy) and five tap water samples collected from Rende (CS, Italy) and Cosenza (CS, Italy). The entire set of samples was collected in August-September 2013 and prepared for analysis as described in experimental section.

Analytes concentrations for all the examined samples were found below LOD. For environmental samples this was expected because were collected in low environmental impact areas, consequently contamination of human urine was not expected. In order to evaluate the versatility and reliability of the proposed method for the analysis of benzothiazole, benzotriazoles and benzosulfonamides, all the sample matrices were spiked at $5 \mu\text{g l}^{-1}$ for all analytes. The accuracy values were calculated according to three replicate experiments for each sample matrix.

The results of accuracy calculated can be considered satisfactory because they ranged from 77.9 to 127.9% in tap water, 86.7 to 129.0 % in river water except for 5-Cl-BTR (138.3%), 69.5 to 109.9 % in urban effluent and 89.8 to 120.8 % in human urine except for BTR (136.2%), 5-MeBTR (139.0%) and 2-SHBTH (141.7%).

3.1.2.4 Conclusions

On the light of the increasing attention focused on the development of high-throughput and versatile analytical protocols allowing the assessment of pollutants distribution and concentration in a broad range of sample matrices, the herein proposed method wants to represent a valid approach for the simultaneous determination of benzothiazole, benzotriazoles and benzosulfonamides in a variety of environmental samples and in urine. For the first time, in this work solid phase microextraction was applied as sample preparation technique for the

determination of these contaminants in order to develop an environmental-friendly procedure that involves only sorption and desorption of the analytes and completely eliminates the use of organic solvents, with evident advantages in terms of time and money saving. The hyphenation of unique features of solid-phase microextraction with the separation capability and high selectivity of a gas-chromatographic/tandem mass spectrometric system allowed the achievement of satisfactory results in terms of precision and accuracy for all the matrices tested. The evaluation of matrix effect for different environmental matrices and human urine revealed a not significant influence in the majority of the cases tested. This allowed the use of simplified calibration procedure promoting the high-throughput of the overall protocol instead of much more tedious and time consuming calibration strategies, such as standard addition and matrix matched calibration, commonly recommended in literature. Critical, in the optimization of this protocol, was the use of multivariate optimization by DoE (Experimental Design) which allowed the establishment of the best working condition for all the tested analytes, notwithstanding their chemical diversity, taking in account possible synergistic effects between the parameters optimized.

3.1.3 Multivariate optimization of SPME, derivatization and tandem mass-spectrometric conditions for the determination of hydrazine in drinking water: a powerful tool for health risk assessment

3.1.3.1 Introduction

Hydrazine, having molecular formula N_2H_4 , is a highly reactive base and reducing agent, which has found a broad range of industrial and military applications. This compound has been used in rocket and spacecraft fuels as well as in agricultural chemicals and pharmaceutical intermediates, in the polymerization of urethane and manufacturing of textile dyes, as an oxygen scavenger or corrosion inhibitor in water boilers and for removal of halogens from wastewater^{107–109}. Moreover, hydrazine can be found as contaminant of drinking water after disinfection processes by chlorination in presence of amines^{110,111}.

Despite the fact that hydrazine has been also employed as intermediate for the synthesis of many drugs and hydrazine sulphate was used as an alternative medical treatment for the loss of appetite (anorexia) and weight loss (cachexia), its toxicity has been described as early as 1908 and it is known to cause irreversible cellular damage¹¹². As revealed by results from in vivo studies, hydrazine and methyl-hydrazine are alkylating agents. The formation of methyl adducts with DNA bases in vivo may be one of the mechanisms by which hydrazines cause DNA damage and gene mutations^{113,114}. Hydrazine neurotoxicity, hepatotoxicity and nephrotoxicity were confirmed in rodents¹¹⁵ and, also, humans' exposure to hydrazine can damage the liver, kidney and central nervous systems^{116,117}.

The vast use of hydrazine implied its increasing environmental occurrence especially in groundwater in proximity of production or usage sites; however the United States Environmental Protection Agency (EPA) has not classified hydrazine as a drinking water contaminant, but has categorized it as a probable human carcinogen (B2)¹¹⁸.

Considering the high health risk related to this compound as well as possible contamination in drinking water, it is critical the development of new, fast and reliable analytical protocols allowing its detection at trace levels and the possibility of high-throughput sample treatment for routine analysis. Determination of hydrazine has been carried out by electrochemical, spectrophotometric, potentiometric, fluorescence and chemiluminescence analysis as well as electrophoresis, at part per million and part per billion levels in environmental samples.^{119–128}

Both liquid- and gas-chromatographic methods prior derivatization were also used to determine hydrazine in different sample matrices.

Several derivatization reagents were used such as naphthalene-2,3-dialdehyde¹²⁹, 5-chlorosalicylaldehyde¹¹⁹, benzaldehyde^{130,131}, 4-chloro-5,7-dinitrobenzofurazan¹³² and cinnamaldehyde¹³³, pentafluorobenzaldehyde^{134,135}, acetone¹³⁶ ethyl chloroformate¹³⁷ and OPA¹³⁸. Most of these derivatization procedures present some drawbacks such as: the need of liquid-liquid extraction steps to isolate the derivatization products, the use of a large volume of sample and solvent and problems during the concentration of the extracts bearing to losses of volatile derivatization products. To date the lowest limits of quantification for the analysis of hydrazine in drinking water were obtained by Davis¹¹¹ et al.. In this work hydrazine was derivatized with acetone in aqueous phase and the derivatized products extracted by liquid-liquid extraction, the instrumental analysis was carried out by GC-CI-MS/MS reaching detection limits of 0.7 ng/L in water samples fortified at 1 ng/L. Notwithstanding the excellent results in terms of LOQ achieved by the aforementioned work the use of liquid-liquid extraction may constitute a bottleneck in the sample preparation process limiting the high throughput of the overall analytical procedure.

Solid phase microextraction has shown over the years its suitability in speeding sample preparation protocols allowing simultaneous extraction and preconcentration of organic compounds from a broad range of matrices such as environmental, biological and food samples. When derivatization has to be carried out solid-phase microextraction avoids the need of further sample pretreatment prior injection in the chromatographic system, extracting derivatized analytes directly from the matrix. In the light of this, this work propose for the first time a SPME-GC-EI-MS/MS protocol for the fast and reliable determination of hydrazine in drinking water using alkyl chloroformates as derivatizing reagents.

A carefully study has been carried out optimizing by multivariate analysis the derivatization reaction conducted with different alkyl chloroformates. Moreover, Experimental Design was also used to optimize tandem mass spectrometric conditions for all the derivatized compounds obtained. The affinity of the different derivated compound obtained towards five SPME coatings was evaluated in order to obtain the best extraction efficiency and finally multivariate optimization was carried out on the parameters affecting SPME process.

3.1.3.2 Experimental section

3.1.3.2.1 Materials

Hydrazine, pyridine, sodium chloride and alkyl chloroformates were obtained from Sigma-Aldrich (Milan, Italy). Labeled hydrazine $^{15}\text{N}_2\text{H}_2$ used as internal standards, was bought from C/D/N Isotopes (Pointe- Claire, Quebec, Canada). The tested solid phase microextraction fibers were purchased from Supelco (Bellefonte, PA, USA) and conditioned as recommended by the manufacturer. Aqueous solutions were prepared using ultrapure water obtained from a Milli-Q plus system (Millipore, Bedford, MA)

3.1.3.2.2 Instrumentation and apparatus

A TSQ Quantum GC (Thermo Fischer Scientific) system constituted by a triple quadrupole mass spectrometer (QqQ) Quantum and a TRACE GC Ultra equipped with a TriPlus autosampler was used for the analysis of the samples. The capillary column used was a Thermo TR-5MS (30 m \times 0.25 mm i.d., 0.25 μm film thickness). The GC oven temperature was initially held at 80 $^\circ\text{C}$ for 1 min, then ramped at 15 $^\circ\text{C min}^{-1}$ to 280 $^\circ\text{C}$, and held at this temperature for 5 min. The carrier gas was helium at 1 ml min^{-1} of purity 99.999% and argon at a pressure of 1.0 mTorr was used as collision gas. For SPME analyses, a Thermo PTV straight liner 0.75mm \times 2.75 mm \times 105 mm was used as GC inlet liner. Analyses were performed in splitless mode and by setting the injector temperature at 250 $^\circ\text{C}$. The QqQ mass spectrometer was operated in electron ionization (EI) in multiple reaction monitoring (MRM) mode. The transfer line and ionization source temperatures were set at 290 $^\circ\text{C}$ and 300 $^\circ\text{C}$, respectively. The emission current was set at 25 μA . The scan width and scan time were set at 0.2 m/z and 0.1 s for all segments. Peak width of Q1 was fixed at 0.7 amu. Instrumental parameters used in EI-MS/MS acquisition are shown in Table 3.11.

**Table 3.11 Electron ionization tandem mass spectrometry (EI-MS/MS) parameters
(Collision energies (eV) are indicated in parenthesis)**

Compound	MRM transition, m/z (collision energy, V)	
	Quantification	Identification
Tetra-derivatized N ₂ H ₂	204→ 76 (9)	204→103 (8)
Tetra-derivatized ¹⁵ N ₂ H ₂	206→ 78 (9)	-

3.1.3.2.3 Samples for derivatization and tandem mass spectrometric parameters multivariate optimization

Derivatization reaction was carried out in 2 ml of drinking water according to the reagent amounts described in Tables 1.1-8 and 1.1-9, 1.5 ml of NaCO₃ were added to have pH 9 in the solution. The system was left to react for 15 minutes at room temperature. Liquid-liquid extraction was carry out using two aliquots of 1ml of methylene chloride. Anhydrification of organic extracts was carried out with sodium sulphate prior the injection in the GC-MS system.

3.1.3.2.4 Samples for SPME-GC-MS/MS analysis

Derivatization procedure was directly carried out in the vial (volume 10 ml) used for autosampler. 5 ml of drinking water were spiked with a proper amount of internal standards solution, then 25 µl of pyridine and 210 µl of propyl chloroformate were added and the mixture, as from the results obtained from multivariate optimization, then the pH was adjusted to 9 adding 1.85 ml of a 2 M solution Na₂CO₃. The mixture was shaken for 15 min, afterwards a proper amount of NaCl was added to reach a percent of 4% (w/w) of salt content in the solution. The vial was then crimped and SPME extraction was performed with 65 µm PDMS/DVB fiber in immersion mode for 30 min at 60°C and the adsorbed analytes were thermally desorbed by introducing the fiber into the injector set at 220 °C for 10 min. A blank analysis has to be performed by using a water solution with derivatizing mixture and without analytes to verify if any peak corresponding to the compounds under investigation is present.

3.1.3.2.5 Optimization of derivatization reaction, tandem mass spectrometric conditions and solid phase microextraction variables

The experimental matrix designs were carried out and evaluated using Statistica 8.0 (StatSoft 2007 Edition, Tulsa, USA).

3.1.3.3 Results and discussion

3.1.3.3.1 Derivatization reaction optimization

Determination of hydrazine by gas-chromatography requires the use of nitrogen selective detectors or in alternative derivatization strategies can be applied in order to generate derivatization products containing carbon atoms and bearing thermal stability and enough volatility to make them suitable for gas-chromatographic determination. As reported, hydrazine was derivatized mainly using carboxylic compounds for the formation of corresponding azines such as p-dimethylaminobenzaldehyde^{139,140}, benzaldehyde^{130,141}, salicylaldehyde¹⁴², 5-chlorosalicylaldehyde¹¹⁹, ortho-phthalaldehyde¹³⁸ and acetone¹¹¹. An alternative approach consists in using alkyl chloroformates for the formation of carbamate derivatives. This fast and simple derivatization strategy proposed by Husek⁵⁹, is well suitable for derivatization of amines¹⁵, aminoacids⁶² and aminoalcohols and carboxylic acids⁶³. Derivatization of hydrazine with ethylchloroformate and the determination of its bi-derivatized product by GC-FID was reported by Khuhawar et al.¹³⁷. An attempt of derivatization was performed in drinking water following derivation procedure described in the aforementioned work and the derivatives extracted by liquid-liquid extraction with chloroform. The gas-chromatographic/mass spectrometric analysis of extracts obtained revealed the presence of three derivatization products (Figure 3.11), conversely to what reported previously¹⁴³.

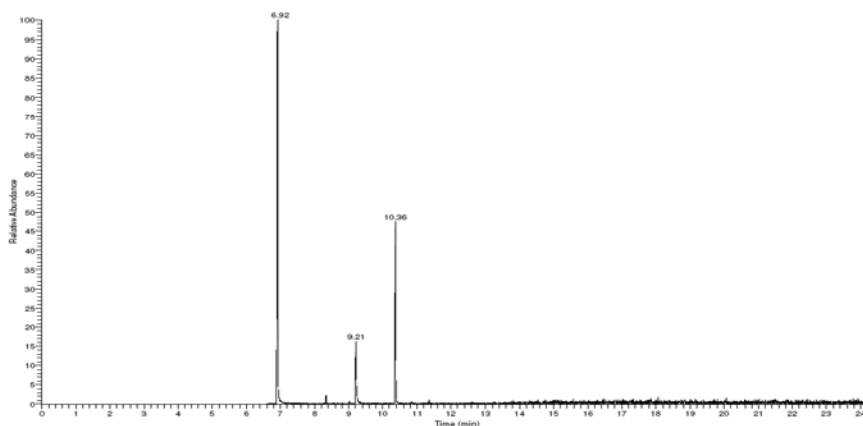


Figure 3.11 Chromatogram obtained from the extracts of derivatization of hydrazine with ethyl chloroformate

From analysis of the mass spectra obtained was possible recognize without ambiguity the derivatized obtained as bi-, tri and tetra-derivatized and identify characteristic fragmentations as summarized in Table 3.12.

Table 3.12 Fragmented ions for the three derivatives obtained derivatizing hydrazine with ethyl chloroformate

Bi-derivatized hydrazine (M.W. = 176 Da)		Tri-derivatized hydrazine (M.W. = 248 Da)		Tetra-derivatized hydrazine (M.W. = 320 Da)	
Ion	m/z	Ion	m/z	Ion	m/z
M^{++}	176	$[M - EtO]^+$	203	$[M - (C_2H_4 + CO_2 + EtO)]^{++}$	203
$[M - EtOH]^{++}$	130	$[M - (C_2H_4 + CO_2)]^{++}$	176	$[M - 2(C_2H_4 + CO_2)]^{++}$	176
$[M - (C_2H_4 + CO_2)]^{++}$	104	$[176 - EtOH]^{++}$	130	$[176 - EtOH]^{++}$	130
$[M - (COOEt)]^+$	103	$[M - 2(C_2H_4 + CO_2)]^{++}$	104	$[M - 3(C_2H_4 + CO_2)]^{++}$	104
$[HOOCNHNH_2]^{++}$	76	$[176 - (COOEt)]^+$	103	$[176 - (COOEt)]^+$	103

The mass spectra obtained for three derivatives are reported in Figure 3.12

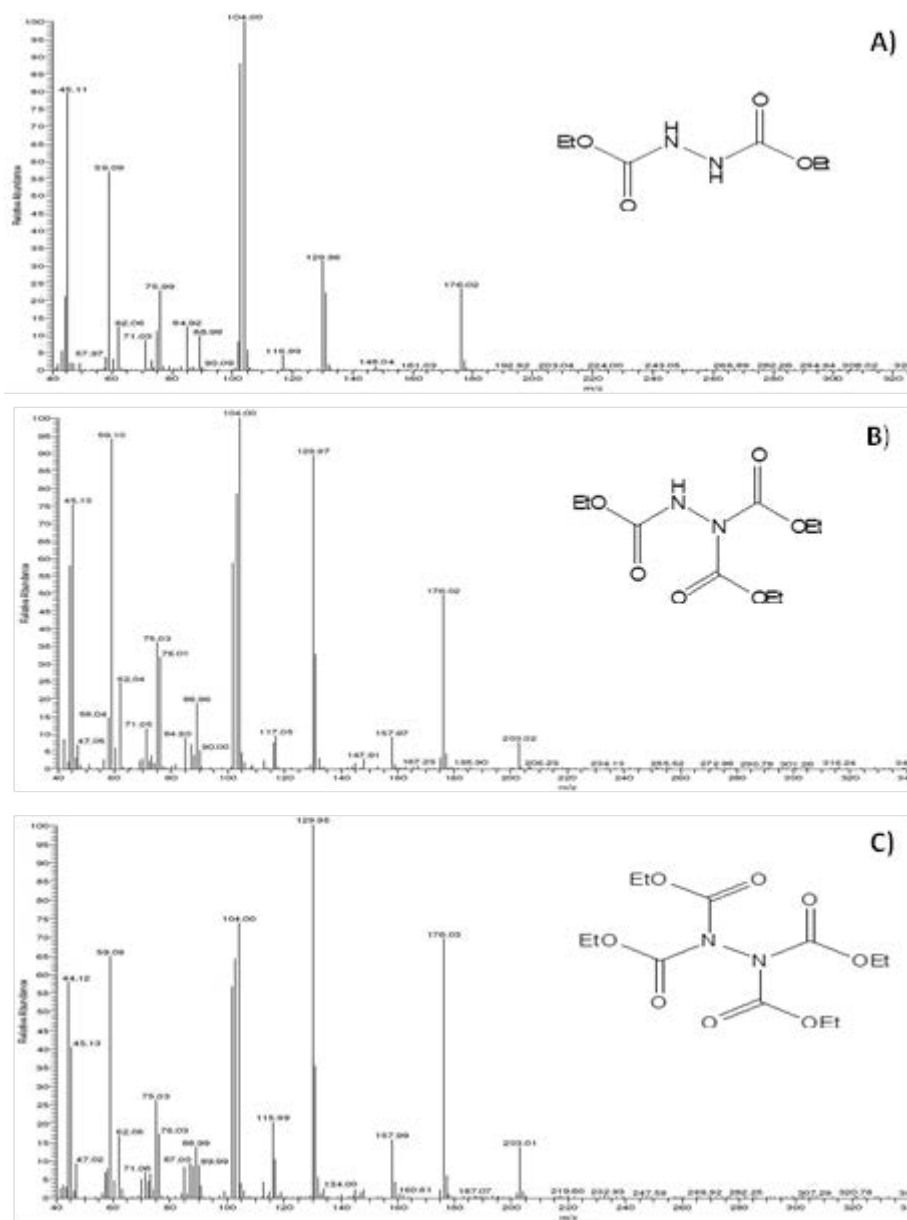


Figure 3.12 Mass spectra and molecular structure of A) bi-derivatized, b) tri-derivatized and c) tetra-derivatized hydrazine obtained with ethyl chloroformate

Analyzing the same extracts by GC-Cl-MS, using methane as ionizing gas, unsatisfactory results were obtained in terms of chromatographic peaks obtained, for this reason electron impact (EI) ionization was chosen as the more suitable ionization method.

Moreover, two other derivatizing reagents were used in order to investigate the effects of the alkyl chain of the derivatization reagent on the extraction efficiency by SPME: propyl and isobutyl chloroformate.

As expected, carrying out the derivatization as mentioned above, three derivatives for each reaction were also obtained. Relative chromatograms (Figure 3.13) and description of the fragmented ions (Table 3.13, Table 3.14) are shown below.

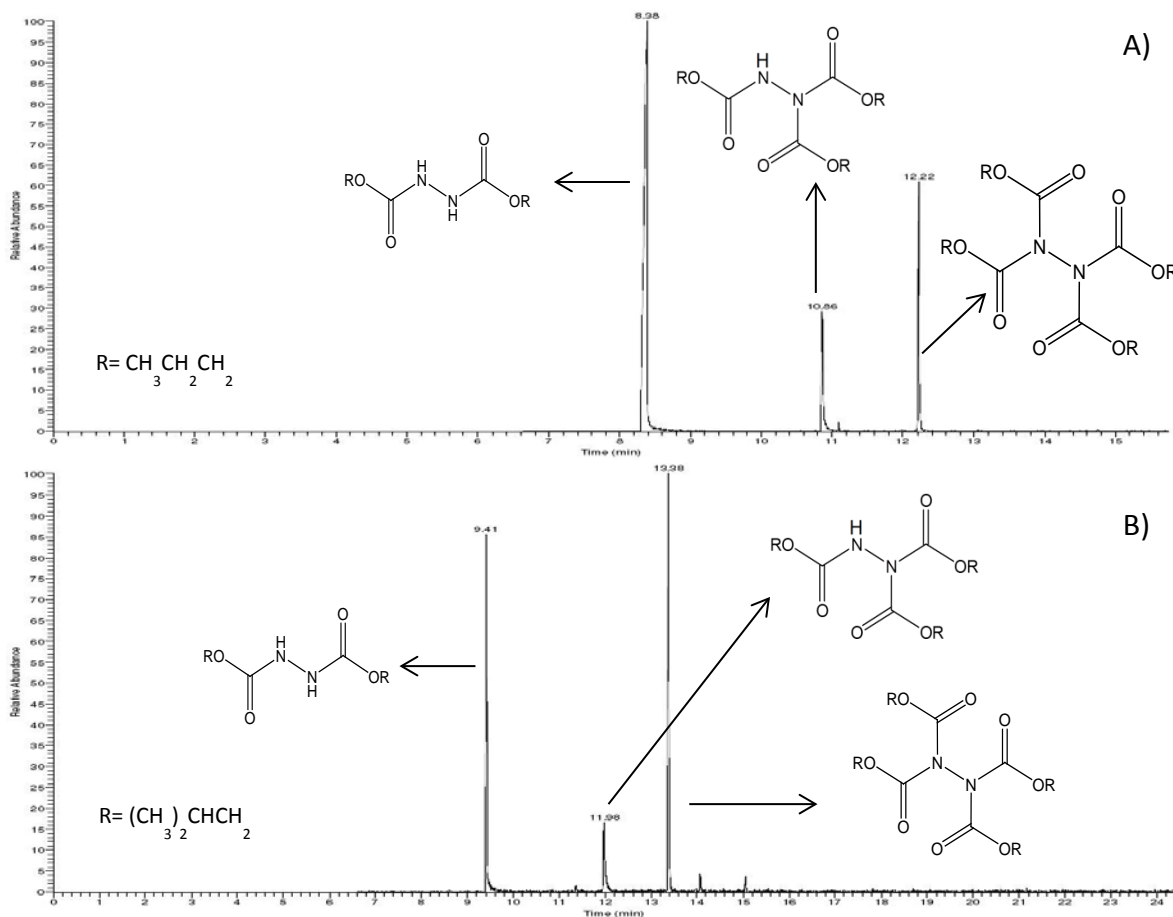


Figure 3.13 Chromatograms obtained from derivatization by A) propyl- and B) isobutyl chloroformate

Table 3.13 Fragmented ions for the three derivatives obtained derivatizing hydrazine with propyl chloroformate

PCF bi-derivatized hydrazine (M.W. = 204 Da)		PCF bi-derivatized hydrazine (M.W. = 290 Da)		PCF bi-derivatized hydrazine (M.W. = 376 Da)	
Ion	m/z	Ion	m/z	Ion	m/z
M ⁺	204	[M - (C ₃ H ₆ + CO ₂)] ⁺	204	[M - 2(C ₃ H ₆ + CO ₂)] ⁺	204
[M - (C ₃ H ₆ + CO ₂)] ⁺	118	[204 - C ₃ H ₆] ⁺	162	[204 - C ₃ H ₆] ⁺	162
[NH ₂ COOC ₃ H ₇] ⁺	103	[204 - C ₃ H ₇ OH] ⁺	144	[204 - C ₃ H ₇ OH] ⁺	144
		[M - 2(C ₃ H ₆ + CO ₂)] ⁺	118	[M - 3(C ₃ H ₆ + CO ₂)] ⁺	118
[HOOCNHNH ₂] ⁺	76	[NH ₂ COOC ₃ H ₇] ⁺	103	[NH ₂ COOC ₃ H ₇] ⁺	103
		[HOOCNHNH ₂] ⁺	76	[HOOCNHNH ₂] ⁺	76

Table 3.14 Fragmented ions for the three derivatives obtained derivatizing hydrazine with isobutyl chloroformate

IBCF bi-derivatized hydrazine (M.W.= 232 Da)		IBCF tri-derivatized hydrazine (M.W. = 332 Da)		IBCF tetra-derivatized hydrazine (M.W. = 432 Da)	
Ione	m/z	Ione	m/z	Ione	m/z
M ⁺	232	[M - (C ₄ H ₈ + CO ₂)] ⁺	232	[M - 2(C ₄ H ₈ + CO ₂)] ⁺	232
[M - C ₄ H ₈] ⁺	176	[232 - C ₄ H ₈] ⁺	176	[232 - C ₄ H ₈] ⁺	176
[M - (C ₄ H ₈ + CO ₂)] ⁺	132	[M - 2(C ₄ H ₈ + CO ₂)] ⁺	132	[M - 3(C ₄ H ₈ + CO ₂)] ⁺	132
[M - 2C ₄ H ₈] ⁺	120	[232 - 2C ₄ H ₈] ⁺	120	[232 - 2C ₄ H ₈] ⁺	120
[M - 2C ₄ H ₈ - OH] ⁺	103	[232 - 2C ₄ H ₈ - OH] ⁺	103	[232 - 2C ₄ H ₈ - OH] ⁺	103
[HOOCNHNH ₂] ⁺	76	[HOOCNHNH ₂] ⁺	76	[HOOCNHNH ₂] ⁺	76

For each derivatizing reagent used, reaction conditions leading to the higher yield for each of the derivatization products obtained were investigate (9 in total).

Univariate optimization of the variables considered for each of the compounds would have been tedious and experimental results would not take into account possible synergic effect between the variables. For this reason a multivariate approach was used. In particular, a full factorial design was used to investigate two factors (amount of pyridine and alkyl chloroformate) considering three levels in an experimental domain ranging from 0.1 to 0.5 ml of pyridine and

0.1-0.6 ml of alkyl chloroformate according with the experimental plan in Table 3.15 consisting of 9 experiments for each derivatization reagent used.

Table 3.15 Design matrix in the full factorial design with three levels for optimization of derivatization reaction

Exp	pyridine (μl)	alkyl chloroformate (μl)
8	500	300
5	250	300
3	100	100
1	100	600
9	500	100
7	500	600
4	250	600
2	100	300
6	250	100

The entire sample set was prepared according to the experimental plan obtained and the organic extracts (methylene chloride as extraction solvent) analyzed by GC-MS. The results obtained revealed higher yields obtained in proximity of the extremity of the experimental domain, following the same trend as the representative response surface shown in Figure 3.14.

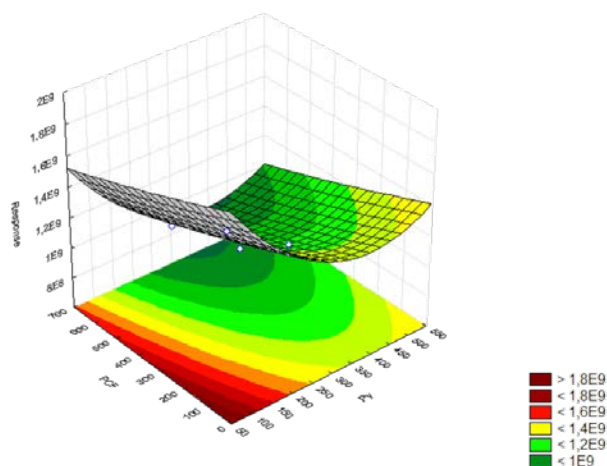


Figure 3.14 Representative response surface for the bi-derivatized product obtained by derivatization reaction with ethyl chloroformate

In the light of this trend, a further investigation was carried out investigating a domain ranging from 10 to 100 μl of both pyridine and alkyl chloroformate according with the experimental plan in Table 3.16

Table 3.16 Design matrix in the full factorial design with three levels for optimization of derivatization reaction

Exp	pyridine (μl)	alkyl chloroformate (μl)
2	10	55
6	55	10
3	10	10
1	10	100
7	55	55
5	55	10
8	100	100
4	100	55
9	100	10

The usefulness of this further optimization also consists in the minimization of the amount of reagents used for the derivatization in order to reduce possible interferences during the extraction by SPME. The results obtained for the organic extracts analyses clearly revealed the poor response of the tri-derivatized product that was not considered for further optimization and quantification.

In Table 3.17 are summarized all the condition leading to highest yield for each bi- and tetra-derivatized products obtained from reaction with ethyl- propyl- and isobutyl chloroformate.

Table 3.17 optimized amount of derivatization reagent obtained by multivariate optimization

Optimized amount of derivatization reagents (μl)		
	Bi-derivatized product	Tetra-derivatized product
Py-ECF	100-39	10-87
Py-PCF	10-10	10-84
Py-IBCF	37-10	10-72

These derivatization conditions were used for further investigations.

3.1.3.3.2 Optimization of tandem mass spectrometric parameters

Tandem mass spectrometry constitutes one of the most powerful tools to improve selectivity and sensitivity of analytical methods especially when the assay of contaminants at trace levels¹⁴⁴ needs to be achieved. In this work DoE optimization was used to perform a thorough investigation of the tandem mass spectrometric conditions leading to the achievement of the lowest limits of detection. At first, proper parent ions for each of the derivates obtained with different alkyl chloroformates were selected so as to achieve the best compromise between selectivity (highest mass to charge ratio) and sensitivity (ion's abundance). The precursors and respective product ions selected for hydrazine bi- and tetra- derivatized are shown in Table 3.18

Table 3.18 Precursor and product ion selected for mass spectrometric multivariate investigation.

Derivatizing reagent	Biderivatized hydrazine		Tetra-derivatized hydrazine	
	Precursor ion (m/z)	Product ion (m/z)	Precursor ion (m/z)	Product ion (m/z)
ECF	176	102, 104, 130	176	102, 104, 130
PCF	204	58, 76, 103, 118, 144, 162	204	58, 76, 103, 118, 144, 162
IBCF	132	57, 76, 103	232	57, 76, 103, 120, 132, 176
	176	57, 76, 103, 120, 121		
	232	57, 76, 103, 120, 132, 176		

Three parameters affecting the intensity of MRM transition were taken into account for the multivariate optimization: collision energy, collision gas pressure and ion source temperature. A full factorial design consisting in twenty seven experiments was performed investigating an experimental domain ranging from 3 to 15 eV of collision energy, 0.6 to 1.4 mTorr of collision gas pressure and 150 to 250 °C of ion source temperature according to the design matrix shown in Table 3.19.

Table 3.19 Design matrix in the full factorial design with three levels and three factors for optimization of derivatization reaction

Experiment #	Collision energy (eV)	Collision gas pressure (mTorr)	Ion source temperature (°C)
7	3	1.4	150
15	9	1	250
6	3	1	250
18	9	1.4	250
21	15	0.6	250
17	9	1.4	200
9	3	1.4	250
23	15	1	200
12	9	0.6	250
22	15	1	150
16	9	1.4	150
10	9	0.6	150
11	9	0.6	200
14	9	1	200
2	3	0.6	200
26	15	1.4	200
19	15	0.6	150
13	9	1	150
1	3	0.6	150
24	15	1	250
25	15	1.4	150
4	3	1	150
27	15	1.4	250
20	15	0.6	200
8	3	1.4	200
5	3	1	200
3	3	0.6	250

The results for each of 39 SRM transitions specified above (Table 3.18) were computed and the best condition determined. The summary of the most sensitive and selective transition selected for further investigations and their optimized work conditions are summarized in Table 3.20.

Table 3.20 Selected SRM transition and their optimized tandem mass spectrometric conditions for bi-derivatized and tetra-derivatized compounds.

Derivatizing reagent	SRM transition	Collision energy (eV)	Collision gas pressure (mTorr)	Ion source temperature (°C)
Bi-derivatized hydrazine				
ECF	176 → 102	6	1	225
PCF	204 → 76	8	0.8	150
IBCF	132 → 57	12	0.6	175
Tetra-derivatized hydrazine				
ECF	176 → 102	8	1.1	220
PCF	204 → 103	8	1.4	168
	204 → 76	9	1.2	169
IBCF	232 → 120	12	0.6	175
	232 → 103	12	0.9	187
	232 → 76	14	0.6	183

The selected SRM transitions in the optimized working condition were used for SPME optimization.

3.1.3.3.3 Optimization of SPME conditions

Solid-phase microextraction has undergone a surge in popularity as a quick and cost effective sample preparation technique in the last two decades. Its versatility consists mainly in the simple design that allows combined preconcentration and extraction and easy coupling with chromatographic systems as well as in the variety of extracting phases that constitute the SPME fiber assembly.¹⁴⁵ The selection of the proper SPME coating is one of the most critical steps in the development of a SPME protocol since the nature of the extraction and the affinity for the analytes of interest are governed by the extracting phase chemistry and polymeric characteristic¹⁴⁶. The affinity of five SPME coatings towards the hydrazine derivatized products was tested. The performance of 85 µm Car/PDMS (carboxen/polydimethylsiloxane), 85 µm PA (polyacrilate), 50/30 µm DVB/Car/PDMS (divinylbenzene/carboxen/polydimethylsiloxane), 65 µm PDMS/DVB (polydimethylsiloxane/divinylbenzene), and 100 µm PDMS (polydimethylsiloxane) were evaluated by direct immersion extraction. The evaluation was

performed taking into account all the optimized derivatization and mass spectrometric conditions aforementioned for the MRM transitions listed in Table 3.20. A noticeable decrease in the amount recovered was noticed relating bi-derivatized product to tetra-derivatized hydrazine peak areas. This observation led to consider only the result obtained for tetra-derivatized hydrazine for further optimizations and quantitative purposes. Data shown in Figure 3.15 clearly show that the best result in terms of peak abundances were obtained extracting the tetra-derivatized compound obtained by propyl chloroformate with PDMS/DVB coating and monitoring the transition 206→74.

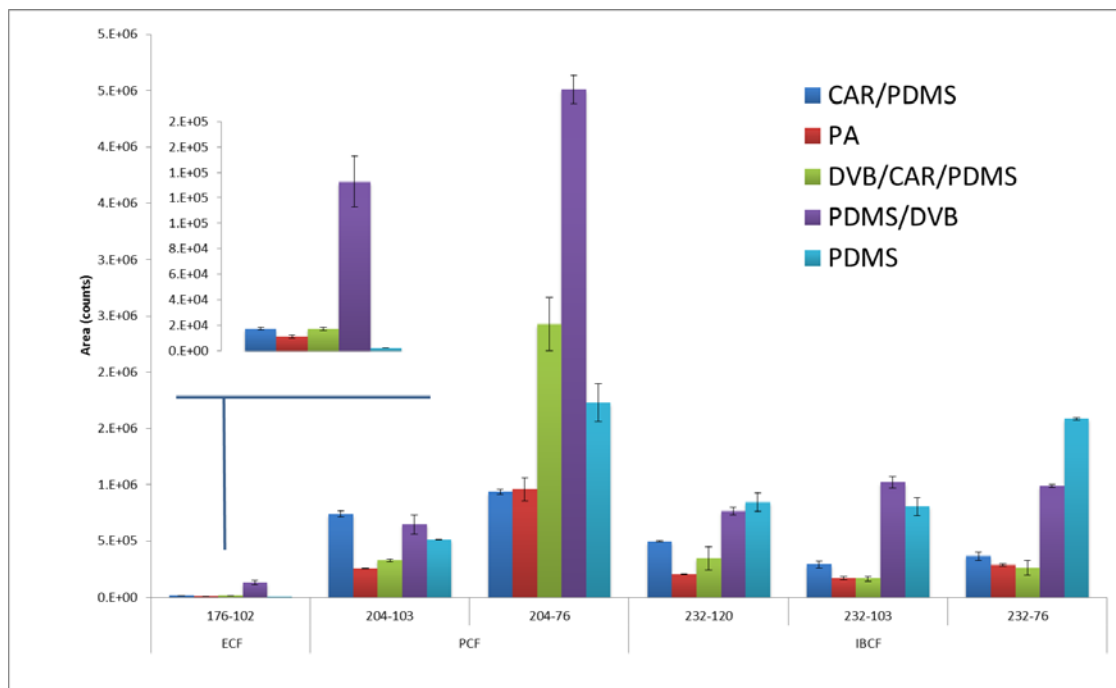


Figure 3.15 Evaluation of SPME coatings performances: peak areas for the three derivation products obtained by performing MRM analyses in immersion mode with five different coatings.

Afterward other parameters affecting SPME process were optimized: adsorption time and temperature, desorption time and temperature, sample pH and salt content and agitation of the sample. Factors affecting the kinetic of extraction and sample pH were optimized by univariate approach. At first extraction time profiles were acquired both agitating the sample and in static conditions in a range between 10 and 40 minutes, using optimized parameters discussed above and sampling from a $1\mu\text{g L}^{-1}$ aqueous solution of hydrazine.

The evaluation of the extraction time profiles revealed the achievement of equilibrium at 30 minutes of extraction for the agitated samples, on the contrary the slower mass diffusion in the samples extracted in static mode, did not provided the achievement of equilibrium even at 40 minutes and consequent lower amount extracted of the target analyte. Thus 30 minutes of extraction agitating the sample were selected as the best working conditions.

Successively three desorption time were tested (3, 5, 10 minutes): the best result in terms of desorption efficiency were achieved at 10 minutes of desorption.

Finally the influence of pH in the extraction of analytes was evaluated. Different pH levels were tested and the highest peak areas were obtained at pH 9 which matches with the pH level leading to highest yields of the derivatization reaction, as aforementioned.

All the parameter optimized as described above were used to conduct the multivariate optimization of parameters affecting the thermodynamics of solid-phase microextraction such as adsorption temperature, desorption temperature and sample salt content. For this purpose a central composite design (CCD) consisting of a factorial design 2^3 with six star points located at $\pm\alpha$ from the center of the experimental domain was performed. The value of the axial distance α for this design was 1.68 in order to establish the rotatability condition. The design was also completed with six experiments in the central point so that the number of degrees of freedom for the lack-of-fit equals that for replications. The complete design, constituted by 20 randomly performed experiments, is shown in Table 3.21 .

Table 3.21 Design matrix in the central composite design (CCD) for optimization of SPME parameters

Experiment #	Desorption Temperature (°C)	Adsorption Temperature (°C)	%NaCl
11	245	40	2.0
1	230	44	0.8
6	260	44	3.2
5	260	44	0.8
9	220	50	2.0
13	245	50	0.0
17 (C)	245	50	2.0
16 (C)	245	50	2.0
14	245	50	4.0
10	270	50	2.0
18 (C)	245	50	2.0
19 (C)	245	50	2.0
15 (C)	245	50	2.0
20 (C)	245	50	2.0
3	230	56	0.8
8	260	56	3.2
4	230	56	3.2
7	260	56	0.8
12	245	60	2.0
2	230	44	3.2

The ranges of the considered parameters were chosen according to preliminary tests: 40-60°C for adsorption temperature, 0.8-4 % for concentration (*w/w*) of NaCl and 220–270 °C for desorption temperature. The optimization of desorption temperature was conducted in order to investigate the potential degradation of the derivatization products bearing a thermolabile carbamate moiety as result of the reaction between the amino group and the alkyl chloroformate. The influence of each variable investigated and possible cross-effect among these factors on the response can be evaluated by the Pareto chart. The bar lengths in these graphs are proportional to the absolute value of the estimated effects and the factors having a significant effect on the response are those

beyond the vertical line representing 95% of the confidence interval. Pareto chart obtained for the derivatized analytes is shown in Figure 3.16.

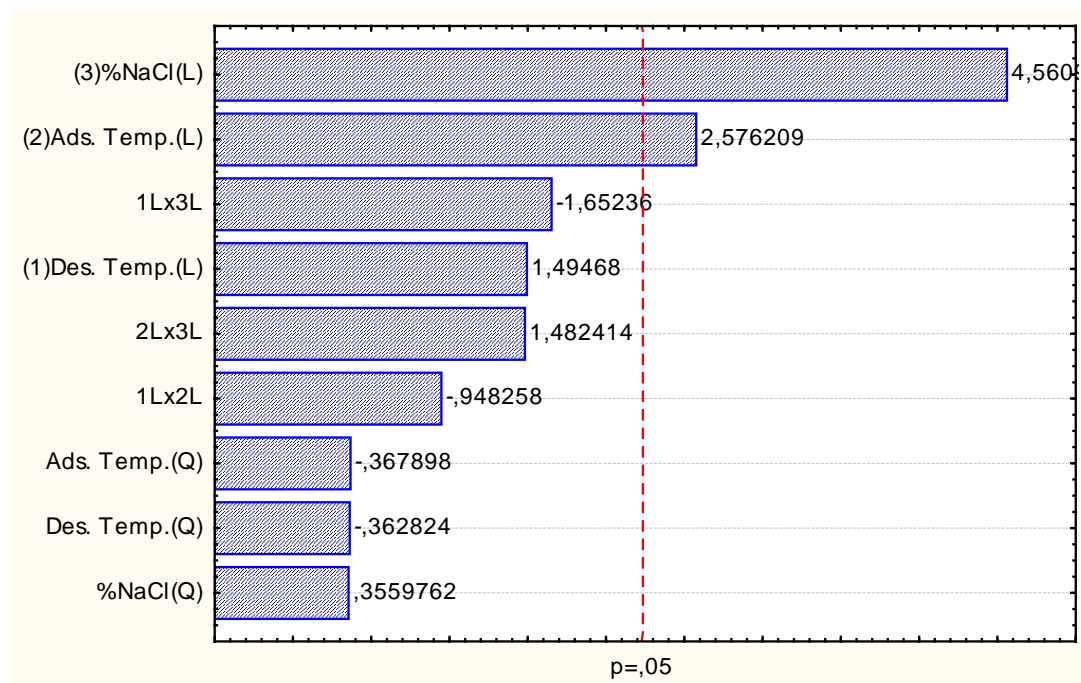


Figure 3.16 Pareto chart obtained from the central composite design for tetra-derivatized hydrazine

As easily deductible from inspection of the Pareto chart, the parameters that affect the most the response are sample salt concentration and adsorption time, the positive coefficient for these parameters indicate that the analyte response increase as their values increase.

The analysis of the response surface (Table 3.17) obtained, reveals that the optimum working conditions for the analytes of interest are 60 °C as adsorption temperature, 4% as salt concentration in the sample (*w/w*) and 220 °C as desorption temperature. However, carry over tests conducted under the fully optimized conditions from a 1 µg L⁻¹ concentrated sample revealed the presence of a peak attributable to the analytes in the successive blank analysis. For this reason, as the best compromise between thermal degradation and desorption efficiency, a temperature of 270 °C was chosen as desorption temperature.

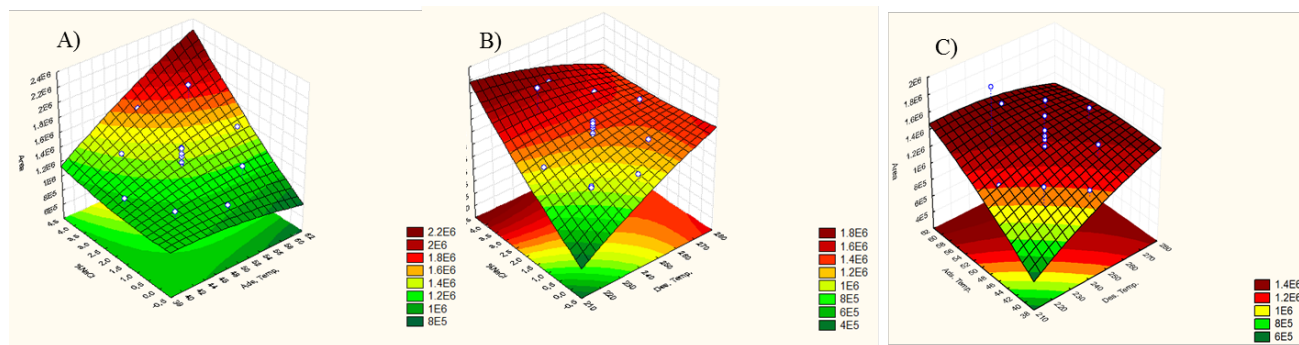


Figure 3.17 Response surfaces estimated from the central composite design for tetra-derivatized hydrazine obtained with propylchloroformate: amount of salt added versus adsorption temperature (A), amount of salt added versus desorption temperature (B) and adsorption temperature versus desorption temperature (C)

3.1.3.4 Conclusions

The use of experimental design for the optimization of derivatization, detection and extraction conditions led to the selection of specific working parameters for the determination of hydrazine in drinking water. The main advantages of the method optimized consist in the minimized use of toxic solvent for the derivatization reaction and the use of SPME allowed performing simultaneous solventless extraction and preconcentration of the analyte by a fully automatized procedure involving the final sample introduction in the chromatographic system. The use of tandem mass spectrometry also allowed the selection of selective and sensitive SRM transitions for derivatized hydrazine and its labeled analogous used as internal standard. Under the optimized conditions a semiquantitative evaluation of limit of detection and quantification was performed. LOQ and LOD were estimated to range from nanogram per liter to subnanogram per liter. Finally a fully validation of the proposed method will need to be carried out.

3.2 Solid Phase Microextraction in Food Analysis: Nutritional Values Assessment and Investigation on Solid and Ionic Liquid Based Coatings

3.2.1 Introduction

Food analysis is important for the evaluation of the nutritional value and quality of fresh and processed products. It also provides means for monitoring food additives and other toxic contaminants. It is however important to mention that sample preparation greatly influences the reliability and accuracy of results obtained from the analysis of food¹⁴⁷. In addition to applying effective sample preparation, appropriate separation and highly selective detection¹⁴⁸ systems are essential for the reliable determination of food constituents so as to avoid possible bias resulting from matrix interferences.

As a result of the complexity of food matrices, a very good sample preparation method will require a careful optimization of all the variables that could affect the extraction and separation of the food components or contaminants. It is also critical to take into account any synergistic effect among the various variables of interest. In this regard, multivariate optimization constitutes a very useful tool for studying complex systems, allowing simultaneous analysis of more than one variable without the need to carry out a large number of experiments.

Compared to other conventional methods such as liquid-liquid extraction (LLE), SPME is generally an environmentally friendly sample preparation method for the analysis of complex sample matrices. It has subsequently been used over the years to various food applications^{62,149–152}. HS-SPME in particular has been the primary choice for the sampling of food matrices over the years. An advantage of HS-SPME is that it prevents deterioration of the coatings since they are not directly exposed to the complex sample medium. However, headspace sampling presents some limitations such as the poor extraction efficiency for polar compounds having medium-to low volatility and the tendency to easily saturate the coating, when the matrix contains significant mixture of polar and very volatile compounds. To overcome this challenge, direct immersion of the fiber into the matrix showed the best results with improved coverage for both polar and very volatile compounds. Generally, with the appropriate coating, direct immersion SPME (DI-SPME) helps to avoid saturation of the coating itself and displacement effects for the most polar analytes extracted. In addition, DI-SPME basically prevents or minimizes changes in metabolites' profile captured, when compared to headspace sampling¹⁵³. For this reason efforts

are been focused on the development on new, robust coatings with enhanced matrix compatibility and suitability for direct immersion sampling of food matrices¹⁵⁴. Moreover, the development and optimization of new coatings able to selectively extract polar compounds, which are originally poorly extracted by commercial SPME coatings, is gaining interest within the scientific researchers^{155,156}.

This aspect of the thesis describes the successful application of SPME coupled to GC-MS/MS for the assessment of nutraceutical values (selenoamino acids) in potatoes by carrying out a pre-extraction derivation step directly within the matrix followed by DI-SPME. The method developed allowed the determination of free selenoaminoacid in selenized potatoes.

Also, the thesis provides further insight on adsorption behavior of solid sorbents in SPME in terms of competitive adsorption and inter-analyte displacement phenomena often occurring in food analysis. The investigation describes the impact of SPME extraction mode on competitive adsorption comparing headspace (HS) and direct immersion (DI) sampling, at different extraction times using different SPME coatings. In addition to assessing SPME commercially available solid sorbents, the recently introduced PDMS-modified coatings were compared to their non-modified analogous. To complement the investigation, a model food matrix was employed to simulate *ex vivo* and *in vivo* sampling conditions. Moreover an evaluation new polymeric Ionic Liquid for the extraction of food metabolites was carried out testing their extraction performances and comparing them to commercially SPME coatings.

3.2.2 Assessment of selenoamino acids levels in selenized potatoes by DI-SPME-GC-MS/MS⁶²

3.2.2.1 Introduction

Selenium (Se) is an essential microelement for humans assumed from vegetables, cereals (enriched or not) and Se-enriched meat¹⁵⁷. Its anti-oxidant and anti-cancer effects were verified at lower doses but it becomes toxic at higher concentrations. The range between deficiency, essentiality and toxicity is very narrow: intakes of less than 0.1 $\mu\text{g selenium g}^{-1}$ by foods result in deficiency, whereas regular consumption of food containing more than 1 $\mu\text{g Se g}^{-1}$ has toxic consequences¹⁵⁸. Selenium levels in food are highly dependent on the amount of Se in soil and on the ability of plants to take up and accumulate this element. In some areas where the amount of selenium in the soil is low, different strategies have been followed in order to supply the population with a sufficient amount of this element. One of the most used is to draw on functional foods obtained by the use of Se-enriched fertilizers. Selenium bioavailability depends on its chemical form. Generally, organic compounds of Se are more bioavailable than the inorganic analogs¹⁵⁹. Inorganic Se forms (selenite and selenate) up taken from soil are converted in vegetables in organic forms such as selenomethionine, selenocystine, γ -glutamyl selenomethylselenocystine, selenomethyl selenocysteine, selenocystathione, seleno-homocysteine and selenomethylselenomethionine¹⁶⁰. In particular selenomethionine (SeMet) is the predominant selenium species in plants and it is highly bioavailable. Moreover, SeMet can be not-specifically incorporated in body proteins and serves as a pool of SeMet, which can be drawn on at times of depletion or increasing need¹⁶¹. Another very interesting Se-organic form is the selenoamino acid selenomethylselenocysteine (SeMeSeCys) which is a good precursor of methylselenol when β -lyase is present. This Se-metabolite seems to be the most active species for cancer reduction. Therefore SeMeSeCys has been widely studied as a potential anticarcinogenic compound^{158,162,163}. Potato is one of the staple foods in many countries and Se fertilization is often used to enrich the selenium content in potato tubers. Several studies were conducted on selenium speciation in this food¹⁶⁴⁻¹⁷⁰ focused on determination and quantification of selenoamino acids and other Se-organic and inorganic compounds. These works are carried out by high performance liquid chromatography (HPLC) in conjunction with electrospray ionization (ESI) and especially with inductively coupled plasma-mass spectrometry (ICP-MS)

detectors. These studies show that, besides the inorganic moiety, SeMet and SeMeSeCys are the seleno aminoacidic species detected in potato flesh and skin. Capillary electrophoresis was also used for speciation of selenocompounds but it lacks of enough sensitivity with complex matrices. Gas chromatography technique was also applied for selenoamino acid speciation coupled with ICP-MS^{171,172}, AED¹⁷³, FPD and MIP-AES¹⁷⁴, and MS^{173,175} due to its high resolution and low instrumental cost. On the other hand, selenoamino acids are nonvolatile species and a derivatization reaction is needed before gas chromatographic analysis. For amino acids derivatization several derivatizing agent were used such as silylation reagents¹⁷⁶, fluorination reagents¹⁷⁷, and alkylchloroformates.^{48,132,137,138} Alkyl chloroformates were preferred because the derivatization reaction occurs simultaneously on amino and carboxylic acid moieties. Moreover, it is rapid at room temperature in aqueous solution instead of organic solvent. Moreover, this derivatization is compatible with the use of solid phase microextraction (SPME) that allows the extraction of analytes directly in the aqueous phase^{64,180}. The only available method for the extraction of selenoamino acids from aqueous matrices by SPME requires the use of not- commercial fiber prepared by authors and the following analyses were performed by a GC-ICP-MS system¹⁷¹.

In the present work, a new analytical method was developed for selenium speciation in potatoes by SPME-GC-triple quadrupole mass spectrometry (SPME-GC-QqQMS). Five commercial SPME fibers and three alkylchloroformates were evaluated and the variables of the SPME process were optimized by the multivariate approach of design of experiment (DoE). Furthermore the capability of tandem mass spectrometry in selected reaction monitoring (SRM) acquisition was investigated and exploited to achieve an unfailing identification and lower limits of detection¹⁴⁴. To the best of our knowledge, this is the first study based on SPME coupled to GC-MS/MS for the quantification of selenoamino acids. The method was applied to analysis of SeAA in selenized and not selenium enriched potatoes.

3.2.2.2 Experimental section

3.2.2.2.1 Chemicals

Selenomethionine and selenomethylselenocysteine standards, pyridine, and sodium chloride were purchased from Sigma-Aldrich (Milan, Italy). Selenoethionine was purchased from Toronto Research Chemicals Inc. (North York, Ontario, Canada). Methyl-, ethyl-, propylchloroformate,

methanol, ethanol and propanol were obtained from Fluka (Milan, Italy). The SPME fibers tested were purchased from Supelco (Bellefonte, PA, USA) and conditioned as recommended by the manufacturer.

3.2.2.2.2 Samples

Potato samples were purchased in local stores. Three different types of commercial potatoes, i.e. selenized, unselenized and iodine enriched potatoes were considered since they are the three most common categories of retail potatoes in Italy.

3.2.2.2.3 Instrumentation and apparatus

GC-MS analyses for the optimization of SPME variables were performed using a Varian (Walnut Creek, CA, USA) Saturn 2000 GC-MS ion-trap system in EI (electron ionization) mode, coupled to a Varian 3400 gas chromatograph equipped with a Varian 8200 autoinjector. The ion trap temperature was set at 210°C with an ionization time of 25 ms, an emission current of 10 μA , and a scan rate of 1,000 ms. The capillary column was a 30 m \times 0.25-mm inner diameter, 0.25- μm film thickness Zebron GC ZB-5 ms [95% polydimethylsiloxane (PDMS), 5% polydiphenylsiloxane]. The gas chromatograph oven temperature was initially held at 80°C for 3 min, then ramped at 12° C min⁻¹ to 250°C, and finally ramped at 50°C min⁻¹ to 280°C and held at this temperature for 5 min. The carrier gas was helium (purity 99.999%) at a flow rate of 1 mL min⁻¹. For SPME analyses, a narrow-bore Supelco 0.8-mm inner diameter gas chromatograph inlet liner was used. Analyses were performed in splitless mode and spectra were acquired in full-scan mode in a mass range of m/z 40–400. GC-MS analyses for calibration and quantification of real samples were carried out using a TSQ Quantum GC (Thermo Fischer Scientific) system constituted by a Quantum triple quadrupole (QqQ) mass spectrometer and a TRACE GC Ultra equipped with an TriPlus autosampler. The capillary column was a 30 m \times 0.25-mm inner diameter, 0.25- μm film thickness Thermo TR-5MS. The injector temperature was set at 270°C and the gas chromatograph oven temperature was programmed as the Saturn 2000 GC-MS system. Helium at a constant flow rate of 1 mL min⁻¹ was used as the carrier gas; argon at a pressure of about 1.0 mTorr was used as the collision gas. The QqQ mass spectrometer was operated in electron ionization and selected reaction monitoring (SRM) mode. The transfer line and ionization source temperatures were set at respectively at 270°C and 250°C. A filament multiplier delay of 16 min was set to prevent instrument damage. The emission

current was set at 25 μA . The scan width and the scan time were set at 0.1 m/z and 0.1 s respectively. The peak width of the first quadrupole was fixed at 0.7 amu. The transitions m/z 325 \rightarrow 188 (collision energy 8 eV) and m/z 311 \rightarrow 208 (collision energy 5 eV) for SeMet and SeMeSeCys and m/z 339 \rightarrow 188 (collision energy 11 eV) for SeEt, used as internal standard, were selected for the quantitative assay in SRM acquisition.

3.2.2.2.4 Analytical procedure

Fresh potatoes sample was blended and the homogenized was freeze-dried for a day at $-60\text{ }^{\circ}\text{C}$. According to Kotrebai et al. ¹⁸¹ 0.4 g of lyophilized potatoes was weight in a 15 mL centrifuge tube and 10 mL of high purity deionized water was added as extraction solvent. The tube was shaken for 1 minute and then the mixture was centrifuged at 4000 rpm for 20 min. Afterwards 1.5 mL of the supernatant solution was pipetted in a 10 mL vial and 30 μL of selenoethionine solution at $100\mu\text{g L}^{-1}$, used as internal standard, was added. Derivatization was carried out by adding 750 μL of a propanol and pyridine mixture (3:1 v/v) to the aqueous potato extract. The solution was then magnetically stirred for 10 min, 156 μL of propylchloroformate was added and the mixture was again stirred for 2 min.

Finally 180 μL of HCl 5M solution and 5.82 mL of high purity deionized water were added. The solution was centrifuged again at 14500 rpm for 20 min and the supernatant was collected in a 10 mL vial and an appropriate amount of NaCl was added in order to obtain a 10% (w/w) solution. SPME analysis was performed with a 50/30 μm divinylbenzene/carboxen/polydimethylsiloxane fiber. The extraction was performed in immersion mode for 20 min. The desorbing step was performed introducing the fiber in the injector set at 270°C for 10 min. In the blank analysis of the fiber, any peak related to analytes under investigation is displayed.

3.2.2.2.5 Calibration procedure

For the quantitative analysis of selenoamino acids a calibration curve was built on four different concentrations covering a range of 0.1-5 $\mu\text{g L}^{-1}$ (0.1, 0.3, 1, 5 $\mu\text{g L}^{-1}$) corresponding to 2-100 $\mu\text{g Kg}^{-1}$ (dry matter, DM) with selenoethionine used as internal standard at $1\mu\text{g L}^{-1}$. Each solution was prepared spiking aqueous solution with a known amount of stock solutions of SeMet, SeMeSeCys and SeEt and adjusting pH and NaCl percentage respectively to 2.5 and 10%. Each experimental value was obtained from the average of three independent experiments.

3.2.2.2.6 Experimental Design

Optimization of SPME parameters by design of experiment was carried out using Statistica 8.0 (2007 edition, Statsoft, Tulsa, USA).

3.2.2.3 Result and discussion

3.2.2.3.1 Derivatization and optimization of SPME conditions

Derivatization step was conducted according to the method proposed by Husek¹⁷⁸. The derivatization procedure involves the addition of few microliters of an alkylchloroformate to a solution of amino acids in aqueous alcohol with pyridine. This method allows simultaneous derivatization of both amino and carboxylic acid groups at room temperature in aqueous medium providing minimal sample handling and high reaction rate. The product of derivatization is the N(O,S)-alkyloxycarbonylalkyl ester as shown in Figure 3.18.

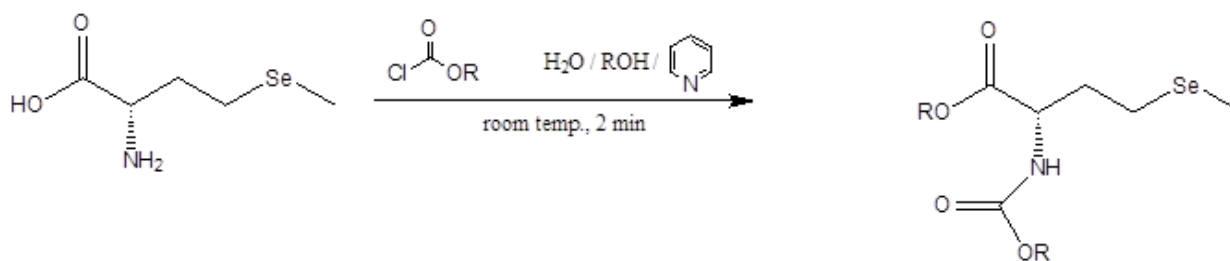


Figure 3.18 Schematic diagram of the derivatization reaction for SeMet

In the study conducted by Caruso *et al.*¹⁷¹, the efficiency of two SPME fibers (polydimethylsiloxane (PDMS) and carboxen/polydimethylsiloxane (Car/PDMS)) in preconcentration of three selenoamino acids (SeMet, SeCys and SeEt) was tested for aqueous samples in both headspace and immersion mode. Analytes were derivatized with ethyl and isobutylchloroformate in a proper mixture of alcohol and pyridine and no results were obtained in headspace mode due to low volatility of the derivatized compounds. On the other hand, the use of Car/PDMS fiber in immersion mode exhibited a progressive deterioration of coating and then, because of these limitations, the not commercial sol-gel PDMS fibers were investigated. In the first part of our work, in order to obtain more volatile compounds, selenoamino acids (SeMet and SeMeSeCys) were derivatized with methylchloroformate in a mixture of methanol and

pyridine and the performance of three SPME fibers with different extraction affinity (polydimethylsiloxane (PDMS), polyacrilate (PA) and divinylbenzene/carboxen/polydimethylsiloxane (DVB/Car/PDMS)) was tested in headspace sampling mode. No results were obtained after 30 min of adsorption of potato extract spiked at 5 mg L^{-1} and other attempts of stirring or heating the solution were unsuccessful. Therefore, sampling by immersion was necessary. Extraction efficiency tests on five commercial available fibers (85 μm Car/PDMS, 85 μm PA, 50/30 μm DVB/Car/PDMS, 65 μm PDMS/DVB, and 100 μm PDMS) were carried out with different extraction times in aqueous solution spiked at 5 mg L^{-1} . Overall, fibers show the best results in terms of chromatographic peak areas after 10 min of adsorption, and then this extraction time was chosen for further analysis. To evaluate the deterioration of SPME fibers due to derivatizing reagents in potato extract mixture, fifteen consecutive analyses were carried out by the investigated fibers for ethyl esterified analytes. A progressive deterioration of the coating was noted and not reproducible data were obtained after fifteen analyses in according with results obtained by Caruso *et al.*¹⁷¹. To avoid coating degradation a simple fourfold dilution of the sample was performed with ultrapure water^{60,61}. Results show that water dilution allows preserving the coating extending fiber lifetime and, as a consequence, to obtain a good compromise between method sensitivity and preservation of polymer fiber. The next step was to address the choice of the SPME fiber and derivatization mixture that provide the best analytical performance. For this purpose, the five commercially available fibers previously tested for coating degradation study were used along with three derivatizing reagents (methylchloroformate, ethylchloroformate, propylchloroformate with the respective mixtures of alcohol and pyridine). Analyses were carried out in immersion mode in potato extract spiked at 5 mg L^{-1} at room temperature and with 10 min of extraction time. The highest peak areas were obtained for both analytes with DVB/Car/PDMS fiber and propylchloroformate as shown in Figure 3.19 and then these fiber and derivatizing reagent were chosen for the following screening and optimization designs.

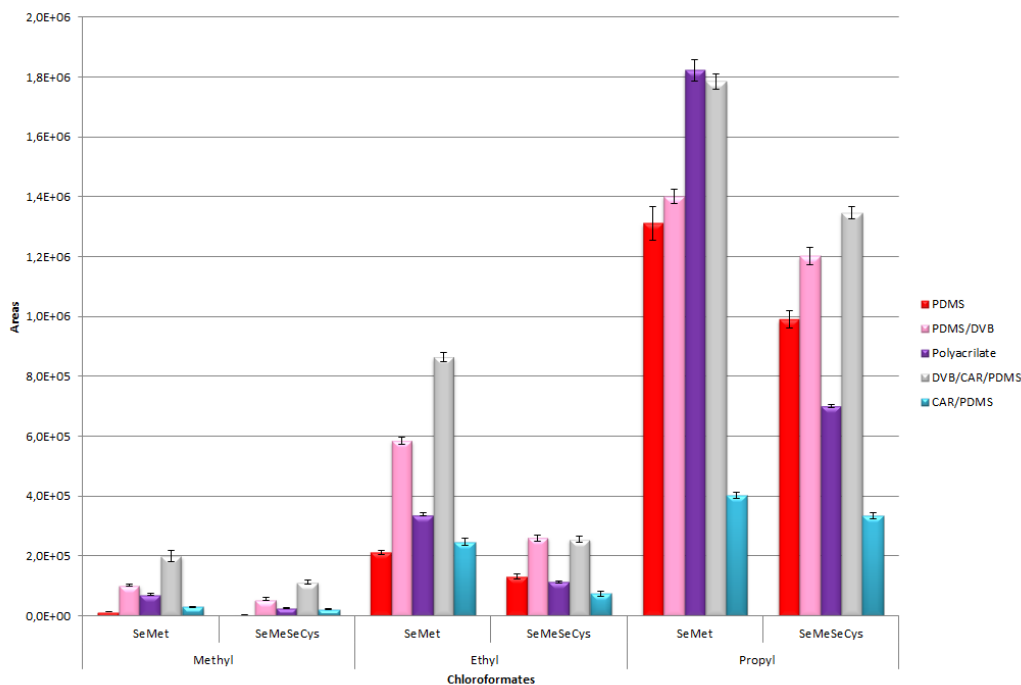


Figure 3.19 Peak areas obtained for SeMet and SeMeSeCys derivatized with three alkylchloroformates and extracted by immersion mode with five SPME fibers.

The experimental parameters studied by the multivariate approach of design of experiment (DoE) to obtain the best experimental conditions of SPME analysis were: desorption temperature, sodium chloride addition and pH. It was decided to include desorption temperature since N(O,S)-propyloxycarbonylpropyl ester derivatives could behave as thermally labile compounds due to the presence of the carbamate moiety. Kinetic variables such as extraction time and agitation effect were left for a further study. A Central composite design (CCD) consisting of a factorial design 2^3 with six star points located at $\pm\alpha$ from the center of the experimental domain was performed for DVB/Car/PDMS fiber using propylchloroformate as derivatizing reagent. The value of the axial distance α for this design was 1.68 in order to establish the rotatability condition. The design was also completed with six experiments in the central point so that the number of degrees of freedom for the lack-of-fit equals that for replications. Therefore, the complete design consisted of 20 randomly performed experiments (design matrix shown in Table 3.22).

Table 3.22 Matrix of the central composite experimental design

Experiment	pH	Desorption temperature (°C)	%NaCl
18(C)	5	250	5
6	6.5	238	8
9	2.5	250	5
16(C)	5	250	5
19(C)	5	250	5
13	5	250	0
3	3.5	262	2
4	3.5	262	8
15(C)	5	250	5
20(C)	5	250	5
11	5	230	5
14	5	250	10
8	6.5	262	8
1	3.5	238	2
12	5	270	5
5	6.5	238	2
10	7.5	250	5
17(C)	5	250	5
7	6.5	262	2
2	3.5	238	8

The ranges of the considered parameters were chosen according to preliminary tests: 2.5–7.5 for pH, 0–10% for concentration of NaCl and 230–270°C for desorption temperature. All the designed experiments were carried out using an aqueous potato extract spiked at 5 mg L⁻¹ for both selenoamino acids. The influence of each factor investigated and possible cross-effect among these factors on the response was evaluated by the Pareto chart. The bar lengths in these charts are proportional to the absolute value of the estimated effects and the vertical line represents 95% of the confidence interval. Therefore, the factors crossing this line had a significant effect on the response. The Pareto charts obtained for SeMet and SeMeSeCys were shown in Figure 3.20.

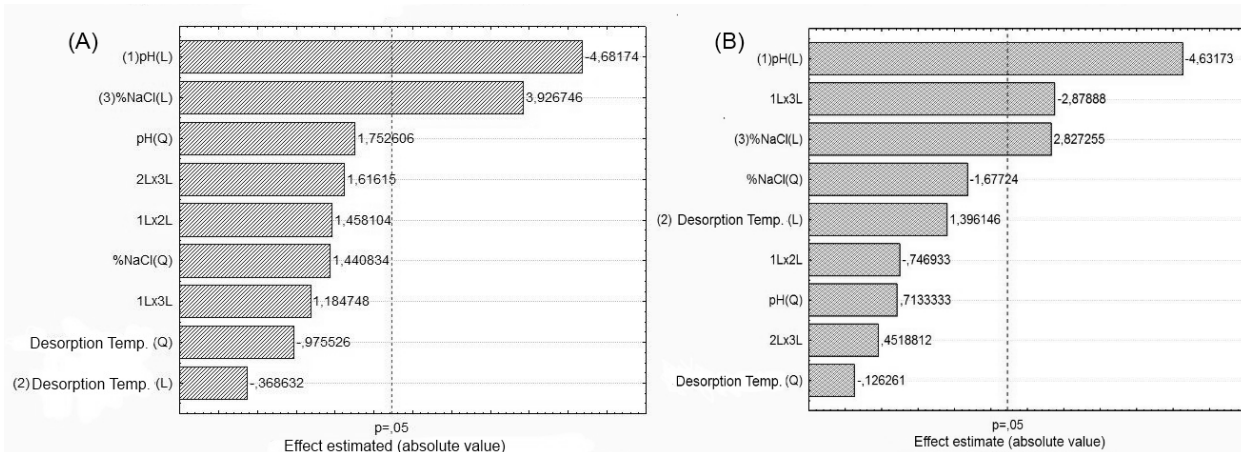


Figure 3.20 Pareto charts obtained from central composite design for A) SeMeSeCys and B) SeMet

As can be seen, concentration of NaCl with positive sign and pH of solution with negative sign were significant ($p < 0.05$) for the response of both analytes whereas desorption temperature can be considered not significant respect to response. Moreover, the interaction term of pH and % NaCl gave also an important effect to the signal of SeMet. To evaluate the trends of the three considered factors, response surfaces were drawn in Figure 3.21.

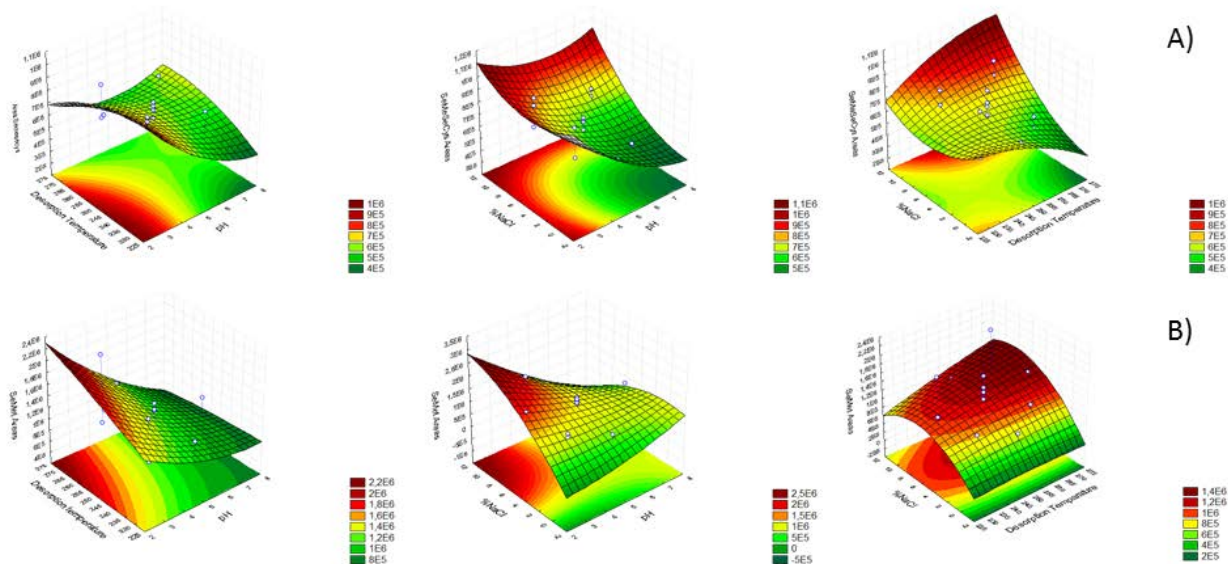


Figure 3.21 Response surfaces obtained for A) SeMeSeCys and B) SeMet from the central composite design: peak area of derivatized selenoamino acids for desorption temperature versus pH, versus pH and desorption temperature versus % NaCl

The optimum working conditions should be a compromise between the responses of the two analytes. In order to convert a multi-response problem into a single-response one, the Derringer's desirability function was used¹⁰⁵. The optimum working conditions in terms of desirability score were achieved at the following values: pH = 2, desorption temperature 270°C, 10% of NaCl. According to the literature^{182,183}, the kinetic variables that potentially affect extraction efficiency, as sample stirring and adsorption time, were tested by univariate approach. A sample of aqueous potato extract spiked at 1 mg L⁻¹ of both analytes was analyzed using the optimized SPME conditions and applying different extraction times (5, 10, 20, 30, 40, 60 min), with and without sample agitation. The best response was obtained stirring the solution during the adsorption and after 40 min of extraction time. The signals of derivatized analytes began to decrease after 40 min of adsorption time. This trend could be justified as a result of modification of the fiber coating due to the relatively high amount of pyridine present in the solution, already observed by Caruso *et al.*¹⁷¹. The chromatograms obtained after 40 min of extraction and acquired in full-scan mode revealed that a large amount of interfering compounds was adsorbed on fiber coating. A lack of reproducibility was noted after a series of analyses carried out in these conditions,

probably due to adsorption of interfering compounds which contaminate irreversibly the coating. Therefore an extraction time of 20 min was selected for further experiments as a compromise among sensitivity, reproducibility and fiber coating extraction efficiency.

3.2.2.3.2 GC-QqQ-MS/MS analysis

A GC-QqQ analytical system permits to carry out experiments in selected reaction monitoring (SRM) that represents a very useful acquisition mode especially when food matrices are involved. Indeed, this mass spectrometric method increases the sensitivity by reducing the noise of acquisition and, at the same time, without losing the capability of identifying the analytes unambiguously. For the analysis in SRM mode, the parent ion has to be properly chosen to obtain the highest sensitivity and specificity and then the full scan spectra of analytes and selenoethionine were acquired. The latter compound was selected as internal standard because it does not occur naturally in potatoes and was already used in another work for selenoamino acids determination in vegetables¹⁷⁹. The mass spectrum of SeMeSeCys propyl derivative presents the typical selenium isotopic pattern for the molecular ion (m/z 311) and this pattern is retained in the other fragments containing selenium (Figure 3.22-A). The fragment at m/z 224 was attributed to $M-COOCH_2CH_2CH_3$ whereas that at m/z 208 (base peak) is due to the loss of the group $NHCOOCH_2CH_2CH_3$ from the molecular ion. The ion at m/z 193 is a species probably obtained by the loss of a CH_3 group from the fragment at m/z 208 whereas the ion at m/z 166 can be interpreted as the product of McLafferty rearrangement on the same ion (m/z 208). Finally, the peak at m/z 138 could arise from the molecular ion by the loss of $NH_2CHCH_2SeCH_3$ group. The mass spectrum of SeMet propyl derivative (Figure 3.22-B) is very similar to that of N-ethoxycarbonylethylester derivative published by Iscioglu *et al.*¹⁷⁵. In particular, the spectrum presents the typical selenium isotopic pattern for the molecular ion (m/z 325) and ion at m/z 238 ($[M-COOCH_2CH_2CH_3]$). The peak at m/z 265 arises from the loss of propanol whereas that at m/z 230 can be attributed to the loss of $SeCH_3$ group from the molecular ion. The intense peak at m/z 203 was attributed to the loss of $CH_2CH_2SeCH_3$ group. The peaks at m/z 188 and 101 could be justified by the loss of a CH_3 group from m/z 203 and the loss of group $COOCH_2CH_2CH_3$ from the ion at m/z 188, respectively. Finally, the base peak (m/z 142) should be due to the loss of $COOCH_2CH_2CH_3$ and $SeCH_3$ groups from molecular ion. The mass spectrum of SeEt ester shows a fragmentation similar to that of SeMet propyl derivative (Figure 3.22-C).

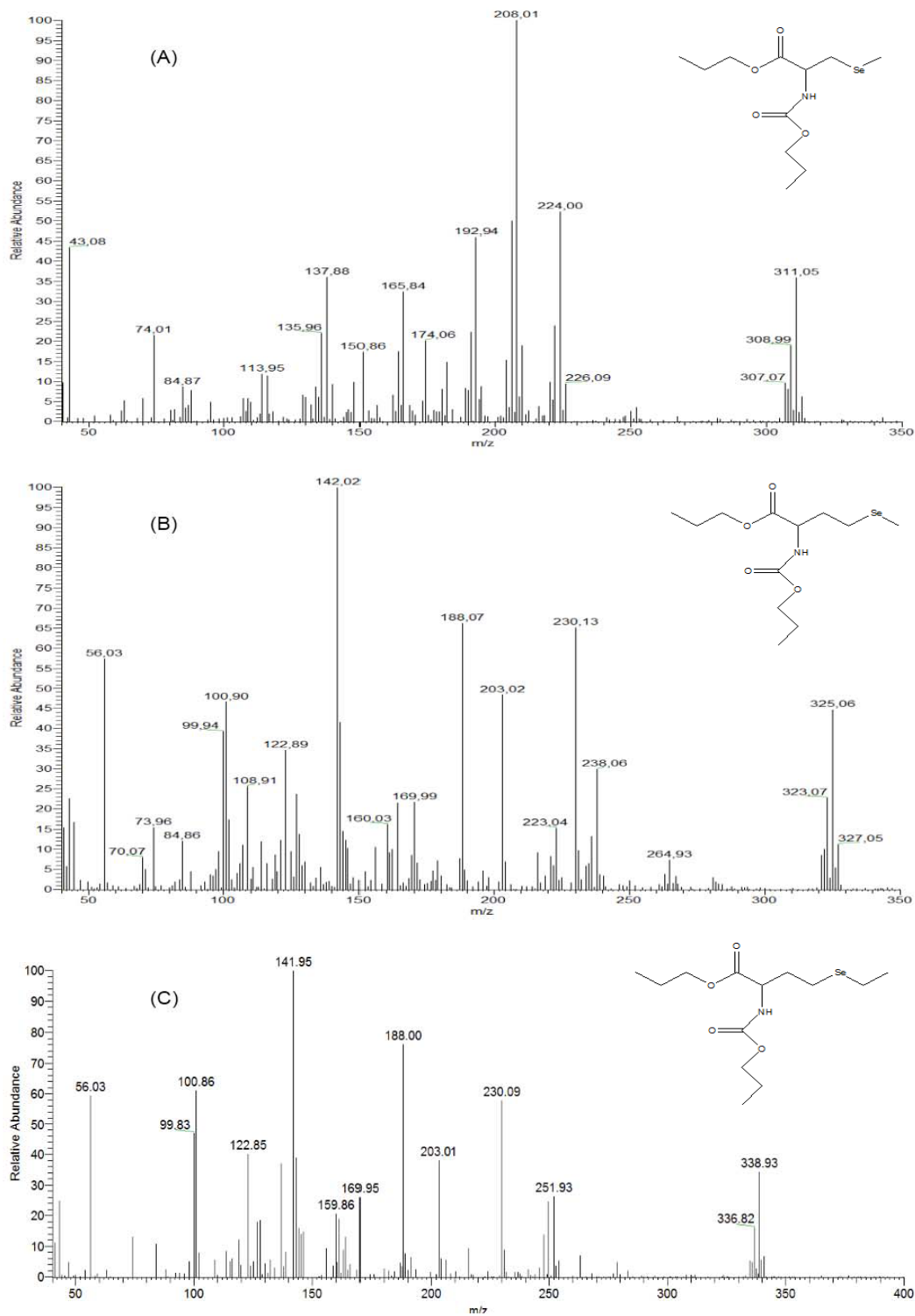


Figure 3.22 Electron ionization (EI) full-scan spectra of (A) SeMeSeCys (B) SeMet and (C) SeEt.

For both analytes and internal standard molecular ions (m/z 311 for SeMeSeCys, m/z 325 for SeMet and m/z 339 for SeEt) were selected as precursor ions and product ion spectra were acquired by collision-induced dissociation (CID) using argon as collision gas (Figure 3.23).

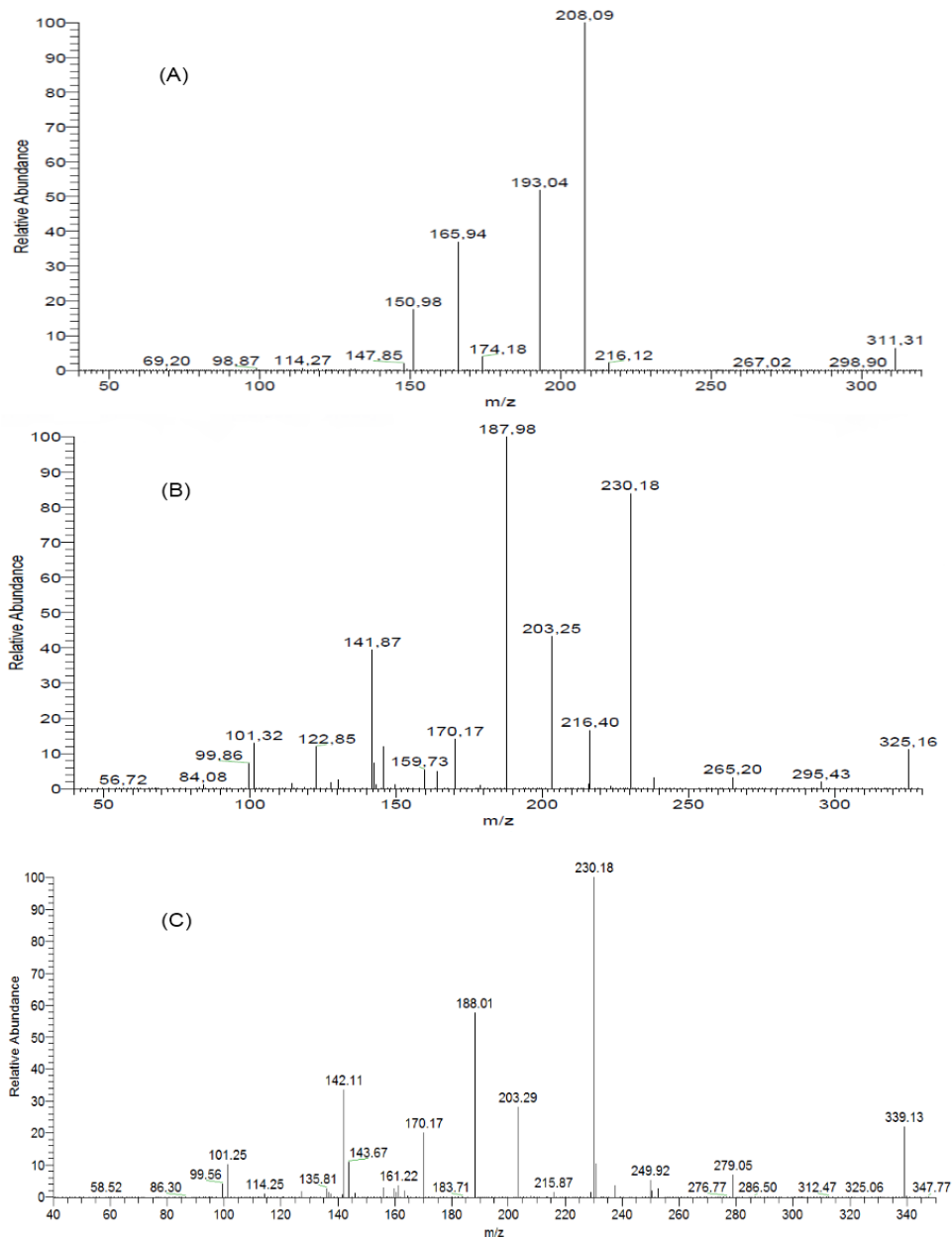


Figure 3.23 EI-MS/MS spectra of SeMeSeCys, SeMet and SeEt with parent ion at m/z 311 (A), m/z 325 (B) and m/z 339 (C).

Two SRM transitions were evaluated for each precursor ion (m/z 311 \rightarrow 208 and m/z 311 \rightarrow 193 for SeMeSeCys; m/z 325 \rightarrow 230 and m/z 325 \rightarrow 188 for SeMet; m/z 339 \rightarrow 230 and m/z 339 \rightarrow 188 for SeEt) by selecting both 70 eV and 40 eV as ionization energy. Collision energies (CEs) were optimized for each SRM transition (Table 3.23).

Table 3.23 SRM transition evaluated and optimum values of collision energy

	Ionization Energy (eV)	SRM transition	Collision Energy (eV)
SeMeSeCys	70	311 \rightarrow 208	5
	40	311 \rightarrow 208	5
	70	311 \rightarrow 193	8
	40	311 \rightarrow 193	11
SeMet	70	325 \rightarrow 230	8
	40	325 \rightarrow 230	8
	70	325 \rightarrow 188	8
	40	325 \rightarrow 188	11
SeEt	70	339 \rightarrow 230	7
	40	339 \rightarrow 230	8
	70	339 \rightarrow 188	11
	40	339 \rightarrow 188	13

The best results in term of peak intensity and signal to noise ratio were obtained selecting the transition m/z 311 \rightarrow 208 for SeMeSeCys, 325 \rightarrow 188 for SeMet and 339 \rightarrow 188 all with 70 eV as ionization energy. Linearity was studied in the range of 0.1–5 $\mu\text{g L}^{-1}$ corresponding to 2–100 $\mu\text{g kg}^{-1}$ (dry matter) in 10% NaCl aqueous solutions containing 1 $\mu\text{g L}^{-1}$ of selenoethionine used as internal standard. Correlation coefficient (R^2) values of 0.9960 and 0.9954 were obtained for SeMeSeCys and SeMet, respectively (Table 3). Recovery and precision were evaluated at two concentrations (0.4 and 2 $\mu\text{g L}^{-1}$ corresponding to 8 and 40 $\mu\text{g kg}^{-1}$ DM) in aqueous potato extract by analyzing a spiked sample three times. Since a matrix free of studied selenoamino acids does not exist, the standard addition method was applied to the same potato sample subjected later to recovery tests.

Table 3.24 Summary of calibration parameters, mean accuracies (%), relative standard deviation RSD (N=3), % in parenthesis and limits of detection (LODs) and limits of quantification (LOQs).

	Calibration range $\mu\text{g Kg}^{-1}$ (DM)	Curve	R^2	8 $\mu\text{g Kg}^{-1}$	40 $\mu\text{g Kg}^{-1}$	LOD $\mu\text{g Kg}^{-1}$ (DM)	LOQ $\mu\text{g Kg}^{-1}$ (DM)
SeMet	2-100	$Y=0.3556x-0.0225$	0.9960	82.3 (9.6)	112.1 (11.9)	0.143	0.292
SeMeSeCys	2-100	$Y=0.4559x-0.0515$	0.9954	99.0 (8.5)	116.3 (13.1)	0.210	0.588

Therefore, after assaying the SeAA naturally present, the remaining amount to achieve concentration values of 8 and 40 $\mu\text{g kg}^{-1}$ dry matter (0.4 and 2 $\mu\text{g L}^{-1}$) was added to the same potato sample. The recovery values (82.3% and 112.1% for SeMeSeCys; 99.0% and 116.3% for SeMet) and the relative standard deviations (9.6% and 11.9% for SeMeSeCys; 8.5% and 13.1% for SeMet) obtained are to be considered in the range generally accepted (Table 3.24). The limit of detection (LOD) and the limit of quantitation (LOQ) were calculated following the directives of IUPAC and the American Chemical Society's Committee on Environmental Analytical Chemistry, that is, as follows for SeMet) obtained are to be considered in the range generally accepted (Table 3.24). The limit of detection (LOD) and the limit of quantitation (LOQ) were calculated following the directives of IUPAC and the American Chemical Society's Committee on Environmental Analytical Chemistry, that is, as follows:

$$S_{LOD} = S_{RB} + 3\sigma_{RB} \quad (3.5)$$

$$S_{LOQ} = S_{RB} + 10\sigma_{RB} \quad (3.6)$$

where S_{LOD} is the signal at the limit of detection, S_{LOQ} is the signal at the limit of quantitation, S_{RB} is the signal of the blank of a potato extract, and δ_{RB} is the standard deviation for the same blank. In particular, the S_{RB} values were determined from the chromatogram baseline immediately before the elution of the SeAA. The LOD and LOQ values obtained on dry matter basis (0.143 and 0.292 $\mu\text{g kg}^{-1}$ for SeMeSeCys; 0.210 and 0.588 $\mu\text{g kg}^{-1}$ for SeMet) can be considered very satisfactory.

3.2.2.4 Application to real samples

The method developed was applied to assay SeMet and SeMeSeCys content in retail potato samples. For each category the survey was spread over three production lots and the amounts of selenoamino acids were compared. Fig. 7 shows the SRM chromatograms for typical samples of not-enriched selenium (A) and selenized potatoes (B). The mean concentration values of free SeMet and SeMeSeCys found in selenized potatoes were $2032 \pm 434 \mu\text{g kg}^{-1}$ and $719 \pm 318 \mu\text{g kg}^{-1}$, respectively. Significant lower contents were found in not-enriched potatoes ($26.4 \pm 6.9 \mu\text{g kg}^{-1}$ of SeMet and $6.94 \pm 3.05 \mu\text{g kg}^{-1}$ of SeMeSeCys) and iodine-added potatoes ($49.7 \pm 14.4 \mu\text{g kg}^{-1}$ of SeMet and $6.92 \pm 1.55 \mu\text{g kg}^{-1}$ of SeMeSeCys). It is worth highlighting that in all samples the selenium enrichment leads to an increase of both free selenoamino acids and their relative ratios are roughly maintained.

3.2.2.5 Conclusion

A method for the assay of the selenoamino acids present in potatoes, selenomethionine and selenomethylselenocysteine, was developed by SPME-GC-QqQ MS analysis following a preliminary derivatization using propylchloroformate/propanol mixture. The variables influencing the efficiency of SPME analysis were reliably optimized by the multivariate approach of experimental design. The joint use of SPME and GC-tandem mass spectrometry in SRM acquisition, applied for the first time in the SeAA determination, permitted to fulfill an important goal of this work: the possibility of analyzing selenoamino acids by employing an available commercial instrument as GC-triple quadrupole MS even in complex matrix such as potatoes. Indeed, the good performances in terms of linearity, recovery, precision, LOD and LOQ values, make the method developed capable of a reliable assay of SeAA, without using not commercial and more complicated systems such as HPLC-ICP-MS and GC-ICP-MS. The application of the proposed method to commercial samples of selenized and not selenium enriched potatoes proved that the Se fertilization increases significantly the concentration of these bioavailable selenoamino acids. The protocol could be applied to other food matrix in order to evaluate the amount of free selenoamino acids in their aqueous extracts.

3.2.3 Headspace versus direct immersion solid phase microextraction (SPME): investigation of inter-analyte displacement phenomena and consideration for food matrices

3.2.3.1 Introduction

Since its introduction solid phase microextraction¹⁸⁰ has constitute one of the most user-friendly, time saving, easily automatable and green sample preparation technique available on the market. SPME has successful spread its fields of applicability to clinical, environmental and food applications.^{9,63,67,68,184,185}

In particular, regarding food-related investigations, this sample preparation technique has allowed the achievements of admirable results in terms of nutraceutical values assessment⁶², traceability purposes^{150,186}, investigation of aroma composition of food and essential oils^{187–189}, and recently also characterization of fruit metabolome¹⁵³.

The potential applications of the technique have been broadened since the introduction of solid adsorbents as SPME coatings by Supelco in 1998. The utility and improved efficiency of these coating were readily confirmed, and their use quickly diffused for copious applications¹⁹⁰. The main advantage in the use of these coating is their better suitability for trace analysis as well as the broader mass molecular range of compounds efficiently sampled¹⁹¹.

The mechanism that governs the extraction process is adsorption on the active surface of the solid coatings that are characterized by having high degree of porosity (meso and micropore) and high specific surface area (ranging approximately from 750 to 950 m² g⁻¹)¹⁹².

The interactions between analytes and active surface of the coating happen by physisorption that involves interaction such as Van der Waals and electrostatic forces. The entire process is exothermic and its activation energy is associated to the analyte's transfer between the solution and the coating. The use of solid sorbent for food analysis applications has gained important attention, especially for untargeted investigations such as metabolomic profiling¹⁵³.

However, the use of solid coating can lead some drawbacks related to selection of the extraction mode and the complexity of the matrix that needs to be analyzed. During the years, most common practice in the use of SPME for food analysis has involved the exposure of the coating in the headspace above the sample matrix^{103,186,188,193–198}. The extraction in the vapor phase has been mainly preferred when complex food matrices have been analyzed in order to prevent the

attachment of high molecular weight compound to the external surface of the coating that can lead to rapid deterioration of the coating, bias in the extraction efficiency and possible formation of artifacts when desorption is performed in gas-chromatographic injector port systems^{154,199}.

Notwithstanding, the advantages of headspace sampling in terms of coating lifetime, when matrices having very complex aroma profile are analyzed, the headspace above the sample is readily enriched by compounds having poor water solubility and high Henry's law constant. Conversely, the kinetic of the mass transfer from the solution to the headspace can have a much slower kinetic for more polar compounds due to their mass resistance to the interface liquid-headspace. This imply that volatiles compounds are extracted faster than semi-volatiles since they are present in higher concentration in the headspace and this lead to faster mass transport rates through the headspace. For this reasons, especially in pre-equilibrium conditions the extraction of semi-volatiles polar compound can be seriously affected and a not accurate profile of the actual chemical composition of the matrix investigate can be obtained. The kinetic for polar and semivolatiles compounds improves drastically in when direct exposure of the coating is performed directly in the matrix bulk. This allows performing extractions that are able to give comprehensive results in terms of analyte coverage¹⁴⁹. Recent studies demonstrated that DVB/PDMS solid coating is much more effective than PDMS (liquid coating) for the extraction of pesticides in grape pulp, however the liquid coating showed much more robustness towards a series of extractions. The solid coating indeed showed a drastic decrease in extraction efficiency due to precocious deterioration of the external coating surface, due to irreversible attachment of matrix interferences.¹⁵⁴ On the light of those results a new matrix-compatible SPME coating was developed. A thin layer of PDMS surrounding the solid adsorbent prevents the rapid fouling of the coating making it suitable for a long series of extraction directly exposing the extraction phase in the food matrix¹⁵⁴. Once highlighted all the advantages in using solid SPME coatings and how new strategies were adopted in order to extend their usage for direct immersion analysis is necessary to mention and call the attention on one of the main drawbacks occurring by the use of this coatings. Adsorption takes place on the active surface of the porous structured coating, hence saturation phenomena are likely to occur when the complex composition of the matrix lead to the adsorption of high concentrations and/or high number of analytes till occupying all the adsorption sites available on the coating. At this point, since the adsorption can be defined a competitive phenomenon,²⁰⁰ compound bearing stronger affinity for the coating start to gradually

displace from the coating less affine analytes. This phenomenon affects calibration procedure by SPME and has been theoretically studied and modeled for a two-analytes system by Gorecki et al.²⁰¹ The occurrence of analytes displacement is a well-known phenomenon when dealing with multi component systems, and it has already been reported in literature for environmental and food application.^{193,202,203}

In food applications, the phenomenon has been mainly reported for HS-SPME: Risticovic *et al.* reported such behavior when profiling apple aroma using a DVB/Car/PDMS coating²⁰⁴, Contini *et al.* reported displacement effects for the analysis of volatile composition of Italian extra virgin olive oil using a PDMS/DVB coating¹⁹³ and Roberts *et al.* also reported such inter-analyte competition towards a Car/PDMS coating for the determination of volatiles flavor compounds from coffee¹⁹⁴.

The present study aims to give a further and complementary contribution to understand the inter-analyte displacement phenomenon, as well as to the optimization of the SPME protocol, especially in food investigations, showing which coating and extraction mode is better suitable to guarantee most accurate results.

Many factors have been taken in consideration in the present study such as extraction time, matrix composition and coating chemistry; however, the most important results were obtained comparing different extraction modes at the same working conditions in order to simulate in-vivo and ex-vivo (both DI and HS) extractions. The outcomes of this study give a better understanding of the phenomenon and reveal the suitability of in-vivo extractions performed with the new PDMS-modified coatings in order to minimize the competitive adsorption and obtain reliable results when studies of complex matrices are performed.

3.2.3.2 Experimental

3.2.3.2.1 Chemicals and Materials

Analyte standards were obtained from Sigma-Aldrich (Oakville, Canada) and they were all of purity > 97 %. HPLC grade methanol and obtained Supelco (Oakville, Canada).

Commercial SPME fibre assemblies in 23-gauge needle sizes and automated formats, 100 µm PDMS (stable flex), 65 µm PDMS/DVB (stableflex), 85 µm Car/PDMS (stableflex), 50/30 µm DVB/Car/PDMS (stableflex), were obtained from Supelco (Oakville, Canada).

The PDMS modified coating where prepared according the procedure described by Souza Silva *et al.*¹⁵⁴

Automated SPME holder and 10- and 20 mL screw cap vials were purchased from Supelco (Oakville, Canada).

The starch gels at different percent of water where prepared using unmodified starch purchased from Sigma-Aldrich (Oakville, Canada). For the preparation of all the samples and the starch gels ultra pure water was used.

3.2.3.2.2 Standards and Samples Preparation

Individual stock solutions (2.5 mg/mL) of each analyte were prepared in methanol and acetone. A stock mixture standard solution and subsequent working dilutions were prepared in methanol, and stored in a freezer at -30°C. The concentration of each analyte was carefully set in order to guarantee enough sensitivity for all analytes with all the coating tested both in DI and HS extractions, without changing the amount spiked in the samples and ensure the same working condition for the evaluation of all the coatings tested.

A summary of all the probe compounds with their physical-chemical characteristic and the quantitation ions are shown in Table 3.25

Table 3.25 Target metabolites and their physicochemical properties: molecular weight, log Kow , boiling point, EI quantification ion.

Analyte	MW (g/mol)	log K _{ow}	B.P. (°C)	Henry's Law constant (atm*m ³ /mol)	Quatitation ion (m/z)
benzene	78.11	2.0	78.8	5.39*10 ⁻³	78
1-pentanol	88.15	1.3	136.9	1.33*10 ⁻⁵	55
ethyl butanoate	116.16	1.8	125.7	4.10*10 ⁻⁴	88
2-hexanone	100.16	1.3	118.7	9.30*10 ⁻⁵	58
benzaldehyde	106.12	1.5	178.1	1.34*10 ⁻⁵	105
acetophenon	202.00	1.6	201.9	9.81*10 ⁻⁶	105
2-undecanone	170.30	4.1	224.1	4.78 *10 ⁻⁴	58
ethyl nonanoate	186.30	4.3	229.7	1.69*10 ⁻³	88
1-undecanol	172.31	4.2	256.2	7.26*10 ⁻⁵	55
eucalyptol	154.25	2.8	174.0	2.04*10 ⁻⁴	154
alpha-pinene	136.24	4.4	157.3	1.07*10 ⁻¹	93

3.2.3.2.3 Preparation of Starch Dispersions and Gels

For the gelatinized systems, an initial pregelatinized starch dispersion was prepared at 2% (w/w) in distilled water (0.02% NaN₃), by mixing for 10 min at room temperature and then heating in a bath at 95 °C for 30 min. After cooling, aliquots of this dispersion were transferred into the 120 mL flasks, and then native starch was added to prepare dispersions at different concentrations (2.5, 5, 10 w/w). This procedure was used to minimize sedimentation of starch granules during the extractions according to the procedure described by Lopes Da Silva *et al.*²⁰⁵. Addition of the aroma compounds was done after this step. The gelatinized samples were prepared by heating dispersions prepared as described above, with or without the aroma compounds, in a bath at 95 °C for 10 min, under gentle stirring, and then cooling to 20 °C. For the preparation of the sample for HS and DI dynamic extraction the gel was blended and aliquots were moved in each vial. The samples for DI static extractions were prepared carrying out the gelatinization of the starch dispersion directly in-vial, so the starch gel was directly analyzed.

3.2.3.2.4 SPME procedure

The sample were prepared and analyzed fresh in order to avoid degradation of the compounds tested as reported by Risticvic *et. al* in DI and HS-SPME²⁰⁴. The extraction temperature and agitation speed were set at 30 °C and 500 rpm respectively. The extraction times evaluated were 15, 30 and 60 min; the incubation time was set at 0, 2 and 20 min for DI-static, DI-dynamic and HS extractions respectively. For the HS extraction the volume of HS was kept equal to the volume of matrix in order to avoid phenomena of concentration or dilution of the analytes in the headspace. For all the coating tested, desorption in the injector port of the GC-MS was performed for 10 min in splitless mode at a desorption temperature set at maximum recommended coating temperature. Desorption efficiency was tested performing blanks of the coatings immediately after the analysis and keeping the coating sealed at 4°C before the blank injection.

3.2.3.2.5 Instrumentation

A Hewlett Packard 6890/5973 GC-MS equipped with a split/splitless injector and a CTC Combipal autosampler for automated SPME (CTC Analytics AG) was used.

The capillary column used for the chromatographic separation was a J&W DB5-MS UI (30 m, 0.25 mm i.d., 0.25 µm film thickness). The column temperature program was initially set at 35 °C for 6 min, ramped at 20 °C/min to 140 °C then, ramped at 40 °C/min to 260°C , where it was held for 2 min giving a total run time of 16.25 min. Helium was used as carrier gas and its flow set at 1.2 ml/min. The mass spectrometer working conditions were: electron ionization (EI) 70eV, mass range 50-350 m/z ion source temperature: 230 °C; quadrupole temperature: 150 °C transfer line temperature: 280°C.

3.2.3.2.6 Result and discussion

The approach presented in this work aims to show how the occurrence of competitive adsorption and displacement effects can vary according to extraction mode (DI or HS), extraction time and coating used.

Competitive adsorption affect only solid SPME sorbents which consist of porous particles suspended into a liquid polymer, e.g., PDMS, for this reason the amount of analytes extracted is limited by the number of sorption sites available for adsorption. If substantially occupied, competition between the analytes occurs, where analytes presenting higher affinity for the

coating will displace analytes bearing lower K_{fs} values²⁰¹. As reported by Gorecki *et al.* a mathematical description of the phenomenon for a two compound system is presented below, where B is the competing analyte toward the adsorption of the compound A.

$$C_{fA}^{\infty} = \frac{C_{fmax}K_A C_{sA}^{\infty}}{1 + K_A C_{sA}^{\infty} + K_B C_{sB}^{\infty}} \quad (3.7)$$

Where C_{fA}^{∞} and C_{fB}^{∞} , C_{sA}^{∞} and C_{sB}^{∞} represent the equilibrium concentrations on the fiber and in the sample of the analyte A and B respectively. K_A and K_B are the adsorption equilibrium constants for the analytes A and B, and C_{fmax} represents the maximum concentration of active sites on the coating.²⁰⁰

As easily deductible and confirmed by the equation above the role of the competitive compound B plays an antagonist role in the adsorption of A since the term $K_B C_{sB}^{\infty}$ appears in the denominator of the equation. The influence of the competitive compound becomes much important as the terms K_B and C_{sB}^{∞} increase. From this it is possible to conclude that the competitive compound can easily affect the adsorption of compounds having low affinity for the coating (low K_A) even at low concentration in the sample when its adsorption equilibrium constant is very high and $K_A C_{sA}^{\infty} \ll K_B C_{sB}^{\infty}$.

These findings can be readily related to real cases scenarios in food analysis: when plant-based biological tissues are crashed during the sample preparation some native and well regulated biological compartment are disrupted. This lead to the release of high concentrations of hydrophobic compounds characterized by high affinities for the coating and high Henry's Law constants. These compounds tend to readily enrich the headspace and occupying most of the active sites of the coating even at short extraction times. For the reasons described above compounds having higher solubility in water, lower affinity for the coating and lower Henry's law constant will poorly enrich the headspace and be easily displaced from the surface of the coating when the difference between the product $K_A C_{sA}^{\infty}$ became much lower than the sum $\sum_1^n K_i C_{si}^{\infty}$ that represent the contribution of each potential competitive interfering analyte i present in the matrix.

Accordingly, in very complex mixtures the amount extracted of a compound having low affinity for the coating can vary with the concentration of all components in the mixture, being them target analytes or other matrix components. Possible strategies to avoid the occurrence of this phenomena consist in diluting the sample¹⁹³, or shortening the extraction time²⁰⁴.

In order to investigate the behavior of the coatings and evaluate displacement effects, an aqueous mixture of the analytes (Table S1) was employed and extractions performed in HS and DI modes for 15, 30 and 60 minutes. The compound selected to induce saturation was α -pinene (high Henry's Law constant and high affinity for the coating). Two other sets of extractions were carried out by increasing the concentration of α -pinene to 10- and 100-fold the initial concentration in the mixture. A third set of extractions were carried out spiking the sample with a concentration of α -pinene above its solubility in water, namely oversaturation (OS).

All other probe analytes were spiked at the same concentrations for direct and headspace sampling experiments and for all the coating tested. This was possible due to a careful investigation to adjust the concentration of the analytes in the mixture in order to have enough sensitivity for all the different coating tested and evaluate the phenomena exactly at the same working condition. Moreover, the volume of HS and DI was kept constant in order to avoid concentration or dilution effects of the vapor phase.

3.2.3.2.7 Rational behind the selection of model analytes

In order to guaranty the relevance of this work to food application, the model analytes were carefully selected among several homologous groups of metabolites frequently encountered in food and environmental sample matrices such as primary alcohols, 2-ketones, ethyl esters, terpene hydrocarbons, oxygenated terpenes and aromatic compounds (Table 1). The compound selected to induce saturation of the coatings was alpha-pinene, a terpene hydrocarbon forming part of the secondary metabolism of most plant-derived foodstuffs, as well as a major contributing constituent of most essential oils²⁰⁶. This compound is characterized by high hydrophobicity ($\log P \approx 4.4$) and high affinity for the coating tested as easily deductible from the fiber constants calculated in studies recently carried out¹⁵³.

Moreover the high Henry's Law constant of this compounds induce its rapid enrichment of the headspace above the sample, even at very mild extraction conditions and short extraction times.

The most common sample preparation protocols for food matrices prior SPME sampling consists in crashing the biological tissue constituting the matrix and move an aliquot of it in glass vials (10 or 20 ml) where the extraction is performed in direct immersion or headspace mode. This procedure provokes the disruption of well-regulated biological compartments of the biological tissue and the consequent releasing of high concentration of hydrophobic compounds that readily enrich the sample headspace. For this reason saturation of the SPME coating and consequent displacement phenomena are most likely to occur in these sampling conditions.

In the light of all of these considerations the model system created consists basically of three classes of compounds:

- a) The saturating compound, alpha-pinene, that for the reasons described above, is well suitable to mimic the release of hydrophobic compounds when biological food tissue are disrupted prior the sampling.
- b) Easily displaceable compounds bearing low to medium polarity ($\log P < 3$) and various functionalities: 1-pentanol, 2-hexanone, ethyl butanoate, benzaldehyde, acetophenone, benzene and eucalyptol.
- c) Other hydrophobic compounds, having similar hydrophobicity of alpha-pinene, that for this reason should not be displaced: 1-undecanol, 2-undecanone and ethyl nonanoate.

The expected behavior of the system consists in the gradually competitive adsorption between alpha-pinene and the compounds comprised in the class b, at the same time the compound of the class c should not be affected by the phenomenon.

3.2.3.2.8 Trends in displacement occurrence for commercially solid coatings

Adsorption capability of the- solid coatings investigated in the present study differs depending on the total surface area, the degree of porosity, the size of the pores, as well as the chemistry of the particle whose surface interactions with the analytes may involve π - π bonding, hydrogen bonding or van der Waals interactions¹⁹¹.

Competitive adsorption profiles were obtained increasing the concentration of alpha-pinene in the mixture, while keeping the concentration of all other analytes at the same levels. Since all conditions were kept the same, except the concentration of α -pinene, it is assumed that no inter-analyte displacement occurs if the amount extracted, in ng, is statistically the same. The trends of competitive adsorption were obtained comparing amounts extracted after further spiking of

alpha-pinene and amounts extracted from a mixture were the extremely low concentrations of alpha-pinene and other hydrophobic compound are not such as to induce displacement. In Figure 3.24 shows the displacement profiles acquired for the three coatings tested both in DI (a) and HS (b)

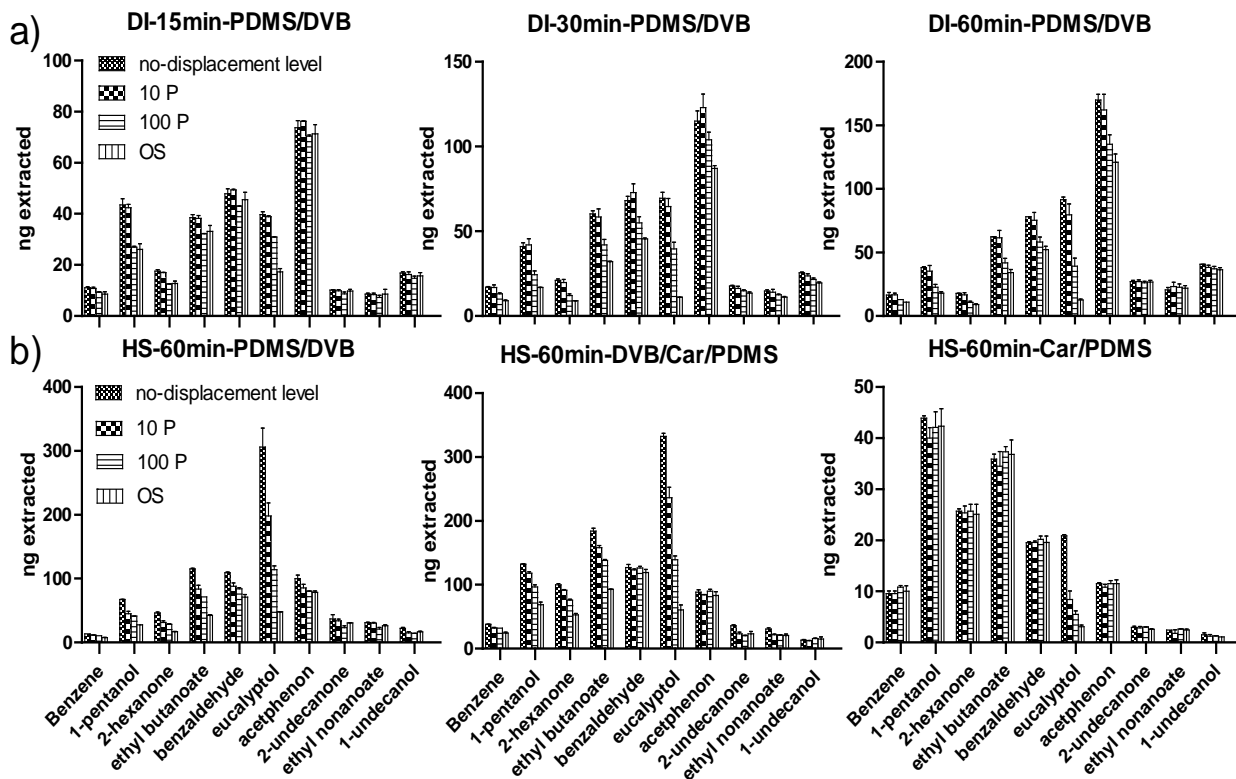


Figure 3.24 Comparison of three commercial SPME coatings (PDMS/DVB, DVB/Car/PDMS, Car/PDMS) in terms of occurrence of inter-analyte displacement for a) direct and b) headspace extractions. Error bars represent standard deviation obtained for three replicates

The results demonstrate that despite of sampling mode, Car/PDMS is less prone to displacement effects as compared to PDMS/DVB and DVB/Car/PDMS in the same working conditions. This behaviour can be explained taking in consideration two factors: specific surface area of the polymer and coating characteristics. Carboxen 1006 particles bear a higher specific surface area compared to DVB (950 vs 750 m^2 g^{-1}), moreover, the commercial SPME fibers Car/PDMS and PDMS/DVB have also different total phase volume that have been calculated being 0.528 mm^3

and 0.440 mm^3 ¹⁹¹. These data lead to formulating the hypothesis that more active sites are available for the adsorption and consequently the value of C_{fmax} , mentioned earlier, will be higher for Car/PDMS than PDMS/DVB coating. This hypothesis is well fit within the experimental data revealing that at the same working conditions and analytes concentrations the competitive adsorption is much less pronounced for Car/PDMS than PDMS/DVB, as evident in Table 3.26 where the relative amount displaced at the at the highest level of alpha-pinene spiked is reported for all the analytes for 60 min HS extraction.

Table 3.26 Comparison between solid coatings tested in terms of relative amount displaced at the highest spiked level of alpha-pinene for HS extraction carried out at the same working conditions.

analyte name	HS extractions		
	PDMS/DVB*	DVB/Car/PDMS*	Car/PDMS*
benzene	42.4	36.1	3.0
1-pentanol	58.5	48.0	9.4
2-hexanone	63.5	47.0	7.5
ethyl butanoate	62.9	49.5	3.1
benzaldehyde	34.3	5.8	4.1
eucalyptol	84.3	81.8	81.8
acetophenon	21.3	6.3	4.9
2-undecanone	n.s.d**	n.s.d**	n.s.d**
ethyl nonanoate	n.s.d**	n.s.d**	n.s.d**
1-undecanol	n.s.d**	n.s.d**	n.s.d**

*: results expressed as relative percent of compound displaced calculated on the nanograms extracted

** : no statically difference has been noticed performing T-test analysis on the amount extracted results

Furthermore, Carboxen 1006 is constituted by micropores narrow enough to retain analytes with a molecular weight greater than 35 g/mol. This implies that the affinity for the coating of low molecular weight and polar compound is much stronger¹⁵³ than for that exhibited by PDMS/DVB making inter-analyte displacement from the Carboxen coating surface less likely to occur. The behavior of the mixed mode DVB/Car/PDMS also deserves further discussion.

This coating has been developed in order to combine the adsorption characteristic of Carboxen and DVB polymers and broadening the molecular weight range of analytes effectively extracted.

In this coating an inner layer of Carboxen is overcoated by a thicker outer layer of DVB particles, glued together by polydimethylsiloxane that was showed do not contribute to the extraction mechanism.

The rationale behind the design of this coating resembles principles used in thermal desorption tubes and purge traps. The larger molecules first interact with the outer and weaker adsorbent DVB and the small molecules diffusing through it and get adsorbed by Carboxen 1006 particles that represent the stronger adsorbent.¹⁹¹ As evidenced in Table 2, DVB/Car/PDMS present a behavior towards competitive adsorption closer to DVB/PDMS than to Car/PDMS, most likely due to the thickness of the different layers of the coating and their total surface areas. The inner 30 μm Carboxen layer presents a total volume of 0.151 mm^3 compared to the outer 50 μm DVB layer with a phase volume of 0.377 mm^3 . Taking into consideration the specific surface area and density of the two porous particles it is approximately possible to calculate the total surface area of the two layers: 372.9 cm^2 for Carboxen layer and 2884 cm^2 for DVB layer. These data show the prevalence of DVB active sites in this coating thus the correlation with the displacement trend observed.

3.2.3.2.9 Effects of extraction time and extraction mode

One strategy to avoid the occurrence of inter-analyte displacement is to reduce the extraction time in order to reduce the amount adsorbed on the solid coating and inhibit competitive adsorption¹⁵³.

Figure 3.25 is shows a representative example of extractions carried out at different times using PDMS/DVB coating, which has been shown to be the solid coating more prone to inter-analyte displacement occurrence.

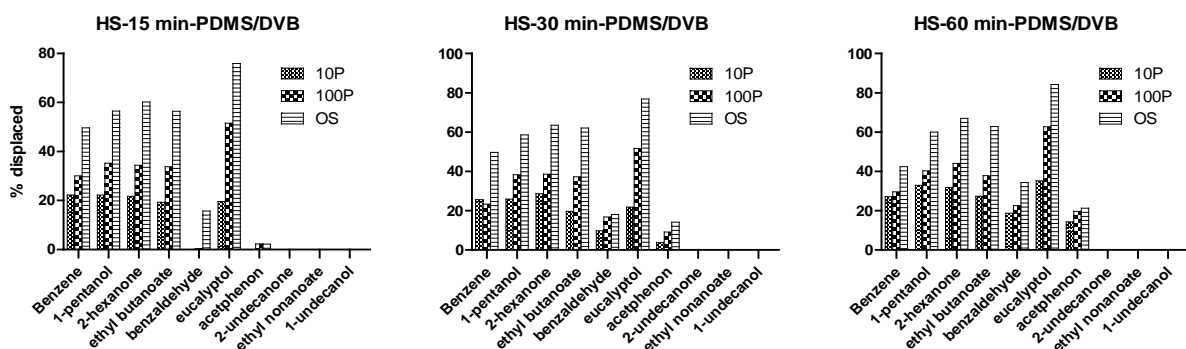


Figure 3.25 Comparison of the trends of inter-analyte displacement at different extraction times (15, 30, 60 minutes). The result are expressed as % of analyte displaced

The results show that, when employing a DVB/PDMS coating, as the extraction time increases, the evidence of competitive adsorption becomes more remarkable since the amount of adsorbates collected increases, occupying more adsorptive active sites in the polymer. It is worth mentioning the influence of the kinetic of the mass transfer on both extraction modes at short extraction times. As can be seen in Figure 3.26, representatively showing the results obtained at the highest level of alpha pinene spiked, the difference in the amount displaced at 15 minutes and 60 minute is more pronounced for DI extractions.

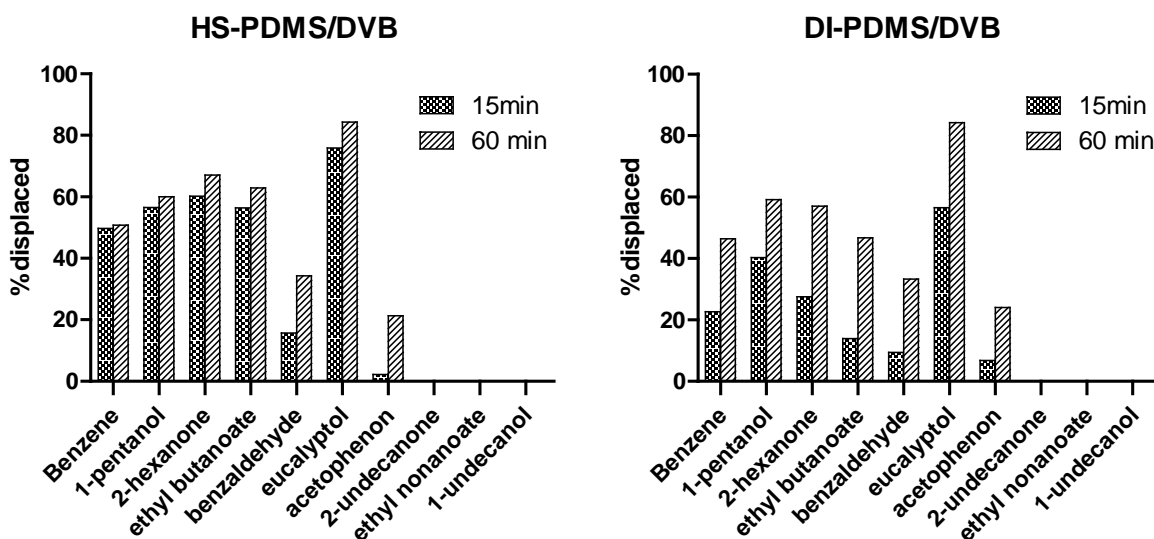


Figure 3.26 Comparison in terms of percent displaced for PDMS-DVB coating at 15 and 60 minutes of extraction in HS and DI mode at the highest level of alpha-pinene spiked.

Again an explanation can be proposed taking in consideration the interphase mass transfer of the saturating analyte. The high Henry's Law constant of α -pinene and possible matrix modification (e.g. salting out effects) makes the compound readily available in the headspace of the sample, where the diffusion coefficient is about orders of magnitude lower than in solution. For this reason, the amount extracted even at shorter extraction time is very close to the saturation threshold for the coating and the amount of analytes displaced closer at different extraction times. For DI extraction, the diffusion kinetic of alpha-pinene in the bulk of the solution is slower according to the diffusion coefficient of the analyte in the matrix, moreover, the mass transfer in the stagnant boundary layer surrounding the coating contribute in slowing down the overall process. This implies that at shorter extraction times the amount of alpha-pinene extracted is much higher for HS than DI extractions.

Nonetheless, for DVB/Car/PDMS and Car/PDMS, less pronounced differences could be noticed in the extraction time window tested, which is in agreement with the abovementioned hypothesis. However, similar trends for PDMS-DVB coating have still been observed.

For the first time in this work, differences in the occurrence of displacement phenomena were studied comparing direct and headspace extraction at the same working conditions. This set of experiment was performed in order to verify which extraction mode is more immune from competitive adsorption and simulate real case scenarios when the real matrices, for example food, are analyzed in both extraction mode; for this reason the concentration in the bulk of the matrix needs to be the same.

As already demonstrate in recent studies¹⁴⁹, direct immersion SPME allows a more balanced and complete metabolite coverage when untargeted metabolomics studies are performed in foodstuff. This work wants to give a further and complementary contribution to the optimization of the sample preparation step showing which extraction mode is better suitable, under the same working condition, to limit or avoid displacement phenomena, guarantying less biased results.

For all the commercial solid coatings tested, even at short extraction times, the amount of analytes displaced by α -pinene resulted to be higher whenever HS extractions are performed compared to DI extractions. As previously mentioned, the most noticeable differences are presented by PDMS/DVB coating. The reason behind the phenomena relies in the physical-chemical characteristic of the displacing compound that wants to simulate the overall behavior of all the highly hydrophobic analytes released after the disruption of plant-based biological tissues.

Figure 3.27 shows the comparison in displacement trends between headspace and direct immersion extraction after 15 minutes of adsorption using a PDMS/DVB coating. The influence of the extraction mode on the competitive adsorption becomes evident at the lower level of α -pinene enrichment: for DI extractions, no statically difference in the response was noticed for all the analytes when the amount extracted from original mixture was compared with the amount extracted from the mixture containing 10 times the original amount of alpha-pinene (level indicated as 10P in the plots). Conversely, for HS extractions, a slight increase in alpha-pinene concentration induced competitive adsorption with the amount of analyte displaced ranging from 19 to 23 %. However, for the analytes bearing higher hydrophobicity (2-undecanoate, ethyl nonanote and 1-undecanol) no displacement effect was observed regardless the extraction mode.

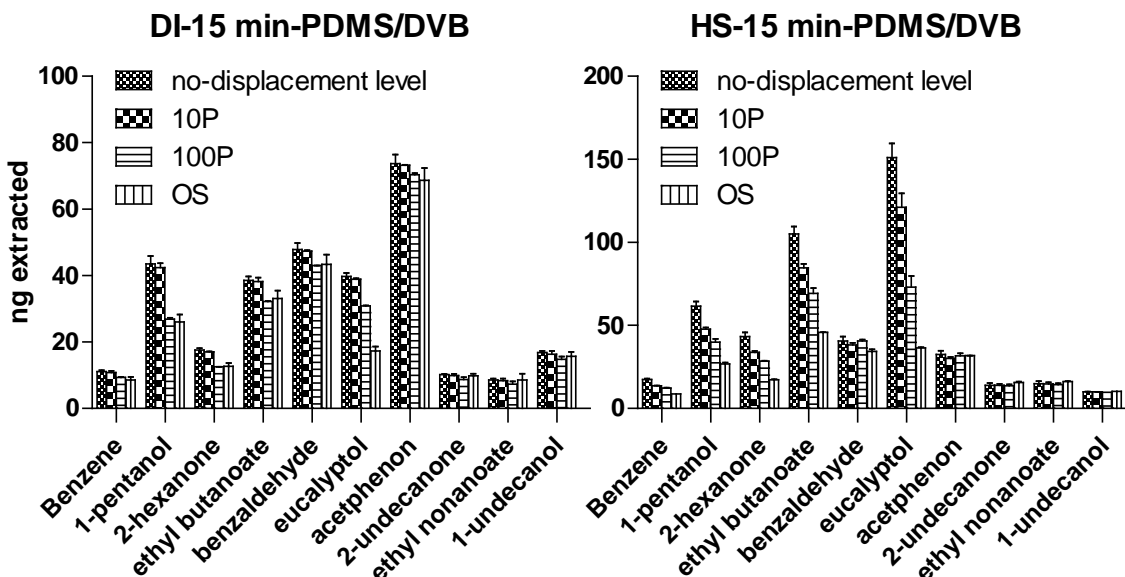


Figure 3.27 Comparison of the trends of inter-analyte displacement for different extraction modes: direct immersion extraction (right) and headspace extraction (left), performed at 15 minutes of extraction in triplicates using PDMS/DVB coating.

Similar trends were also observed when comparing the two extraction modes at different extraction times: when the enrichment of α -pinene is kept at the lower level, the amount of analytes extracted did not change significantly for 30 and 60 minute of direct immersion extraction. Conversely, for HS extractions at the same working conditions, the relative amount of

analytes displaced ranged from 3.8 to 28.6%, and from 14.4 to 35.6% at 30 and 60 minutes of extraction, respectively.

DVB/Car/PDMS and Car/PDMS also show similar trends, but the extent of the phenomena and differences noticed between the two extractions modes are much less pronounced because of the coatings characteristic as aforementioned. Table 3.27, summarizes representative results for DVB/Car/PDMS and Car/PDMS.

Table 3.27 Differences in displacement occurrence in direct immersion (DI) and headspace (HS) mode for DVB/Car/PDMS and Car/PDMS coatings

Analytes	DVB/Car/PDMS*		Car/PDMS*	
	DI	HS	DI	HS
benzene	n.s.d**	13.13	n.s.d**	n.s.d**
1-pentanol	n.s.d**	18.15	n.s.d**	10.12
2-hexanone	n.s.d**	11.47	n.s.d**	7.15
ethyl butanoate	n.s.d**	9.67	n.s.d**	9.37
benzaldehyde	n.s.d**	8.68	n.s.d**	n.s.d**
eucalyptol	n.s.d**	10.52	n.s.d**	37.54
acetophenon	n.s.d**	9.15	n.s.d**	n.s.d**
2-undecanone	n.s.d**	n.s.d**	n.s.d**	n.s.d**
ethyl nonanoate	n.s.d**	n.s.d**	n.s.d**	n.s.d**
1-undecanol	n.s.d**	n.s.d**	n.s.d**	n.s.d**

*: results expressed as relative percent of compound displaced calculated on the nanograms extracted after 15 minutes of extraction

** : no statically difference has been noticed performing T-test analysis on the amount extracted results

From these findings it can be concluded that DI represents a more convenient choice than HS in order to prevent the occurrence of competitive adsorption when complex media containing a plethora of compounds, like food matrices. Such compounds might be characterized by high Henry's law constants, medium to high molecular weight, low polarity, and be present or released by enzymatic activity upon the disruption of biological compartment of vegetable tissues. Moreover, as already demonstrated in recent studies, direct immersion SPME offers a

more balanced and complete analyte coverage when untargeted metabolomics studies are performed in foodstuff¹⁵³.

3.2.3.2.10 Evaluation of new PDMS-modified PDMS/DVB and DVB/Car/PDMS coatings

Recently, in order to overcome issues related to solid coatings compatibility in DI-SPME-GC analysis of complex food matrices, matrix-compatible coatings have been developed. The innovation related to these coatings consists in the implementation of a thin and smooth layer of PDMS surrounding the solid sorbent. The PDMS outerlayer helps to prevent the attachment of matrix components such as carbohydrates onto the coating that could lead to irreversible damaging of the solid sorbent after a limited number of analyses. Because of the proved appropriateness for the direct immersion extraction in complex matrices, these coating are well suitable for direct monitoring in living systems, especially for metabolomics investigation purposes. For this reason, the new matrix-compatible coatings were also tested for inter-analyte displacement occurrence. Two different PDMS-modified, PDMS/DVB and DVB/Car/PDMS, were tested at three different extraction times (15, 30 ad 60 min) in HS and DI modes, at the same working conditions previously employed.

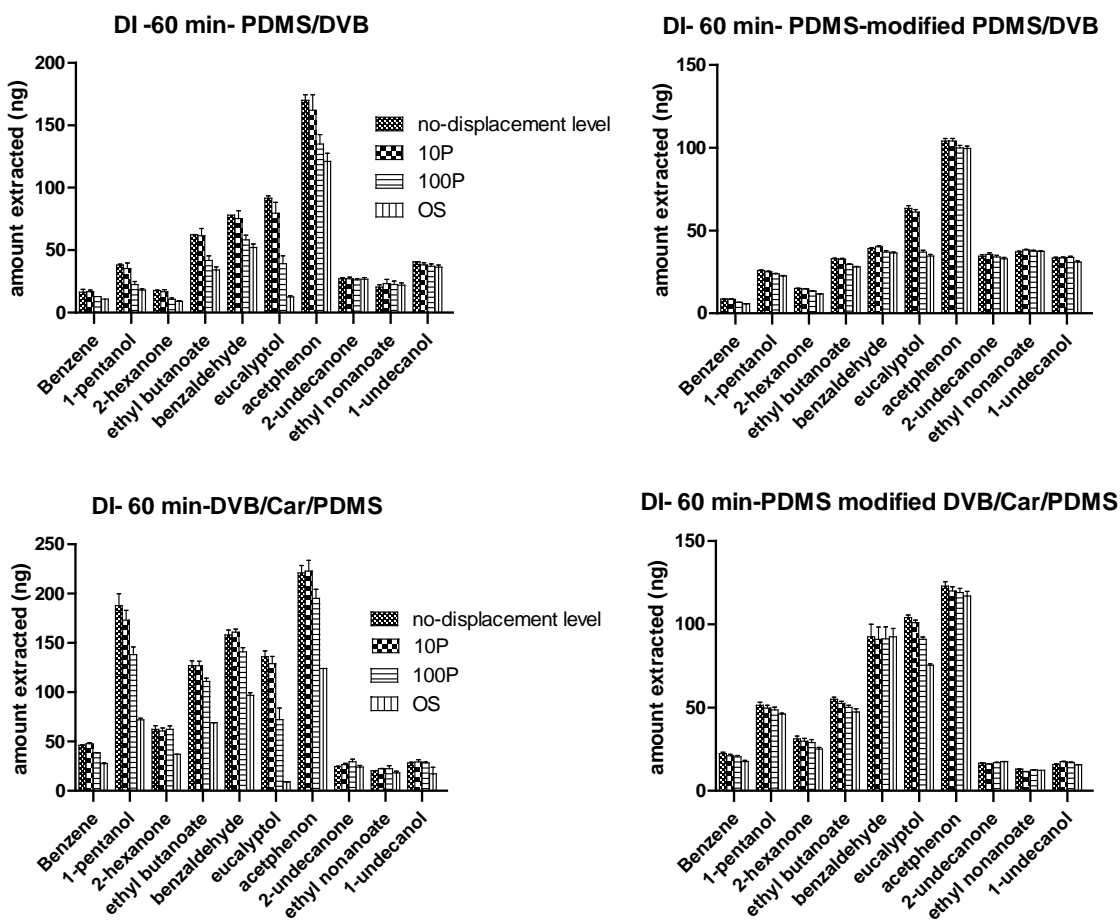


Figure 3.28 Comparison of commercial coatings and PDMS-modified coatings for displacement occurrence in direct immersion analysis

Figure 3.28 shows the difference in the displacement occurrence for the PDMS-modified coatings compared to the corresponding commercial coating for DI extractions.

As can be deduced the occurrence of the phenomenon is much less pronounced for the PDMS modified coating and the explanation for this may rely in two synergic phenomena:

- The slower kinetic of the extraction process for the PDMS-overcoated coatings due to the presence of the thin PDMS layer surrounding the solid porous polymer. The effect must be due to the further diffusion of the analytes in the outer PDMS layer before reaching the active adsorptive surface.
- The potential inhibition of water adsorption by the solid coating induced by the overcoating PDMS layer. As reported by Gorecki et al.²⁰⁰, water adsorption from the

matrix bulk can compete for the active adsorptive sites on the coating. The role of the outer PDMS layer may play a critical role in the inhibition of this phenomenon.

According to studies conducted by Mishima et al.²⁰⁷, related to permselectivity of PDMS membranes, organic analytes dissolved in aqueous media are prone to be hydrated by water molecules whose free motion is prevented by the vicinity with the solute. When permeation in the polymer occurs, molecules constituting the bulk of the sample will be excluded whereas water molecules involved in the hydration will be absorbed by the polymer. Findings of this research showed that, when the concentration of organic solutes increases in the bulk of the PDMS polymer, the diffusion of water molecules is prevented. This phenomenon can give a possible explanation to the effect noticed for the PDMS overcoated for which the outer polymeric layer can actually prevent or drastically limit water molecules from occupying active sites of the porous coating increasing its capacity.

These studies point out the enhanced capacity of the PDMS-modified coating may result in the reduction of inter-analyte displacement phenomena as compared to commercial solid coatings at the same working condition.

Interestingly, even for HS extractions the PDMS-modified coatings showed a consistent reduction in the phenomenon occurrence even at high extraction times, as shown in Figure 3.29.

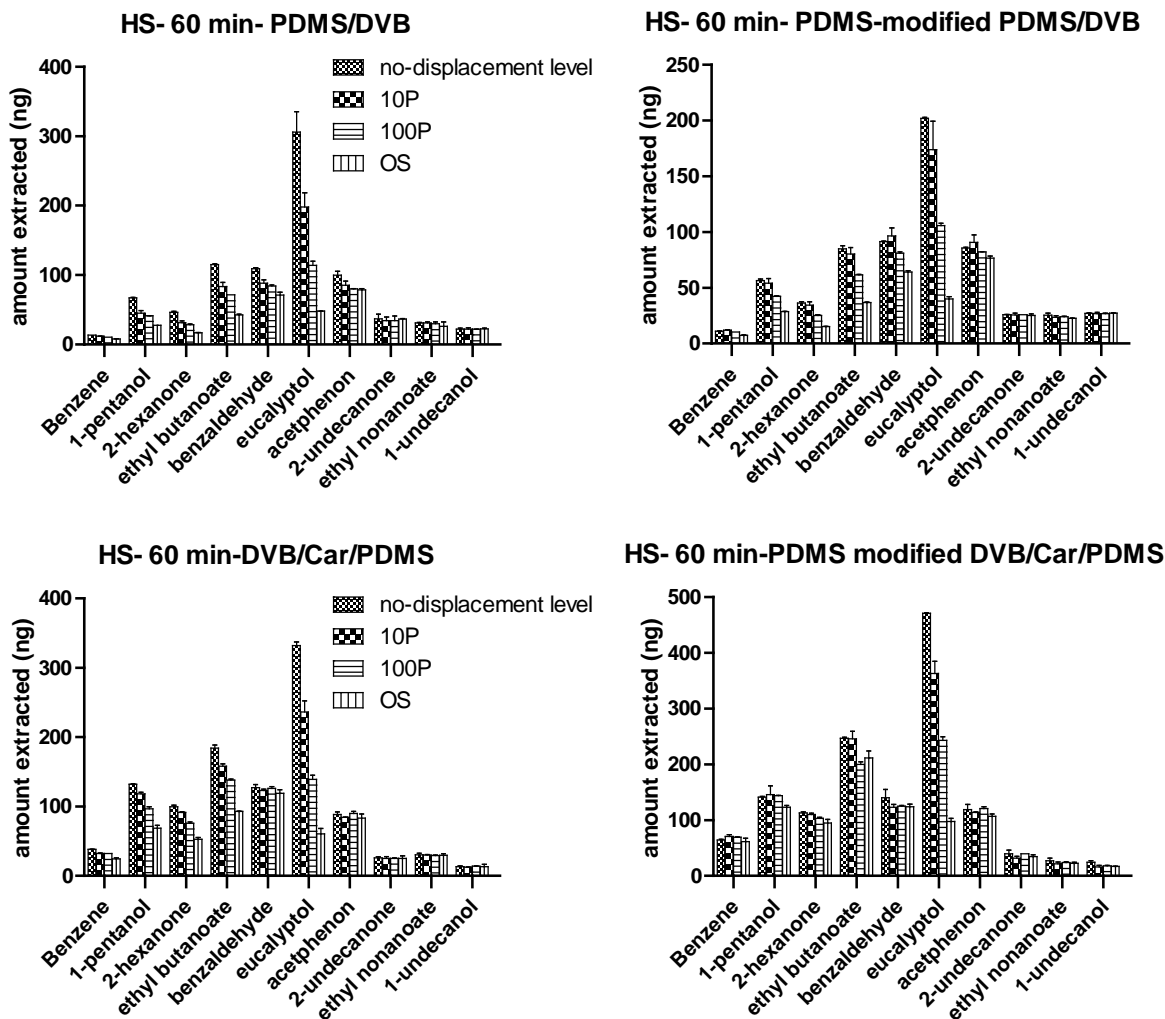


Figure 3.29 Comparison of commercial coatings and PDMS-modified coatings for displacement occurrence in headspace analysis

It is worth to mention that the reduction in the amount displaced for the PDMS-modified coatings is very pronounced for HS extractions especially for the PDMS-modified DVB/Car/PDMS coating, this confirms its suitability for unbiased analysis of complex matrices in both direct immersion and headspace applications.

In Table 6 are summarized the results expressed in relative percent of compounds displaced at the highest level of alpha-pinene spiked at 60 minutes of extraction, that among the working condition tested represent the most favorable for displacement occurrence.

Table 3.28 Differences in displacement occurrence in direct immersion (DI) and headspace (HS) mode for DVB/Car/PDMS and Car/PDMS coatings

Analyte	PDMS/DVB *		DVB/Car/PDMS*	
	commercial	PDMS-modified	commercial	PDMS-modified
benzene	42.4	32.4	36.1	4.7
1-pentanol	58.5	49.3	48.0	12.5
2-hexanone	63.5	57.7	47.0	16.1
ethyl butanoate	62.9	56.7	49.5	14.1
benzaldehyde	34.3	30.0	5.8	n.s.d**
eucalyptol	84.3	80.2	81.8	79.3
acetophenon	21.3	10.6	6.3	n.s.d**
2-undecanone	n.s.d**	n.s.d**	n.s.d**	n.s.d**
ethyl nonanoate	n.s.d**	n.s.d**	n.s.d**	n.s.d**
1-undecanol	n.s.d**	n.s.d**	n.s.d**	n.s.d**

*: results expressed as relative percent of compound displaced calculated on the nanograms extracted after 60 minutes of extraction

** : no statically difference has been noticed performing T-test analysis on the amount extracted results

3.2.3.2.11 Evaluation of matrix effects using starch based food models

Subsequent to the assessment of the solid coatings behavior towards saturation and inter-analyte displacement phenomena in aqueous samples, the effect of a matrix, which can closely simulate texture and consistency of fruits and vegetables, has been investigated. For this purpose a starch gel system, largely used as a food model in studies related to aroma release was employed.²⁰⁵

208209210

Starch gel systems are constituted by two types of molecules: linear and helical amylose and branched amylopectin. Amylose chain have the ability to interact with aroma compounds forming complexes that can be defined as a “combination of ligand and ligand-induced helicated amylose”²¹¹. These reversible complexes result from nonspecific interactions between the ligand and amylose and are formed during the gelatinization of starch or during the subsequent cooling. For this study unmodified starch containing amylopectin, native lipids and protein was used in order to better simulate the composition of many fruits and vegetables.

It has been shown that content of native lipids improve the formation of inclusion complexes for hydrophobic compounds. Amylose helices formed in starch gel systems can assume different conformation and also forming different types of complexes where the ligand can be located in the helical cavity or on the helix surface.²¹¹

For this reason the system chosen was well suitable to simulate the encapsulation of hydrophobic compounds in native biological compartment present in real vegetable tissues.

Taking into account the characteristic of the matrix used, in this part of the work the three extraction modes and sample preparation techniques were simulated, frequently used in SPME for food analysis:

- Headspace (HS) extractions: were performed crashing the matrix and extracting in the headspace above it. The procedure for the preparation of the sample recall common practices used in food analysis with SPME¹⁵³.
- Dynamic Direct Immersion (D-DI): this extraction mode wants to simulate ex-vivo analysis of food, when the sample is crashed, collected in the vial, the coating directly exposed in the matrix bulk and the sample or the SPME fiber are under agitation conditions .
- Static Direct Immersion (S-DI): this extraction mode aims to simulate in-vivo extractions in vegetables systems since the tissue is not disrupted and the extraction is performed in static conditions, also no matrix modification has been performed.

Testing these three extraction modes is critical to evaluate the phenomenon when complex matrices are involved, since various mass transfer mechanisms drive the extraction process.

For headspace extractions the main rate limiting step is the diffusion of the analytes from the bulk of the matrix to the headspace: disrupting the starch gel system induces to the release of the compounds entrapped in it especially the most hydrophobic that readily will enrich the vapor phase above the matrix. Also, the high water percent of the food model system will lead to a slower mass transfer of the more hydrophilic compounds in the vapor phase. That means that in pre-equilibrium conditions a not balanced distribution of all the analytes is present in the headspace that will be much more enriched of hydrophobic volatiles compounds, enhancing the possibility of displacement of the polar compound whose concentration is much lower because of the mass transfer rate from the sample to the headspace.

The dynamic direct immersion sampling (D-DI) has faster mass transfer kinetic since in this case the coating is directly exposed to the matrix bulk and the overall mass transfer to the extracting phase is limited by the diffusion of the analytes through the boundary layer surrounding the coating that it is also dependent on the degree of agitation used and the texture of the matrix. Even if the matrix used include high percent of water the overall migration of the analytes trough the bulk cannot be compared to pure aqueous samples since the gel system plays an important rule on the mobility of the analytes as well as it happens in real vegetable matrix. This sampling mode also involves the disruption of the tissue before the extraction process, thus freer motion of the analytes is allowed by the rupture of the amylose helices and other possible aggregates formed with amylopectins, proteins and native lipids constituting the unmodified starch. Conversely to the fiber-headspace-matrix system, the diffusivities of small molecular weight hydrophilic compound will be faster than for higher molecular weight hydrophobic compounds, implying a better balanced distribution of the analytes on the coating even in pre-equilibrium conditions.

The in-vivo simulating static direct immersion mode provides the slowest mass transfer kinetic among the sampling modes tested. When in-vivo analysis is performed on plant-based systems the entire biological environment surrounding the coating can be assumed to be static, and the biostructural integrity of the plant-based living system is not perturbed.

Same statement is not valid for animal systems *in-vivo* study where biological fluids streams make the extraction happen in dynamic conditions.

In order to mimic the in-vivo extractions, the sample preparation required special attention.

The aim was to avoid any perturbation of the starch gel system after the cooling procedure. For this reason the gelatinization process was carried out directly in the sampling vial in such a way that the gel system did not have to be disrupted or perturbed. Then the coating was exposed into the matrix bulk in static conditions.

3.2.3.2.12 Evaluation of sampling mode and extraction time

To evaluate he phenomena in equilibrium and pre-equilibrium conditions for all the extraction mode tested, extraction time profile were acquired using a gel system (2.5% of starch *w/w*) at pH of 6.8, up to 24 hours. The equilibrium extraction time selected was 6 hours and 30 minutes as

set as pre-equilibrium extraction time. Sets of extractions were performed in D-DI, S-DI and HS mode according to the same displacement inducing procedure described above.

At pre-equilibrium conditions the results shown in Figure 3.30, confirm that DI extraction reveals a more representative coverage among analytes of different polarities, especially regarding polar analytes towards hydrophobic compounds, in agreement with results obtained comparing HS and DI metabolomics studies on apples¹⁴⁹.

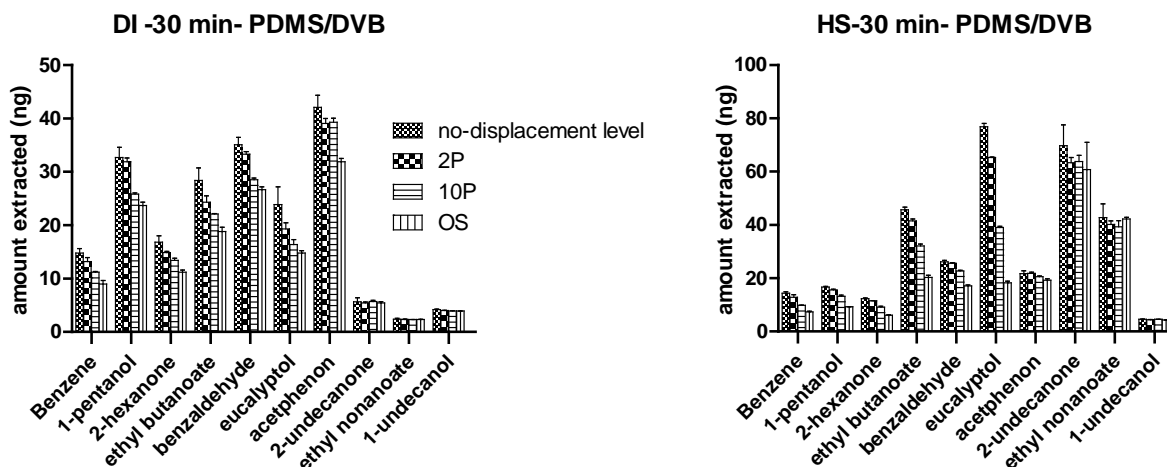


Figure 3.30 Comparison of extraction mode at 30 minutes of extraction for PDMS/DVB coating

Once again, it can be observed that displacement is potentially enhanced in headspace mode, even at pre-equilibrium conditions, due to the faster uptake of hydrophobic compounds on the coating. One of the main goals of this work is showing that, is the most suitable option for metabolomics studies of complex matrices in order to avoid or limit the occurrence of displacement phenomena and ensure unbiased data collection.

Figure 3.31 shows the comparison of extraction modes and extraction times for the three matrix models. From the results obtained it can be seen that static direct immersion extraction (S-DI), simulating in-vivo sampling in plant based systems ,in pre-equilibrium conditions, drastically reduces the inter-analyte displacement phenomenon as compared to other extraction modes. Indeed, even at equilibrium conditions and the highest level of α -pinene spiked, the amount of analytes displaced reached up to 35% versus 80% for D-DI and HS extractions.

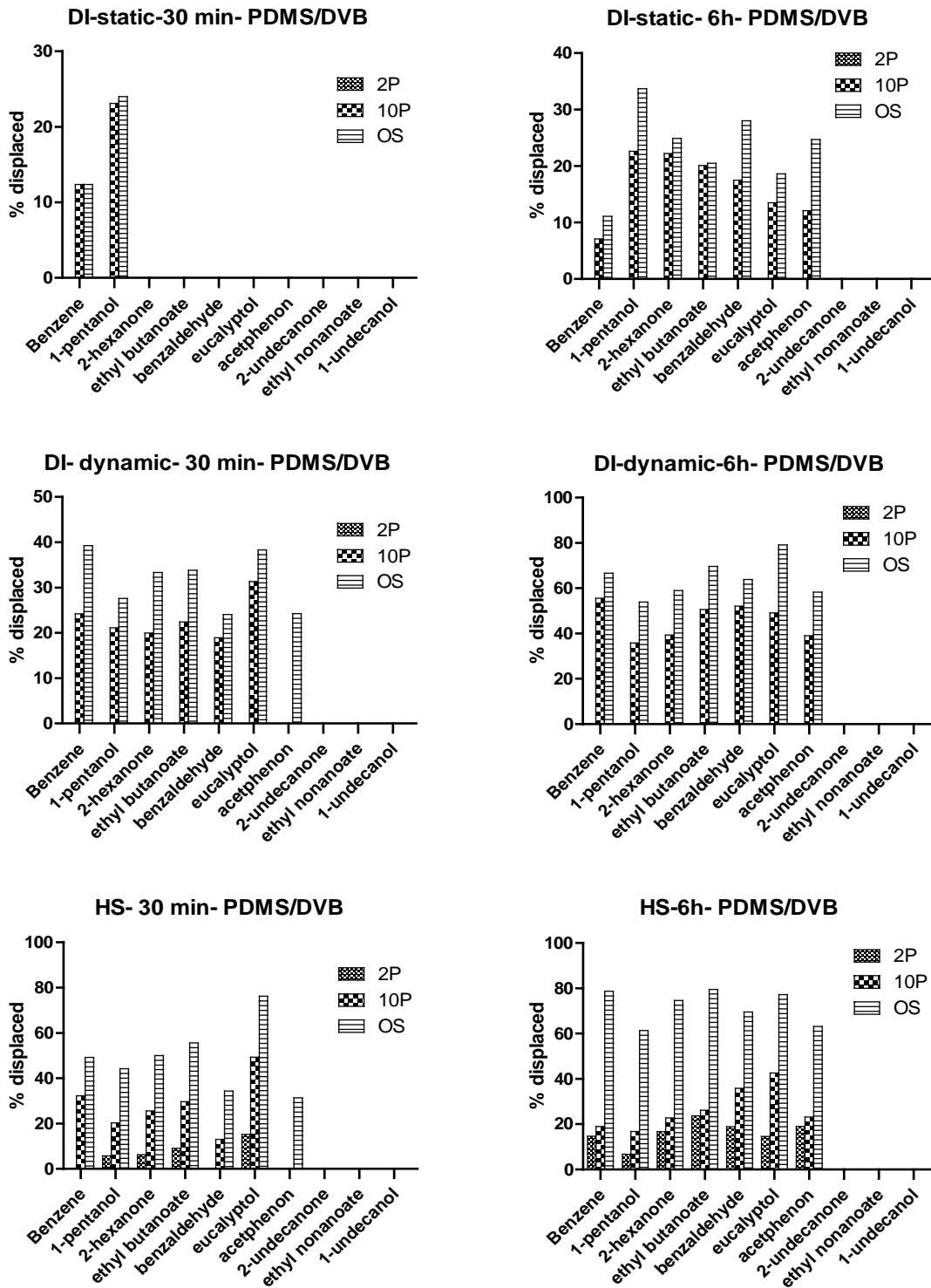


Figure 3.31 Comparison of extraction mode in pre-equilibrium and equilibrium extractions

Figure 3.32 summarizes the results obtained for all experiments pertaining the matrix effects. The static direct immersion at pre-equilibrium condition yields relative amount displaced ranging between 0 and 15% for 8 out of 10 analytes. . Conversely, in pre-equilibrium HS extractions only 4 out of 10 analytes show relative displacement lower than 15%. Moreover, three of these compounds had not been affected by displacement, within the working conditions tested, due to their polarity (2-undecanone, ethyl nonanoate ad 1-undecanol).

For equilibrium extractions, it has been confirmed that static direct extraction inhibited the occurrence of inter-analyte displacement likely due to the entrapment of the more non polar analytes in inclusion complex of the matrix used, similarly to real case scenarios when the most hydrophobic compounds are not released from native biological compartments until the biological tissue is somehow disrupted.

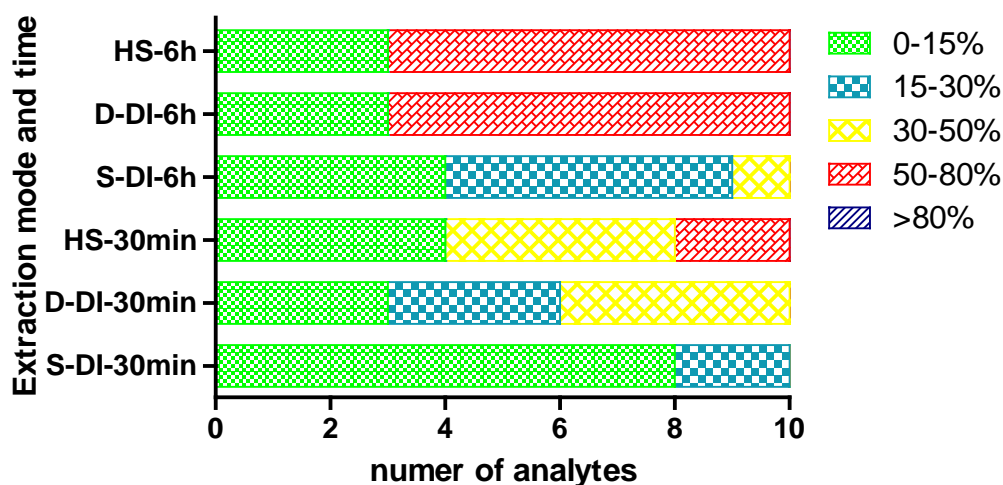


Figure 3.32 Comparison of extraction mode and time for SPME extractions carried out in starch gel matrix. The results shown are expressed in relative % of compound displaced and refer to all the 10 metabolites tested at the highest level of alpha-pinene spiked in the matrix.

These results show that DI static sampling can provide the best solution to avoid occurrence of displacement phenomena compared to DI dynamic (with agitation) and headspace. This behavior will be much more pronounced in the real case scenario of food analysis since the in-vivo sampling actually avoid the extensive disruption of biological compartment present in the vegetable tissue (no blending or grinding of the plant material) and consequent release of

hydrophobic compounds that easily induce coating saturation and displacement of the most polar ones.

3.2.3.2.13 Evaluation of different matrix composition and pH

Other parameters related to matrix composition, such as water content of and pH were also evaluated in this work as potential factors affecting the occurrence of displacement phenomena.

Three different starch/water ratios (w/w) were evaluated taking into account the different water content of fruits and vegetables ranging from 98 to 80%. Three different starch gels were prepared at 2.5, 5 and 10% of native starch powder in water. The extractions were performed for 30 minutes. Different amounts of starch in the system affect the diffusivity of the analytes in the media especially for higher molecular weight compounds. This implies different kinetic of uptake on the coating that favors the adsorption of small polar molecules over larger hydrophobic ones.

As presented in Table 3.29 such effect is especially remarkable for the matrix model containing the higher amount of starch. Regarding the experiments at pH 3.8 and 6.8, the results obtained differ in a range comprised between 0.3 to 10%. Therefore, within the range tested, it can be assumed that pH has no remarkable effect on the inter-analyte displacement phenomenon.

Table 3.29 Evaluation of different extraction modes for different starch gels systems

Analyte	2.5% (w/w)			5% (w/w)			10% (w/w)		
	DI-static	DI-dynamic	HS	DI-static	DI-dynamic	HS	DI-static	DI-dynamic	HS
benzene	12.40	39.29	49.20	n.s.d**	26.3	48.0	n.s.d**	17.1	36.8
1-pentanol	24.00	27.59	44.20	n.s.d**	24.1	57.4	n.s.d**	13.1	52.4
2-hexanone	n.s.d**	33.37	50.00	n.s.d**	25.5	48.5	n.s.d**	23.7	47.0
ethyl butanoate	n.s.d**	33.84	55.60	n.s.d**	20.9	49.9	n.s.d**	20.1	42.8
benzaldehyde	n.s.d**	24.05	34.40	n.s.d**	13.0	29.6	n.s.d**	10.3	29.1
eucalyptol	n.s.d**	38.30	76.20	n.s.d**	32.7	70.2	n.s.d**	26.0	66.1
acetophenon	n.s.d**	24.29	31.40	n.s.d**	10.7	22.7	n.s.d**	8.8	17.7
2-undecanone	n.s.d**	n.s.d**	n.s.d**	n.s.d**	n.s.d**	n.s.d**	n.s.d**	n.s.d**	n.s.d**
ethyl nonanoate	n.s.d**	n.s.d**	n.s.d**	n.s.d**	n.s.d**	n.s.d**	n.s.d**	n.s.d**	n.s.d**
1-undecanol	n.s.d**	n.s.d**	n.s.d**	n.s.d**	n.s.d**	n.s.d**	n.s.d**	n.s.d**	n.s.d**

3.2.3.3 Conclusions

The thorough investigation of competitive adsorption phenomena performed in the present study allowed the identification of main challenges associated with the implementation of solid sorbents in SPME sampling of complex multi-component systems. In addition, approaches to be implemented in order to minimize the occurrence of inter-analyte displacement phenomena have also been evaluated and discussed. In the best of our knowledge, for the first time in this work the behaviors of commercially available SPME solid coatings were evaluated concomitantly to their PDMS-modified analogs, under the same experimental conditions. Furthermore, static direct immersion extraction, applied mainly for *in-vivo* sampling in plant-based systems, was demonstrated to be the most appropriate sampling mode towards the inhibition of the displacement phenomena. In conclusion, direct sampling in tissues represents the best option for an unbiased and trustworthy results for qualitative and quantitative analysis of plant-based material, from target to untargeted studies.

3.2.4 Evaluation of new Polymerized Ionic Liquid coatings in SPME for analysis of food metabolites

3.2.4.1 Introduction

Solid phase microextraction process is governed by the shape, size and chemistry of the extracting phase that also plays an essential role in the selectivity of the extraction¹⁴⁶. In this regard, various extracting phases with different polarities and polymeric characteristics are currently commercially available¹⁴⁶. However, the commercially available extraction phases do not provide the necessary coverage for the various analyte polarities. Thus, efforts are currently focused in the development of new coatings amenable to different sampling objectives and with exclusive characteristics¹⁵⁵.

Generally, analysis of certain polar compounds using SPME, especially for food analysis, has always been a challenge. This is because most of the commercially available coatings show significant selectivity for a particular class of compounds, and thus not applicable for non-targeted global food metabolomics study. It is therefore pertinent to further develop SPME coating chemistry, especially for generally non-selective determination of various polar compounds in food matrices. Ionic liquids, due to their unique chemical properties, may be considered as potential candidates to address some of the limitations of commercially available coatings.

In recent years, ionic liquids (ILs) have gained increasing interest in the analytical chemistry community because their unique physical and chemical properties. Ionic Liquids are organic salts, which consist largely of organic cations paired with organic or inorganic anions. The structure of ILs can be controlled to produce the desired chemical properties. Typically, ILs tend to have negligible vapor pressure, elevated thermal stability, tunable viscosity and miscibility with other solvents, as well as the capability of undergoing numerous solvation interactions. In particular, as extracting phases, selectivity of ILs can be improved by introducing functional groups that impart specific chemical functionality and thus enhance specific extracting capability. This implies that ILs offer researchers the advantage of modifying the surface chemistry to tailor their extraction efficiency to either a specific group of analytes or to a broader range of analytes.

Due to their tunable physical and chemical properties, polymeric ionic liquids PILs have been recently used as extracting phases for SPME²¹² with promising potentialities compared to commercial SPME coatings. PIL-based coatings continue to attract significant interest for the determination of volatiles in food matrices by HS-SPME. For example, PIL-based coatings prepared by AIBN polymerization, have been applied to the determination of wines and coffee aroma composition^{213,214}.

This part of the thesis describes the evaluation of two different PILs coatings, poly([ViBHDIM][NTf₂]) and Poly([DDMGlu][MTFSI]), and the comparison of their extraction performances with commercially available SPME coatings (PA and PDMS). The study was carried out in headspace extraction mode using a group of selected analytes representing different chemical classes of metabolites commonly found in fruit. In addition, the approach offers an opportunity to identify the type of coating, (PILs or commercial SPME fiber), that will be applicable for non-targeted global metabolites study in fruits.

3.2.4.2 Experimental section

3.2.4.2.1 Chemicals

Analytical standards (purity > 97 %) and HPLC grade methanol were obtained Supelco (Oakville, Canada). Commercial SPME fibre assemblies in 23-gauge needle sizes and automated formats, 7 µm PDMS (stable flex), 85 µm PA (stableflex), automated SPME holder and 20 mL screw cap vials were also purchased from Supelco (Oakville, Canada).

3.2.4.2.2 Instrumentation and apparatus

A Hewlett Packard 6890/5973 GC-MS equipped with a split/splitless injector and a CTC Combipal[®] autosampler (CTC Analytics AG) for automated SPME was used. The capillary column used for the chromatographic separation was a J&W DB5-MS UI (30 m, 0.25 mm i.d., 0.25 µm film thickness). The column temperature program was initially set at 35 °C for 6 min, ramped at 20 °C/min to 140 °C then, ramped at 40 °C/min to 260°C, where it was held for 2 min giving a total run time of 16.25 min. Helium was used as carrier gas and the flow rate was set at 1.2 ml/min. The mass spectra were acquired in SIM mode selecting characteristic quantitation ion for each analyte (Table 3.30).

Table 3.30 Analytes of interest and their physical-chemical properties

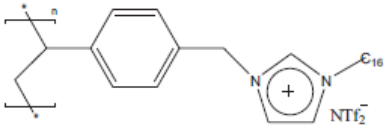
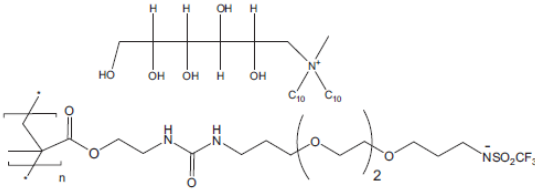
Analyte	MW (g/mol)	log K _{ow}	B.P. (°C)	Henry's Law constant (atm*m ³ /mol)	Quatitation ion (m/z)
benzene	78.11	2.0	78.8	5.39*10 ⁻³	78
1-pentanol	88.15	1.3	136.9	1.33*10 ⁻⁵	55
ethyl butanoate	116.16	1.8	125.7	4.10*10 ⁻⁴	88
2-hexanone	100.16	1.3	118.7	9.30*10 ⁻⁵	58
benzaldehyde	106.12	1.5	178.1	1.34*10 ⁻⁵	105
acetophenon	202.00	1.6	201.9	9.81*10 ⁻⁶	105
2-undecanone	170.30	4.1	224.1	4.78 *10 ⁻⁴	58
ethyl nonanoate	186.30	4.3	229.7	1.69*10 ⁻³	88
1-undecanol	172.31	4.2	256.2	7.26*10 ⁻⁵	55
eucalyptol	154.25	2.8	174.0	2.04*10 ⁻⁴	154
alpha-pinene	136.24	4.4	157.3	1.07*10 ⁻¹	93

The mass spectrometer working conditions were: electron ionization (EI) 70eV, mass range 50-350 m/z ion source temperature: 230 °C; quadrupole temperature: 150 °C transfer line temperature: 280°C.

3.2.4.2.3 Preparation of PIL-Based coatings

The chemical structures of PIL-based coatings are shown in Table 3.31. The synthesis and preparation of the PIL-based coatings used in this work was carried out in the Chemistry Department, University of Toledo, Ohio, USA.

Table 3.31 Structures, abbreviations, and film thicknesses of all sorbent coatings employed in the study.

Coating	Abbreviation (thickness)	Structure
Poly(1-vinylbenzyl-3-hexadecylimidazolium) bis[(trifluoromethyl)sulfonyl]imide	Poly([VBHDIM][NTf ₂]) (≈10 μm)	
N,N-Didecyl-N-methyl-d-glucaminium poly(2-methyl-acrylic acid 2-[1-(3-(2-[2-(3-trifluoromethanesulfonylamino-propoxy)-ethoxy]-ethoxy)-propylamino)-vinylamino]-ethyl ester)	Poly([DDMGlu][MTFSI]) (≈10 μm)	

The synthesis of Poly([VBHDIM][NTf₂]) was carried out as previously published in literature^{213,215}. The synthesis of the poly([DDMGlu][MTFSI]) PIL was performed by combining two previously reported synthetic procedures^{216,217}. It is expedient to state that further details on the synthesis and preparation of the PILs are beyond the scope of this thesis.

3.2.4.2.4 SPME procedure

In a 20-ml headspace vial containing 9 ml of ultrapure water with 20% (w/w) of NaCl, 100 μl of the stock working mixture of the analytes were spiked. Due to the fact that analytes have the potential of undergoing degradation,²⁰⁴ the samples were all freshly prepared prior to the analysis. For the entire sample set, the extraction temperature, stirring rate and incubation time were kept at 30°C, 500rpm and 20 minutes respectively. The coatings were desorbed in the GC-MS injection port for 10 min at 250 °C (commercial coatings) and 175 °C (Ionic Liquid based coatings), in splitless mode. Desorption efficiency was tested by repeating injections with the same coatings immediately after the previous analysis.

3.2.4.2.5 Calibration Procedure

The working solutions for liquid injections were prepared in methanol from individual stock solutions; a series of dilutions at 12 concentration levels from 10 to 40000 μg L⁻¹ was prepared. The solutions were kept at -30 °C and protected from light by keeping them in amber vials. HS-

SPME-GC-MS calibration curves covering the entire concentration ranges stated earlier are reported in Table 3.32. A 60-min extraction time was carried out while maintaining the experimental procedure described earlier.

Table 3.32 Concentration levels of the analytes of interest

Calibration level	Sample concentration ^a ($\mu\text{g L}^{-1}$)	Sample concentration ^b ($\mu\text{g L}^{-1}$)	Sample concentration ^c ($\mu\text{g L}^{-1}$)
1	0.5	2	10
2	1	4	20
3	2	8	40
4	5	20	100
5	10	40	200
6	20	80	400
7	25	100	500
8	100	400	2000
9	200	800	4000
10	250	1000	5000
11	500	2000	10000
12	1000	4000	20000

a) Concentration levels for benzene, alpha-pinene, 2-undecanone, ethyl nonanoate, 1-undecanol
b) Concentration levels for 2-hexanone, ethyl butanoate, benzaldehyde, acetophenon, eucalyptol
c) Concentration levels for 1-pentanol

3.2.4.3 Result and discussion

The compounds used for this investigation belong to different chemical classes and ranges from low to medium polarity as well as low to medium-high molecular weight. The selection of the compounds was based on their presence as metabolites in fruit¹⁵³. The scope of this investigation is to evaluate the extraction efficiency of two new PILs-based coatings, poly([VBHDIM][NTf₂]) and poly([DDMGlu][MTFSI]), and compare their performances with two commercially available SPME fibers. In addition, the investigation offers an opportunity to assess the suitability of these coatings for the determination of food composition. To ensure effective comparison of the extraction efficiencies of the PILs and commercially available coatings, both their composition and thickness were taken in account. The thickness of the PILs coatings was approximately 10 μm , thus the commercially available PDMS (7 μm) coating was selected for the evaluation.

Since PILs were generally polar, a relatively polar commercial fiber, polyacrylate, 85 μm (PA), was also included in this study.

Firstly, extraction time profiles were obtained for the entire set of analytes under the same working conditions. Equilibrium conditions for the extraction process were reached for all the analytes within 60 minutes for all the coatings. Subsequently, all the further experiments were carried out using 60 min extraction time. All extractions were carried out in headspace mode in order to reduce any potential matrix impact on the coating efficiency and robustness.

3.2.4.3.1 Analytical performances

HS-SPME-GC-MS calibration curves were obtained under the aforementioned conditions at equilibrium time using all the coatings used in the current investigation. The calibration levels and corresponding concentrations of all the analytes are specified in Table 3.32. Liquid injections of working solutions of the analytes in methanol into the GC-MS were used to convert the SPME detector responses from the headspace extractions into amounts extracted (pg). All experiments were carried out triplicate.

Table 3.33 Summary of analytical performances and reproducibility values (% RSD) for all the coatings tested

Analyte	Linear range (µg L ⁻¹)	Linearity (R ²)	Curve equation	%RDS*(¹)	% RSD*(²)	% RSD*(³)
Poly([VBHDIM][NTf ₂])						
benzene	0.5-500	0.9998	y=16.9x+9.4	5.4	6.0	1.6
1-pentanol	10-10000	0.9997	y=1.2x-51.63	13.2	0.4	0.4
2-hexanone	2-2000	0.9996	y=5.0x+196.9	10.0	0.4	0.3
ethyl butanoate	2-2000	0.9996	y=12.0x+251.5	8.4	0.7	0.3
α-pinene	0.5-250	0.9996	y=155.5x+119.65	4.4	3.9	2.9
benzaldehyde	2-1000	0.9997	y=6.9x-48.9	5.7	1.6	0.6
eucalyptol	2-400	0.9997	y=47.6x-142.4	4.3	5.3	0.3
acetophenone	2-2000	0.9998	y=7.6x+137.1	4.4	2.0	0.9
2-undecanoate	0.5-10	0.9977	y=2793.9x+289.1	5.7	1.2	5.2
ethyl nonanoate	0.5-10	0.9957	y=2496.9x+75.0	13.6	1.1	1.2
1-undecanol	0.5-25	0.9955	y=2541.5x+616.0	10.1	1.4	7.5
*Obtained from triplicate extractions at calibration level 3 ⁽¹⁾ ,6 ⁽²⁾ ,10 ⁽³⁾						
PA						
benzene	0.5-100	0.9998	y=108.1x+84.6	3.8	0.9	2.2
1-pentanol	10-2000	0.9999	y=15.1x+23.9	1.2	1.4	5.7
2-hexanone	2-400	0.9998	y=25.6x+236.4	1.6	2.0	2.3
ethyl butanoate	2-400	0.9998	y=64.4x+815.9	0.5	4.3	7.6
α-pinene	0.5-100	0.9991	y=560.9x+573.3	5.3	8.4	6.5
benzaldehyde	2-400	0.9997	y=87.2x+399.5	4.4	5.7	7.2
eucalyptol	2-400	0.9992	y=163.3x+901.0	5.4	8.9	3.5
acetophenone	2-400	0.9996	y=85.5x+499.9	4.6	1.4	6.1
2-undecanoate	0.5-5	0.9994	y=2608.9x-1087.1	3.5	4.0	3.8
ethyl nonanoate	0.5-5	0.9992	y=2560.6x+6028.6	0.9	9.8	3.3
1-undecanol	0.5-5	0.9935	y=10662.2x+2931.9	3.3	14.4	4.1
*Obtained from triplicate extractions at calibration level 3 ⁽¹⁾ ,6 ⁽²⁾ ,8 ⁽³⁾						
Poly([DDMglu][MTFSI])						
benzene	1-500	0.9993	y=0.6x+3.6	7.3	5.2	2.3
1-pentanol	20-10000	0.9953	y=0.2x-8.9	26.5	2.3	4.0
2-hexanone	20-2000	0.9972	y=0.3+1.8	13.9	3.3	4.4
ethyl butanoate	4-2000	0.9969	y=0.7x+6.0	5.7	2.7	9.8
α-pinene	1-500	0.9961	y=8.0x-48.7	13.6	3.4	4.7
benzaldehyde	40-1000	0.9908	y=0.5x-20.0	<LLOQ	5.4	4.0
eucalyptol	4-2000	0.9962	y=2.7x-65.2	38.4	6.4	2.4
acetophenone	20-1000	0.9982	y=0.6x+3.7	<LLOQ	3.4	4.4
2-undecanoate	1-250	0.9993	y=109.7x-204.7	22.6	0.7	4.1
ethyl nonanoate	1-250	0.9979	y=113.1x-492.4	22.4	1.2	6.2
1-undecanol	1-200	0.9993	y=142.4x-19.7	33.6	4.2	0.9
*Obtained from triplicate extractions at calibration level 3 ⁽¹⁾ ,6 ⁽²⁾ ,10 ⁽³⁾						

PDMS 7 μ m						
benzene	1-500	0.9998	y=7.8x+26.6	2.0	2.1	3.5
1-pentanol	20-10000	0.9942	y=2.4x-34.21	4.5	5.9	4.2
2-hexanone	4-2000	0.9972	y=2.3+158.8	2.6	4.0	3.1
ethyl butanoate	4-2000	0.9913	y=33.8x+21.4	1.1	2.8	2.6
α -pinene	1-250	0.9990	y=34.4x+76.1	2.2	6.6	2.3
benzaldehyde	4-1000	0.9983	y=3.1x+140.0	2.7	3.0	4.0
eucalyptol	4-1000	0.9929	y=33.2x-709.4	5.5	4.1	3.6
acetophenone	4-1000	0.9978	y=9.8x+293.8	5.7	3.0	2.7
2-undecanoate	1-20	0.9984	y=893.7x+427.1	3.1	1.8	3.7
ethyl nonanoate	1-20	0.9997	y=1277.4x+71.6	3.1	5.0	9.5
1-undecanol	1-25	0.9980	y=565.6x+988.4	11.9	4.1	0.1

*Obtained from triplicate extractions at calibration level 3⁽¹⁾,6⁽²⁾,10⁽³⁾

The linearity given by the PILs-coating can be considered satisfactory when compared to commercial fibers. The values obtained ranged from 0.9955 to 0.9998 for poly([VBHDIM][NTf₂]) and 0.9908 to 0.9913 for poly([DDMGlu][MTFSI]). Moreover, poly([VBHDIM][NTf₂]) was able to achieve lower LLOQ for all the analytes extracted compared to poly([DDMGlu][MTFSI]) and PDMS, and comparable LLOQ to PA. From the reproducibility results obtained (Table 3.33) the RSD% of the poly([VBHDIM][NTf₂]) coating for all analytes ranges from 0.3 to 13.6% over all the concentration levels tested. For poly([DDMGlu][MTFSI]), however, relatively higher RSD% values ranging from 7.6 to 38.4% were obtained at the lower concentration. It is worth to underline that generally PILs-based coatings provided broader linear ranges compared to the commercial coatings, particularly for 2-undecanone, 1-undecanol and ethyl nonanoate by comparing poly([VBHDIM][NTf₂]) with PA, and poly([DDMGlu][MTFSI]) with PDMS.

3.2.4.3.2 Comparison of coatings in terms of extraction sensitivity

A better understanding of the characteristic selectivity of each functionalized PIL-based fiber can be ascertained by comparing the extraction efficiencies of the coatings, taking into account their sensitivities expressed as the calibration slopes obtained by SPME sampling^{214,218}. As shown in Table 3.33, the PA fiber exhibited the highest sensitivity for all selected analytes based on the slopes obtained for all analytes. With respect to the PDMS fiber, the extraction efficiency was either comparable to (poly([VBHDIM][NTf₂])) or an order magnitude higher than the PIL-based fiber. The relatively higher extraction efficiency of the PA fiber can be attributed to the relatively larger film thickness (85 μ m) as well as the favorable analyte interactions with the fiber. The

good affinity of PA coating for the analytes can be explained in terms of functional groups: all the analytes chosen in this study (except α -pinene) contain oxygen as the electronegative heteroatom, which can interact favorably with polar coatings such as PA via dipole-dipole and hydrogen bonding interactions. However, such conclusion may not be entirely accurate since the thickness of the coatings was not considered. Obviously, the PA coating with a relatively larger coating thickness (85 μm) will demonstrate higher extraction efficiency compared to the other coatings. To correct for any possible bias, the coatings thickness must be carefully considered. Thus, due to the fact that the fibers have different coating thickness, the comparison of their efficiencies was carried out through normalization. Therefore, for effective evaluation of the commercial fibers and the PIL-based fibers, the slope of the calibration curve was divided by the thickness of the coatings in order to normalize the sensitivities obtained, as shown in Figure 3.33 Comparison of the film thickness normalization of the slope calculated from detector response for all coatings in the extraction of selected analytes. By this approach, the normalized extraction efficiency provides a better comparison between all fiber coatings regardless of extraction phase volume.

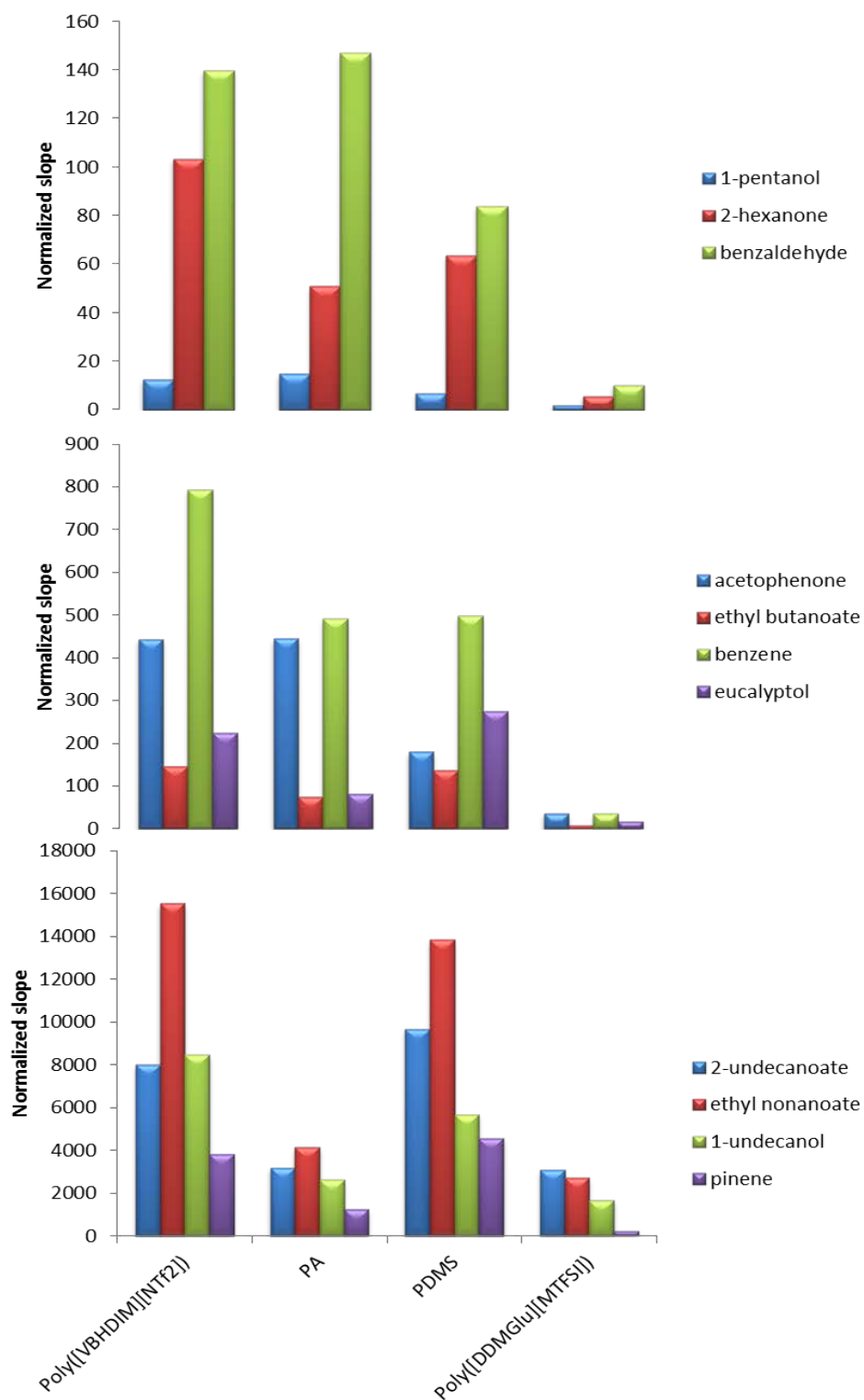


Figure 3.33 Comparison of the film thickness normalization of the slope calculated from detector response for all coatings in the extraction of selected analytes

Taking into account the normalized extraction efficiencies poly([VBHDIM][NTf₂]) PIL showed better performances compared to the other coatings for 2-hexanone, benzene, ethyl nonanoate and 1-undecanol. Also, the aforementioned PIL coating showed comparable efficiencies to PA for benzaldehyde, 1-pentanol, acetophenone and to PDMS for ethyl butanoate, eucalyptol, 2-undecanoate and α -pinene. The higher selectivity of the PILs-coating for benzene is in agreement with studies previously reported²¹⁵, demonstrating that this fiber coating is highly selective for large polyaromatic molecules due to the enhanced π - π stacking and high dispersion interaction. The results obtained for acetophenone and benzaldehyde may be due to the inductive effect of aromatic ring substituents that partially deactivate the π electrons leading to less pronounced affinity with the coating. The poly([VBHDIM][NTf₂]) coating showed an efficiency that can be defined as between PA and PDMS coatings' performances. The poly([DDMGlu][MTFSI]) PIL fiber generally exhibited lower efficiencies for all the analytes except for 2-undecanoate, where it is becomes comparable to PA.

3.2.4.4 Conclusions

The analytical performances of two PIL-based SPME sorbent coatings, poly([VBHDIM][NTf₂]) and poly([DDMGlu][MTFSI]), have been evaluated for the analysis of metabolites commonly found in fruit and belonging to different chemical classes. The two PIL-based fibers exhibited satisfactory performances in terms of linearity and reproducibility compared to commercial SPME fibers. The extraction efficiency of both PIL coatings was also compared with the commercial SPME coating. In spite of the important differences in film thicknesses among the fibers, the extraction performances could be considered satisfactory using the PIL coatings. The poly([VBHDIM][NTf₂]) coating showed good selectivity towards aromatic compounds and its extraction efficiency is comparable to the performance of PA and PDMS coatings.

From the results obtained, the PIL coatings, specifically poly([VBHDIM][NTf₂]), demonstrate that by careful manipulation of their functionalities and chemistry, PIL-SPME fibers can be applied successfully to the analysis of food components. This is because generally, the poly([VBHDIM][NTf₂]) effectively extracted all the analytes and thus makes it a potential coating of choice for a global non-targeted food metabolomics studies. The significant differences in the performances of the poly([VBHDIM][NTf₂]) and poly([DDMGlu][MTFSI])

may be attributed to the differences in their chemical properties. Although, PA coating showed relatively good extraction efficiencies for some analytes, its selectivity is very pronounced for certain class of compounds, and thus may not be an appropriate coating for food metabolomics study.

3.3 References

- (1) Xia, J.; Broadhurst, D. I.; Wilson, M.; Wishart, D. S. *Metabolomics* 2013, 9, 280–299.
- (2) Rifai, N.; Gillette, M. a; Carr, S. a *Nat. Biotechnol.* 2006, 24, 971–83.
- (3) Lee, M. S.; Kerns, E. H. *Mass Spectrom. Rev.* 18, 187–279.
- (4) Meng, Z.; Veenstra, T. D. *Proteomics. Clin. Appl.* 2007, 1, 747–57.
- (5) Perchalski, R. J.; Yost, R. A.; Wilder, B. J. *Anal. Chem.* 1982, 54, 1466–1471.
- (6) Yost, R. A.; Fetterolf, D. D. *Mass Spectrom. Rev.* 1983, 2, 1–45.
- (7) Tiller, P. R.; Cunniff, J.; Land, A. P.; Schwartz, J.; Jardine, I.; Wakefield, M.; Lopez, L.; Newton, J. F.; Burton, R. D.; Folk, B. M.; Buhrman, D. L.; Price, P.; Wu, D. J. *Chromatogr. A* 1997, 771, 119–125.
- (8) Zhu, X.; Desiderio, D. M. *Mass Spectrom. Rev.* 1996, 15, 213–240.
- (9) Cudjoe, E.; Togunde, P.; Pawliszyn, J. *Bioanalysis* 2012, 4, 2605–2619.
- (10) Bojko, B.; Cudjoe, E.; Gómez-Ríos, G. A.; Gorynski, K.; Jiang, R.; Reyes-Garcés, N.; Risticvic, S.; Silva, É. A. S.; Togunde, O.; Vuckovic, D.; Pawliszyn, J. *Anal. Chim. Acta* 2012, 750, 132–151.
- (11) Cudjoe, E.; Bojko, B.; de Lannoy, I.; Saldivia, V.; Pawliszyn, J. *Angew. Chemie Int. Ed.* 2013, 52, 12124–12126.
- (12) Kataoka, H.; Saito, K. *J. Pharm. Biomed. Anal.* 2011, 54, 926–50.
- (13) Richardson, S. D. *Anal. Chem.* 2012, 84, 747–78.
- (14) Rosenfeld, J. M. *Sample Preparation for Hyphenated Analytical Techniques*; Rosenfeld, J. M., Ed.; Blackwell Publishing Ltd.: Oxford, UK, 2004.
- (15) Naccarato, A.; Gionfriddo, E.; Sindona, G.; Tagarelli, A. *Anal. Chim. Acta* 2014, Accepted Manuscript.
- (16) Kagedal, B.; Goldstein, D. S. *J. Chromatogr. B Biomed. Sci. Appl.* 1988, 429, 177–233.
- (17) Nakagawara, A.; Ikeda, K.; Tsuneyoshi, M.; Daimaru, Y.; Enjoji, M. *Cancer* 1985, 55, 2794–2798.
- (18) Durstewitz, D.; Kelc, M.; Gunturkun, O. *J. Neurosci.* 1999, 19, 2807–2822.

- (19) Wang, Y.-L.; Wei, J.-W.; Sun, A. Y. *Neurochem. Res.* 1993, 18, 1293–1297.
- (20) Barron, J. J. *Clin. Pathol.* 2010, 63, 669–74.
- (21) Castleberry, R. P. *Eur. J. Cancer* 1997, 33, 1430–1437.
- (22) Harro, J.; Orelund, L. *Brain Res. Rev.* 2001, 38, 79–128.
- (23) Rosano, T.; Swift, T.; Hayes, L. *Clin. Chem.* 1991, 37, 1854–1867.
- (24) Machida, M.; Sakaguchi, A.; Kamada, S.; Fujimoto, T.; Takechi, S.; Kakinoki, S.; Nomura, A. *J. Chromatogr. B* 2006, 830, 249–254.
- (25) Sabbioni, C.; Saracino, M. A.; Mandrioli, R.; Pinzauti, S.; Furlanetto, S.; Gerra, G.; Raggi, M. A. *J. Chromatogr. A* 2004, 1032, 65–71.
- (26) Rozet, E.; Morello, R.; Lecomte, F.; Martin, G. B.; Chiap, P.; Crommen, J.; Boos, K. S.; Hubert, P. *J. Chromatogr. B. Analyt. Technol. Biomed. Life Sci.* 2006, 844, 251–60.
- (27) Oppolzer, D.; Moreno, I.; da Fonseca, B.; Passarinha, L.; Barroso, M.; Costa, S.; Queiroz, J. A.; Gallardo, E. *Biomed. Chromatogr.* 2013, 27, 608–14.
- (28) Thomas, D. H.; Taylor, J. D.; Barnaby, O. S.; Hage, D. S. *Clin. Chim. Acta.* 2008, 398, 63–9.
- (29) Kumar, A.; Hart, J. P.; McCalley, D. V. *J. Chromatogr. A* 2011, 1218, 3854–61.
- (30) Auger, J.; Boulay, R.; Jaillais, B.; Delion-Vancassel, S. *J. Chromatogr. A* 2000, 870, 395–403.
- (31) Fotopoulou, M. A.; Ioannou, P. C. *Anal. Chim. Acta* 2002, 462, 179–185.
- (32) Alberts, G.; Boomsma, F.; Man in 't Veld, A. J.; Schalekamp, M. A. D. H. *J. Chromatogr. B Biomed. Sci. Appl.* 1992, 583, 236–240.
- (33) Iizuka Hideaki, Ishige Takayuki, Ohta Yuri, Y. T. In *Advances in Experimental Medicine and Biology*; Springer US, 1999; pp. 821–826.
- (34) Sakaguchi, Y.; Yoshida, H.; Hayama, T.; Itoyama, M.; Todoroki, K.; Yamaguchi, M.; Nohta, H. *J. Chromatogr. A* 2011, 1218, 5581–6.
- (35) Liu, L.; Li, Q.; Li, N.; Ling, J.; Liu, R.; Wang, Y.; Sun, L.; Chen, X. H.; Bi, K. *J. Sep. Sci.* 2011, 34, 1198–204.

- (36) Carvalho, V. M. J. *Chromatogr. B. Analyt. Technol. Biomed. Life Sci.* 2012, 883-884, 50–8.
- (37) Moriarty, M.; Lehane, M.; O'Connell, B.; Keeley, H.; Furey, A. *Talanta* 2012, 90, 1–11.
- (38) Sirén, H.; Mielonen, M.; Herlevi, M. J. *Chromatogr. A* 2004, 1032, 289–297.
- (39) Gosetti, F.; Mazzucco, E.; Gennaro, M. C.; Marengo, E. *Anal. Bioanal. Chem.* 2013, 405, 907–16.
- (40) El-Beqqali, A.; Kussak, A.; Abdel-Rehim, M. J. *Sep. Sci.* 2007, 30, 421–424.
- (41) Moriarty, M.; Lee, A.; O'Connell, B.; Kelleher, A.; Keeley, H.; Furey, A. *Anal. Bioanal. Chem.* 2011, 401, 2481–93.
- (42) Peterson, Z. D.; Collins, D. C.; Bowerbank, C. R.; Lee, M. L.; Graves, S. W. J. *Chromatogr. B* 2002, 776, 221–229.
- (43) Vuorensola, K.; Sirén, H. J. *Chromatogr. A* 2000, 895, 317–327.
- (44) Bouri, M.; Lerma-García, M. J.; Salghi, R.; Zougagh, M.; Ríos, A. *Talanta* 2012, 99, 897–903.
- (45) Zhang, X.; Xu, S.; Lim, J.-M.; Lee, Y.-I. *Talanta* 2012, 99, 270–6.
- (46) Xu, Z.; Okada, J.; Timerbaev, A. R.; Hirokawa, T. J. *Sep. Sci.* 2009, 32, 4143–7.
- (47) Bacaloni, a; Insogna, S.; Sancini, a; Ciarrocca, M.; Sinibaldi, F. *Biomed. Chromatogr.* 2013, 27, 987–93.
- (48) Xu, X.; Zhang, H.; Shi, H.; Ma, C.; Cong, B.; Kang, W. *Anal. Biochem.* 2012, 427, 10–7.
- (49) Diao, P.; Yuan, H.; Huo, F.; Chen, L.; Xiao, D.; Paa, M. C.; Choi, M. M. F. *Talanta* 2011, 85, 1279–84.
- (50) Chicharro, M.; Sánchez, A.; Zapardiel, A.; Rubianes, M. D.; Rivas, G. *Anal. Chim. Acta* 2004, 523, 185–191.
- (51) Klett, O.; Nischang, I.; Nyholm, L. *Electrophoresis* 2002, 23, 3678–82.
- (52) Chen, D. C.; Zhan, D. Z.; Cheng, C. W.; Liu, a C.; Chen, C. H. J. *Chromatogr. B. Biomed. Sci. Appl.* 2001, 750, 33–9.
- (53) Vuorensola, K.; Kokkonen, J.; Sirén, H.; Ketola, R. A. *Electrophoresis* 2001, 22, 4347–54.

- (54) Park, N.-H.; Hong, J. Y.; Shin, H. J.; Hong, J. J. *Chromatogr. A* 2013, 1305, 234–43.
- (55) Llop, A.; Borrull, F.; Pocurull, E. *Anal. Chim. Acta* 2010, 665, 231–6.
- (56) Singh, D. K.; Sanghi, S. K.; Gowri, S.; Chandra, N.; Sanghi, S. B. *J. Chromatogr. A* 2011, 1218, 5683–5687.
- (57) Zhao, Y.-Y.; Jing, Z.-Z.; Wang, H.; Zhang, H.-S.; Yu, J.-X. *Anal. Chim. Acta* 2002, 468, 255–261.
- (58) Zhao, Y.-Y.; Cai, L.-S.; Jing, Z.-Z.; Wang, H.; Yu, J.-X.; Zhang, H.-S. *J. Chromatogr. A* 2003, 1021, 175–181.
- (59) Husek, P. *J. Chromatogr. B. Biomed. Sci. Appl.* 1998, 717, 57–91.
- (60) Myung, S. W.; Kim, M.; Min, H. K.; Yoo, E. a.; Kim, K. R. *J. Chromatogr. B. Biomed. Sci. Appl.* 1999, 727, 1–8.
- (61) Cavaliere, B.; Macchione, B.; Monteleone, M.; Naccarato, A.; Sindona, G.; Tagarelli, A. *Anal. Bioanal. Chem.* 2011, 400, 2903–12.
- (62) Gionfriddo, E.; Naccarato, A.; Sindona, G.; Tagarelli, A. *Anal. Chim. Acta* 2012, 747, 58–66.
- (63) Monteleone, M.; Naccarato, A.; Sindona, G.; Tagarelli, A. *Anal. Chim. Acta* 2013, 759, 66–73.
- (64) Lord, H.; Pawliszyn, J. *J. Chromatogr. A* 2000, 885, 153–193.
- (65) Kataoka, H. *Anal. Sci.* 2011, 27, 893.
- (66) Cavaliere, B.; Macchione, B.; Sindona, G.; Tagarelli, A. *J. Chromatogr. A* 2008, 1205, 137–143.
- (67) Monteleone, M.; Naccarato, A.; Sindona, G.; Tagarelli, A. *J. Chromatogr. A* 2012, 1251, 160–8.
- (68) Cavaliere, B.; Monteleone, M.; Naccarato, A.; Sindona, G.; Tagarelli, A. *J. Chromatogr. A* 2012, 1257, 149–57.
- (69) Kataoka, H. *J. Chromatogr. A* 1996, 733, 19–34.
- (70) Commission Decision (2002/657/EC) of 12 August 2002 implementing Council Directive 96/23/EC concerning the performance of analytical methods and the interpretation of results, *Off. J. Eur. Commun.*, L221/8, 17 August 2002.

- (71) Matuszewski, B. K.; Constanzer, M. L.; Chavez-Eng, C. M. *Anal. Chem.* 2003, 75, 3019–3030.
- (72) Wick, A.; Fink, G.; Ternes, T. a *J. Chromatogr. A* 2010, 1217, 2088–103.
- (73) Richardson, S. D. *Anal. Chem.* 2012, 84, 747–78.
- (74) Jover, E.; Matamoros, V.; Bayona, J. M. *J. Chromatogr. A* 2009, 1216, 4013–9.
- (75) Babić-Samardžija, K.; Hackerman, N. J. *Solid State Electrochem.* 2005, 9, 483–497.
- (76) Reemtsma, T.; Miehe, U.; Duennbier, U.; Jekel, M. *Water Res.* 2010, 44, 596–604.
- (77) Kiss, A.; Fries, E. *Environ. Sci. Pollut. Res. Int.* 2009, 16, 702–10.
- (78) Kloepfer, A.; Jekel, M.; Reemtsma, T. *Environ. Sci. Technol.* 2005, 39, 3792–8.
- (79) Matamoros, V.; Jover, E.; Bayona, J. M. *Water Sci. Technol.* 2010, 61, 191–8.
- (80) Ni, H.-G.; Lu, F.-H.; Luo, X.; Tian, H.-Y.; Zeng, E. Y. *Environ. Sci. Technol.* 2008, 42, 1892–7.
- (81) Kloepfer, A.; Jekel, M.; Reemtsma, T. *J. Chromatogr. A* 2004, 1058, 81–88.
- (82) De Groote, P.; Jonas, A. M.; Devaux, J.; Godard, P. J. *Polym. Sci. Part B Polym. Phys.* 2001, 39, 2022–2034.
- (83) Heberer, T.; Stan, J. *FRESENIUS Environ. Bull.* 1994, 3, 639–643.
- (84) Stavrić, B.; Klassen, R. J. *Assoc. Off. Anal. Chem.* 1975, 58, 427.
- (85) Van Leerdam, J. a.; Hogenboom, A. C.; van der Kooi, M. M. E.; de Voogt, P. *Int. J. Mass Spectrom.* 2009, 282, 99–107.
- (86) Loos, R.; Gawlik, B. M.; Locoro, G.; Rimaviciute, E.; Contini, S.; Bidoglio, G. *Environ. Pollut.* 2009, 157, 561–568.
- (87) Giger, W.; Schaffner, C.; Kohler, H.-P. E. *Environ. Sci. Technol.* 2006, 40, 7186–7192.
- (88) Loos, R.; Locoro, G.; Comero, S.; Contini, S.; Schwesig, D.; Werres, F.; Balsaa, P.; Gans, O.; Weiss, S.; Blaha, L.; Bolchi, M.; Gawlik, B. M. *Water Res.* 2010, 44, 4115–4126.
- (89) Cancilla, D. A.; Baird, J. C.; Rosa, R. *Bull. Environ. Contam. Toxicol.* 2003, 70, 868–75.

- (90) Breedveld, G. D.; Roseth, R.; Sparrevik, M.; Hartnik, T.; Hem, L. J. *Water, Air Soil Pollut. Focus* 2003, 3, 91–101.
- (91) Voutsas, D.; Hartmann, P.; Schaffner, C.; Giger, W. *Environ. Sci. Pollut. Res. - Int.* 2006, 13, 333–341.
- (92) Weiss, S.; Reemtsma, T. *Anal. Chem.* 2005, 77, 7415–20.
- (93) Weiss, S.; Jakobs, J.; Reemtsma, T. *Environ. Sci. Technol.* 2006, 40, 7193–7199.
- (94) Pena, M. T.; Vecino-Bello, X.; Casais, M. C.; Mejuto, M. C.; Cela, R. *Anal. Bioanal. Chem.* 2012, 402, 1679–95.
- (95) Carpinteiro, I.; Abuin, B.; Ramil, M.; Rodríguez, I.; Cela, R. *Anal. Bioanal. Chem.* 2012, 402, 2471–8.
- (96) Céspedes, R.; Lacorte, S.; Ginebreda, A.; Barceló, D. *Anal. Bioanal. Chem.* 2006, 385, 992–1000.
- (97) Domínguez, C.; Reyes-Contreras, C.; Bayona, J. M. *J. Chromatogr. A* 2012, 1230, 117–22.
- (98) Liu, Y.-S.; Ying, G.-G.; Shareef, A.; Kookana, R. S. *J. Chromatogr. A* 2011, 1218, 5328–35.
- (99) Asimakopoulos, A. G.; Bletsou, A. a; Wu, Q.; Thomaidis, N. S.; Kannan, K. *Anal. Chem.* 2013, 85, 441–8.
- (100) Richter, D.; Massmann, G.; Dünnebier, U. *Water Res.* 2008, 42, 1369–1378.
- (101) Richter, D.; Dünnebier, U.; Massmann, G.; Pekdeger, A. *J. Chromatogr. A* 2007, 1157, 115–21.
- (102) Mazzotti, F.; Di Donna, L.; Macchione, B.; Maiuolo, L.; Perri, E.; Sindona, G. *Rapid Commun. Mass Spectrom.* 2009, 23, 1515–8.
- (103) Cavaliere, B.; De Nino, A.; Hayet, F.; Lazez, A.; Macchione, B.; Moncef, C.; Perri, E.; Sindona, G.; Tagarelli, A. *J. Agric. Food Chem.* 2007, 55, 1454–62.
- (104) Pawliszyn, J.; Kudlejova, L.; Risticovic, S.; Vuckovic, D. In *Handbook of Solid Phase Microextraction*; 2012; pp. 201–249.
- (105) Box, G.; Hunter, W.; Hunter, S. *Statistics for Experimenters: An Introduction to Design, Data Analysis, and Model Building*; John Wiley & Sons, 1978.

- (106) Naccarato, A.; Moretti, S.; Sindona, G.; Tagarelli, A. *Anal. Bioanal. Chem.* 2013, 405, 8267–76.
- (107) Budavari, S. *The Merck Index – An Encyclopedia of Chemicals, Drugs and Biologicals.*; Merck and Co., Inc.: New York, 1996; p. 816.
- (108) *Kirk-Othmer Encyclopedia of Chemical Technology*; John Wiley & Sons, Inc.: Hoboken, NJ, USA, 2000.
- (109) Ashford, R. D. *Ashford's Dictionary of Industrial Chemicals*; Wavelength Publications Ltd.: London, England, 1994; p. 474.
- (110) Yagil, G.; Anbar, M. J. *Am. Chem. Soc.* 1962, 84, 1797–1803.
- (111) Davis, W. E.; Li, Y. *Anal. Chem.* 2008, 80, 5449–53.
- (112) Wells, H. G. *J. Exp. Med.* 1908, 10, 457–64.
- (113) Parodi, S.; Flora, S. De; Cavanna, M.; Pino, A.; Robbiano, L.; Bennicelli, C.; Brambilla, G. *Cancer Res.* 1981, 41, 1469–1482.
- (114) Zeilmaker, M. J.; Horsfall, M. J.; van Helten, J. B. M.; Glickman, B. W.; Mohn, G. R. *Mol. Carcinog.* 1991, 4, 180–188.
- (115) Lambert, C. E.; Shank, R. C. *Carcinogenesis* 1988, 9, 65–70.
- (116) Toth, B. *Hydrazines and Cancer: A Guidebook on the Carciogenic Activities of Hydrazines, Related Chemicals, and Hydrazine Containing Natural Products*; CRC Press, 2004; p. 264.
- (117) Morris, J.; Densem, J. W.; Wald, N. J.; Doll, R. *Occup. Environ. Med.* 1995, 52, 43–45.
- (118) Hydrazine/Hydrazine sulfate (CASRN 302-01-2) | IRIS | US EPA <http://www.epa.gov/iris/subst/0352.htm> (accessed Nov 18, 2013).
- (119) Chen, X.; Xiang, Y.; Li, Z.; Tong, A. *Anal. Chim. Acta* 2008, 625, 41–6.
- (120) Safavi, A.; Karimi, M. A. *Talanta* 2002, 58, 785–92.
- (121) Lv, J.; Huang, Y.; Zhang, Z. *Anal. Lett.* 2001, 34, 1323–1330.
- (122) He, Z. K.; Fuhrmann, B.; Spohn, U. *Anal. Chim. Acta* 2000, 409, 83–91.
- (123) Safavi, A.; Baezzat, M. . *Anal. Chim. Acta* 1998, 358, 121–125.

- (124) Ganesh, S.; Khan, F.; Ahmed, M. K.; Pandey, S. K. *Talanta* 2011, 85, 958–963.
- (125) Guo, L.; Matysik, F.-M.; Gläser, P.; Engewald, W. *Electrophoresis* 2005, 26, 3341–8.
- (126) Liu, Z.; Zou, H.; Ye, M. *Electrophoresis* 2001, 22, 1298–304.
- (127) Yang, M.; Li, H. L. *Talanta* 2001, 55, 479–84.
- (128) Mori, M.; Tanaka, K.; Xu, Q.; Ikedo, M.; Taoda, H.; Hu, W. J. *Chromatogr. A* 2004, 1039, 135–139.
- (129) Smolenkov, A. D.; Rodin, I. A.; Shpigun, O. A. *J. Anal. Chem.* 2012, 67, 98–113.
- (130) Elias, G.; Bauer, W. F. J. *Sep. Sci.* 2006, 29, 460–464.
- (131) Gyllenhaal, O.; Grönberg, L.; Vessman, J. J. *Chromatogr. A* 1990, 511, 303–315.
- (132) Evgen'ev, M. I.; Evgen'eva, I. I.; Ismailova, R. N. *J. Anal. Chem.* 2000, 55, 933–937.
- (133) Seifart, H. I.; Gent, W. L.; Parkin, D. P.; van Jaarsveld, P. P.; Donald, P. R. J. *Chromatogr. B Biomed. Sci. Appl.* 1995, 674, 269–275.
- (134) Riggs, A. S.; Borth, D. M.; Tutty, D. G.; Yu, W. S. J. *AOAC Int.* 2008, 91, 5–12.
- (135) Preece, N. E.; Forrow, S.; Ghatineh, S.; Langley, G. J.; Timbrell, J. A. J. *Chromatogr. B Biomed. Sci. Appl.* 1992, 573, 227–234.
- (136) Selim, S.; Warner, C. R. J. *Chromatogr. A* 1978, 166, 507–511.
- (137) Khuhawar, M. Y.; Zardari, L. A. *Anal. Sci.* 2008, 24, 1493–6.
- (138) Oh, J. A.; Park, J. H.; Shin, H. S. *Anal. Chim. Acta* 2013, 769, 79–83.
- (139) George, M.; Nagaraja, K. S.; Balasubramanian, N. *Talanta* 2008, 75, 27–31.
- (140) Zarei, A. R. *Anal. Biochem.* 2007, 369, 161–7.
- (141) Gyllenhaal, O.; Grönberg, L.; Vessman, J. J. *Chromatogr. A* 1990, 511, 303–315.
- (142) Kester, P. E.; Danielson, N. D. *Chromatographia* 1984, 18, 125–128.
- (143) Khuhawar, M. Y.; Zardari, L. A. 2006, 14, 323–328.
- (144) Aiello, D.; De Luca, D.; Gionfriddo, E.; Naccarato, A.; Napoli, A.; Romano, E.; Russo, A.; Sindona, G.; Tagarelli, A. *Eur. J. Mass Spectrom.* 2011, 17, 1–31.

- (145) Pawliszyn, J. In *Handbook of Solid Phase Microextraction*; 2012; pp. 61–97.
- (146) Pawliszyn, J.; Shirey, R. E. In *Handbook of Solid Phase Microextraction*; 2012; pp. 99–133.
- (147) Kataoka, H.; Lord, H. L.; Pawliszyn, J. J. *Chromatogr. A* 2000, 880, 35–62.
- (148) Aiello, D.; De Luca, D.; Gionfriddo, E.; Naccarato, A.; Napoli, A.; Romano, E.; Russo, A.; Sindona, G.; Tagarelli, A. *Eur. J. mass Spectrom. Chichester Engl.* 2011, 17, 1–31.
- (149) Risticvic, S.; DeEll, J. R.; Pawliszyn, J. J. *Chromatogr. A* 2012, 1251, 208–18.
- (150) Risticvic, S.; Carasek, E.; Pawliszyn, J. *Anal. Chim. Acta* 2008, 617, 72–84.
- (151) Pawliszyn, J.; Kudlejova, L.; Risticvic, S. In *Handbook of Solid Phase Microextraction*; 2012; pp. 291–334.
- (152) Innocente, N.; Marchesini, G.; Biasutti, M. *Food Chem.* 2011, 124, 1249–1257.
- (153) Risticvic, S. *Univ. Waterloo, PhD Thesis* 2012.
- (154) Souza-Silva, E. A.; Pawliszyn, J. *Anal. Chem.* 2012, 84, 6933–6938.
- (155) Souza Silva, E. A.; Risticvic, S.; Pawliszyn, J. *TrAC Trends Anal. Chem.* 2013, 43, 24–36.
- (156) Spietelun, A.; Pilarczyk, M.; Kloskowski, A.; Namieśnik, J. *Chem. Soc. Rev.* 2010, 39, 4524–37.
- (157) Navarro-Alarcon, M.; Cabrera-Vique, C. *Sci. Total Environ.* 2008, 400, 115–41.
- (158) Whanger, P. D. *J. Am. Coll. Nutr.* 2002, 21, 223–232.
- (159) Thomson, C. D. *Eur. J. Clin. Nutr.* 2004, 58, 391–402.
- (160) Thiry, C.; Ruttens, A.; De Temmerman, L.; Schneider, Y.-J.; Pussemier, L. *Food Chem.* 2012, 130, 767–784.
- (161) Dumont, E.; Vanhaecke, F.; Cornelis, R. *Anal. Bioanal. Chem.* 2006, 385, 1304–23.
- (162) Brummell, D. A.; Watson, L. M.; Pathirana, R.; Joyce, N. I.; West, P. J.; Hunter, D. A.; McKenzie, M. J. *J. Agric. Food Chem.* 2011, 59, 10987–94.
- (163) Weekley, C. M.; Aitken, J. B.; Musgrave, I. F.; Harris, H. H. *Biochemistry* 2012, 51, 736–8.

- (164) Ferri, T.; Favero, G.; Frascioni, M. *Microchem. J.* 2007, 85, 222–227.
- (165) Cuderman, P.; Kreft, I.; Germ, M.; Kovacevic, M.; Stibilj, V. J. *J. Agric. Food Chem.* 2008, 56, 9114–20.
- (166) Infante, H. G.; Borrego, A. A.; Peachey, E.; Hearn, R.; O'Connor, G.; Barrera, T. G.; Ariza, J. L. G. *J. Agric. Food Chem.* 2009, 57, 38–45.
- (167) Liang, L.; Mo, S.; Zhang, P.; Cai, Y.; Mou, S.; Jiang, G.; Wen, M. *J. Chromatogr. A* 2006, 1118, 139–143.
- (168) Pan, F.; Tyson, J. F.; Uden, P. C. *J. Anal. At. Spectrom.* 2007, 22, 931.
- (169) Montes-Bayón, M.; Molet, M. J. D.; González, E. B.; Sanz-Medel, A. *Talanta* 2006, 68, 1287–93.
- (170) Turakainen, M.; Hartikainen, H.; Ekholm, P.; Seppänen, M. M. *J. Agric. Food Chem.* 2006, 54, 8617–22.
- (171) Vonderheide, A. P.; Montes-Bayon, M.; Caruso, J. A. *Analyst* 2002, 127, 49–53.
- (172) Łobiński, R.; Adams, F. C. *Spectrochim. Acta Part B At. Spectrosc.* 1997, 52, 1865–1903.
- (173) Haberhauer-Troyer, C.; Álvarez-Llamas, G.; Zitting, E.; Rodríguez-González, P.; Rosenberg, E.; Sanz-Medel, A. *J. Chromatogr. A* 2003, 1015, 1–10.
- (174) Beatriz De La Calle-Guntias, M.; Brunori, C.; Scerbo, R.; Chiavarini, S.; Quevauviller, P.; Adams, F.; Morabito, R. J. *J. Anal. At. Spectrom.* 1997, 12, 1041–1046.
- (175) Işcioglu, B.; Henden, E. *Anal. Chim. Acta* 2004, 505, 101–106.
- (176) Hope, J. L.; Prazen, B. J.; Nilsson, E. J.; Lidstrom, M. E.; Synovec, R. E. *Talanta* 2005, 65, 380–388.
- (177) Deng, C.; Shang, C.; Hu, Y.; Zhang, X. *J. Chromatogr. B* 2002, 775, 115–120.
- (178) Hušek, P. *J. Chromatogr. A* 1991, 552, 289–299.
- (179) Duan, J.; Hu, B. *J. Mass Spectrom.* 2009, 44, 605–12.
- (180) Arthur, C. L.; Pawliszyn, J. *Anal. Chem.* 1990, 62, 2145–2148.
- (181) Kotrebai, M.; Tyson, J. F.; Uden, P. C.; Birringer, M.; Block, E. *Anal. Commun.* 1999, 36, 249–252.

- (182) Carrillo, J. D.; Garrido-López, Á.; Tena, M. T. J. *Chromatogr. A* 2006, 1102, 25–36.
- (183) Llompart, M.; Lourido, M.; Landín, P.; García-Jares, C.; Cela, R. J. *Chromatogr. A* 2002, 963, 137–148.
- (184) Souza-Silva, E. A.; Lopez-Avila, V.; Pawliszyn, J. J. *Chromatogr. A* 2013.
- (185) Bojko, B.; Gorynski, K.; Gomez-Rios, G. A.; Knaak, J. M.; Machuca, T.; Spetzler, V. N.; Cudjoe, E.; Hsin, M.; Cypel, M.; Selzner, M.; Liu, M.; Keshavjee, S.; Pawliszyn, J. *Anal. Chim. Acta* 2013.
- (186) Feudo, G. Lo; Macchione, B.; Naccarato, A.; Sindona, G.; Tagarelli, A. *Food Res. Int.* 2011, 44, 781–788.
- (187) Pankow, J. F.; Luo, W.; Melnychenko, a. N.; Barsanti, K. C.; Isabelle, L. M.; Chen, C.; Guenther, a. B.; Rosenstiel, T. N. *Atmos. Meas. Tech.* 2012, 5, 345–361.
- (188) Belliardo, F.; Bicchi, C.; Cordero, C.; Liberto, E.; Rubiolo, P.; Sgorbini, B. J. *Chromatogr. Sci.* 2006, 44, 416–29.
- (189) Jeleń, H. H.; Majcher, M.; Dziadas, M. *Anal. Chim. Acta* 2012, 738, 13–26.
- (190) Risticvic, S.; Niri, V. H.; Vuckovic, D.; Pawliszyn, J. *Anal. Bioanal. Chem.* 2009, 393, 781–95.
- (191) Pawliszyn, J. *Handbook of Solid Phase Microextraction*; Pawliszyn, J., Ed.; Elsevier.; 2012.
- (192) Nongonierma, A.; Voilley, A.; Cayot, P.; Le Quéré, J.-L.; Springett, M. *Food Rev. Int.* 2006, 22, 51–94.
- (193) Contini, M.; Esti, M. *Food Chem.* 2006, 94, 143–150.
- (194) Roberts, D. D.; Pollien, P.; Milo, C. J. *Agric. Food Chem.* 2000, 48, 2430–7.
- (195) Dunemann, F.; Ulrich, D.; Boudichevskaia, a.; Grafe, C.; Weber, W. E. *Mol. Breed.* 2009, 23, 501–521.
- (196) Zhang, Y.; Zhang, J. *Anal. Chim. Acta* 2008, 627, 212–8.
- (197) Bianco, G.; Novario, G.; Zianni, R.; Cataldi, T. R. I. *Anal. Bioanal. Chem.* 2009, 393, 2019–27.
- (198) Setkova, L.; Risticvic, S.; Pawliszyn, J. J. *Chromatogr. A* 2007, 1147, 213–23.

- (199) Feinberg, M. J. *Chromatogr. A* 2007, 1158, 174–83.
- (200) Górecki, T.; Yu, X.; Pawliszyn, J. *Analyst* 1999, 124, 643–649.
- (201) Górecki, T.; Martos, P.; Pawliszyn, J. *Anal. Chem.* 1998, 70, 19–27.
- (202) Lestremau, F.; Desauziers, V.; Fanlo, J.-L. *Anal. Bioanal. Chem.* 2004, 378, 190–6.
- (203) Alvarez, E. G.; Valcárcel, M. *Talanta* 2009, 77, 1444–53.
- (204) Risticovic, S.; Pawliszyn, J. *Anal. Chem.* 2013, 85, 8987–8995.
- (205) Lopes Da Silva, J. A.; Castro, S. M.; Delgadillo, I. J. *Agric. Food Chem.* 2002, 50, 1976–1984.
- (206) Mercier, B.; Prost, J.; Prost, M. *Int. J. Occup. Med. Environ. Health* 2009, 22, 331–42.
- (207) Mishima, S.; Nakagawa, T. *J. Appl. Polym. Sci.* 2000, 78, 1304–1311.
- (208) Savary, G.; Guichard, E.; Doublier, J.-L.; Cayot, N. *Food Res. Int.* 2006, 39, 372–379.
- (209) Savary, G.; Guichard, E.; Doublier, J.-L.; Cayot, N.; Moreau, C. J. *Agric. Food Chem.* 2006, 54, 665–71.
- (210) Zafeiropoulou, T.; Evageliou, V.; Gardeli, C.; Yanniotis, S.; Komaitis, M. *Food Hydrocoll.* 2012, 28, 105–109.
- (211) Arvisenet, G.; Le Bail, P.; Voilley, a; Cayot, N. *J. Agric. Food Chem.* 2002, 50, 7088–93.
- (212) Ho, T. D.; Canestraro, A. J.; Anderson, J. L. *Anal. Chim. Acta* 2011, 695, 18–43.
- (213) Zhao, F.; Meng, Y.; Anderson, J. L. *J. Chromatogr. A* 2008, 1208, 1–9.
- (214) López-Darias, J.; Anderson, J. L.; Pino, V.; Afonso, A. M. *Anal. Bioanal. Chem.* 2011, 401, 2965–76.
- (215) Meng, Y.; Anderson, J. L. *J. Chromatogr. A* 2010, 1217, 6143–6152.
- (216) Juger, J.; Meyer, F.; Vidal, F.; Chevrot, C.; Teyssié, D. *Tetrahedron Lett.* 2009, 50, 128–131.
- (217) Joshi, M. D.; Chalumot, G.; Kim, Y.; Anderson, J. L. *Chem. Commun.* 2012, 48, 1410–2.
- (218) Meng, Y.; Pino, V.; Anderson, J. L. *Anal. Chem.* 2009, 81, 7107–12.

